Thesis

Topological insulators and superconductors: classification of topological crystalline phases and axion phenomena

Ken Shiozaki

Department of Physics, Kyoto University

December, 2014

Abstract

This thesis presents two topics of topological insulators and superconductors. One is a classification of topological crystalline insulators and superconductors which are topological phases protected by space group symmetries. Another topic is a study of axion phenomena in topological phases.

Chap. 1 is an overview of topological insulators and superconductors. Topological insulators and superconductors are classes of topological phases of free fermions. The momentum space topology of the Bloch and Bogoliubov de Gennes Hamiltonian characterizes topologically stable properties of the ground state against perturbation, leading robust low-energy gapless excitations localized at boundaries and defects of insulators and superconductors. The exploration of axion phenomena is a significant application of topological phases in which the band topology plays an essential role.

Chap. 2 gives a self-contained introduction of the band topology. We review a usual band theory with a careful description of symmetries, which include the time-reversal symmetry, the particle-hole symmetry, and space group symmetries. The existence of an energy gap in a band structure induces a classification of band insulators and superconductors: there are distinct classes characterized by topological invariants that remain unchanged against smooth variations of the band structure with preserving the energy gap.

Chap. 3 provides the complete classification of topological crystalline phases with order-two point group symmetries. Those symmetries include Z_2 global spin flip, reflection, two-fold rotation, inversion, and their magnetic symmetries. Bulk topological insulators and superconductors, defect gapless states, and topological semimetals are discussed in a unified framework. We find that the topological periodic table shows a periodicity in the number of flipped coordinates under the order-two spatial symmetry, in addition to the Bott periodicity in the space dimensions. We give a number of concrete examples in Chap. 4.

The theme of Chap. 5 is about a physical implication of topological invariants. In the case of chiral symmetric systems in odd spatial dimensions such as time-reversal invariant topological superconductors and topological insulators with sublattice symmetry, the relation between bulk topological invariants and experimentally observable physical quantities has not been well understood. We clarify that the winding number which characterizes the bulk Z nontriviality of these systems can appear in electromagnetic and thermal responses in a certain class of heterostructure systems. It is also found that the Z nontriviality can be detected in a certain polarization induced by magnetic field.

In Chap. 6, we argue dynamical axion phenomena in superconductors and superfluids in terms of the gravitoelectromagnetic topological action, in which the axion field couples with mechanical rotation under finite temperature gradient. The dynamical axion is induced by relative phase fluctuations between topological and s-wave superconducting orders. We show that an antisymmetric spin-orbit interaction which induces parity-mixing of Cooper pairs enlarges the parameter region in which the dynamical axion fluctuation appears as a low-energy excitation. We propose that the

dynamical axion increases the moment of inertia, and in the case of ac mechanical rotation, i.e. a shaking motion with a finite frequency ω, as ω approaches the dynamical axion fluctuation mass, the observation of this effect becomes feasible.

Contents

List of publications

Published papers related to the thesis

1. Ken Shiozaki and Masatoshi Sato
   Topology of crystalline insulators and superconductors
   Phys. Rev. B **90**, 165114 (2014).

2. Ken Shiozaki and Satoshi Fujimoto
   Electromagnetic and Thermal Responses of Z Topological Insulators and Superconductors in odd Spatial Dimensions
   Phys. Rev. Lett. **110**, 076804 (2013).

3. Ken Shiozaki and Satoshi Fujimoto
   Dynamical axion in topological superconductors and superfluids
   Phys. Rev. B **89**, 054506 (2014).

Published papers not included in the thesis

4. Ken Shiozaki and Satoshi Fujimoto
   Green's function method for line defects and gapless modes in topological insulators: Beyond the semiclassical approach
   Phys. Rev. B **85**, 085409 (2012).

5. Ken Shiozaki, Takahiro Fukui, and Satoshi Fujimoto
   Index theorem for topological heterostructure systems
   Phys. Rev. B **86**, 125405 (2012).

Chapter 1

Overview: topological phases of free fermions

In this Chapter, before presenting a detailed discussion of topological insulators and superconductors, we give a basic concept of "topological phases of matter". Topological insulators and superconductors are classes of topological phases of free fermions. We give an overview of the topological band theory by using concrete examples in Sec. 4 - Sec. 7. The topological band theory offers a systematic description of gapless boundary states, gapless states localized at defects, topological fermi points, and adiabatic pumps. They are related closely to each other. Realization of the axion physics is a significant feature of topological phases, which is briefly explained in Sec. 8. We collect some experimental realizations of topological insulators and superconductors in Sec. 9. The last three sections, Sec. 10- Sec. 12 are devoted to short introductions of Chap. 3 - Chap. 6.

1 Topological phases of matter

Phases of matter are usually characterized by symmetry breaking and order parameters. Magnetism, superconductivity, and superfluidity provide fundamental examples. Consider a magnetic phase transition with broken Z_2 symmetry. In the high temperature disordered phase, the Z_2 symmetry in the spin space is not broken. At the critical temperature T_c, the Z_2 symmetry is spontaneously broken, and the system shows magnetism associated with a finite Z_2 breaking order parameter.

However, there are distinguishable phases with the same symmetry and without (local) order parameters. Such phases occur in gapped quantum phases at zero temperature. Integer quantum Hall states and fractional quantum Hall states offer typical examples. Those phases indicate different characters from ordinarily phases such as existences of boundary gapless states, ground state degeneracy depending on real-space topology, and bulk low-energy excitation with fractional charge and statistics. [1]

A possible definition of such unusual phases is an operational one described as follows. We consider a family of Hamiltonians $\{H(\lambda)\}_{\lambda\in\Lambda}$ where λ represents all possible parameters in given degrees of freedom and symmetries. The parameter space Λ is categorized into three types on a viewpoint of ground state property of $H(\lambda)$ as: [1]

(i-a) gapped phases without breaking symmetry,

[1] Here we consider bulk quantum phases, where the energy gap from the finite size effect is neglected.

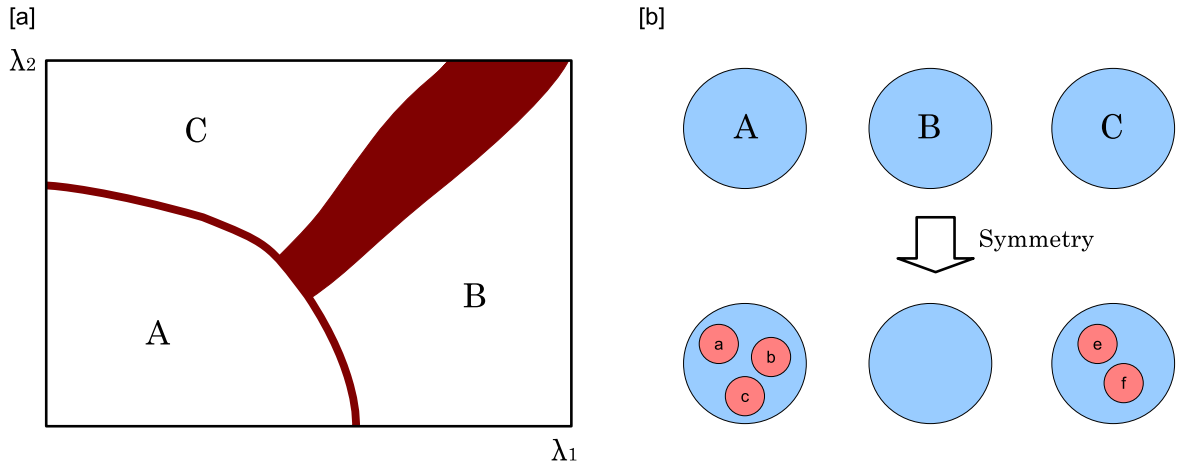

Figure 1.1: [a] A example of a topological phase diagram. λ_1, λ_2 represent the parameters of Hamiltonian. White regions A, B, C represent distinct topological phases. Red regions represent gapped symmetry-broken phases or gapless phases. [b] The effect of symmetry attachment to topological phases. Topological phases may be divided into more multiple phases (A and C), or disappeared (B).

(i-b) gapped phases with breaking symmetry,

(ii) gapless phases.

We can define an equivalence relation in (i-a) phases as follows: H_1 and H_2 are equivalent if and only if H_1 can be continuously deformed into H_2 without breaking the symmetry or closing the energy gap. Then the gapped phases without breaking symmetry are divided into some equivalent classes which are separated by the gapless phases or symmetry breaking phases. The equivalent classes are referred to as topological phases. In Fig. 1.1 [a] we show a schematic picture of a topological phase diagram.

In topological phases, symmetry plays an important role. Symmetries restrict possible forms of Hamiltonians, which gives a finer classification of topological phases. Let us consider the effect of symmetry attachment. Assume that there are topological phases $A, B, C, \ldots$ in a symmetry class S_0. Then, in the symmetry class $S_1 = S_0 + S'$, due to the restriction on parameters by the symmetry S', the topological phases may be divided into different phases: $A \mapsto A\text{-}a, A\text{-}b, A\text{-}c, \ldots$, or forbidden: $A \mapsto$ empty. In Fig. 1.1 [b] we show a schematic picture of the role of symmetry in topological phases.

2 Topological insulators and superconductors

Topological insulators and superconductors [2, 3] are topological phases of free fermions, in other words, topological phases of one-particle states. Band insulators, superconductors and superfluids (within a mean field approximation) belong to this category. Topological insulators and superconductors are the main topic of this thesis.

If there is the lattice translational symmetry, Hamiltonians are characterized by the Bloch Hamiltonians $\mathcal{H}(\boldsymbol{k})$ with the Bloch momentum $\boldsymbol{k}$ which is a good quantum number. Then, the characterization of topological phases is simplified to the homotopy classification of the map $\mathcal{H}(\boldsymbol{k})$ from Brillouin zone (BZ) to matrix space with a finite energy gap. [4, 5, 6] We can apply mathematical tools of topology, especially the K-theory, [7, 8, 9] to the classification of topological insulators and superconductors. [2]

Since the bulk has a finite energy gap from the ground state a signature of nontrivial topology cannot be seen in the bulk. All possible signatures of nontrivial topology occur only at real space boundaries of matters or interfaces between topologically distinct phases. [3] On the boundary of topologically nontrivial insulators and superconductors there should be gapless states which are robust against disorder and perturbation. Topological defects such as vortex and monopole defects and edge and screw dislocations also provide gapless states which are robust against disorder. [10, 11] Also, even if there is no gapless state at the boundary due to symmetry breaking (for example, the time-reversal symmetry breaking perturbation at the boundary, or obviously breaking of crystalline symmetries from the existence of the boundary), some topological nontrivialities may be captured in the variation of the charge polarization and the magnetoelectric polarization near the boundary, which leads to topologically robust electromagnetic and thermal responses. [12, 13]

Some topological invariants characterizing topological phases are directly related to experimentally observable quantities. For example, the Chern (TKNN) number, which characterizes 2-dimensional time-reversal symmetry-broken topological phases, is nothing but the (thermal) Hall conductivity. [14, 15, 16] The 3-dimensional Chern-Simons invariant, which characterizes 3-dimensional time-reversal or inversion symmetric topological insulators, gives the topological magnetoelectric coefficient. [4] [13] However, not all topological invariants are related to some physical observable quantities.

A common physical meaning of topological invariants is the "bulk-boundary correspondence": If a bulk insulating phase shows some nontrivial topology, there should be gapless states localized at the real space boundary. Moreover, the structure of the boundary gapless states is characterized by the bulk topological invariant. Thus the bulk topological data are entirely reflected in the boundary gapless states. We give a concrete example in Sec. 4.

3 Topological crystalline insulators and superconductors

Crystalline symmetries are distinguished from global symmetries in topological phases. Here, crystalline symmetries are space group symmetries which consist of spatially non-local transformation. Global symmetries are spatially local symmetries such as the time-reversal symmetry, the particle-hole symmetry, and the on-site spin $SU(2)$ symmetry. Topological insulators and superconductors

[2] The full translational symmetry is not essential for topological insulators and superconductors. The analysis of the Anderson delocalization of the boundary of topological insulators and superconductors shows the same classification as the homotopy classification of bulk Bloch Hamiltonian $\mathcal{H}(\boldsymbol{k})$. [4] The present thesis does not deal with disorder effect and assume the translational symmetry when we consider a classification of topological phases.

[3] For topologically ordered states (i.e., topological phases with a long-range entanglement), the bulk can show a signature of nontrivial topology via low-energy excitations with a fractional charge and statistics, which is essentially many-particle physics. [1] Free fermion topological phases we consider in this thesis does not show such bulk topological signatures.

[4] The 3-dimensional Chern-Simons invariant is also referred to as the magnetoelectric polarization or the axion theta angle.

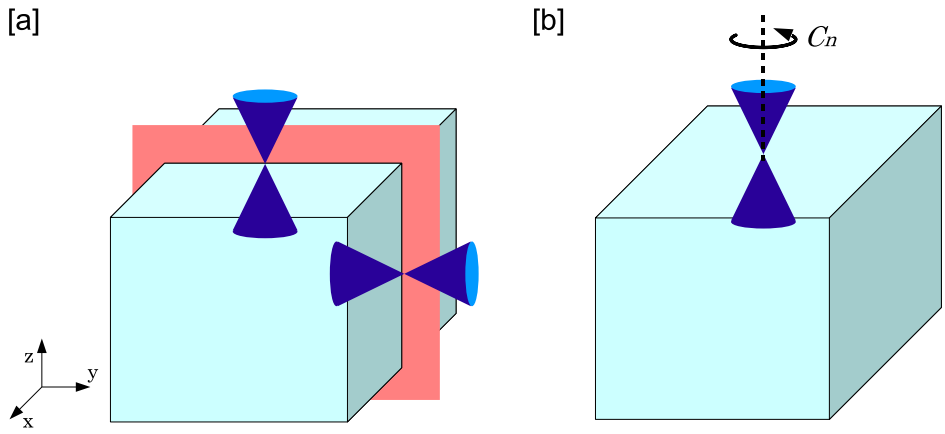

Figure 1.2: Boundary gapless states on the topological crystalline insulators. [a] For mirror reflection symmetry M_{yz}, symmetry respected surfaces are $y = const.$ and $z = const.$ surfaces. $x = const.$ surface is not closed under the reflection transformation. [b] For C_n rotation symmetry along z-axis, the $z = const.$ surface is only possible symmetry respected surface.

protected by crystalline symmetries are called the "topological crystalline insulators and superconductors". [17, 18]

A physical difference between global and crystalline symmetries is stability against the disorder effects such as existence of impurities, lattice defects, and boundaries. It is naively expected that the gapless boundary modes in topological crystalline insulators and superconductors are fragile against disorders because these specific symmetries are microscopically sensitive to small perturbations. But recent studies of topological crystalline insulators have shown that if the symmetries are preserved on average, then for some symmetry classes the existence of gapless boundary states is rather robust. [19, 20, 21, 22] Moreover, surface gapless states protected by the mirror reflection crystal symmetry have been observed experimentally. [23, 24, 25, 26] Such recent developments motivate us to classify the topological crystalline insulators and superconductors, and reveal their low-energy physics.

It is required for the existence of boundary gapless states that the boundary does not break the crystalline symmetry. For example, consider the mirror reflection symmetry $M_{yz} : (x, y, z) \to (-x, y, z)$. The symmetry respecting surfaces are parallel to x-axis (Fig. 1.2 [a]). Another example is the C_n rotation symmetry along the z-axis. The symmetry respecting surface is the $z = const.$ plane (Fig. 1.2 [b]). The allowed space group symmetries which are compatible with the existence of the boundary are the 2-dimensional space group symmetries in 3-dimensional materials (and so the 1-dimensional space group symmetries in 2-dimensional materials). [5]

[5] The entanglement spectrum can detect topological nontrivialities for the boundary non-respecting space group symmetries. See, for example, [27].

4 Boundary gapless states

As stated previously, topological insulators and superconductors show the boundary gapless states which reflect nontrivial topology of the bulk.

4.1 Example: anomalous Hall insulator

Let us illustrate the relation between bulk topology and boundary gapless states by an concrete model known as the anomalous Hall insulator. [28] Consider a two band model in 2-dimensions,

$$\mathcal{H}(k_x, k_y) = \varepsilon(k_x, k_y) + \boldsymbol{R}(k_x, k_y) \cdot \boldsymbol{\sigma}, \tag{1.4.1}$$

where $\boldsymbol{\sigma} = (\sigma_x, \sigma_y, \sigma_z)$ are the Pauli matrices. (k_x, k_y) stand on the 2-dimensional BZ torus $T^2 = S^1 \times S^1$. The energy eigenvalues of (1.4.1) are given by

$$E_\pm(k_x, k_y) = \varepsilon(k_x, k_y) \pm |\boldsymbol{R}(k_x, k_y)|. \tag{1.4.2}$$

We assume a finite energy gap in the overall BZ, which implies $\boldsymbol{R}(k_x, k_y) \neq \boldsymbol{0}$ for all $(k_x, k_y) \in T^2$. Then we can introduce a unit vector $\boldsymbol{n}(k_x, k_y) := \boldsymbol{R}(k_x, k_y)/|\boldsymbol{R}(k_x, k_y)|$ which is not singular in T^2. The topology of the two band model is evaluated by the homotopy classification of the map $\boldsymbol{n} : T^2 \to S^2$, [6] which is characterized by the winding number

$$N = \frac{1}{8\pi} \int_{T^2} d^2\boldsymbol{k} \epsilon_{\mu\nu\rho} \epsilon_{ij} n_\mu \partial_{k_i} n_\nu \partial_{k_j} n_\rho. \tag{1.4.3}$$

N counts how many times T^2 winds S^2, [7] and is invariant under a continuous change of the Hamiltonian $\mathcal{H}(\boldsymbol{k})$ until the bulk energy gap is closed. Hence, two band models show $\mathbb{Z}$ topological phases.

If N is a nonzero integer, there should be N chiral gapless states at the boundary. To see this, let us consider the following two orbital square lattice model with the hopping that flips the orbitals (For example, see [13]),

$$H = \sum_i \left[c^\dagger_{i+\hat{x}} \frac{\sigma_z + i\sigma_x}{2} c_i + c^\dagger_{i+\hat{y}} \frac{\sigma_z + i\sigma_y}{2} c_i + h.c. \right] + m \sum_i c^\dagger_i \sigma_z c_i. \tag{1.4.4}$$

The Bloch Hamiltonian of (1.4.4) is

$$\mathcal{H}(k_x, k_y) = \sin k_x \sigma_x + \sin k_y \sigma_y + (m + \cos k_x + \cos k_y)\sigma_z, \tag{1.4.5}$$

and the winding number is given by

$$N = \begin{cases} 1 & \text{for } -2 < m < 0 \\ -1 & \text{for } 0 < m < 2 \\ 0 & \text{for } |m| > 2 \end{cases} \tag{1.4.6}$$

We consider an infinite plane geometry for $y > 0$ as shown in Fig. 1.3 [a]. k_x is a good quantum number since the lattice translational symmetry along x-direction is remained. In Fig. 1.3 [b-e], we show the energy eigenvalues with respect to k_x for distinct values of m. In Fig. 1.3 [c] ([d]), there is a right (left) mover chiral gapless state localized at the boundary, which reflects the bulk topological invariant $N = 1(-1)$. [8] [9]

[6] The potential term $\varepsilon(k_x, k_y)$ merely contributes an energy shift, and does not affect the topology.

[7] There is no winding from a sub circle $S^1 \subset T^2$ to S^2 since S^1 cannot wind in S^2.

[8] The right and left mover are determined by the group velocity $\partial E(k_x)/\partial k_x$ of the gapless states.

[9] Strictly speaking, the bulk topology protects the difference of the number between right and left mover chiral

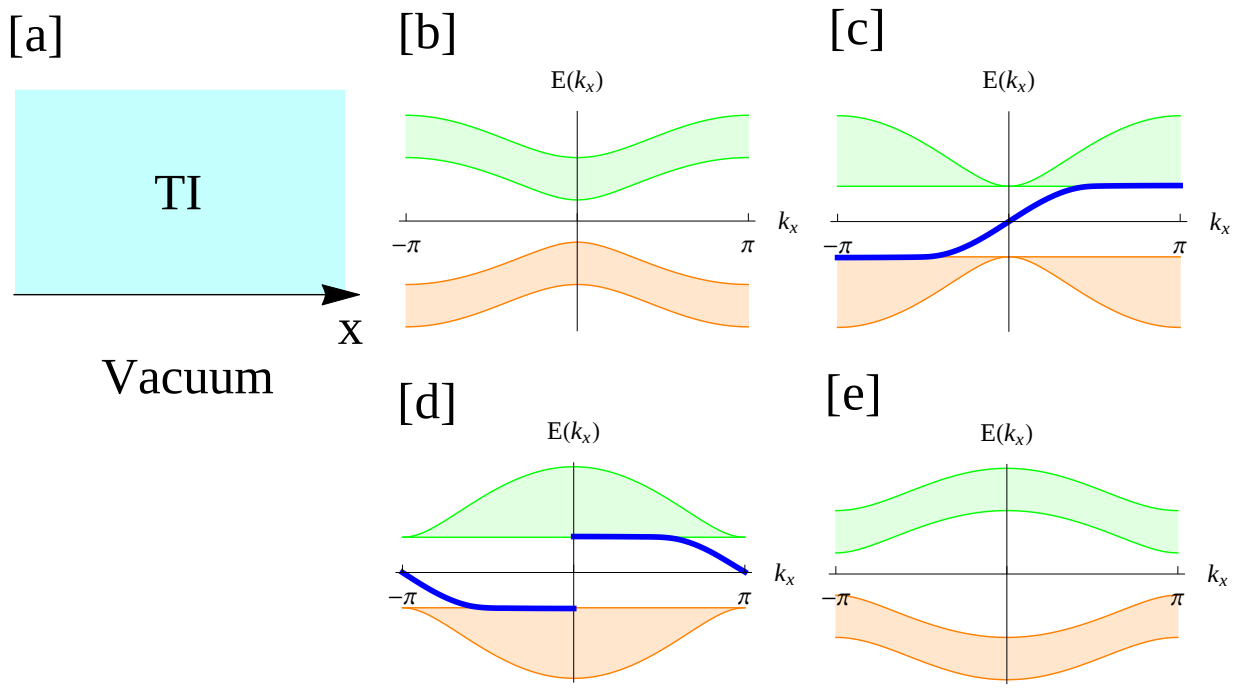

Figure 1.3: [a] The anomalous Hall insulator for $y > 0$ and the vacuum for $y < 0$. [b-e] The energy eigenvalues for the infinite plane geometry [a] with [b] $m = -3$, [c] $m = -1$, [d] $m = 1$, and [d] $m = 3$. Thick blue lines in [c] and [d] are chiral gapless boundary states localized at the interface between the anomalous Hall insulator and the vacuum.

4.2 Bulk-boundary correspondence

In previous subsection, we saw the relation between the bulk topology (homotopy of $\mathcal{H}(k_x, k_y)$) and the existence of the chiral gapless states at the boundary. This is an example of the bulk-boundary correspondence, which states:

- If a bulk Hamiltonian $\mathcal{H}(\boldsymbol{k})$ has nontrivial topology, then there should be gapless states localized at the boundary which reflect the bulk topological invariant.

There are many papers about the bulk-boundary correspondence. See, [29, 30, 31], for example.

5 Defect gapless states

Topological band theory is also applied to gapless states localized at defects. Here the defects include topological defects such as domain wall, vortex, monopole defects, and also lattice dislocations.

---

gapless excitations.

5.1 Example: Jackiw-Rossi vortex zero mode

We start up with a concrete example known as the Jackiw-Rossi model. Consider a 2-dimensional Dirac model with a single vortex: [32, 33]

$$\mathcal{H} = -i\gamma_1\partial_x - i\gamma_2\partial_y + \Delta(r)\cos\phi\ \gamma_3 \pm \Delta(r)\sin\phi\ \gamma_4 \tag{1.5.1}$$

where γ_μ-s are Dirac matrices satisfying $\{\gamma_\mu, \gamma_\nu\} = \delta_{\mu\nu}$, ϕ is the azimuth angle, and we assume $\Delta(r \to \infty) \to \Delta_0 > 0$. The prefactor of the fourth term $\pm$ corresponds to the chirality of the vortex. We set $\gamma_5 = i\gamma_1\gamma_2\gamma_3\gamma_4$. Due to the finite mass gap Δ_0, there is no low-energy excitation far from the vortex, i.e., "insulator". Near the vortex there may be discrete in-gap excitations. It is known that the Hamiltonian (1.5.1) has a zero energy state $\phi_0(x, y)$ localized at the vortex of which the wave function is

$$\phi_0(x, y) \propto \xi_\pm e^{\pm i\phi} e^{-\int_0^r dr'\Delta(r')} \tag{1.5.2}$$

with the fixed chirality of γ_5: $\gamma_5\xi_\pm = \pm\xi_\pm$ (or $\gamma_5\xi_\pm = \mp\xi_\pm$). [10]

The zero energy state ϕ_0 is shifted from the zero under the perturbation such as $\mathcal{H}_{pert} = V$ or $V'\gamma_5$. If we assume the "chiral symmetry" $\{\mathcal{H}, \gamma_5\} = 0$, those perturbations are forbidden, and we expect the zero energy states are stable under perturbations preserving the chiral symmetry. This is true from the following reason: Noticing $[\mathcal{H}, \gamma_5] = 0$ on the subspace spanned by zero energy states under the chiral symmetry, we can find that an zero energy state are also an eigen state of γ_5. [11] A pair of zero energy states with positive and negative chiralities $\{|\phi_0^+\rangle, |\phi_0^-\rangle\}$ can be gapped out without breaking the chiral symmetry because of the existence of the chiral symmetry preserving perturbation $\alpha |\phi_0^+\rangle \langle\phi_0^-| + h.c.$, $\{\alpha |\phi_0^+\rangle \langle\phi_0^-| + h.c., \gamma_5\} = 0$. Thus,

$$\mathrm{Ind}(\mathcal{H}) := N^+ - N^-, \tag{1.5.3}$$

the difference between the number of positive and negative chiral zero modes, may be stable under perturbations with the chiral symmetry. $\mathrm{Ind}(\mathcal{H})$ is referred to as the analytic index of $\mathcal{H}$. More strictly, the index theorem for the open infinite system [34, 35] states that the analytic index is completely determined by an certain topological index as

$$\mathrm{Ind}(\mathcal{H}) = \frac{1}{2\pi i}\oint_{|\boldsymbol{r}|\to\infty} d\Phi(\phi) \tag{1.5.4}$$

where the r.h.s is the total phase winding of the gap function $\Delta(\boldsymbol{r})e^{i\Phi(\phi)}$ at the infinite region $r \to \infty$. [12] Thus, the number of zero energy states near the vortex does not depend on microscopic structure, determined only by the topological information far away from the vortex, which

[10] The sign of chirality of the zero energy state depends on the definition of the gamma matrices. The essential point is the one-to-one correspondence between the chirality of the phase winding $\pm$ in Eq. (1.5.1) and the chirality of the zero energy states.

[11] If $|\phi\rangle$ is a zero energy state, we get $[\mathcal{H}, \gamma_5]|\phi\rangle = -2\gamma_5\mathcal{H}|\phi\rangle = 0$.

[12] The assumptions on the index theorem (1.5.4) are

- (i) The Dirac theory
- (ii) The existence of the chiral symmetry $\{\mathcal{H}, \Gamma\} = 0$
- (iii) $|\Delta(\boldsymbol{r})| > 0$ for $r \to \infty$

However, the condition (iii) can be weaken to

is symbolically written as

$$\text{Analytic index} = \text{Topological index}. \tag{1.5.5}$$

This is the same spirit as the bulk-boundary correspondence.

5.2 Bulk-defect correspondence

It is suggested that the index theorem (1.5.4) is generalized to non Dirac systems such as lattice systems or Hamiltonians including higher order derivatives, and also for any symmetry classes. The generalized conjecture is known as the "bulk-defect correspondence" [10] explained below. Let $\mathcal{H}(\hat{\boldsymbol{k}}, \hat{\boldsymbol{r}})$ be a Hamiltonian describing a defect. The momentum and position operators $\hat{\boldsymbol{k}}$ and $\hat{\boldsymbol{r}}$ do not commute because the translation symmetry is broken due to the defect. We assume that there is no gapless excitation far from the defect. We set a closed sphere S^D surrounding the defect, where $(D+1)$ is the defect co-dimensions. For example, in the case of the point defect in 2-spatial dimensions as given by (1.5.1), the defect surrounding sphere is the circle S^1. Without loss of generality, we can assume that ξ_{var}, which is the characteristic length of the spatial variation of the defect Hamiltonian on the sphere S^D, is sufficiently slower than ξ_{gap}: $\xi_{var} \ll \xi_{gap}$, where ξ_{gap} is the characteristic length determined by the finite energy gap far from the defect. This simplification implies that the semiclassical Hamiltonian on the sphere $\mathcal{H}(\boldsymbol{k}, \boldsymbol{s}) := \mathcal{H}(\boldsymbol{k}, \boldsymbol{r}(\boldsymbol{s}))$ is fully gapped. [13] The semiclassical Hamiltonian $\mathcal{H}(\boldsymbol{k}, \boldsymbol{s})$ defines the map from the base space $T^d \times S^D$ to the "space of gapped Hamiltonian matrices", which is a similar situation to the bulk-boundary correspondence. The bulk-defect correspondence says:

- If a semiclassical Hamiltonian $\mathcal{H}(\boldsymbol{k}, \boldsymbol{s})$ is topologically nontrivial, then there should be gapless states localized at the defect. Also, the structure of the gapless states reflects the topological invariants of the semiclassical Hamiltonian $\mathcal{H}(\boldsymbol{k}, \boldsymbol{s})$.

5.3 Defect gapless state as a boundary gapless state

Actually, the topological classification of defect gapless states is reduced to the classification of boundary gapless states. [14]

For example, let us consider the classification of zero energy bound states localized at a point defect in 3-dimensions with a symmetry class S. The topological classification is determined by the homotopy classification of symmetry compatible Hamiltonians $\mathcal{H}_{3D}(k_x, k_y, k_z, \theta, \phi)$ where (θ, ϕ) are the parameters for a sphere S^2 surrounding a point defect. The K-theory classification shows the topological classification of $\mathcal{H}_{3D}(k_x, k_y, k_z, \theta, \phi)$ is the same as that of the one-lower dimensional subsystem; i.e. the classification of zero energy states localized at a point defect in 2-dimensions with

- (iii') There is no gapless excitation at $r \to \infty$,

which allows the vortex Hamiltonian $\mathcal{H}$ to be more complicated systems such as heterostructure systems. [35, 36] Moreover, any systems satisfying the condition (iii') is adiabatically (i.e., without closing the finite energy gap at $r \to \infty$) changed into a Hamiltonian satisfying the condition (iii). As a result, without loss of generality, we can assume the condition (iii) for defect gapless states. [11, 36]

[13] Even if the condition $\xi_{var} \ll \xi_{gap}$ is not satisfied, the Hamiltonian $\mathcal{H}(\hat{\boldsymbol{k}}, \hat{\boldsymbol{r}})$ can be adiabatically changed into that satisfying this condition. This is justified by a way similar to the footnote 12. The Hamiltonian on the sphere $\mathcal{H}(\boldsymbol{k}, \boldsymbol{s})$ is also referred to as the adiabatic Hamiltonian. [11]

[14] Strictly speaking, this reduction is true for so called "strong indices" which represent topological nontriviality over the base space of the one-point compactification $T^d \times S^D \to S^{d+D}$.

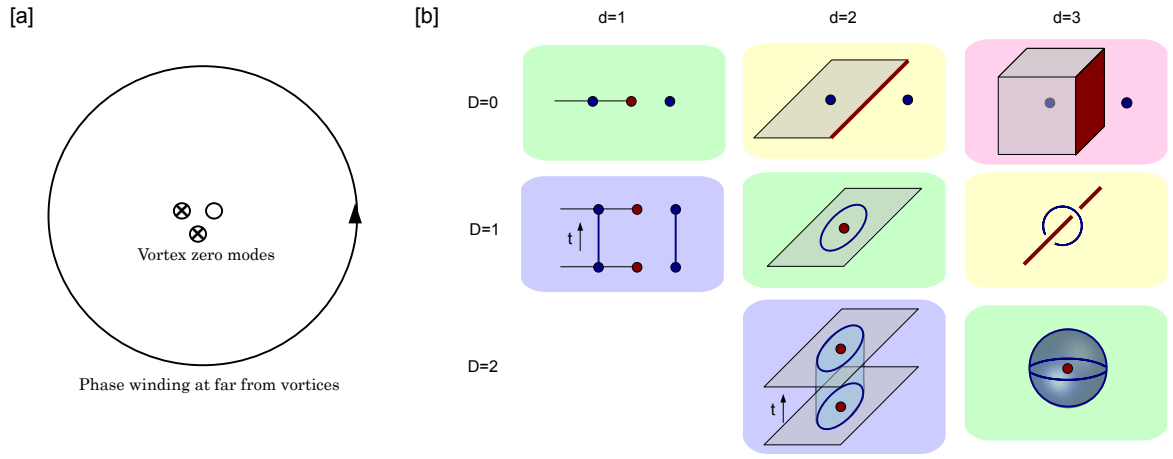

Figure 1.4: [a] The number of vortex zero modes is determined by the phase winding at far from the vortices. [b] Various defect gapless states. d is the space dimensions and $(D+1)$ is the defect codimensions. A defect with codimension $(D+1)$ is enclosed by a D-dimensional sphere S^D. The same background color regions (the same defect dimensions $d-D-1$) indicate the same topological classifications. [6, 11]

the same symmetry class S, of which the semiclassical Hamiltonian is $\mathcal{H}_{2D}(k_x, k_y, \phi)$ where ϕ is the parameter for a circle S^1 surrounding the defect. Furthermore, the classification of $\mathcal{H}_{2D}(k_x, k_y, \phi)$ is the same as the classification of zero energy states localized at a point defect in 1-dimension with the same symmetry class S, i.e., boundary gapless states of 1-dimensional insulators, $\mathcal{H}_{1D}(k_x)$.

We can always iterate such reduction to a lower-dimensional sub-system up to a boundary state of a $(D+1)$ dimensional insulator with the same symmetry class S. In other words, the topological classification of defect gapless states with a defect dimension (d, D), where d is a spatial dimension and $(D+1)$ is a defect co-dimension, is determined only by the defect dimension itself $\delta - 1 = d - D - 1$. [6, 11]

We summarize the above discussion by the following statement dubbed "a defect gapless state as a boundary state": [37]

- The topological classification of defect gapless states localized at a $(\delta-1)$-dimensional defect is the same as the topological classification of boundary gapless states of a δ-dimensional insulator with the same symmetry class. [15]

[15] If a symmetry class S includes a crystalline symmetry, it is required for the topological protection of gapless states that the *δ-dimensional insulator*, of which the boundary composes the $(\delta-1)$-dimensional defect, is invariant under the crystalline symmetry transformations. [38] Note that the invariance of the *$(\delta-1)$-dimensional defect* under the crystalline symmetry does not imply topological protection of the gapless states. We will discuss this point in detail in Sec. 5.2 of Chap. 3.

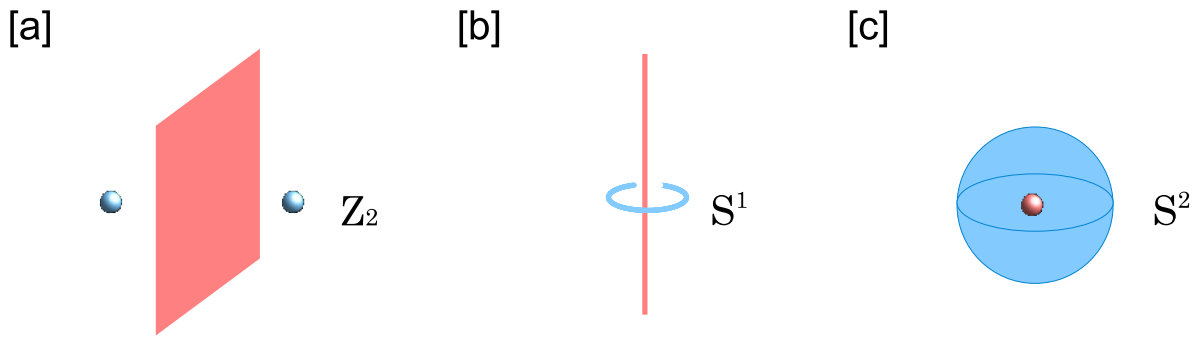

Figure 1.5: Fermi singularities (red regions) and each subspace M surrounding the fermi singularity. [a] A fermi surface and two points $M \cong \mathbb{Z}_2$. [b] A line node and $M \cong S^1$. [c] A point node and $M \cong S^2$.

6 Topological fermi point

The idea of band topology is also applicable to gapless phases with a nontrivial topological charge in the momentum space. [39, 10] Fermi points, lines, and surfaces are singularities of a Hamiltonian $\mathcal{H}(\boldsymbol{k})$ in the BZ. Here the singularity means $\det[\mathcal{H}(\boldsymbol{k})] = 0$. At the singular point, the energy gap of the Hamiltonian $\mathcal{H}(\boldsymbol{k})$ should be closed, which breaks the construction of topological invariants over all around the BZ. However, we can define topological invariants over a closed subspace M which surrounds the fermi point, or general singular regions [16] where the Hamiltonian $\mathcal{H}(\boldsymbol{k})$ is non-singular on M. Nontrivial topology over the closed subspace M indicates the existences of a stable fermi point inner-side, *and also outer-side* regions of M. [17] Fig. 1.5 shows a fermi surface ([a]), a line node ([b]), a point node ([c]), and their corresponding subspaces M.

6.1 Example: Weyl semimetal

A famous example is the Weyl semimetal or the Weyl superconductor of which the fermi point is protected by the first Chern number ch_1 over the sphere S^2 surrounding the fermi point. The low-energy effective model around the fermi point of the Weyl fermions is written as

$$\mathcal{H}(\boldsymbol{k}) = k_x\sigma_x + k_y\sigma_y + k_z\sigma_z \tag{1.6.1}$$

The closed sphere S^2 surrounding the fermi point ($\boldsymbol{k} = \boldsymbol{0}$) is given by $|\boldsymbol{k}| = k$. On the sphere S^2, the Hamiltonian $\mathcal{H}(\boldsymbol{k})|_{|\boldsymbol{k}|=k}$ is fully gapped, thus we can define the first Chern number

$$ch_1 = \frac{i}{2\pi}\int_{S^2} \mathrm{tr}\mathcal{F}, \tag{1.6.2}$$

[16] In the presence of symmetries, the subspace M have to be closed under the symmetry group transformations.

[17] This is essentially the Nielsen-Ninomiya no go theorem. [39] On the other hand, if a momentum space is open, the nontrivial topology on M indicates the existence of a stable fermi point only inner-side of M. An example where the momentum space is open is the Dirac theory of which the Bloch Hamiltonian is given by $\mathcal{H}(\boldsymbol{k}) = \gamma_1 k_1 + \cdots + \gamma_d k_d$.

where $\mathcal{F}$ is the Berry curvature of the occupied state of the Hamiltonian $\mathcal{H}(\boldsymbol{k})$ on S^2. We can show $ch_1 = -1$ for the Weyl fermion (1.6.1), which implies the existence of a stable fermi point inner-side of S^2, i.e. the Weyl point.

7 Adiabatic pump

Consider a time-dependent Hamiltonian $H(t)$ which has a finite energy gap Δ between the ground state and the first excited state. If the time dependence of $H(t)$ is much slower than $1/\Delta$, we can take the adiabatic approximation for time evolution of the ground state. Let $L = \{\ell(s) \in \Lambda | 0 \leq s \leq 1, \ell(0) = \ell(1)\}$ be a loop in the parameter space Λ of the Hamiltonian. Correspondingly, we get a time-dependent Hamiltonian $H(t) := H(\ell(t/T))$ $(0 \leq t \leq T)$ with $H(T) = H(0)$. The adiabatic cycle is defined by a limit $T \to \infty$ for the fixed loop L.

The Thouless adiabatic charge pump [40] is the integrated conserved current during an adiabatic cycle. The adiabatic charge pump is quantized into an integer value and it is topologically robust against perturbation. The topological band theory provides the classification of such topological adiabatic charge pump in insulators. The fermion parity pump during an adiabatic cycle in superconductors are also characterized by the topological band theory. [11]

In this thesis, we do not deal with the adiabatic pump. However, the adiabatic pump is a significant notion in topological phases since the adiabatic charge pump is related to the bulk-boundary correspondence (Ex. [13]), and the adiabatic fermion parity pump is related to the non-abelian statistics of the Majorana fermions. [11] In the following, we briefly illustrate the adiabatic charge pump by using a concrete example.

7.1 Example: adiabatic charge pump

We give an example of the adiabatic charge pump. [40] Consider the following 1-dimensional spinless model as shown in Fig 1.6 [a], [18]

$$H = \sum_i \Big(\frac{t}{2} a_i^\dagger a_{i+1} + \frac{\delta}{2} (-1)^i a_i^\dagger a_{i+1} + h.c. \Big) + \sum_i \Delta (-1)^i a_i^\dagger a_i. \tag{1.7.1}$$

In the bulk with the translational symmetry, the Bloch Hamiltonian is written by

$$\mathcal{H}(k_x) = t \cos(k_x a)\sigma_x - \delta \sin(k_x a)\sigma_y + \Delta \sigma_z, \quad k_x \in [-\frac{\pi}{2a}, \frac{\pi}{2a}] \tag{1.7.2}$$

with the boundary condition in the BZ $\mathcal{H}(\pi/2a) = \sigma_z \mathcal{H}(-\pi/2a)\sigma_z$. Here t is the hopping, δ is the bond order, Δ is the staggered potential, $\boldsymbol{\sigma} = (\sigma_x, \sigma_y, \sigma_z)$ are the Pauli matrices for even and odd sites, and $a = x_{i+1} - x_i$. [19] The energy eigenvalues of (1.7.2) are given by

$$E_\pm(k_x) = \pm \sqrt{t^2 \cos^2(k_x a) + \delta^2 \sin^2(k_x a) + \Delta^2}. \tag{1.7.4}$$

[18] This model is known as the Rice-Mele model. [41]

[19] Here we chose the Fourier transformation as

$$a_{2i} = \sum_{-\frac{\pi}{2a} < k_x < \frac{\pi}{2a}} a_{e,k_x} e^{ik_x x_{2i}}, \quad a_{2i+1} = \sum_{-\frac{\pi}{2a} < k_x < \frac{\pi}{2a}} a_{o,k_x} e^{ik_x (x_{2i}+a)}. \tag{1.7.3}$$

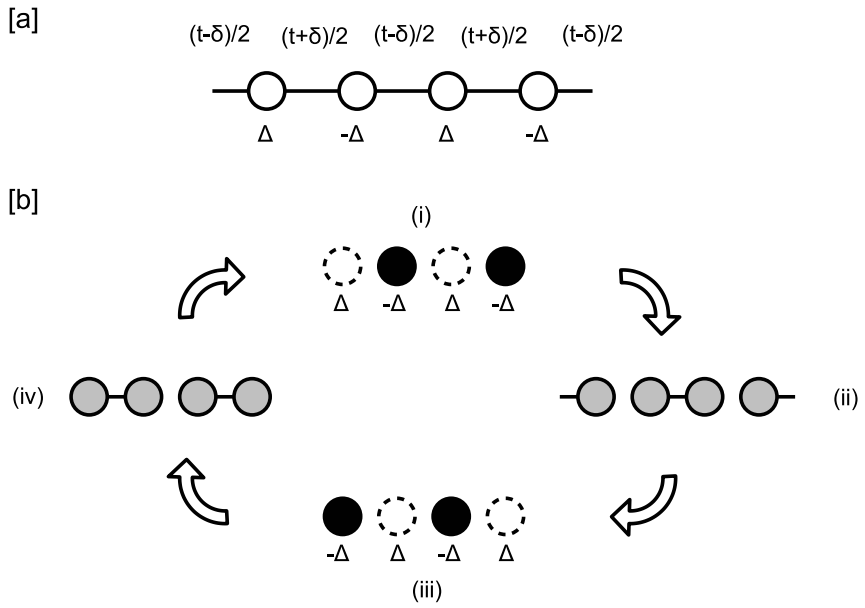

Figure 1.6: [a] The Rice-Mele model. [b] An adiabatic cycle which indicates a topological charge pump.

Thus the gapless parameter regions in the space (t, δ, Δ) are given by $(t, 0, 0)$ and $(0, \delta, 0)$. Note that the spatial parameters $(t, \delta = \pm t, \Delta = 0)$ and $(0, 0, \Delta)$ show the flat bands composed of the localized orbitals.

Let us consider the following adiabatic cycle (i) $\to$ (ii) $\to$ (iii) $\to$ (iv) $\to$ (i) as shown in Fig. 1.6 [b]:

(i) $t = \delta = 0$, $\Delta > 0$: localized at the even site.

(ii) $t + \delta = 0, \Delta = 0$: localized at the $(2i-1)-(2i)$ bond.

(iii) $t = \delta = 0$, $\Delta < 0$: localized at the odd site.

(iv) $t - \delta = 0, \Delta = 0$: localized at the $(2i)-(2i+1)$ bond.

Under the above cycle, the system returns to the initial, but there is a charge pumping from the left to the right unit cell, as shown in Fig 1.6 [b]. More generally, a pumped fermion number is computed by the integral of the adiabatic current [42, 40, 43]

$$J_{ad}(\tau) = 2a \int_{BZ} \frac{dk_x}{2\pi} j_{ad}(k_x, \tau) = \frac{2a}{2\pi} \int_{-\frac{\pi}{2\pi}}^{\frac{\pi}{2a}} dk_x \left[\frac{\partial E_-(k_x, \tau)}{\hbar \partial k_x} - i\mathcal{F}_{k_x\tau}(k_x, \tau) \right] \tag{1.7.5}$$

where τ is the adiabatic parameter labeling the adiabatic process and $\mathcal{F}_{k_x\tau}$ is the Berry curvature of the occupied bands of the adiabatic Hamiltonian $\mathcal{H}(k_x, \tau)$. The pumped fermion number par an

adiabatic cycle is

$$N = \frac{1}{2a}\oint d\tau J_{ad}(\tau) = -\frac{i}{2\pi}\int dk_x d\tau \mathcal{F}_{k_x\tau}(k_x,\tau) = -ch_1. \tag{1.7.6}$$

Here ch_1 is the first Chern number which is a topological invariant and does not depend on microscopic structure of the adiabatic cycle. The first Chern number ch_1 reflects the topology of the adiabatic Hamiltonian $\mathcal{H}(k_x,\tau)$, and determines the pumped fermion number at the adiabatic cycle.

8 Axion physics

The axion was introduced as a hypothetical particle to resolve the strong CP problem in quantum chromodynamics. The axion field θ is a pseudoscalar under the time-reversal and the parity transformation, and may couples to the electromagnetic field via the action,

$$S_{\rm top} = \frac{\alpha}{4\pi^2}\int d^3x dt \theta(x,t)\boldsymbol{E}\cdot\boldsymbol{B}. \tag{1.8.1}$$

Here $\alpha = e^2/\hbar c$ is the fine structure constant. Because $\frac{\alpha}{4\pi^2\hbar}\int d^3x dt \boldsymbol{E}\cdot\boldsymbol{B} = N$ is a topological invariant which does not depend on a detail of the electromagnetic field, the axion field $\theta(x)$ takes values in a circle S^1, [20] and a constant axion field $\theta(x,t) = \theta_0$ cannot contribute dynamics. A spatially or temporally inhomogeneous background axion field or a fluctuation of the axion field show meaningful effects. The electrodynamics associated with the axion field is called the axion electrodynamics. [44]

Some topological insulators provide the axion electrodynamics. In the bulk we can define the static axion field θ for a given insulator by

$$\theta = \frac{1}{4\pi}\int {\rm tr}\Big[\mathcal{A}d\mathcal{A} + \frac{2}{3}\mathcal{A}^3\Big] \pmod{2\pi} \tag{1.8.2}$$

where $\mathcal{A}(\boldsymbol{k})$ is the Berry connection of the Bloch Hamiltonian $\mathcal{H}(\boldsymbol{k})$. The time-reversal symmetry or the inversion symmetry quantizes θ by 0 or π because the axion field θ is a pseudoscalar. In fact, in the presence of these symmetries the axion field θ is nothing but the topological invariant characterizing the topological phases of the bulk insulators. Consider an interface between $\theta = 0$ and $\theta = \pi$ phases. If there is no gapless excitation at the interface due to symmetry breaking perturbation, θ is changed from 0 to π without singularity, which leads to the quantum Hall effect and the Kerr rotation from the action (1.8.1). [13]

Thermal and quantum fluctuations of the axion field θ also yield various interesting phenomena. It is proposed that some magnetic fluctuations induce the dynamical axion field, which leads to the axionic polariton under an applied magnetic field [45] and a magnetic instability under an applied electrostatic field. [46]

9 Experimental realizations

In this section we collect experimental realizations of topological insulators and superconductors and gapless topological phases.

[20] Note that $\exp\left(\frac{i}{\hbar}S_{\rm top}[\theta+2\pi]\right) = \exp\left(\frac{i}{\hbar}S_{\rm top}[\theta]\right)$.

9.1 Integer quantum Hall effect

A familiar example of topological insulators is the integer quantum Hall effect, [47] where the Hall conductivity $\sigma_{\rm H}$ shows plateaus along increasing an applied magnetic field, and is quantized into integer values $\sigma_{\rm H} = \frac{e^2}{h}N$. The quantized $\sigma_{\rm H}$ is nothing but the topological invariant characterizing the ground states.

9.2 Quantum spin Hall effect

After the theoretical discovery of the quantum spin Hall effect by Kane and Mele [48, 49], it was proposed that a HgTe quantum well shows the quantum spin Hall effect [50], and experimentally observed. [51]

9.3 Time-reversal symmetric $\mathbb{Z}_2$ topological insulators

The parity criterion of time-reversal symmetric $\mathbb{Z}_2$ topological insulators with the inversion symmetry [52] provides a useful way to determine $\mathbb{Z}_2$ topological invariant for various realistic materials, and a good scenario of topological phase transition, i.e., a band inversion at symmetric points. After a theoretical proposal, [52] a surface Dirac fermion is observed by the Angle-resolved photo emission spectroscopy (ARPES) measurement in $Be_{1-x}Sb_x$. Various materials have been confirmed to be 3-dimensional $\mathbb{Z}_2$ topological insulators. See, for example, Ando [53].

9.4 Time-reversal symmetric topological superconductor and superfluid

3-dimensional time-reversal symmetric superconductors and superfluids are classified by $\mathbb{Z}$. A nontrivial phase with $n \in \mathbb{Z}$ topological invariant shows n number of surface Majorana fermions. It is known that ^{3}He-B phase is a topological superfluid with $n = 1$. [54, 4] The $Cu_xBe_2Se_3$ superconductor is a candidate for a topological superconductor [55, 56]

9.5 Time-reversal broken topological superconductor in 2D

Topological nontriviality in 2-dimensional superconductors requires the broken time-reversal symmetry. A topologically nontrivial phase shows chiral gapless Majorana fermions at the boundary. More interestingly, vortex zero modes of topological superconductors with the odd Chern number indicates non-abelian braiding statistics [37, 57] which may serve as qubits for quantum computation. [58, 59] Sr_2RuO_4 is a promising candidate for a 2-dimensional chiral superconductor. [60]

9.6 Topological crystalline insulator with mirror symmetry

3-dimensional $\mathbb{Z}_2$ topological insulators have odd number of surface Dirac fermions. Even number of surface Dirac fermions are not stable against nonmagnetic disorder which may induce a scattering between a pair of Dirac fermions. However, crystalline symmetry may forbid such gap-generating scattering term. In fact, the mirror symmetry with the time-reversal symmetry shows $\mathbb{Z}$ topological classification, and a $n \in \mathbb{Z}$ phase indicates stable $2n$ number of surface Dirac fermions. [17] This is an example of topological crystalline insulators. [18]

After the proposal that SeTe shows a nontrivial topological crystalline insulator with the mirror symmetry [23], a pair of surface Dirac fermions is experimentally observed [24, 25, 26].

9.7 Dirac semimetals

Dirac semimetals are 3-dimensional analog of graphene. There is a gapless Dirac fermion in the bulk which has a nontrivial topological charge and is stable against disorder. The Dirac semimetals offer a platform for engineering other exotic phases such as Weyl semimetals, axion insulators, and topological superconductors. Recently, Na_3Bi [61] and Cd_3As_2 [62, 63, 64] were experimentally confirmed as the Dirac semimetals.

9.8 Weyl superconductor and superfluid

Weyl semimetals and superconductors/superfluids have a pair of stable point nodes with the first Chern number in the BZ. Weyl semimetals have not yet been found experimentally. The ^{3}He-A phase is known as a Weyl superfluid. [10] A superconducting phase of URu_2Si_2 is a candidate for a time-reversal broken chiral superconductor, [65, 66] indicating a Weyl superconductor with the topological charge $ch_1 = 2$ for each point node.

10 Classification of topological crystalline phases with order-two point group symmetry

The classification of topological crystalline insulators and superconductors for general space group symmetries is a difficult issue. There are 230 distinct space group symmetries in three spatial dimensions, which implies 230 distinct problems in the topological classification. Moreover, by combining with the time-reversal symmetry and the particle-hole symmetry, possible symmetry classes increase in each element of space group symmetries. The 1651 magnetic space group symmetries are parts of possible symmetry classes. An algorithmic way to classify the topological phases for general crystalline symmetries is not yet known.

In the cases of order-two (magnetic) point group symmetries, we can systematically classify topological phases. [38] In Chap. 3, we give a detailed description of this topic. The order-two point group symmetries include $\boldsymbol{Z}_2$ global, mirror reflection, two-fold rotation, inversion, and their magnetic point group symmetries. See Fig. 1.7. A peculiarity of the order-two point group symmetries is that Hamiltonians which are compatible with the order-two point group symmetries can be represented by the Dirac Hamiltonians,

$$H(k_1, \ldots, k_d) = \sum_{\mu=1}^{d} k_\mu \gamma_\mu + m\gamma_{d+1}, \tag{1.10.1}$$

as explained below. Let us consider an order-two point group transformation $\hat{U}$ which flips $d_\parallel$ coordinates:

$$\hat{U} : (x_1, \ldots, x_{d_\parallel}, x_{d_\parallel+1}, \ldots, x_d) \mapsto (-x_1, \ldots, -x_{d_\parallel}, x_{d_\parallel+1}, \ldots, x_d). \tag{1.10.2}$$

If there is an additional Dirac matrix Γ which satisfies the following conditions:

$$\begin{aligned} &\{\Gamma, \gamma_\mu\} = 0, \quad (\mu = 1, \ldots, d_\parallel), \\ &[\Gamma, \gamma_\mu] = 0, \quad (\mu = d_\parallel, \ldots, d+1), \end{aligned} \tag{1.10.3}$$

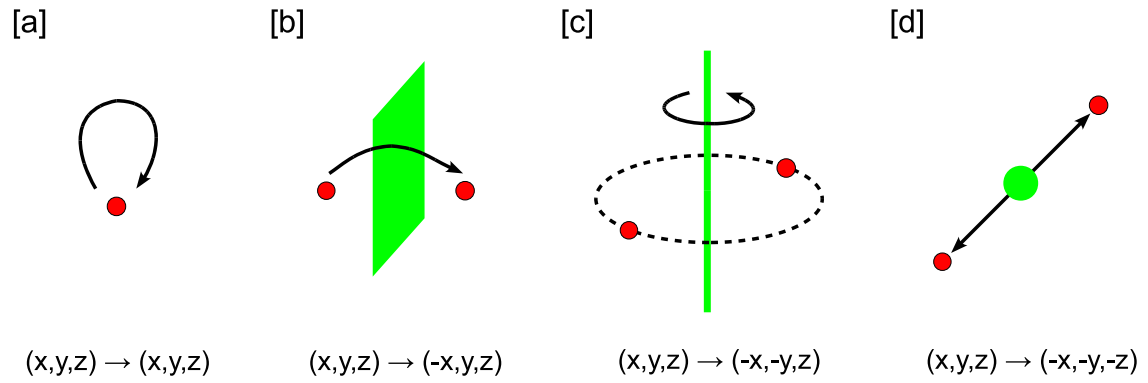

Figure 1.7: Order-two point group symmetries: [a] global Z_2, [b] reflection, [c] two-fold rotation, [d] inversion.

the order-two point group symmetry $\hat{U}$ is represented by the Dirac Hamiltonian as

$$\Gamma H(k_1, \ldots, k_{d_\parallel}, k_{d_\parallel+1}, \ldots, k_d)\Gamma^{-1} = H(-k_1, \ldots, -k_{d_\parallel}, k_{d_\parallel+1}, \ldots, k_d). \tag{1.10.4}$$

The above observation suggests that the classification problem of topological phases with order-two point group symmetries can be replaced by a problem only in terms of the Dirac matrices. In fact, this expectation is true, which is explained in Chap. 3. The replaced problem can be systematically solved as the extension problem of the Clifford algebras. [5, 67, 68, 38]

We find that the topological periodic table shows a novel periodicity in the number of flipped coordinates under the order-two point group symmetry, in addition to the Bott-periodicity in the space dimensions. Various symmetry protected topological phases and gapless modes will be identified and discussed in a unified framework. In addition, we also present a topological classification of Fermi points in the crystalline insulators and superconductors. The bulk topological classification and the Fermi point classification show the bulk-boundary correspondence in terms of the K-theory:

$$\begin{array}{c} \text{Classification of bulk topological phases in } (d+1) \text{ dimensions} \\ \Longleftrightarrow \quad \text{Classification of stable fermi point in } d \text{ dimensions.} \end{array} \tag{1.10.5}$$

In Chap. 4, we give the periodic tables with an additional order-two point group symmetry, and illustrate how the topological tables work by using concrete examples.

11 Chiral topological phases and winding number

The relation between bulk topological invariants and experimentally observable physical quantities is a fundamental issue of topological phases. For instance, the first Chern number appears as the quantized Hall conductivity in the quantum Hall effect [14], and the $\mathbb{Z}_2$ invariant of a time-reversal invariant topological insulator in 3-dimensions can be detected in axion electromagnetic responses [13].

However, for the case of topological phases characterized by $\mathbb{Z}$ invariants in odd spatial dimensions, this point has not yet been fully understood. These classes include time-reversal symmetry broken topological insulators with sublattice symmetry in one and 3-dimensions (class AIII), time-reversal invariant topological superconductors in 3-dimensions (class DIII, e.g. ^{3}He, $Cu_xBi_2Se_3$ [69, 56], Li_2Pt_3B [70]), and time-reversal invariant topological insulators and superconductors of spinless fermions in 1-dimension (class BDI, e.g. Su-Schrieffer-Heeger model [71], Kitaev Majorana chain model [72]). It is noted that all of these classes possess the chiral symmetry (the sublattice symmetry); i.e. the Bloch and BdG Hamiltonian $\mathcal{H}(\boldsymbol{k})$ satisfies the relation

$$\Gamma\mathcal{H}(\boldsymbol{k})\Gamma^{-1} = -\mathcal{H}(\boldsymbol{k}) \tag{1.11.1}$$

with Γ a unitary operator. This implies that if $|\psi(\boldsymbol{k})\rangle$ is an eigen state of $\mathcal{H}(\boldsymbol{k})$ with an energy $E(\boldsymbol{k})$, then, $\Gamma|\psi(\boldsymbol{k})\rangle$ is also an eigen state with an energy $-E(\boldsymbol{k})$. The chiral symmetry is indeed the origin of the bulk $\mathbb{Z}$ topological invariant referred to as the winding number:

$$\begin{aligned} N_1 &= \frac{1}{4\pi i}\int_{BZ} \text{tr}\ \Gamma[\mathcal{H}^{-1}d\mathcal{H}], \quad \text{for 1 dimension,} \\ N_3 &= \frac{1}{48\pi^2}\int_{BZ} \text{tr}\ \Gamma[\mathcal{H}^{-1}d\mathcal{H}]^3, \quad \text{for 3 dimensions.} \end{aligned} \tag{1.11.2}$$

A chiral symmetric topological insulator with the winding number N possesses N flavors of gapless Dirac (Majorana) fermions at the boundary, which are stable against impurity scatterings as long as the chiral symmetry is preserved. A general framework which relates the winding number to electromagnetic or thermal responses is still lacking, and desired.

In Chap. 5, we present two approaches for the solution of this issue. One is based on the idea that the winding number can be detected in electromagnetic and thermal responses of a certain class of heterostructure systems. We clarify the condition for the heterostructure systems in which the $\mathbb{Z}$ non-trivial character of the bulk systems can appear. The other one is to introduce a novel bulk physical quantity which can be directly related to the winding number. This quantity is referred to as "chiral charge polarization". We show that for 3-dimensional class AIII topological insulators, the chiral charge polarization is induced by an applied magnetic field, which is an analogy with topological magnetoelectric effect.

12 Dynamical axion in superconductors and superfluids

In Chap. 6, we argue a possibility of dynamical axion phenomena in superconductors and superfluids. The dynamical axion is fluctuating field which varies the (thermal) magnetoelectric polarization (1.8.2) of the BdG Hamiltonian $\mathcal{H}_{\text{BdG}}(\boldsymbol{k})$. To vary the magnetoelectric polarization θ, both the time-reversal symmetry and the inversion symmetry have to be broken. For example, in the case of a ^{3}He-B phase like time-reversal invariant p-wave topological superconductor, the imaginary s-wave superconducting fluctuation induces the dynamical axion field. [73] For centrosymmetric crystals, such an inversion-symmetry-breaking fluctuation survives only in the narrow parameter region where the magnitude of the even and odd parity channel attractive interactions are close to each other. If there is an inversion-symmetry-breaking spin-orbit interaction from noncentrosymmetric crystal structure, the dynamical axion is more feasible since the parity-mixing of Cooper pairs enables a relative phase fluctuation (Leggett mode [74]) between the even and odd parity superconducting orders.

In the case of superconductors and superfluids, since charge is not conserved, it is difficult to detect topological characters in electromagnetic responses. However, thermal responses can be good probes for topological nontriviality because energy is still conserved. A proposed action describing the thermal axion phenomena is the following gravitoelectromagnetic θ term, [75, 76]

$$S_\theta = \frac{\pi k_B^2 T^2}{12h} \int d^3\boldsymbol{x} dt \theta(t, \boldsymbol{x}) \boldsymbol{E}_E \cdot \boldsymbol{B}_E, \tag{1.12.1}$$

where $\boldsymbol{E}_E$ and $\boldsymbol{B}_E$ couple with the "energy polarization" [76] and the "energy magnetization" [77], respectively. The topological action (1.12.1) describes a thermal topological magnetoelectric effect, i.e., the energy magnetization induced by the gravitational field: $\boldsymbol{M}_E = \theta \frac{\pi k_B^2 T^2}{12h} \boldsymbol{E}_E$, and the energy polarization induced by the gravitomagnetic field; $\boldsymbol{P}_E = \theta \frac{\pi k_B^2 T^2}{12h} \boldsymbol{B}_E$. [76]

We consider dynamical axion phenomena in superconductors and superfluids in three spatial dimensions in terms of the gravitoelectromagnetic topological action (1.12.1), in which the axion field couples with mechanical rotation under finite temperature gradient. [76] We propose that the dynamical axion increases the moment of inertia, and in the case of ac mechanical rotation, i.e. a shaking motion with a finite frequency ω, as ω approaches the dynamical axion fluctuation mass, the observation of this effect becomes feasible.

Chapter 2

Band topology

In this chapter, we collect some mathematical formulations and basic results of the classification of free fermion topological phases. We introduce the Bloch and Bogoliubov-de Gennes (BdG) Hamiltonian for free fermions. Symmetry plays a central role for topological classifications. We formulate symmetry transformations of the time-reversal symmetry (TRS), the particle-hole symmetry (PHS), the chiral symmetry (CS), and space group symmetries. We illustrate the K-theory [7, 8, 9] description of the band topology for class A (no symmetry) systems, and comment on the K-theory with symmetries. We give the topological classification for the Altland-Zirnbauer (AZ) symmetry classes (TRS, PHS, and CS) [78] by using the Clifford algebra and the suspension isomorphism of the K-theory. Finally, we give the topological periodic table and analytic formulae for topological invariants.

1 Bloch Hamiltonian

1.1 Free fermion

Let $\{|i\rangle\}_{i\in I}$ be a basis of a one-particle Hilbert space, and $\psi_i^\dagger/\psi_i$ be the associate complex fermion creation/annihilation operators of one-particle states $|i\rangle$. A general Hamiltonian $\hat{H}$ is written as

$$\hat{H} = \sum_{ij\in I} \psi_i^\dagger \mathcal{H}_{ij} \psi_j + \frac{1}{4} \sum_{ijkl\in I} \psi_i^\dagger \psi_j^\dagger V_{ij,kl} \psi_l \psi_k + \cdots . \tag{2.1.1}$$

Our interest is free fermions. A Hamiltonian of free fermions is described by a quadratic form:

$$\hat{H} = \sum_{ij\in I} \psi_i^\dagger \mathcal{H}_{ij} \psi_j, \tag{2.1.2}$$

where $\mathcal{H}_{ij}$ satisfies the hermite condition $\mathcal{H}_{ij}^* = \mathcal{H}_{ji}$. We also consider superconductors and superfluids. Within the mean field approximation, a Hamiltonian is given by

$$\hat{H} = \sum_{ij\in I} \psi_i^\dagger \mathcal{H}_{ij} \psi_j + \frac{1}{2} \sum_{ij\in I} \psi_i^\dagger \Delta_{ij} \psi_j^\dagger + \frac{1}{2} \sum_{ij\in I} \psi_i \Delta_{ji}^* \psi_j \tag{2.1.3}$$

with Δ_{ij} the gap function. Δ_{ij} satisfies $\Delta_{ij} = -\Delta_{ji}$ from the fermion anticommutation relation $\{\psi_i, \psi_j\} = \{\psi_i^\dagger, \psi_j^\dagger\} = 0$. If we introduce the Nambu spinor Ψ_i by

$$\Psi_i = \begin{pmatrix} \psi_i \\ \psi_i^\dagger \end{pmatrix}, \tag{2.1.4}$$

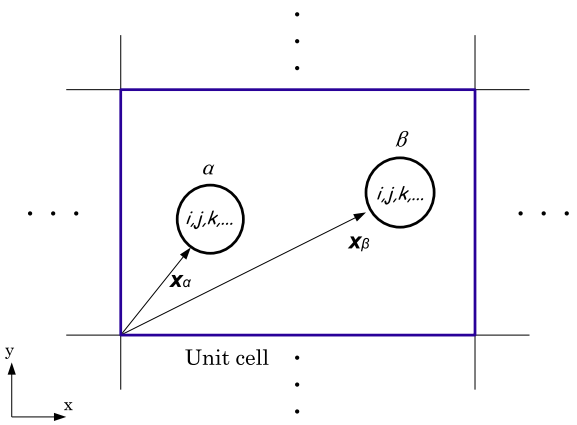

Figure 2.1: Degrees of freedom within a unit cell. $\{\alpha, \beta, \dots\}$ represent the positions of atoms. $\{i, j, \dots\}$ represent the internal degrees of freedom inner-side of an atom.

the Hamiltonian is written as

$$\hat{H} = \frac{1}{2} \sum_{ij \in I} \Psi_i^\dagger [\mathcal{H}_{BdG}]_{ij} \Psi_j + const. \tag{2.1.5}$$

where

$$[\mathcal{H}_{BdG}]_{ij} = \begin{pmatrix} \mathcal{H}_{ij} & \Delta_{ij} \\ \Delta^*_{ji} & -\mathcal{H}_{ji} \end{pmatrix} = \begin{pmatrix} \mathcal{H}_{ij} & \Delta_{ij} \\ [\Delta^\dagger]_{ij} & -[\mathcal{H}^T]_{ij} \end{pmatrix} \tag{2.1.6}$$

is the BdG Hamiltonian.

1.2 Bloch and BdG Hamiltonian

Let us move on to crystalline systems. Let $|\boldsymbol{R}\alpha i\rangle$ be one-particle states of a crystal. $\boldsymbol{R} \in BL \cong \mathbb{Z}^d$ represents a center of unit cells which are elements of the Bravais lattice (BL). Here d is the space dimensions. Concretely, $\boldsymbol{R} = \sum_{\mu=1}^d n_\mu \boldsymbol{a}_\mu$ with $\{n_\mu\}_{\mu=1,\dots d} \in \mathbb{Z}^d$ and $\boldsymbol{a}_\mu$ the lattice vectors. α labels a localized position of atoms in a unit cell, and i expresses internal degrees of freedom inner-side of a α-atom, such as spin, orbital, and Nambu degrees of freedom. See Fig. 2.1. The quadratic form $\mathcal{H}$ is a matrix in the space spanned by the basis $|\boldsymbol{R}\alpha i\rangle$. The lattice translation symmetry of the crystal means $\mathcal{H}_{\alpha i,\beta j}(\boldsymbol{R}, \boldsymbol{R}') = \mathcal{H}_{\alpha i,\beta j}(\boldsymbol{R}+\boldsymbol{a}, \boldsymbol{R}'+\boldsymbol{a})$ with the lattice vector $\boldsymbol{a} \in BL$, which implies $\mathcal{H}_{\alpha i,\beta j}(\boldsymbol{R}, \boldsymbol{R}') = \mathcal{H}_{\alpha i,\beta j}(\boldsymbol{R}-\boldsymbol{R}')$. The good quantum number associated with the lattice translation symmetry is called the Bloch wave number or momentum $\boldsymbol{k}$.

To transform into the momentum space we introduce the Fourier transformation as

$$|\boldsymbol{k}\alpha i\rangle = \sum_{\boldsymbol{R} \in BL} e^{i\boldsymbol{k}\cdot(\boldsymbol{R}+\boldsymbol{x}_\alpha)} |\boldsymbol{R}\alpha i\rangle \,, \tag{2.1.7}$$

where $\boldsymbol{x}_\alpha$ is localized position of the α-atom in a unit cell. $|\boldsymbol{k}\alpha i\rangle$ is periodic in Brillouin zone (BZ) up to a phase factor depending on α:

$$|\boldsymbol{k}+\boldsymbol{G}\alpha i\rangle = e^{i\boldsymbol{G}\cdot\boldsymbol{x}_\alpha} |\boldsymbol{k}\alpha i\rangle \tag{2.1.8}$$

where $\boldsymbol{G}$ is a reciprocal lattice vector which is generated by the basis $\{\boldsymbol{G}_\mu\}_{\mu=1,\dots,d}$ satisfying $\boldsymbol{G}_\mu \cdot \boldsymbol{a}_\nu = 2\pi\delta_{\mu\nu}$. Correspondingly, the Hamiltonian is

$$\hat{H} = \Omega \int_{BZ} \frac{d^d k}{(2\pi)^d} \psi^\dagger_{\alpha i}(\boldsymbol{k}) \mathcal{H}_{\alpha i,\beta j}(\boldsymbol{k}) \psi_{\beta j}(\boldsymbol{k}), \tag{2.1.9}$$

where $\mathcal{H}_{\alpha i,\beta j}(\boldsymbol{k})$ is the Bloch Hamiltonian which satisfies the following periodicity in the BZ,

$$\mathcal{H}_{\alpha i,\beta j}(\boldsymbol{k}+\boldsymbol{G}) = e^{-i\boldsymbol{G}\cdot\boldsymbol{x}_\alpha} \mathcal{H}_{\alpha i,\beta j}(\boldsymbol{k}) e^{i\boldsymbol{G}\cdot\boldsymbol{x}_\beta}. \tag{2.1.10}$$

The BZ is the d-dimensional torus for the Bravais lattice BL. $\Omega = \prod_{\mu=1}^d a_\mu, (a_\mu = |\boldsymbol{a}_\mu|)$ is the volume of a unit cell.

For superconductors and superfluids, we introduce the Nambu spinor of the momentum space,

$$\Psi_{\alpha i}(\boldsymbol{k}) = \sum_{\boldsymbol{R}\in\Pi} \Psi_{\alpha i}(\boldsymbol{R}) e^{-i\boldsymbol{k}\cdot(\boldsymbol{R}+\boldsymbol{x}_\alpha)} = \sum_{\boldsymbol{R}\in\Pi} \begin{pmatrix} \psi_{\alpha i}(\boldsymbol{R}) \\ \psi^\dagger_{\alpha i}(\boldsymbol{R}) \end{pmatrix} e^{i\boldsymbol{k}\cdot\boldsymbol{R}} = \begin{pmatrix} \psi_{\alpha i}(\boldsymbol{k}) \\ \psi^\dagger_{\alpha i}(-\boldsymbol{k}) \end{pmatrix}. \tag{2.1.11}$$

The BdG Hamiltonian is written as

$$\mathcal{H}_{BdG}(\boldsymbol{k}) = \begin{pmatrix} \mathcal{H}(\boldsymbol{k}) & \Delta(\boldsymbol{k}) \\ \Delta^\dagger(\boldsymbol{k}) & -\mathcal{H}^T(-\boldsymbol{k}) \end{pmatrix}. \tag{2.1.12}$$

1.2.1 Periodic basis

For dealing with the band topology, it is sometimes useful to introduce the periodic basis $|\boldsymbol{k}\alpha i\rangle'$ defined by

$$|\boldsymbol{k}\alpha i\rangle' = \sum_{\boldsymbol{R}\in BZ} e^{i\boldsymbol{k}\cdot\boldsymbol{R}} |\boldsymbol{R}\alpha i\rangle. \tag{2.1.13}$$

Of course, this basis does not take into account localized positions of α-atoms. More concretely, (2.1.13) corresponds to a different system S' from the original system. The system S' is given by the translations of the position of α-atoms as $\boldsymbol{x}_\alpha \mapsto \boldsymbol{0}$. In the momentum space, this translations are written by the following $\boldsymbol{k}$-dependent unitary transformation

$$\mathcal{H}_{\alpha i,\beta j}(\boldsymbol{k}) = e^{-i\boldsymbol{k}\cdot\boldsymbol{x}_\alpha} \mathcal{H}'_{\alpha i,\beta j}(\boldsymbol{k}) e^{i\boldsymbol{k}\cdot\boldsymbol{x}_\beta}. \tag{2.1.14}$$

By definition, the periodic basis $|\boldsymbol{k}\alpha i\rangle'$ satisfies the periodicity condition

$$|\boldsymbol{k}+\boldsymbol{G}\alpha i\rangle' = |\boldsymbol{k}\alpha i\rangle', \tag{2.1.15}$$

$$\mathcal{H}'_{\alpha i,\beta j}(\boldsymbol{k}+\boldsymbol{G}) = \mathcal{H}'_{\alpha i,\beta j}(\boldsymbol{k}). \tag{2.1.16}$$

Hamiltonians have the same form as (2.1.9),

$$\hat{H} = \Omega \int_{BZ} \frac{d^d k}{(2\pi)^d} \psi'^\dagger_{\alpha i}(\boldsymbol{k}) \mathcal{H}'_{\alpha i,\beta j}(\boldsymbol{k}) \psi'_{\beta j}(\boldsymbol{k}). \tag{2.1.17}$$

The classification of band topology is given by the (stable) homotopy classification of maps $\mathcal{H}(\boldsymbol{k})$ from the BZ (or a closed subspace) to some matrix space. Since the homotopy classification does not change under the unitary transformation (2.1.15), it is useful to choose the periodic basis $|\boldsymbol{k}\alpha i\rangle'$ in advance.

2 Symmetry

Symmetry plays an essential role in band topology. Symmetries restrict the forms of the Bloch Hamiltonians $\mathcal{H}(\boldsymbol{k})$, which changes the homotopy classifications. Symmetries are divided into global and crystalline symmetries. The global symmetries are non-spatial symmetries which act only on local internal degrees of freedom i and do not act on $\boldsymbol{R}$ and α. Examples of the global symmetries include the time-reversal symmetry (TRS), the particle-hole symmetry (PHS), and the global spin $SU(2)$ symmetry. On the other hand, the crystalline symmetries are spatial symmetries which transform localized positions, i.e., $\boldsymbol{R}$ and α. The crystalline symmetries are specified by the space group symmetries or magnetic space group symmetries. [1]

2.1 Altland-Zirnbauer symmetry class

The existence of global symmetry divides a Hilbert space into the direct sum of irreducible representations of the symmetry group. Here we assume the global unitary symmetries, such as the $SU(2)$ spin symmetry, are already diagonalized, and we consider remaining symmetries in irreducible blocks. The remaining symmetries are antiunitary symmetry or *anti-symmetry* which exchanges the occupied and unoccupied states. Those symmetries form the Altland-Zirnbauer (AZ) ten-fold symmetry classes, as explained below. [78, 79]

2.1.1 Time-reversal symmetry

A time-reversal transformation is defined in the second quantized formalism by an antiunitary transformation

$$\hat{T}\psi_i\hat{T}^\dagger = [U_T]_{ij}\psi_j,\ \hat{T}i\hat{T}^\dagger = -i \tag{2.2.1}$$

with a unitary matrix $[U_T]_{ij}$, $U_T U_T^\dagger = U_T^\dagger U_T = 1$. Here we suppressed the degrees of freedom $\{\boldsymbol{R}, \alpha\}$ because the time-reversal transformation does not change them. TRS is an order-two symmetry, which implies that $\hat{T}^2$ is a pure phase factor $\hat{T}^2 = z = e^{i\theta}$ in the Fock space. Due to the anti-linearity of $\hat{T}$, we give

$$z\hat{T} = \hat{T}^3 = \hat{T}z = z^*\hat{T}, \tag{2.2.2}$$

thus z is real $z = \pm 1$. The existence of the TRS means $\hat{T}\hat{H}\hat{T}^\dagger = \hat{H}$. For free fermions, the TRS is written as $U_T^\dagger \mathcal{H}^* U_T = \mathcal{H}$. In the Bloch basis $\psi_{\alpha i}(\boldsymbol{k}) = \sum_{\boldsymbol{R}} \psi_{\alpha i}(\boldsymbol{R}) e^{-i\boldsymbol{k}\cdot(\boldsymbol{R}+\boldsymbol{x}_\alpha)}$, the momentum $\boldsymbol{k}$ is flipped by anti-linearity of $\hat{T}$, so we get

$$T\mathcal{H}(\boldsymbol{k})T^{-1} = \mathcal{H}(-\boldsymbol{k}),\quad T = U_T\mathcal{K},\ T^2 = \pm 1. \tag{2.2.3}$$

Basic examples of $T^2 = \pm 1$ are a half integer spin system and an integer spin systems. For a spin 1/2 system the time-reversal transformation is $T = is_y\mathcal{K}$ where s_y is the y-component of the Pauli matrices for the spin space and $\mathcal{K}$ represents the complex conjugate. For a spinless system the time-reversal transformation is $T = \mathcal{K}$.

[1] The magnetic space group symmetries are combined symmetries with the time-reversal transformation and a space group transformation

2.1.2 Particle-hole symmetry

The PHS is associated with the BdG Hamiltonians. First, we argue the properties of the PHS for the Hamiltonians without pairing terms, i.e., $\hat{H} = \sum \psi_i^\dagger \mathcal{H}_{ij} \psi_j$. The particle-hole transformation is defined in the second quantized formalism as a unitary transformation that changes creation and annihilation operators as

$$\hat{C}\psi_i\hat{C}^\dagger = [U_C]_{ij}^* \psi_j^\dagger, \quad \hat{C}i\hat{C}^\dagger = i \tag{2.2.4}$$

with a unitary matrix $[U_C]_{ij}$, $U_C U_C^\dagger = U_C^\dagger U_C = 1$. A successive transformation gives $\hat{C}^2\psi_i[\hat{C}^\dagger]^2 = [U_C]_{ij}^*[U_C]_{jk}\psi_k$, and the order-two of PHS means $U_C^* U_C$ is a pure phase $U_C^* U_C = z = e^{i\theta}$. Then, in the same way as the TRS,

$$U_C z = U_C U_C^* U_C = U_C z^* \tag{2.2.5}$$

implies $z = \pm 1$. The PHS means $\hat{C}\hat{H}\hat{C}^\dagger = \hat{H}$. For free fermions we get

$$U_c^\dagger \mathcal{H}^T U_c = -\mathcal{H}. \tag{2.2.6}$$

The BdG Hamiltonians are always accompanied by the PHS since the Nambu spinor $\Psi_i = (\psi_i, \psi_i^\dagger)$ satisfies $\Psi = \tau_x \Psi^\dagger$ by definition, where $\boldsymbol{\tau}$ is the Pauli matrix for the Nambu space. Thus, the PHS for the BdG Hamiltonian is

$$\tau_x \mathcal{H}_{BdG}^T \tau_x = -\mathcal{H}_{BdG}, \tag{2.2.7}$$

which is a realization of $U_C^* U_C = 1$.

Some additional symmetries allow another type of the PHS. Consider the $SU(2)$ symmetric BdG Hamiltonian

$$\mathcal{H}_{BdG} = \begin{pmatrix} \varepsilon\sigma_0 & \delta i\sigma_y \\ -i\sigma_y\delta^\dagger & -\varepsilon^T\sigma_0 \end{pmatrix} \tag{2.2.8}$$

with the Nambu spinor $\Psi = (\psi_\uparrow, \psi_\downarrow, \psi_\uparrow^\dagger, \psi_\downarrow^\dagger)$, the Hamiltonian is recast into

$$\hat{H} = \sum (\psi_\uparrow^\dagger \;\; \psi_\downarrow) \begin{pmatrix} \varepsilon & \delta \\ \delta^\dagger & -\varepsilon^T \end{pmatrix} \begin{pmatrix} \psi_\uparrow \\ \psi_\downarrow^\dagger \end{pmatrix} + const. \tag{2.2.9}$$

The reduced BdG Hamiltonian $\mathcal{H}_{BdG} = \begin{pmatrix} \varepsilon & \delta \\ \delta^\dagger & -\varepsilon^T \end{pmatrix}$ satisfies the PHS

$$\tau_y \mathcal{H}_{BdG}^T \tau_y = -\mathcal{H}_{BdG}. \tag{2.2.10}$$

This is an realization of $U_C^* U_C = -1$.

For the Bloch basis $\psi_{\alpha i}(\boldsymbol{k}) = \sum_{\boldsymbol{R}} \psi_{\alpha i}(\boldsymbol{R}) e^{-i\boldsymbol{k}\cdot(\boldsymbol{R}+\boldsymbol{x}_\alpha)}$, the momentum $\boldsymbol{k}$ is flipped because of the definition of Nambu spinor $\Psi_{\alpha i}(\boldsymbol{k}) = (\psi_{\alpha i}(\boldsymbol{k}), \psi_{\alpha i}^\dagger(-\boldsymbol{k}))$. General PHSs take the following form:

$$C\mathcal{H}(\boldsymbol{k})C^\dagger = -\mathcal{H}(-\boldsymbol{k}), \quad C = U_C\mathcal{K}, \quad C^2 = \pm 1. \tag{2.2.11}$$

Table 2.1: AZ symmetry classes. The top two rows are complex AZ classes, and the bottom eight rows are real AZ classes. The first column represents the names of the AZ classes. The second to fourth columns indicate the absence (0) or the presence (± 1) of TRS, PHS and CS, respectively, where ± 1 means the sign of $T^2 = \pm 1$ and $C^2 = \pm 1$. The fifth column shows examples of physical realizations.

AZ class	TRS	PHS	CS	Physical realizations
A	0	0	0	No symmetry, superconductors with S_z conservation
AIII	0	0	1	Sublattice symmetry, superconductors with TRS and S_z conservation
AI	+1	0	0	Time reversal symmetry for integer spin systems
BDI	+1	+1	1	Spinless superconductors with TRS
D	0	+1	0	Superconductors
DIII	−1	+1	1	Superconductors with TRS
AII	−1	0	0	Time reversal symmetry for half integer spin systems
CII	−1	−1	1	
C	0	−1	0	Superconductors with $SU(2)$ symmetry
CI	+1	−1	1	Superconductors with TRS and $SU(2)$ symmetry

2.1.3 Chiral symmetry

The chiral symmetry (CS) is a unitary *anti-symmetry* of the one-particle Hamiltonian,

$$\Gamma \mathcal{H}(\boldsymbol{k}) \Gamma^\dagger = -\mathcal{H}(\boldsymbol{k}). \tag{2.2.12}$$

The CS emerges in the combined symmetry with TRS and PHS, $\Gamma = TC$. A pure CS does not realize as a global transformation in condensed matter context.

However, a CS approximately emerges as the sublattice symmetry of which the transformation acts as $\hat{\Gamma} : (\psi_A, \psi_B) \to (\psi_A, -\psi_B)$ where A and B are labels for the two-sublattice. The chiral symmetry implies

$$\hat{H} = \sum (\psi_A^\dagger \quad \psi_B^\dagger) \begin{pmatrix} 0 & V \\ V^\dagger & 0 \end{pmatrix} \begin{pmatrix} \psi_A \\ \psi_B \end{pmatrix}, \tag{2.2.13}$$

i.e., the absence of the terms within the same sublattice like as $V_{ij} \psi_{A,i}^\dagger \psi_{A,j} + h.c.$

2.1.4 Tenfold way

As a result, we get the tenfold symmetry classes, which is called the Altland-Zirnbauer (AZ) symmetry classes. Table 2.1 shows AZ symmetry classes and possible condensed matter realizations.

2.2 Space group symmetry

In this subsection we introduce space group symmetry and its representation on the Bloch basis. In this thesis, we do not deal with the topological classification of all the space group symmetric

topological crystalline insulators and superconductors. We only classify the topological crystalline phases protected by order-two point group symmetries in the Chap. 3. However, it is useful to summarize the relation between space group symmetry and the classification problem of topological crystalline insulators and superconductors, since the classification of space group symmetric topological crystalline insulators and superconductors is unsolved yet.

2.2.1 Symmorphic and nonsymmorphic space group

Let C be a given crystalline structure. The crystal C determines the Bravais lattice $BL(C)$, the space group $G(C)$, and the point group $P(C)$. The Bravais lattice $BL(C)$ is identified with the abelian group for the lattice transformation symmetry. The space group $G(C)$ is the symmetry group that does not change the crystal C. The point group $P(C)$ is the projection from $G(C)$ by "forgetting" the translations, and those element $p \in P(C)$ does not change the Bravais Lattice: $\boldsymbol{R} \in BL(C) \Rightarrow p\boldsymbol{R} \in BL(C)$.

An element of the space group $g \in G(C)$ consists of a point group element $p \in P(C)$ and an translation $\boldsymbol{a}$. $g \in G(C)$ is written by the Seitz notation $g = \{p|\boldsymbol{a}\}$:

$$\{p|\boldsymbol{a}\} : \boldsymbol{x} \mapsto p\boldsymbol{x} + \boldsymbol{a}. \tag{2.2.14}$$

The group structure of the space group $G(C)$ is written as

$$\{p|\boldsymbol{a}\} \cdot \{p'|\boldsymbol{a}'\} = \{pp'|\boldsymbol{a} + p\boldsymbol{a}'\}. \tag{2.2.15}$$

The inverse of $\{p|\boldsymbol{a}\}$ is

$$\{p|\boldsymbol{a}\}^{-1} = \{p^{-1}| - p^{-1}\boldsymbol{a}\}. \tag{2.2.16}$$

By using the lattice translation $BL(C)$, we can restrict $\boldsymbol{a}$ in the unit cell torus $T_u(C) = \mathbb{R}^d/BL(C)$ [2] for each $p \in P(C)$, which gives a one-to-one correspondence between the point group $P(C)$ and the translation by $p \mapsto \boldsymbol{a}_p \in T_u(C)$ *as a set*. So we get representative elements of the space group $G(C)$ by $\{p|\boldsymbol{a}_p\}$. However, $\{p|\boldsymbol{a}_p\}$ does not preserve the group structure in general: $\{p|\boldsymbol{a}_p\} \cdot \{p'|\boldsymbol{a}_{p'}\} \stackrel{?}{=} \{pp'|\boldsymbol{a}_{pp'}\}$, or equivalently,

$$\boldsymbol{a}_p + p\boldsymbol{a}_{p'} \stackrel{?}{=} \boldsymbol{a}_{pp'}. \tag{2.2.17}$$

If it is possible to choose $\boldsymbol{a}_p$ for all $p \in P(C)$ satisfying $\boldsymbol{a}_p + p\boldsymbol{a}_{p'} = \boldsymbol{a}_{pp'}$, the space group $G(C)$ is *symmorphic*. If not, i.e., there is a pair $p, p' \in P(C)$ such that

$$\boldsymbol{\nu}(p, p') := \boldsymbol{a}_p + p\boldsymbol{a}_{p'} - \boldsymbol{a}_{pp'} \in \Pi(C) \quad \text{with } \boldsymbol{\nu}(p, p') \neq \boldsymbol{0}, \tag{2.2.18}$$

the space group $G(C)$ is *nonsymmorphic*. [3]

[2] Note that the unit cell torus $T_u(C)$ is different from the BZ.

[3] The space group can be considered as the following group extension,

$$1 \to BL(C) \to G(C) \to P(C) \to 1. \tag{2.2.19}$$

$p \mapsto \{p|\boldsymbol{a}_p\} \in G(p)$ gives a section as a set. The symmorphic space group corresponds to that the above short exact sequence is split (split means an existence of a section preserving the group structure). The nonsymmorphic space group corresponds to a non-split group extension.

Let us consider the meaning of $\boldsymbol{\nu}(p,p') \in BL(C)$. Under the space group transformation by $\{p|\boldsymbol{a}_p\}$, an α-atom localized at $\boldsymbol{R}+\boldsymbol{x}_\alpha$ is mapped into $p(\boldsymbol{R}+\boldsymbol{x}_\alpha)+\boldsymbol{a}_p$. There should be a β-atom at the mapped position, which implies

$$\boldsymbol{\Delta}_{\beta\alpha}(p) := p\boldsymbol{x}_\alpha + \boldsymbol{a}_p - \boldsymbol{x}_\beta \in BL(C). \tag{2.2.20}$$

The mapped unit cell is specified by $p\boldsymbol{R}+\boldsymbol{\Delta}_{\beta\alpha}(p)$ because

$$p(\boldsymbol{R}+\boldsymbol{x}_\alpha)+\boldsymbol{a}_p = p\boldsymbol{R}+\boldsymbol{x}_\beta+\boldsymbol{\Delta}_{\beta\alpha}(p). \tag{2.2.21}$$

For the successive transformation $\{p|\boldsymbol{a}_p\}\cdot\{p'|\boldsymbol{a}_{p'}\}$, the α-atom is mapped into

$$p(p'\boldsymbol{R}+\boldsymbol{x}_\beta+\boldsymbol{\Delta}_{\beta\alpha}(p'))+\boldsymbol{x}_\gamma+\boldsymbol{\Delta}_{\gamma\beta}(p) = pp'\boldsymbol{R}+\boldsymbol{x}_\gamma+\boldsymbol{\Delta}_{\gamma\alpha}(pp')+\boldsymbol{\nu}(p,p'), \tag{2.2.22}$$

where the unit cell is mapped to $\boldsymbol{R}\mapsto pp'\boldsymbol{R}+\boldsymbol{\Delta}_{\gamma\alpha}(pp')+\boldsymbol{\nu}(p,p')$. This can be compared with the single transformation by $\{pp'|\boldsymbol{a}_{pp'}\}$ where the unit cell is mapped to $\boldsymbol{R}\mapsto pp'\boldsymbol{R}+\boldsymbol{\Delta}_{\gamma\alpha}(pp')$. Thus $\boldsymbol{\nu}(p,p')$ indicates the difference of the mapped unit cell between the successive transformation $\{p|\boldsymbol{a}_p\}\cdot\{p'|\boldsymbol{a}_{p'}\}$ and the single transformation $\{pp'|\boldsymbol{a}_{pp'}\}$.

2.2.2 Internal degrees of freedom

The space group is the symmetry group associated with the pattern of the crystal. But realistic materials have internal degrees of freedom such as spin and orbital, which induces an additional structure in the space group action.

Let $|\boldsymbol{R}\alpha i\rangle$ be the one-particle basis of a crystal C. The action of $\{p|\boldsymbol{a}_p\}$ on the basis $|\boldsymbol{R}\alpha i\rangle$, which is denoted by $\hat{U}(p)$, is written as

$$\hat{U}(p)\,|\boldsymbol{R}\alpha i\rangle = \sum_{\beta j} |p\boldsymbol{R}+\boldsymbol{\Delta}_{\beta\alpha}(p)\beta j\rangle\, U_{\beta j,\alpha i}(p). \tag{2.2.23}$$

Here the unitary matrix $U_{\beta j,\alpha i}(p)$ represents the transformation of the internal degrees of freedom between α and β atoms. The successive transformation $\{p|\boldsymbol{a}_p\}\cdot\{p'|\boldsymbol{a}_{p'}\}$ shows

$$\hat{U}(p)\hat{U}(p')\,|\boldsymbol{R}\alpha i\rangle = \sum_{\gamma\beta lj} |pp'\boldsymbol{R}+\boldsymbol{\Delta}_{\gamma\alpha}(pp')+\boldsymbol{\nu}(p,p')\gamma l\rangle\, U_{\gamma l,\beta j}(p)U_{\beta j,\alpha i}(p'). \tag{2.2.24}$$

On the other hand, the single transformation by $\{pp'|\boldsymbol{a}_{pp'}\}$ shows

$$\hat{U}(pp')\,|\boldsymbol{R}\alpha i\rangle = \sum_{\gamma l} |pp'\boldsymbol{R}+\boldsymbol{\Delta}_{\gamma\alpha}(pp')\gamma l\rangle\, U_{\gamma l,\alpha i}(pp'). \tag{2.2.25}$$

Now, there are two sources that may generate an obstruction of group structure. The first one comes from $\boldsymbol{\nu}(p,p')$ which was previously explained. The second one comes from the transformations of the internal degrees of freedom $U_{\alpha i,\beta j}(p)$: A representation of the point group may be projective:

$$\sum_{\beta j} U_{\alpha i,\beta j}(p)U_{\beta j,\gamma l}(p') = e^{i\phi(p,p')}U_{\alpha i,\gamma l}(pp'). \tag{2.2.26}$$

Here $e^{i\phi(p,p')}$ satisfies the 2-cocycle condition from the associativity $(U(p_1)U(p_2))U(p_3) = U(p_1)(U(p_2)U(p_3))$,

$$e^{i\phi(p_1,p_2)}e^{i\phi(p_1p_2,p_3)} = e^{i\phi(p_1,p_2p_3)}e^{i\phi(p_2,p_3)}. \tag{2.2.27}$$

A redefinition of the phases $U_{\alpha i,\beta j}(p) \mapsto e^{i\theta(p)}U_{\alpha i,\beta j}(p)$ gives the equivalence relation (coboundary condition)

$$e^{i\phi(p_1,p_2)} \sim e^{i\phi(p_1,p_2)}e^{i\theta(p_1)}e^{i\theta(p_1)}e^{-i\theta(p_1p_2)}. \tag{2.2.28}$$

The above conditions (2.2.27) and (2.2.28) imply that the projective representation is classified by the second group cohomology $H^2(P(C), U(1))$ where the group action on $U(1)$ is trivial: $P(C) \ni p : e^{ix} \mapsto e^{ix}$.

A familiar example of the nontrivial projective representation for internal degrees of freedom is the rotation transformation with a spin-orbit interaction. Consider the point group $C_{2v} = \{1, C_2, m_x, m_y\} \cong \mathbb{Z}_2 \times \mathbb{Z}_2$ where the mirror reflection transformations $U(m_x)$ and $U(m_y)$ flip the spin: $U(m_x) = s_x, U(m_y) = s_y$. We choose $U(C_2 = m_xm_y) = -i\sigma_z$. Then we observe $U(m_x)U(m_y) = -U(m_y)U(m_x) = -U(C_2)$, in which the relative phase factor cannot be removed by any redefinition of the $U(p)$.

In summary, general forms of successive transformations are

$$\begin{aligned}\hat{U}(p)\hat{U}(p')\left|\boldsymbol{R}\alpha i\right\rangle &= e^{i\phi(p,p')}\sum_{\beta j}\left|pp'\boldsymbol{R} + \boldsymbol{\Delta}_{\beta\alpha}(pp') + \boldsymbol{\nu}(p,p')\beta j\right\rangle U_{\beta j,\alpha i}(pp') \\ &= e^{i\phi(p,p')}\hat{U}(pp')\left|\boldsymbol{R} + (pp')^{-1}\boldsymbol{\nu}(p,p')\alpha i\right\rangle.\end{aligned} \tag{2.2.29}$$

For the second quantized formalism, the space group action on the fermion creation/annihilation operators is given by the replacement $|\boldsymbol{R}\alpha i\rangle$ by $\psi^\dagger_{\alpha i}(\boldsymbol{R})$,

$$\begin{aligned}\hat{U}(p)\psi^\dagger_{\alpha i}(\boldsymbol{R})\hat{U}^\dagger(p) &= \sum_{\beta j}\psi^\dagger_{\beta j}(p\boldsymbol{R} + \boldsymbol{\Delta}_{\beta\alpha}(p))U_{\beta j,\alpha i}(p), \\ \hat{U}(p)\psi_{\alpha i}(\boldsymbol{R})\hat{U}^\dagger(p) &= \sum_{\beta j}U^\dagger_{\alpha i,\beta j}(p)\psi_{\beta j}(p\boldsymbol{R} + \boldsymbol{\Delta}_{\beta\alpha}(p)).\end{aligned} \tag{2.2.30}$$

The successive transformations are

$$\begin{aligned}\hat{U}(p)(\hat{U}(p')\psi^\dagger_{\alpha i}(\boldsymbol{R})\hat{U}^\dagger(p'))\hat{U}^\dagger(p) &= e^{i\phi(p,p')}\hat{U}(pp')\psi^\dagger_{\alpha i}(\boldsymbol{R} + (pp')^{-1}\boldsymbol{\nu}(p,p'))\hat{U}^\dagger(pp'), \\ \hat{U}(p)(\hat{U}(p')\psi_{\alpha i}(\boldsymbol{R})\hat{U}^\dagger(p'))\hat{U}^\dagger(p) &= e^{-i\phi(p,p')}\hat{U}(pp')\psi_{\alpha i}(\boldsymbol{R} + (pp')^{-1}\boldsymbol{\nu}(p,p'))\hat{U}^\dagger(pp').\end{aligned} \tag{2.2.31}$$

2.2.3 Bloch state representation

The space group action on the Bloch basis is immediately given by (2.2.23) and (2.2.29):

$$\hat{U}(p)\left|\boldsymbol{k}\alpha i\right\rangle = e^{-ip\boldsymbol{k}\cdot\boldsymbol{a}_p}\sum_{\beta j}\left|p\boldsymbol{k}\beta j\right\rangle U_{\beta j,\alpha i}(p), \tag{2.2.32}$$

$$\hat{U}(p)\hat{U}(p')\left|\boldsymbol{k}\alpha i\right\rangle = e^{i\phi(p,p')}e^{-ipp'\boldsymbol{k}\cdot\boldsymbol{\nu}(p,p')}\hat{U}(pp')\left|\boldsymbol{k}\alpha i\right\rangle. \tag{2.2.33}$$

The obtained representation can be labeled by the point group $P(C)$ only, and may be projective in the cases where

(i) the transformation of internal degrees of freedom is projective.

(ii) the space group is nonsymmorphic.

The former obstruction is characterized by the second group cohomology $\{[e^{i\phi(p,p')}]\} \in H^2(P(C), U(1))$. The latter obstruction is described by $\boldsymbol{\nu}(p,p') \in BL(C)$, and it is also characterized by the group cohomology $H^1(P(C), T_u(C)) = H^2(P(C), BL(C))$ where the point group $P(C)$ acts on the unit cell torus $T_u(C)$ and the Bravais lattice $BL(C)$ in the natural way. (See, for example [80].) [4] [5]

The representation of the space group on the Bloch basis is

$$[U(p,\boldsymbol{k})]_{\alpha i,\beta j} := e^{-ip\boldsymbol{k}\cdot\boldsymbol{a}_p} U_{\alpha i,\beta j}(p) \tag{2.2.34}$$

which is not periodic in BZ in general. For topological classification, the periodic Bloch basis (2.1.13) may be useful. On the basis (2.1.13), the space group is represented as

$$\hat{U}(p)\,|\boldsymbol{k}\alpha i\rangle' = \sum_{\beta j} |p\boldsymbol{k}\beta j\rangle'\, e^{-ip\boldsymbol{k}\cdot\boldsymbol{\Delta}_{\beta\alpha}(p)} U_{\beta j,\alpha i}(p), \tag{2.2.35}$$

and the successive transformation is the same form as the usual Bloch basis,

$$\hat{U}(p)\hat{U}(p')\,|\boldsymbol{k}\alpha i\rangle' = e^{i\phi(p,p')} e^{-ipp'\boldsymbol{k}\cdot\boldsymbol{\nu}(p,p')} \hat{U}(pp')\,|\boldsymbol{k}\alpha i\rangle'\,. \tag{2.2.36}$$

Here

$$[U'(p,\boldsymbol{k})]_{\alpha i,\beta j} := e^{-ip\boldsymbol{k}\cdot\boldsymbol{\Delta}_{\alpha\beta}(p)} U_{\alpha i,\beta j}(p) \tag{2.2.37}$$

is periodic over BZ because $\boldsymbol{\Delta}_{\beta\alpha}(p) \in BL(C)$.

For the second quantized formalism, the space group actions on the fermion creation/annihilation operators are given by the replacement $|\boldsymbol{k}\alpha i\rangle$ by $\psi^\dagger_{\alpha i}(\boldsymbol{k})$,

$$\begin{aligned} \hat{U}(p)\psi^\dagger_{\alpha i}(\boldsymbol{k})\hat{U}^\dagger(p) &= \sum_{\beta j} \psi^\dagger_{\beta j}(p\boldsymbol{k}) U_{\beta j,\alpha i}(p,\boldsymbol{k}), \\ \hat{U}(p)\psi_{\alpha i}(\boldsymbol{k})\hat{U}^\dagger(p) &= \sum_{\beta j} U^\dagger_{\alpha i,\beta j}(p,\boldsymbol{k}) \psi_{\beta j}(p\boldsymbol{k}). \end{aligned} \tag{2.2.38}$$

The successive transformations shows

$$U(p,p'\boldsymbol{k})U(p',\boldsymbol{k}) = e^{i\phi(p,p')} e^{-ipp'\boldsymbol{k}\cdot\boldsymbol{\nu}(p,p')} U(pp',\boldsymbol{k}). \tag{2.2.39}$$

2.3 Symmetry of Bloch and BdG Hamiltonian

Let us compute the space group symmetry for the Bloch Hamiltonian. We observe

$$\hat{U}(p)\hat{H}\hat{U}^\dagger(p) = \Omega \int \frac{d^dk}{(2\pi)^d} \sum_{\alpha i\beta j} \psi^\dagger_{\alpha i}(p\boldsymbol{k}) [U(p,\boldsymbol{k})\mathcal{H}(\boldsymbol{k})U^\dagger(p,\boldsymbol{k})]_{\alpha i,\beta j} \psi^\dagger_{\beta j}(p\boldsymbol{k}). \tag{2.2.40}$$

[4] Note that an element of the Bravais lattice $BL(C)$ can be identified with a map from the Brillouin zone torus BZ to $U(1)$. We can show $\{e^{-ipp'\boldsymbol{k}\cdot\boldsymbol{\nu}(p,p')}\}_{p,p'\in P(C)}$ is a representative element of the second group cohomology $H^2(P(C), BL(C))$.

[5] The existence of a nontrivial phase $e^{i\phi(p,p')}e^{-ipp'\boldsymbol{k}\cdot\boldsymbol{\nu}(p,p')}$ induces some *twisting* to the K-theory. [81, 82]

The space group symmetry $\hat{U}(p)\hat{H}\hat{U}^\dagger(p) = \hat{H}$ implies

$$U(p,\boldsymbol{k})\mathcal{H}(\boldsymbol{k})U^\dagger(p,\boldsymbol{k}) = \mathcal{H}(p\boldsymbol{k}), \tag{2.2.41}$$

with

$$U(p,p'\boldsymbol{k})U(p',\boldsymbol{k}) = e^{i\phi(p,p')}e^{-ipp'\boldsymbol{k}\cdot\boldsymbol{\nu}(p,p')}U(pp',\boldsymbol{k}). \tag{2.2.42}$$

The BdG Hamiltonian has a gap function part

$$\hat{\Delta} = \frac{1}{2}\Omega\int\frac{d^dk}{(2\pi)^d}\sum_{\alpha i\beta j}\psi^\dagger_{\alpha i}(\boldsymbol{k})\Delta_{\alpha i,\beta j}(\boldsymbol{k})\psi^\dagger_{\beta j}(-\boldsymbol{k}) + h.c. \tag{2.2.43}$$

The space group transformation on $\hat{\Delta}$ is given by

$$\hat{U}(p)\hat{\Delta}\hat{U}^\dagger(p) = \frac{1}{2}\Omega\int\frac{d^dk}{(2\pi)^d}\sum_{\alpha i\beta j}\psi^\dagger_{\alpha i}(p\boldsymbol{k})[U(p,\boldsymbol{k})\Delta(\boldsymbol{k})U^T(p,-\boldsymbol{k})]_{\alpha i,\beta j}\psi^\dagger_{\beta j}(-p\boldsymbol{k}) + h.c., \tag{2.2.44}$$

which implies that the gap function is transformed as

$$\Delta(\boldsymbol{k}) \mapsto \widetilde{\Delta}(\boldsymbol{k}),\ \widetilde{\Delta}(p\boldsymbol{k}) := U(p,\boldsymbol{k})\Delta(\boldsymbol{k})U^T(p,-\boldsymbol{k}). \tag{2.2.45}$$

If the gap function does not break the space group symmetry: $\widetilde{\Delta}(\boldsymbol{k}) = \Delta(\boldsymbol{k})$, the BdG Hamiltonian preserves the space group symmetry:

$$U_{BdG}(p,\boldsymbol{k})\mathcal{H}_{BdG}(\boldsymbol{k})U^\dagger_{BdG}(p,\boldsymbol{k}) = \mathcal{H}_{BdG}(p\boldsymbol{k}). \tag{2.2.46}$$

Here we introduced

$$U_{BdG}(p,\boldsymbol{k}) = \begin{pmatrix} U(p,\boldsymbol{k}) & 0 \\ 0 & U^*(p,-\boldsymbol{k}) \end{pmatrix} \tag{2.2.47}$$

with satisfying

$$U_{BdG}(p,p'\boldsymbol{k})U_{BdG}(p',\boldsymbol{k}) = e^{i\tau_z\phi(p,p')}e^{-ipp'\boldsymbol{k}\cdot\boldsymbol{\nu}(p,p')}U_{BdG}(pp',\boldsymbol{k}), \tag{2.2.48}$$

where τ_z is the z-component of the Pauli matrix for the Nambu space. Note that the space group transformation $U_{BdG}(p,\boldsymbol{k})$ commutes with the particle-hole transformation: $U_{BdG}(p,-\boldsymbol{k})C = CU_{BdG}(p,\boldsymbol{k})$ with $C = \tau_x\mathcal{K}$.

Pairing order parameters may spontaneously break the space group symmetry: $\widetilde{\Delta}(\boldsymbol{k}) \neq \Delta(\boldsymbol{k})$. However, in special cases we can restore the space group symmetry of the BdG Hamiltonian, [83] which is explained in the next subsection.

2.4 Restore the space group symmetry of the BdG Hamiltonian

Consider the cases when the gap function $\Delta(\boldsymbol{k})$ shows a $\boldsymbol{k}$-independent 1-dimensional representation of the space group such as

$$\widetilde{\Delta}(p\boldsymbol{k}) = U(p,\boldsymbol{k})\Delta(\boldsymbol{k})U^T(p,-\boldsymbol{k}) = e^{i\theta(p)}\Delta(p\boldsymbol{k}) \tag{2.2.49}$$

with $e^{i\theta(p)}e^{i\theta(p')} = e^{i\theta(pp')}$. With respect to the phase factor $e^{i\theta(p)}$, we introduce a global U(1) phase transformation

$$\hat{U}(\theta(p)/2)\psi^\dagger_{\alpha i}(\boldsymbol{R})\hat{U}^\dagger(\theta(p)/2) = \psi^\dagger_{\alpha i}(\boldsymbol{R})e^{-i\theta(p)/2}, \tag{2.2.50}$$

then the combined transformation $\hat{U}(\theta(p)/2)\hat{U}(p)$ preserves the gap function:

$$(\hat{U}(\theta(p)/2)\hat{U}(p))\hat{\Delta}(\hat{U}(\theta(p)/2)\hat{U}(p))^\dagger = \hat{\Delta}. \tag{2.2.51}$$

Correspondingly, we introduce the combined space group transformation on the BdG Hamiltonian,

$$\tilde{U}_{BdG}(p,\boldsymbol{k}) = \begin{pmatrix} U(p,\boldsymbol{k}) & 0 \\ 0 & e^{i\theta(p)}U^*(p,-\boldsymbol{k}) \end{pmatrix}. \tag{2.2.52}$$

We can restore the space group symmetry of the BdG Hamiltonian

$$\tilde{U}_{BdG}(p,\boldsymbol{k})\mathcal{H}_{BdG}(\boldsymbol{k})\tilde{U}^\dagger_{BdG}(p,\boldsymbol{k}) = \mathcal{H}_{BdG}(p\boldsymbol{k}). \tag{2.2.53}$$

An important point is that the phase factor $e^{i\theta(p)}$ in $\tilde{U}_{BdG}(p,\boldsymbol{k})$ changes the commutation relation with the particle-hole transformation as

$$C\tilde{U}_{BdG}(p,\boldsymbol{k}) = e^{i\theta(p)}\tilde{U}_{BdG}(p,-\boldsymbol{k})C, \tag{2.2.54}$$

which induces a twisting of the group action.

2.4.1 Example: spin-singlet superconductors with C_4 symmetry

Assume normal state has the C_4 symmetry $C_4 : (x,y,z) \mapsto (-y,x,z)$. Here we restrict spin-singlet superconductors.

For s-wave, $\Delta(\boldsymbol{k}) = \Delta_0$ is invariant under the C_4 transformation.

For $(d_{zx} \pm id_{zy})$-wave, $\Delta(\boldsymbol{k}) = k_zk_x \pm ik_zk_y$ breaks the the C_4 transformation as $\widetilde{\Delta}(\boldsymbol{k}) = \Delta(C_4^{-1}\boldsymbol{k}) = \mp i\Delta(\boldsymbol{k})$, which implies $e^{i\theta(C_4)} = \mp i$ and shows $C\tilde{U}_{BdG}(p,\boldsymbol{k}) = \mp i\tilde{U}_{BdG}(p,-\boldsymbol{k})C$.

For $(d_{x^2-y^2} + id_{xy})$-wave, $\Delta(\boldsymbol{k}) = k_x^2 - k_y^2 + ik_xk_y$ break the C_4 transformation as $\widetilde{\Delta}(\boldsymbol{k}) = \Delta(C_4^{-1}\boldsymbol{k}) = -\Delta(\boldsymbol{k})$, which implies $e^{i\theta(C_4)} = -1$ and shows $C\tilde{U}_{BdG}(p,\boldsymbol{k}) = -\tilde{U}_{BdG}(p,-\boldsymbol{k})C$.

3 Topology of gapped Hamiltonian

Now we arrived at the position where the most essential factor for band topology is introduced. That is a projection onto sub energy bands, which is well-defined for the gapped structure of insulators and superconductors. There are some stages where topological classification is acted. The homotopy classification, the vector bundle classification, and the K-theory classification provide slightly distinct classifications of band topology in a mathematical and physical sense. The most "stable" one is the K-theory classification, which is also the most calculable. We illustrate the topological classification for class A systems, and only briefly comment on the cases with symmetry.

3.1 Energy gap and projection

Let $\{|u_a(\boldsymbol{k})\rangle\}$ be the eigen states of a Hamiltonian $\mathcal{H}(\boldsymbol{k})$:

$$\mathcal{H}(\boldsymbol{k})\,|u_a(\boldsymbol{k})\rangle = E_a(\boldsymbol{k})\,|u_a(\boldsymbol{k})\rangle\,. \tag{2.3.1}$$

Index a runs over $\{1,\ldots,N\}$ where N is the number of all the degrees of freedom within a unit cell. $|u_a(\boldsymbol{k})\rangle$ is called as the Bloch state. We label a such that $E_a \le E_{a+1}$.

Let X be a subspace of the Brillouin zone BZ. X may be BZ itself. If there is a finite gap in the energy spectrum between lower n bands and higher $(N-n)$ bands on the subspace X,

$$E_a(\boldsymbol{k}) < E_b(\boldsymbol{k}), \quad (a = 1,\ldots n, b = n+1,\ldots N, \boldsymbol{k} \in X), \tag{2.3.2}$$

then the total Hilbert space $\mathbb{C}^N$ is decomposed into the two subspace on X as

$$\mathbb{C}^N = \mathbb{C}^{N-n} \oplus \mathbb{C}^n = (1 - P(\boldsymbol{k}))\mathbb{C}^N \oplus P(\boldsymbol{k})\mathbb{C}^N, \ (\boldsymbol{k} \in X). \tag{2.3.3}$$

where $P(\boldsymbol{k})$ is the projection onto the lower energy states,

$$P(\boldsymbol{k}) := \sum_{a=1}^{n} |u_a(\boldsymbol{k})\rangle \langle u_a(\boldsymbol{k})|\,, \ (\boldsymbol{k} \in X). \tag{2.3.4}$$

Such a situation is naturally realized in band insulators and fully gapped superconductors with $X = BZ$, or stable fermi points or nodes where X is a closed subspace surrounding the fermi points or nodes.

The decomposition (2.3.3) may induce a nontrivial classification under the equivalence relation $\mathcal{H}_1(\boldsymbol{k}) \sim \mathcal{H}_2(\boldsymbol{k})$ if and only if $\mathcal{H}_1(\boldsymbol{k})$ can be smoothly deformed into $\mathcal{H}_2(\boldsymbol{k})$ with preserving the finite energy gap on X. Notice that if we do not impose the gapped condition in the energy spectrum of $\mathcal{H}(\boldsymbol{k})$, there is no classification in the Hamiltonians $\mathcal{H}(\boldsymbol{k})$ since any Hamiltonian can be smoothly deformed into an atomic insulator.

The projection $P(\boldsymbol{k})$ on X defines the rank n complex vector bundle $E \to X$ by

$$E := \cup_{\boldsymbol{k}\in X} P(\boldsymbol{k})\mathbb{C}^N. \tag{2.3.5}$$

E is a sub bundle of the trivial bundle $X \times \mathbb{C}^N$.

3.2 Homotopy classification

Let us consider a classification of gapped Hamiltonians $\mathcal{H}(\boldsymbol{k})$ over X. We fix N the number of degrees of freedom in a unit cell, and also fix n the number of occupied states. Without loss of generality, we can assume flat band Hamiltonians in which the energy eigenvalues are ± 1. A Hamiltonian $\mathcal{H}(\boldsymbol{k})$ is diagonalized by a $N \times N$ unitary matrix $U(\boldsymbol{k}) \in U(N)$ as

$$\mathcal{H}(\boldsymbol{k}) = U(\boldsymbol{k}) \begin{pmatrix} 1_{(N-n)\times(N-n)} & 0 \\ 0 & -1_{n\times n} \end{pmatrix} U^\dagger(\boldsymbol{k}). \tag{2.3.6}$$

There is redundancy in $U(\boldsymbol{k})$ from a redefinition as

$$U(\boldsymbol{k}) \mapsto U(\boldsymbol{k}) \cdot \begin{pmatrix} V(\boldsymbol{k}) & 0 \\ 0 & W(\boldsymbol{k}) \end{pmatrix}, \quad V(\boldsymbol{k}) \in U(N-n),\ W(\boldsymbol{k}) \in U(n). \tag{2.3.7}$$

Then, the Hamiltonians $\mathcal{H}(\boldsymbol{k})$ with n occupied states in N total bands are uniquely characterized by a map $X \to G_n(\mathbb{C}^N)$ where $G_n(\mathbb{C}^N)$ is the complex Grassmannian

$$G_n(\mathbb{C}^N) = \frac{U(N)}{U(n) \times U(N-n)} \tag{2.3.8}$$

which is a topological space for the way of selections of a $(N-n)$-dimensional sub vector space in the total vector space $\mathbb{C}^N$. The topological classification of Hamiltonians $\mathcal{H}(\boldsymbol{k})$ over X with n occupied states and $(N-n)$ unoccupied states is evaluated by the set of homotopy classes $[X, G_n(\mathbb{C}^N)]$.

For example, consider 2-band insulators over 2-dimensional sphere $X = S^2$, the set of the homotopy classes of the Hamiltonians is given by

$$[S^2, G_1(\mathbb{C}^2)] = \mathbb{Z}. \tag{2.3.9}$$

$\mathbb{Z}$ is characterized by the winding number. Note that $G_1(\mathbb{C}^2) = CP^1 = S^2$.

The following two examples are instructive. Consider 2-band insulators over 3-dimensional sphere $X = S^3$. The homotopy class is given by

$$[S^3, G_1(\mathbb{C}^2)] = [S^3, S^2] = \mathbb{Z}. \tag{2.3.10}$$

A generator of $\mathbb{Z}$ is the Hopf map $S^3 \to S^2$. [84] On the other hand, 3-band insulators with a one occupied state over 3-dimensional sphere $X = S^3$ do not show the nontrivial band,

$$[S^3, G_1(\mathbb{C}^3)] = [S^3, CP^2] = 0. \tag{2.3.11}$$

Compared with (2.3.10), the Hopf map insulator, which belongs to an nontrivial homotopy class of $[S^3, S^2]$, is unstable under adding unoccupied states.

To give the stable classification under adding unoccupied states, we move on to the vector bundle classification.

3.3 Vector bundle classification

As explained previously, the occupied states of n bands determine a rank n complex vector bundle over X by $E = \cup_{\boldsymbol{k} \in X} P(\boldsymbol{k})\mathbb{C}^N$. Let $\mathrm{Vext}^n_{\mathbb{C}}(X)$ be the set of isomorphic classes of rank n complex vector bundles. We denote the vector bundles E_1 and E_2 are isomorphic by $E_1 \approx E_2$. The stable classification of rank n complex vector bundles against adding unoccupied states is given by the homotopy classification of maps $X \to G_n(\mathbb{C}^N)$ with a sufficiently large N, which is called the classifying space for $U(n)$,

$$BU(n) = \lim_{N \to \infty} G_n(\mathbb{C}^N). \tag{2.3.12}$$

The classifying space $BU(n)$ corresponds to the Hamiltonian $\mathcal{H}(\boldsymbol{k})$ with n-occupied states and a sufficiently large number of unoccupied states. There is a bijection

$$\mathrm{Vext}^n_{\mathbb{C}}(X) \cong [X, BU(n)]. \tag{2.3.13}$$

Let $\mathrm{Vext}_{\mathbb{C}}(X) = \sqcup_{n=0}^{\infty} \mathrm{Vext}^n_{\mathbb{C}}(X)$ be the set of isomorphic classes of vector bundles over X. The Whitney sum of vector bundles $E_1 \oplus E_2$ induces an abelian semigroup structure in $\mathrm{Vext}_{\mathbb{C}}(X)$ via

$[E_1]+[E_2]=[E_1\oplus E_2]$. For the Hamiltonian notation, the Whitney sum corresponds to the direct sum of Hamiltonians $\mathcal{H}_1\oplus\mathcal{H}_2=\begin{pmatrix}\mathcal{H}_1(\boldsymbol{k}) & 0\\ 0 & \mathcal{H}_2(\boldsymbol{k})\end{pmatrix}$.

Note that $\mathrm{Vect}_{\mathbb{C}}(X)$ does not have its inverse because there is no meaning of a "rank $(-n)$ vector bundle" or "$(-n)$ number of occupied states". We introduce a notion of "stable equivalence" in the next subsection, which induces an inverse in $\mathrm{Vect}_{\mathbb{C}}(X)$ and gives an abelian group structure.

3.4 K-theory classification

The vector bundle classification gives the classification of isomorphic classes of occupied states. However, in realistic cases, there may be other occupied states E' in a low energy region which can mix with occupied states E under a smooth deformation. So it is natural to weaken the equivalence relation to the "stable equivalence" $\sim$ defined by

$$E_1\sim E_2 \overset{def}{\Longleftrightarrow} E_1\oplus E'\approx E_2\oplus E' \text{ for some } E'. \tag{2.3.14}$$

The complex K-theory over X, $KU(X)$, is the abelian group of the equivalence classes in $\mathrm{Vect}_{\mathbb{C}}(X)$ under $\sim$,

$$KU(X):=\{(E_1,E_2)\in \mathrm{Vect}_{\mathbb{C}}(X)\times \mathrm{Vect}_{\mathbb{C}}(X)\}/(E_1,E_2)\approx (E_1\oplus E', E_2\oplus E'). \tag{2.3.15}$$

The unit of the abelian group $KU(X)$ is given by the same pair of E, $(E,E)\sim 0$. The inverse of a $[(E_1,E_2)]$ is given by $[(E_1,E_2)]^{-1}=[(E_2,E_1)]$ because $[(E_1,E_2)]+[(E_2,E_1)]\sim[(E_1\oplus E_2, E_2\oplus E_1)]\sim 0$. Now $KU(X)$ is the abelian group of formal differences $[E_1]-[E_2]$

Physical implication of $[E_1]-[E_2]\in KU(X)$ is obvious. $[E_1]-[E_2]$ represents the difference between the two occupied states E_1 and E_2, which is stable against adding occupied states.

From the Swan's theorem: every vector bundle E is a summand of a trivial bundle, [6] we have

$$[E_1]-[E_2]=[E_1\oplus\widetilde{E}_2]-[E_2\oplus\widetilde{E}_2]=[E_1\oplus\widetilde{E}_2]-[n]. \tag{2.3.16}$$

Thus an element of $KU(X)$ can be always described by $[E]-[n]$ the difference between an occupied states E and trivial vacuum n, which provides an interpretation that an element $[E]-[n]\in KU(X)$ corresponds to the difference between the occupied states E and vacuum.

It is useful to introduce the reduced K-theory over X, $\widetilde{KU}(X)$. The rank of vector bundle, $E\mapsto rank(E)\in\mathbb{Z}$, induces a homomorphism $KU(X)\to\mathbb{Z}$ by $[E_1]-[E_2]\mapsto rank(E_1)-rank(E_2)$. $\widetilde{KU}(X)$ is defined by the kernel of the $rank$:

$$\widetilde{KU}(X):=\ker\Big[rank: KU(X)\to\mathbb{Z}\Big]. \tag{2.3.17}$$

The element of $\widetilde{KU}(X)$ is represented by the formal difference $[E]-[n]$ where $rank(E)=n$, i.e., the K-theory for the same number of the occupied states.

[6] I.e., for a vector bundle E, there is a vector bundle $\widetilde{E}$ such that the Whitney sum is the trivial bundle, $E\oplus\widetilde{E}\approx n$.

3.4.1 Stabilization

Let us see an implication of the stable equivalence. Consider two different isomorphic classes E_1 and E_2 in $\mathrm{Vect}_{\mathbb{C}}(X)$. From the stable equivalence, E_1 and E_2 may be not distinguished in the K-theory $KU(X)$. We give an example.

To see a simple example, we consider the real K-theory $KO(X)$ which is defined for real vector bundles in which the structure group is the orthogonal group $O(n)$. [7] We denote isomorphic classes of real vector bundles over X by $\mathrm{Vect}_{\mathbb{R}}(X)$. Consider the base space is $X = S^2$. It is known that the tangent bundle over S^2, $[TS^2] \in \mathrm{Vect}_{\mathbb{R}}(X)$ is not isomorphic to the trivial bundle $S^2 \times \mathbb{R}^2$. There is an obvious isomorphism $TS^2 \oplus NS^2 \approx S^2 \times \mathbb{R}^3$ where $NS^2 \approx S^2 \times \mathbb{R}$ is the cotangent bundle over S^2 which is isomorphic to the trivial line bundle. We denote the isomorphic class of the trivial line bundle by [1] and its n multiple by $[n]$. $TS^2 \oplus NS^2 \approx S^2 \times \mathbb{R}^3$ leads to an equivalence relation of the real K-theory

$$[TS^2] - [2] = [TS^2 \oplus NS^2] - [3] = [3] - [3] = 0. \tag{2.3.18}$$

Thus the tangent bundle over S^2, which is a nontrivial bundle, is stably equivalent to the trivial bundle $S^2 \times \mathbb{R}^2$. The K-theory does not distinguish between the tangent bundle TS^2 and the rank 2 trivial bundle $S^2 \times \mathbb{R}^2$.

3.4.2 Hamiltonian and homotopy representation

We constructed the K-theory by stable classes of vector bundles. But it is useful to reformulate by using Hamiltonians. We follow the Kitaev's [5] approach. From (2.3.13) and (2.3.14), the K-theory classification provides the classification stable against adding both unoccupied and occupied states: For gapped Hamiltonian matrices $\mathcal{H}_1(\boldsymbol{k}), \mathcal{H}_2(\boldsymbol{k})$ with the same rank, the stable equivalence $\sim$ for $\mathcal{H}_1(\boldsymbol{k}), \mathcal{H}_2(\boldsymbol{k})$ is defined as

$$\mathcal{H}_1(\boldsymbol{k}) \sim \mathcal{H}_2(\boldsymbol{k}) \overset{def}{\Leftrightarrow} \mathcal{H}_1(\boldsymbol{k}) \oplus \mathcal{H}'(\boldsymbol{k}) \approx \mathcal{H}_2(\boldsymbol{k}) \oplus \mathcal{H}'(\boldsymbol{k}) \text{ for some } \mathcal{H}'(\boldsymbol{k}). \tag{2.3.19}$$

where $\oplus$ is direct sum of the matrix and $\approx$ is the homotopy equivalence. The K-theory over X is defined as the same manner as (2.3.20),

$$KU(X) := \text{Set of pairs } \{(\mathcal{H}_1(\boldsymbol{k}), \mathcal{H}_2(\boldsymbol{k}))\}/\sim . \tag{2.3.20}$$

An element of $KU(X)$ is a formal difference $[\mathcal{H}_1(\boldsymbol{k})] - [\mathcal{H}_2(\boldsymbol{k})]$.

Let us consider a homotopy representation of $KU(X)$. Consider rank s two Hamiltonians $\mathcal{H}_1, \mathcal{H}_2$. Let n_i and m_i $(i = 1, 2)$ be the number of the occupied and unoccupied states, respectively. Note that $n_1 + m_1 = n_2 + m_2 = s$. The stable equivalent index is $k = n_1 - n_2 (= -m_1 + m_2)$ only. Since $[\mathcal{H}_1] - [\mathcal{H}_2] = [\mathcal{H}_1 \oplus (-\mathcal{H}_2)] - [\mathcal{H}_2 \oplus (-\mathcal{H}_2)]$ it is sufficient to consider pairs where the second matrix is trivial. The space of the $KU(X)$ is given by the first matrix $\mathcal{H}_1 \oplus (-\mathcal{H}_2)$ where the total rank is $2s$ and $s + k$ occupied states,

$$\mathcal{C}_0 = \cup_{k \in \mathbb{Z}} \lim_{s \to \infty} \frac{U(2s)}{U(s+k) \times U(s-k)}. \tag{2.3.21}$$

[7] Similarly, the K-theory for the quaternionic vector bundle, in which the structure group is the symplectic group $Sp(n)$, is the quaternionic K-theory $KSp(X)$.

(2.3.21) is called the classifying space $\mathcal{C}_0$. $\lim_{s\to\infty}$ corresponds the stable equivalence. $k \in \mathbb{Z}$ characterizes disconnected parts of $\mathcal{C}_0$. We obtain the homotopy representation of $KU(X)$:

$$KU(X) \cong [X, C_0]. \tag{2.3.22}$$

Especially, the K-theory over point is given by

$$KU(pt) = [pt, C_0] = \pi_0(C_0) = \mathbb{Z}. \tag{2.3.23}$$

3.5 Band topology with symmetry

So far, we did not consider symmetry in band topology. Symmetries include the TRS, PHS, CS, and space group symmetries, and magnetic space group symmetries. Symmetries restrict the form of Hamiltonians $\mathcal{H}(\boldsymbol{k})$ explained in Subsection 2.3, and induce some group actions on the complex vector bundle and the K-theory.

Here we briefly sketch the symmetry group action on the vector bundle picture. The symmetry of Hamiltonian is written as

$$U(p, \boldsymbol{k})\mathcal{H}(\boldsymbol{k})U^{-1}(p, \boldsymbol{k}) = \mathcal{H}(p\boldsymbol{k}) \tag{2.3.24}$$

where $U(p, \boldsymbol{k})$ is unitary or anti-unitary. [8] The above equation implies the symmetry of the projection

$$U(p, \boldsymbol{k})P(\boldsymbol{k})U^{-1}(p, \boldsymbol{k}) = P(p\boldsymbol{k}), \tag{2.3.25}$$

then we get the group action on the fiber between $\boldsymbol{k}$ and $p\boldsymbol{k}$: $E_{\boldsymbol{k}} \ni v \mapsto U(p, \boldsymbol{k})v \in E_{p\boldsymbol{k}}$. This map is well-defined since

$$E_{p\boldsymbol{k}} = P(p\boldsymbol{k})\mathbb{C}^N = U(p, \boldsymbol{k})P(\boldsymbol{k})U^{-1}(p, \boldsymbol{k})\mathbb{C}^N = U(p, \boldsymbol{k})E_{\boldsymbol{k}}. \tag{2.3.26}$$

Thus we get the vector bundle with the group action. And also we get the K-theory with group action. In Fig. 2.2 we show a picture of the group action on the vector bundle.

Some physical symmetries fit into well known K-theory. In the following, we give some examples.

3.5.1 Symmorphic space group and equivariant K-theory

First, we introduce a notion of G-space X. Let G be a group and X be a topological space that G acts on. The G-space X is a topological space X with group action

$$g : x \mapsto g \cdot x, \ (g \in G, x \in X) \tag{2.3.27}$$

with satisfying

$$1 \cdot x = x, \quad (g_1 \cdot g_2) \cdot x = g_1 \cdot (g_2 \cdot x). \tag{2.3.28}$$

[8] We omit the anti-symmetry $U(p, \boldsymbol{k})\mathcal{H}(\boldsymbol{k})U^{-1}(p, \boldsymbol{k}) = -\mathcal{H}(p\boldsymbol{k})$ such as the PHS and CS, for simplicity. To deal with the anti-symmetry we have to introduce a grading of vector bundle $E^- \oplus E^+$ where $E^{\pm}$ represents the vector bundle consists of the unoccupied/occupied states.

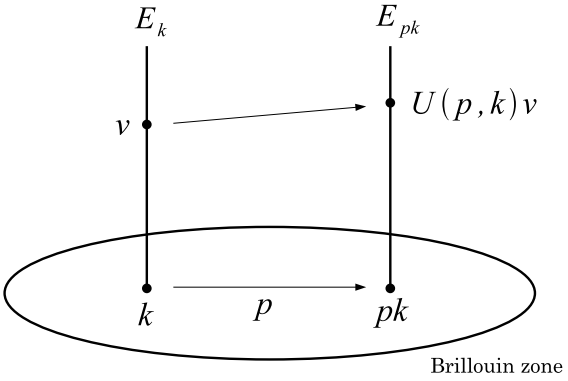

Figure 2.2: The symmetry group action on the vector bundle.

A G-vector bundle $\pi : E \to X$ is a G-space E with group action G preserving the projection, i.e., $g\pi = \pi g$. The G-vector bundle is referred to as the G-equivariant vector bundle. And its stable equivalence version is the G-equivariant K-theory. [85, 86]

Let us consider a topological insulator with a symmorphic space group symmetry. And also we assume the group transformation of the internal degrees of freedom is trivial. In this set up, the compatibility of group action is satisfied:

$$U(p, p'\boldsymbol{k})U(p', \boldsymbol{k}) = U(pp', \boldsymbol{k}) \tag{2.3.29}$$

where $U(p, \boldsymbol{k})$ is unitary and $p \in P$ is an element of the point group P. The above property fits into the G-equivariant vector bundle. The isomorphic classes of the G-equivariant vector bundle is denoted by $\mathrm{Vect}_G(X)$, and its stable equivalent version is denoted by $K_G(X)$, the G-equivariant K-theory over X.

On the other hand, If the space group is nonsymmorphic, or the transformation of internal degrees of freedom shows a nontrivial projective representation, the group action on the fiber $E_{\boldsymbol{k}} \to E_{p\boldsymbol{k}}$ does not satisfy the compatibility condition:

$$U(p, p'\boldsymbol{k})U(p', \boldsymbol{k}) = e^{i\phi(p,p')}e^{-pp'\boldsymbol{k}\cdot\boldsymbol{\nu}(p,p')}U(pp', \boldsymbol{k}). \tag{2.3.30}$$

The corresponding K-theory is the twisted equivariant K-theory. [81, 82]

3.5.2 Time-reversal symmetry and 'Real' and 'Quaternionic' K-theory

Consider the TRS

$$T\mathcal{H}(\boldsymbol{k})T^{-1} = \mathcal{H}(-\boldsymbol{k}),\ T^2 = \pm 1. \tag{2.3.31}$$

Here T is antiunitary. $T^2 = 1$ is class AI TRS and $T^2 = -1$ is class AII TRS. The above TRS induces an $\mathbb{Z}_2$ group action on the BZ:

$$E_{\boldsymbol{k}} \ni v \mapsto Tv \in E_{-\boldsymbol{k}}. \tag{2.3.32}$$

The corresponding K-theory is so called the Atiyah's 'Real' K-theory $KR(X,\tau)$ for class AI [87], and the 'Quaternionic' K-theory $KQ(X,\tau)$. [88] Here (X,τ) is a space with involution $\tau^2(x)=x$. [9]

3.5.3 Twisted equivariant K-theory

Topological insulators and superconductors protected by general symmetries are formulated by the twisted equivariant K-theory over BZ. [81, 82] In this formulation, the symmetries besides the symmorphic space group without nontrivial projective representations for internal degrees of freedom are accompanied with some twisting of group actions. The twisting informations are determined by ([81])

(i) $U(p,\boldsymbol{k})$ is unitary or antiunitary. Let us label it by the homomorphism $\phi: P\to\{\pm 1\}$:

$$U(p,\boldsymbol{k})z=\begin{cases} zU(p,\boldsymbol{k}), & \phi(p)=1 \text{ (unitary)} \\ z^*U(p,\boldsymbol{k}), & \phi(p)=-1 \text{ (antiunitary)} \end{cases} \tag{2.3.33}$$

(ii) $U(p,\boldsymbol{k})$ is symmetry or anti-symmetry. Let us label it by the homomorphism $c: P\to\{\pm 1\}$:

$$U(p,\boldsymbol{k})\mathcal{H}(\boldsymbol{k})U^{-1}(p,\boldsymbol{k})=c(p)\mathcal{H}(p\boldsymbol{k}), \tag{2.3.34}$$

(iii) The nontrivial phase in the successive symmetry group action:

$$U(p_1,p_2\boldsymbol{k})U(p_2,\boldsymbol{k})=e^{i\Phi(p_1,p_2;\boldsymbol{k})}U(p_1p_2,\boldsymbol{k}). \tag{2.3.35}$$

where the phase $e^{i\phi(p_1,p_2,\boldsymbol{k})}$ satisfies

$$e^{i\Phi(p_1,p_2;p_3\boldsymbol{k})}e^{i\Phi(p_1p_2,p_3;\boldsymbol{k})}=e^{i\phi(p_1)\Phi(p_2,p_3;\boldsymbol{k})}e^{i\Phi(p_1,p_2p_3;\boldsymbol{k})} \tag{2.3.36}$$

from the associativity condition

$$\{U(p_1,p_2p_3\boldsymbol{k})U(p_2,p_3\boldsymbol{k})\}U(p_3,\boldsymbol{k})=U(p_1,p_2p_3\boldsymbol{k})\{U(p_2,p_3\boldsymbol{k})U(p_3,\boldsymbol{k})\}. \tag{2.3.37}$$

For many symmetry classes, especially, nonsymmorphic space group and its combination with the TRS and PHS, the classification of topological insulators and superconductors have not yet been completed.

4 Altland-Zirnbauer symmetry class and extension problem of Clifford algebra

In this section, we consider the classification of 0-dimensional systems with the AZ symmetries. The symmetry constraints are represented by the Clifford algebra. The degrees of freedom of the symmetry-allowed 0-dimensional Hamiltonians $\mathcal{H}$ can be considered as the extension problem of the Clifford algebra, which counts how many ways the Clifford generators add to. [5, 67, 68] The extension problem defines the classifying spaces $\mathcal{C}_p$ and $\mathcal{R}_p$, which will be explained below. Disconnected parts of the classifying spaces give the classification of the topological insulators and superconductors in 0-dimension.

[9] Note that the 'Real' and 'Quaternionic' K-theory is different from the ordinary real K-theory $KO(X)$ and quaternionic K-theory $KSp(X)$ where the TRS locally act on the BZ: $T\mathcal{H}(\boldsymbol{k})T^{-1}=\mathcal{H}(\boldsymbol{k})$.

4.1 Complex AZ class

The complex Clifford algebra Cl_p is the algebra with $\mathbb{C}$ coefficient, and is generated by a set of generators $\{e_1, e_2, \ldots, e_p\}$ with anticommutation relation

$$\{e_i, e_j\} = e_i e_j + e_j e_i = 2\delta_{ij}. \tag{2.4.1}$$

The basis as a vector space are spanned by

$$e_1^{n_1} e_2^{n_2} \ldots e_p^{n_p}, \quad n_i = 0, 1. \tag{2.4.2}$$

Thus the dimension as a vector space is 2^p. [10]

Symmetry operators in complex AZ classes, namely no operator in class A and the chiral operator Γ in class AIII, can be considered as generators of the complex Clifford algebra, Cl_0 and Cl_1, respectively. Since a flattened Hamiltonian $\mathcal{H}$ satisfies $\mathcal{H}^2 = 1$, and it also anticommutes with Γ in class AIII, it extends the Clifford algebra as

$$Cl_p = \{e_1, e_2, \ldots, e_p\} \to Cl_{p+1} = \{\mathcal{H}, e_1, e_2, \ldots, e_p\}, \tag{2.4.3}$$

where $p = 0$ for class A and $p = 1$ for class AIII. ($Cl_0 = \{\emptyset\}$, $Cl_1 = \{e_1 = \Gamma\}$.) The set of possible maps from Cl_p to Cl_{p+1} defines the classifying space $\mathcal{C}_p$, which obeys the Bott periodicity

$$\mathcal{C}_p \simeq \mathcal{C}_{p+2}. \tag{2.4.4}$$

Let us see some examples of the extension problem.

For 0-dimensional class A systems, a Hamiltonian $\mathcal{H}$ has no symmetry, so the space C_0 is the same as the space of Hamiltonians, this is nothing but the classifying space $C_0 = \cup_{m\in\mathbb{Z}} \lim_{n\to\infty} \frac{U(2n)}{U(n+m)\times U(n-m)}$ previously introduced. We have $\pi_0(\mathcal{C}_0) = \mathbb{Z}$ which counts the difference of the occupied states between a pair of Hamiltonians $[\mathcal{H}_1] - [\mathcal{H}_2] \in KU(pt)$. So the 0-dimensional class A insulators are classified by $\mathbb{Z}$.

For 0-dimensional class AIII system, a Hamiltonian $\mathcal{H}$ has the CS, $\Gamma\mathcal{H}\Gamma = -\mathcal{H}$. The space C_1 is the same as the space of Hamiltonians preserving the CS. We can choose $\Gamma = \sigma_z = \begin{pmatrix} 1 & 0 \\ 0 & -1 \end{pmatrix}$, then Hamiltonians have the following forms,

$$\mathcal{H} = \begin{pmatrix} 0 & U_{n\times n} \\ U^\dagger_{n\times n} & 0 \end{pmatrix} \tag{2.4.5}$$

with $U_{n\times n} \in U(n)$. The space C_1 is the same as the infinite unitary group $C_1 = U = \lim_{n\to\infty} U(n)$. $\mathcal{C}_1$ does not have disconnected parts: $\pi_0(\mathcal{C}_1) = 0$, which means there is no nontrivial classification in 0-dimensional class AIII systems.

We can see an example of the Bott periodicity $C_2 \cong C_0$. Assume the Hamiltonian has two chiral symmetry $\Gamma_i\mathcal{H}\Gamma_i = -\mathcal{H}, (i = 1, 2)$ where Γ_1 and Γ_2 anticommute, $\{\Gamma_1, \Gamma_2\} = 0$. The space of symmetry preserving Hamiltonians is classifying space C_2 which is the degrees of freedom of the extension

$$\{\Gamma_1, \Gamma_2\} \to \{\mathcal{H}, \Gamma_1, \Gamma_2\}. \tag{2.4.6}$$

[10] Note that the basis $e_1^{n_1} e_2^{n_2} \ldots e_p^{n_p}$ must be independent. For Cl_3 case, $\{e_1 = \sigma_x, e_2 = \sigma_y, e_3 = \sigma_z\}$ satisfy the anticommutation relation, but is not independent because of $e_1 e_2 = i\sigma_z = ie_3$. An appropriate basis are $\{e_1 = \sigma_x \otimes 1, e_2 = \sigma_y \otimes 1, e_3 = \sigma_z \otimes \sigma_x\}$.

We can choose $\Gamma_1 = 1 \otimes \sigma_x, \Gamma_2 = 1 \otimes \sigma_y$ with $\{\sigma_x, \sigma_y\} = 0$, then the symmetry preserving Hamiltonian has the form

$$\mathcal{H} = \widetilde{\mathcal{H}} \otimes \sigma_0. \tag{2.4.7}$$

Thus, the space of symmetry preserving Hamiltonian $\mathcal{H}$ is the same as the space of the Hamiltonian $\widetilde{\mathcal{H}}$ which has no symmetry, i.e., the classifying space C_0.

In the same way, we can show the Bott periodicity $C_{n+2} \cong C_n$.

4.2 Real AZ class

The real Clifford algebra $Cl_{p,q}$ is the algebra with $\mathbb{R}$ coefficient, and is generated by a set of generators $\{e_1, e_2, \ldots, e_p; e_{p+1}, \ldots e_{p+q}\}$ with $\{e_i, e_j\} = 2\delta_{ij}(i \neq j)$, $e_i^2 = -1(i = 1, \ldots, p)$, and $e_i^2 = 1(i = p+1, \ldots, p+q)$. The basis as a vector space are spanned by

$$e_1^{n_1} e_2^{n_2} \ldots e_{p+q}^{n_{p+q}}, \quad n_i = 0, 1. \tag{2.4.8}$$

Thus the dimension of the vector space is 2^{p+q}.

Since the symmetry operators of the real AZ classes can be considered as generators of the real Clifford algebra, the classifying spaces of real AZ classes are derived by the counting the distinct symmetry-allowed 0-dimensional Hamiltonians $\mathcal{H}$, which defines the extension problem of the Clifford algebra:

$$Cl_{p,q} = \{e_1, \ldots, e_p; e_{p+1}, \ldots, e_{p+q}\} \to Cl_{p+1,q} = \{i\mathcal{H}, e_1, \ldots, e_p; e_{p+1}, \ldots, e_{p+q}\}, \tag{2.4.9}$$

or

$$Cl_{p,q} = \{e_1, \ldots, e_p; e_{p+1}, \ldots, e_{p+q}\} \to Cl_{p,q+1} = \{e_1, \ldots e_p; \mathcal{H}, e_{p+1}, \ldots, e_{p+q}\}. \tag{2.4.10}$$

The classifying space obtained in the former case is $\mathcal{R}_{p+2-q}$, and that obtained in the latter case is $\mathcal{R}_{q-p}$. The Bott periodicity implies $\mathcal{R}_p \simeq \mathcal{R}_{p+8}$.

In a way similar to the complex Clifford algebra, we can identify the classifying space $\mathcal{R}_p (p = 0, \ldots, 7)$ for the eight real AZ classes. The Tab. 2.2 show the extension problem and the classifying spaces for the AZ classes, and disconnected parts of the classifying spaces.

5 Dimensional shift of Hamiltonians

As explained in the last section, the 0-dimensional Hamiltonian with AZ symmetries are described as the extension problem of the Clifford algebra and classification is given by the counting disconnected part of the corresponding classifying space. In the next step, we would like to know topological classification of finite dimensional systems.

For general symmetry class and space dimensions, the topological classification may be very hard task. However, for some symmetry classes, we can construct a K-group isomorphism between different space dimensions. The following discussion is based on the Teo and Kane [11].

Table 2.2: AZ symmetry classes and their classifying spaces. The top two rows are complex AZ classes, and the bottom eight rows are real AZ classes. The first column represents the names of the AZ classes. The second and third columns indicate the extension of Clifford algebras. The fourth column shows classifying spaces $\mathcal{C}_s$ or $\mathcal{R}_s$ which is concretely written in the fifth column. [8, 9] The sixth column shows disconnected parts of the classifying spaces.

AZ class	Generator	Extension	$\mathcal{C}_s/\mathcal{R}_s$	classifying space	$\pi_0(\mathcal{C}_s)/\pi_0(\mathcal{R}_s)$
A	$\emptyset \to \{\mathcal{H}\}$	$Cl_0 \to Cl_1$	$\mathcal{C}_0$	$\cup_{m\in\mathbb{Z}} \lim_{n\to\infty} \frac{U(2n)}{U(n+m)\times U(n-m)}$	$\mathbb{Z}$
AIII	$\{\Gamma\} \to \{\mathcal{H}, \Gamma\}$	$Cl_1 \to Cl_2$	$\mathcal{C}_1$	$\lim_{n\to\infty} U(n)$	0
AI	$\{\emptyset; T, iT\} \to \{i\mathcal{H}; T, iT\}$	$Cl_{0,2} \to Cl_{1,2}$	$\mathcal{R}_0$	$\cup_{m\in\mathbb{Z}} \lim_{n\to\infty} \frac{O(2n)}{O(n+m)\times O(n-m)}$	$\mathbb{Z}$
BDI	$\{iCT; C, iC\} \to \{iCT; \mathcal{H}, C, iC\}$	$Cl_{1,2} \to Cl_{1,3}$	$\mathcal{R}_1$	$\lim_{n\to\infty} O(n)$	$\mathbb{Z}_2$
D	$\{\emptyset; C, iC\} \to \{\emptyset; \mathcal{H}, C, iC\}$	$Cl_{0,2} \to Cl_{0,3}$	$\mathcal{R}_2$	$\lim_{n\to\infty} \frac{O(2n)}{U(n)}$	$\mathbb{Z}_2$
DIII	$\{\emptyset; C, iC, iCT\} \to \{\emptyset; \mathcal{H}, C, iC, iCT\}$	$Cl_{0,3} \to Cl_{0,4}$	$\mathcal{R}_3$	$\lim_{n\to\infty} \frac{U(2n)}{Sp(n)}$	0
AII	$\{T, iT; \emptyset\} \to \{i\mathcal{H}, T, iT; \emptyset\}$	$Cl_{2,0} \to Cl_{3,0}$	$\mathcal{R}_4$	$\cup_{m\in\mathbb{Z}} \lim_{n\to\infty} \frac{Sp(2n)}{Sp(n+m)\times Sp(n-m)}$	$2\mathbb{Z}$
CII	$\{C, iC, iCT; \emptyset\} \to \{C, iC, iCT; \mathcal{H}\}$	$Cl_{3,0} \to Cl_{3,1}$	$\mathcal{R}_5$	$\lim_{n\to\infty} Sp(n)$	0
C	$\{C, iC; \emptyset\} \to \{C, iC; \mathcal{H}\}$	$Cl_{2,0} \to Cl_{2,1}$	$\mathcal{R}_6$	$\lim_{n\to\infty} \frac{Sp(n)}{U(n)}$	0
CI	$\{C, iC; iCT\} \to \{C, iC; \mathcal{H}, iCT\}$	$Cl_{2,1} \to Cl_{2,2}$	$\mathcal{R}_7$	$\lim_{n\to\infty} \frac{U(n)}{O(n)}$	0

5.1 Dimension-raising map

First we introduce the suspension which creates a one-higher dimensional space from a give space X. The suspension SX of the space X is defined by the quotient space

$$SX := (X \times I)/\{(x_1, 0) \sim (x_2, 0) \text{ and } (x_1, 1) \sim (x_2, 2) \text{ for all } x_1, x_2 \in X\}, \tag{2.5.1}$$

where $I = [0, 1]$ is the unit interval. Thus, X is stretched into a cylinder $X \times I$ and then both ends $(0, 1 \in I)$ are collapsed to points. See the Fig. 2.3 [a].

For a sphere $X = S^d$, the suspension is the one-higher dimensional sphere

$$SS^d = S^{d+1} \ (d \geq 0) \tag{2.5.2}$$

as shown in Fig. 2.3 [b]. Here S^0 is considered as two points $\{\pm 1\}$ which correspond to 0-dimensional systems. So we can construct any dimensional sphere by iteration of suspension from two points $S^0 = \{\pm 1\}$.

Let us introduce a map from a Hamiltonian on X, $\mathcal{H}(x)$ $(x \in X)$, to a Hamiltonian on the suspension SX. If the original Hamiltonian $\mathcal{H}(x)$ supports the CS Γ, then the map is

$$\mathcal{H}_{\rm nc}(x, \theta) = \sin\theta \mathcal{H}_{\rm c}(x) + \cos\theta\Gamma, \quad \theta \in [0, \pi]\,, \tag{2.5.3}$$

and if not, it is

$$\mathcal{H}_{\rm c}(x, \theta) = \sin\theta \mathcal{H}_{\rm nc}(x) \otimes \sigma_z + \cos\theta \mathbf{1} \otimes \sigma_y, \quad \theta \in [0, \pi]\,. \tag{2.5.4}$$

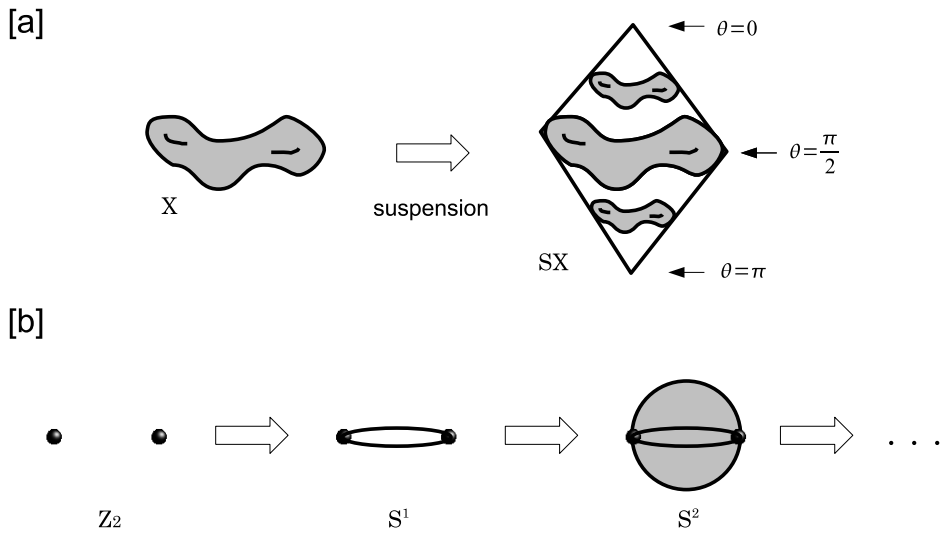

Figure 2.3: [a] Suspension SX of X. Two end points $0, 1 \in I$ are collapsed to points. [b] A sequence of suspensions for spheres.

Since the mapped Hamiltonian $\mathcal{H}(x, \theta)$ is independent of $x \in X$ at $\theta = 0$ and $\theta = \pi$, the base space $(x, \theta) \in S \times [0, \pi]$ of the mapped Hamiltonian can be identified as the suspension SX. The dimension-raising map interchanges a Hamiltonian with the CS and a Hamiltonian without the CS.

If the original Hamiltonian $\mathcal{H}(x)$ has symmetries $\{U(p, x)\}_{p\in P}$, these symmetries are also mapped to symmetries $\{\widetilde{U}(p, x)\}_{p\in P}$ on the suspension SX. Then, the maps (2.5.3) and (2.5.4) induce homomorphisms from the K-theory over X with symmetries $\{U(p, x)\}_{p\in P}$ to the K-theory over SX with symmetry $\{\widetilde{U}(p, x)\}_{p\in P}$. This homomorphism is not isomorphism in general. However, for special cases we can also construct the inverse homomorphism from SX to S. Especially, topological insulators and superconductors with the AZ class symmetries show isomorphism explained in subsection 6.4. An inverse map from the K-theory over SX to that over X is constructed in the next subsection.

5.2 Dimension-lowering map

A dimension-lowering map can be constructed as follows. Consider a Hamiltonian $\mathcal{H}(x, \theta)$ defined on a suspension SX of X. Here θ denotes unit interval $[0, \pi]$ of SX, which points the north pole (south pole) of SX at $\theta = 0$ ($\theta = \pi$), and x parametrizes X, so the Hamiltonian satisfies

$$\mathcal{H}(x, \theta = 0) = \text{const.}, \quad \mathcal{H}(x, \theta = \pi) = \text{const}', \tag{2.5.5}$$

By using continuous deformation, we can also flatten the Hamiltonian as

$$\mathcal{H}^2(x, \theta) = 1. \tag{2.5.6}$$

The above parametrization (x, θ) provides a natural dimensional reduction $SX \to X$ by fixing θ, say $\theta = \pi/2$. This procedure, however, does not ensure providing the inverse map of Eqs.(2.5.3) and (2.5.4), because the flattened Hamiltonian does not have the form of the right hand side of Eqs.(2.5.3) or (2.5.4) in general.

To fix the form of the flattened Hamiltonian, following Teo and Kane [11], we introduce an artificial "action" $S[\mathcal{H}]$ of the Hamiltonian,

$$S[\mathcal{H}] = \int dx d\theta \ \mathrm{Tr}[\partial_\theta \mathcal{H} \partial_\theta \mathcal{H}]. \tag{2.5.7}$$

By continuous deformation of the Hamiltonian, the value of action can reduce to reach its minimal value, where $\mathcal{H}$ satisfies the saddle point equation with the constraint of $\mathcal{H}^2 = 1$, i.e. $\partial_\theta^2 \mathcal{H} + \mathcal{H} = 0$. [11] Imposing the boundary condition (2.5.5), we can fix the form of the Hamiltonian as the saddle point solution,

$$\mathcal{H}(x, \theta) = \sin\theta \mathcal{H}_1(x) + \cos\theta \mathcal{H}_2, \tag{2.5.8}$$

where the flatness condition $\mathcal{H}^2(x, \theta) = 1$ implies

$$\mathcal{H}_1^2(x) = 1, \quad \mathcal{H}_2^2 = 1, \quad \{\mathcal{H}_1(x), \mathcal{H}_2\} = 0. \tag{2.5.9}$$

Then, by fixing $\theta = \pi/2$, we have a dimensional reduction from $\mathcal{H}(x, \theta)$ to $\mathcal{H}_1(x)$.

The last relation of Eq.(2.5.9) means that $\mathcal{H}_2$ act as CS on $\mathcal{H}_1(x)$. Therefore, if the original Hamiltonian $\mathcal{H}(x)$ does not support CS, Eq.(2.5.8) defines a dimensional reduction from non-chiral to chiral Hamiltonians. On the other hand, if the original Hamiltonian has CS Γ, then $\mathcal{H}_1(x)$ hosts a couple of CSs, Γ and $\mathcal{H}_2$, with $\{\Gamma, \mathcal{H}_2\} = 0$. Hence, $\mathcal{H}_1(x)$ has redundancy due to the commutation relation $[\mathcal{H}_1(x), \Gamma\mathcal{H}_2] = 0$. In the basis where $\Gamma = \mathbf{1} \otimes \sigma_x$ and $\mathcal{H}_2 = \mathbf{1} \otimes \sigma_y$, the redundancy of $\mathcal{H}_1(x)$ is resolved as $\mathcal{H}_1(x) = \mathcal{H}_3(x) \otimes \sigma_z$, and thus we obtain

$$\mathcal{H}(x, \theta) = \sin\theta \mathcal{H}_3(x) \otimes \sigma_z + \cos\theta \mathbf{1} \otimes \sigma_y \tag{2.5.10}$$

In this manner, a chiral Hamiltonian $\mathcal{H}(x, \theta)$ is mapped to a non-chiral one $\mathcal{H}_3(x)$.

6 Defect Hamiltonians and dimensional hierarchy of AZ classes

As explained in Sec. 5, topologically protected defect gapless states are classified by an adiabatic Hamiltonian

$$\mathcal{H}(\boldsymbol{k}, \boldsymbol{r}). \tag{2.6.1}$$

Here the base space of the Hamiltonian is composed of momentum $\boldsymbol{k}$, defined in the d-dimensional Brillouin zone T^d, and real-space coordinates $\boldsymbol{r}$ of a D-dimensional sphere S^D surrounding a defect. For instance, the Hamiltonian of a point defect in 3-dimensions is given by $\mathcal{H}(k_x, k_y, k_z, r_1, r_2)$, where (r_1, r_2) are the coordinates of a 2-dimensional sphere S^2 surrounding the point defect. Another example is a line defect in 3-dimensions, in which the Hamiltonian is $\mathcal{H}(k_x, k_y, k_z, r_1)$ where r_1 is a parameter of a circle S^1 enclosing the line defect. The case of $D = 0$ corresponds to a uniform system.

[11] This procedure is known as the Morse theory. [89]

As mentioned above, the exact base space is $T^d \times S^D$, but instead we consider a simpler space S^{d+D} in the following. This simplification does not affect on "strong" topological nature of the system. Although the difference of the base space may result in "weak" topological indices of the system, they can be obtained as"strong" topological indices in lower dimensions, as will be argued in section 6 in Chap. 3. Therefore, generality is not lost by the simplification.

6.1 Altland-Zirnbauer Symmetry Classes

The AZ symmetries, TRS, PHS, and CS, imply

$$\begin{aligned} &T\mathcal{H}(\boldsymbol{k},\boldsymbol{r})T^{-1} = \mathcal{H}(-\boldsymbol{k},\boldsymbol{r}), \\ &C\mathcal{H}(\boldsymbol{k},\boldsymbol{r})C^{-1} = -\mathcal{H}(-\boldsymbol{k},\boldsymbol{r}), \\ &\Gamma\mathcal{H}(\boldsymbol{k},\boldsymbol{r})\Gamma^{-1} = -\mathcal{H}(\boldsymbol{k},\boldsymbol{r}), \end{aligned} \tag{2.6.2}$$

respectively, where T and C are anti-unitary operators and Γ is a unitary operator.

Below, we choose a convention that T and C commutes with each other, i.e. $[T, C] = 0$: Because Eq.(2.6.2) yields $[TCT^{-1}C^{-1}, \mathcal{H}(\boldsymbol{k},\boldsymbol{r})] = 0$ for any Hamiltonians with TRS and PHS, the unitary operator $TCT^{-1}C^{-1}$ should be proportional to the identity, $TCT^{-1}C^{-1} = e^{i\beta}1$. The phase β can be removed by a re-definition of the relative phase between T and C without changing the sign of T^2 and C^2, which leads to $[T, C] = 0$.

We denote the K-group over S^{d+D} with the AZ symmetries (2.6.2) by

$$K_{\mathbb{C}}(s, d, D) \quad (s = 0, 1 \bmod 2) \tag{2.6.3}$$

for complex AZ classes and

$$K_{\mathbb{R}}(s, d, D) \quad (s = 0, \ldots 7 \bmod 8) \tag{2.6.4}$$

for real AZ classes. [12] Here s represents the AZ classes.

6.2 Dimension-raising map for defect Hamiltonians

Here we introduce a map from a Hamiltonian on a $(d + D)$-dimensional sphere $(\boldsymbol{k},\boldsymbol{r}) \in S^{d+D}$ to a Hamiltonian on S^{d+D+1} by suspension (2.5.3) and (2.5.4). If the original Hamiltonian $\mathcal{H}(\boldsymbol{k},\boldsymbol{r})$ supports CS Γ, then the map is

$$\mathcal{H}_{\rm nc}(\boldsymbol{k},\boldsymbol{r},\theta) = \sin\theta\mathcal{H}_{\rm c}(\boldsymbol{k},\boldsymbol{r}) + \cos\theta\Gamma, \quad \theta \in [0,\pi]\,, \tag{2.6.5}$$

and if not, it is

$$\begin{aligned} &\mathcal{H}_{\rm c}(\boldsymbol{k},\boldsymbol{r},\theta) = \sin\theta\mathcal{H}_{\rm nc}(\boldsymbol{k},\boldsymbol{r}) \otimes \sigma_z + \cos\theta\mathbf{1} \otimes \sigma_y, \quad \theta \in [0,\pi]\,. \\ &\{\Gamma\mathcal{H}(\boldsymbol{k})\} = 0, \quad \Gamma = \sigma_x. \end{aligned} \tag{2.6.6}$$

The dimension-raising map interchanges a Hamiltonian with CS and a Hamiltonian without CS.

[12] Strictly speaking, the K-groups (2.6.3) and (2.6.4) are the reduced K-theory introduced in (2.3.17) which omits obvious 0-dimensional K-group.

6.3 Dimension-lowering map for defect Hamiltonians

A dimension-lowering map $S^{d+D+1} \to S^{d+D}$ can be constructed by the way in subsection 5.2:

$$\mathcal{H}(\boldsymbol{k}, \boldsymbol{r}, \theta) = \sin\theta \mathcal{H}_1(\boldsymbol{k}, \boldsymbol{r}) + \cos\theta \mathcal{H}_2, \tag{2.6.7}$$

with

$$\mathcal{H}_1^2(\boldsymbol{k}, \boldsymbol{r}) = 1, \quad \mathcal{H}_2^2 = 1, \quad \{\mathcal{H}_1(\boldsymbol{k}, \boldsymbol{r}), \mathcal{H}_2\} = 0. \tag{2.6.8}$$

Then, by fixing $\theta = \pi/2$, we have a dimensional reduction from $\mathcal{H}(\boldsymbol{k}, \boldsymbol{r}, \theta)$ to $\mathcal{H}_1(\boldsymbol{k}, \boldsymbol{r})$

If the original Hamiltonian $\mathcal{H}(\boldsymbol{k}, \boldsymbol{r})$ does not support CS, Eq.(2.6.7) defines a dimensional reduction from non-chiral to chiral Hamiltonians. If the original Hamiltonian has CS $\Gamma = \mathbf{1} \otimes \sigma_x$, we obtain

$$\mathcal{H}(\boldsymbol{k}, \boldsymbol{r}, \theta) = \sin\theta \mathcal{H}_3(\boldsymbol{k}, \boldsymbol{r}) \otimes \tau_z + \cos\theta \mathbf{1} \otimes \tau_y, \tag{2.6.9}$$

and a chiral Hamiltonian $\mathcal{H}(\boldsymbol{k}, \boldsymbol{r}, \theta)$ is mapped to a non-chiral one $\mathcal{H}_3(\boldsymbol{k}, \boldsymbol{r})$.

6.4 Dimensional hierarchy of AZ classes

In this section, we review the topological classification for AZ symmetry classes.[4, 5, 11] We provide the periodic table for the topological insulator and superconductor by using the K-group isomorphic map between different dimensions and symmetries. Following Teo and Kane [11], we argue the dimensional hierarchy of the K-groups,

$$K_{\mathbb{C}}(s, d, D) = K_{\mathbb{C}}(s+1, d+1, D) = K_{\mathbb{C}}(s+1, d, D+1) \tag{2.6.10}$$

for complex AZ classes and

$$K_{\mathbb{R}}(s, d, D) = K_{\mathbb{R}}(s+1, d+1, D) = K_{\mathbb{R}}(s-1, d, D+1) \tag{2.6.11}$$

for real AZ classes. We prove (2.6.10) and (2.6.11) below. For topological insulators and superconductors in ten AZ symmetry classes, the following relations summarize their classification [5, 6, 11]

$$K_{\mathbb{C}}(s; d, D) = K_{\mathbb{C}}(s-d+D; 0, 0) = \pi_0(\mathcal{C}_{s-d+D}), \quad (s = 0, 1 \,(\mathrm{mod}\ 2)) \tag{2.6.12}$$

$$K_{\mathbb{R}}(s; d, D) = K_{\mathbb{R}}(s-d+D; 0, 0) = \pi_0(\mathcal{R}_{s-d+D}), \quad (s = 0, 1, \cdots, 7 \,(\mathrm{mod}\ 8)) \tag{2.6.13}$$

where $\mathcal{C}_s$ ($\mathcal{R}_s$) is the classifying space of s complex (real) AZ class in Table 2.2. The case of $D = 0$ corresponds to the bulk topological classification, and the presence of topological defects shifts the dimension of the system. (2.6.12) and (2.6.13) provide the periodic table of topological insulators and superconductors (Tab. 2.4). [4, 5, 6, 11]

6.4.1 Complex AZ classes

The complex AZ classes consist of two symmetry class, class A for Hamiltonians with no symmetry and class AIII for those with the presence of CS. The symmetry classes are labeled by $s = 0, 1 \,(\mathrm{mod}\ 2)$ as in Table 2.2. For the complex AZ classes, because of the absence of antiunitary symmetry, momentum $\boldsymbol{k}$ and coordinates $\boldsymbol{r}$ are not distinguished from each other, and thus $K_{\mathbb{C}}(s, d, D) = K_{\mathbb{C}}(s, d+D, 0)$.

The dimensional raising maps, Eqs. (2.6.5) and (2.6.6), interchange Hamiltonians with CS and those without CS, and thus they define a K-group homomorphism $K_{\mathbb{C}}(s, d+D, 0) \mapsto K_{\mathbb{C}}(s+1, d+D+1, 0)$, where s is also shifted by 1. At the same time, the dimensional lowering maps, Eqs. (2.6.7) and (2.6.9) define the inverse of the K-group homomorphism, i.e. $K_{\mathbb{C}}(s+1; d+D+1, 0) \mapsto K_{\mathbb{C}}(s; d+D, 0)$. Consequently, we obtain the K-group isomorphism Eq.(2.6.10).

6.4.2 Real AZ classes

The real AZ classes consist of eight symmetry classes which specified by the presence of TRS and/or PHS. The eight symmetry classes are labeled by $s = 0, \ldots, 7 \pmod 8$ as shown in Table 2.2. In this paper, we take a convention that T and C commute with each other: $[T, C] = 0$. In this rule, the chiral operator Γ (that is a Hermitian matrix) is given by

$$\Gamma = \begin{cases} TC & (s = 1, 5) \\ iTC & (s = 3, 7) \end{cases} , \tag{2.6.14}$$

where the following relation holds,

$$T\Gamma T^{-1} = C\Gamma C^{-1} = \begin{cases} \Gamma & (s = 1, 5) \\ -\Gamma & (s = 3, 7) \end{cases} . \tag{2.6.15}$$

For real AZ classes hosting CS ($s = 1, 3, 5, 7$), one can raise the dimension of the base space by using Eq.(2.6.5). The mapped Hamiltonian $\mathcal{H}(\boldsymbol{k}, \boldsymbol{r}, \theta)$ supports either TRS or PHS, but does not have both. The remaining symmetry depends on the type of θ one considers: If one increases the dimension d of the momentum space, the parameter θ should transform as $\theta \to \pi - \theta$ under TRS and PHS. In contrast, if one raises the dimension D of the position space, θ does not transform under these symmetries. We call the former θ as $\boldsymbol{k}$-type, and the latter as $\boldsymbol{r}$-type. The difference in the transformation law of θ results in the difference of the remaining symmetry. For instance, consider the BDI class ($s = 1$) and $\boldsymbol{k}$-type θ. In this case, because of Eq.(2.6.15), one finds that the mapped Hamiltonian, $\mathcal{H}(\boldsymbol{k}, \boldsymbol{r}, \theta) = \sin\theta\mathcal{H}(\boldsymbol{k}, \boldsymbol{r}) + \cos\theta(TC)$, supports PHS. For real AZ classes without CS ($s = 0, 2, 4, 6$), the dimensional raising map is provided by Eq.(2.6.6). The mapped Hamiltonian $\mathcal{H}(\boldsymbol{k}, \boldsymbol{r}, \theta)$ has the CS, $\{\mathbf{1} \otimes \sigma_x, \mathcal{H}(\boldsymbol{k}, \boldsymbol{r}, \theta)\} = 0$. It also realizes TRS or PHS of the original Hamiltonian $\mathcal{H}(\boldsymbol{k}, \boldsymbol{r})$, in the form of $T \otimes \sigma_a$ or $C \otimes \sigma_a$, where the choice of σ_a ($a = 0, z$) depends on the type of θ. The mapped Hamiltonian also has the rest of AZ symmetries, which is obtained by combination of these symmetries.

We summarize the AZ symmetries of the mapped Hamiltonian for each real AZ class in the lower part of Table 2.3. From this table, one finds that the dimensional raising maps, Eqs. (2.6.5) and (2.6.6), shift the label s of AZ classes by ± 1, and thus they define K-group homomorphic maps, $K_{\mathrm{R}}(s, d, D) \mapsto K_{\mathrm{R}}(s+1, d+1, D)$ and $K_{\mathrm{R}}(s, d, D) \mapsto K_{\mathrm{R}}(s-1, d, D+1)$.

In a manner similar to complex AZ classes, the dimensional lowering maps, Eqs. (2.6.7) and (2.6.9), define the inverse of the K-group homomorphism, $K_{\mathrm{R}}(s+1, d+1, D) \mapsto K_{\mathrm{R}}(s, d, D)$ and $K_{\mathrm{R}}(s-1, d, D+1) \mapsto K_{\mathrm{R}}(s, d, D)$: Here note that Eqs. (2.6.7) and (2.6.9) determine uniquely how TRS and/or PHS of higher dimensional Hamiltonians act on the lower dimensional ones. As a result, we have the K-group isomorphism, Eq.(2.6.11).

Table 2.3: Isomorphism from $K_{\mathbb{R}}(s,d,D)$ to $K_{\mathbb{F}}(s+1,d+1,D)$ and $K_{\mathbb{F}}(s-1,d,D+1)$, ($\mathbb{F}=\mathbb{C},\mathbb{R}$).

AZ class	Hamiltonian mapping	Type of θ	Mapped AZ class	TRS	PHS	Chiral
A	$\sin\theta\mathcal{H}(\boldsymbol{k},\boldsymbol{r})\otimes\sigma_z+\cos\theta\mathbf{1}\otimes\sigma_y$	$\boldsymbol{k}/\boldsymbol{r}$	AIII			$\mathbf{1}\otimes\sigma_x$
AIII	$\sin\theta\mathcal{H}(\boldsymbol{k},\boldsymbol{r})+\cos\theta\Gamma$	$\boldsymbol{k}/\boldsymbol{r}$	A			
AI/AII	$\sin\theta\mathcal{H}(\boldsymbol{k},\boldsymbol{r})\otimes\sigma_z+\cos\theta\mathbf{1}\otimes\sigma_y$	$\boldsymbol{k}$	BDI/CII	$T\otimes\sigma_0$	$T\otimes\sigma_x$	$\mathbf{1}\otimes\sigma_x$
		$\boldsymbol{r}$	CI/DIII	$T\otimes\sigma_z$	$T\otimes\sigma_y$	$\mathbf{1}\otimes\sigma_x$
BDI/CII	$\sin\theta\mathcal{H}(\boldsymbol{k},\boldsymbol{r})+\cos\theta(TC)$	$\boldsymbol{k}$	D/C		C	
		$\boldsymbol{r}$	AI/AII	T		
D/C	$\sin\theta\mathcal{H}(\boldsymbol{k},\boldsymbol{r})\otimes\sigma_z+\cos\theta\mathbf{1}\otimes\sigma_y$	$\boldsymbol{k}$	DIII/CI	$C\otimes\sigma_y$	$C\otimes\sigma_z$	$\mathbf{1}\otimes\sigma_x$
		$\boldsymbol{r}$	BDI/CII	$C\otimes\sigma_x$	$C\otimes\sigma_0$	$\mathbf{1}\otimes\sigma_x$
DIII/CI	$\sin\theta\mathcal{H}(\boldsymbol{k},\boldsymbol{r})+\cos\theta(iTC)$	$\boldsymbol{k}$	AII/AI	T		
		$\boldsymbol{r}$	D/C		C	

7 Topological invariants

In this section, we summarize the notation and the definition of topological invariants used in this thesis.

7.1 Topological invariants in zero-dimension

Here, we introduce topological invariants in zero dimension. A Hamiltonian $\mathcal{H}$ in zero dimension is merely a constant matrix, so adding extra trivial bands to the Hamiltonian makes any change of the Hamiltonian possible. This means that no well-defined topological number of a single Hamiltonian is possible in the meaning of the stable-equivalence. We need a couple of Hamiltonians $(\mathcal{H}_+,\mathcal{H}_-)$ to define a topological number. We say that two coupled Hamiltonians, $(\mathcal{H}_{1+},\mathcal{H}_{1-})$ and $(\mathcal{H}_{2+},\mathcal{H}_{2-})$, are stable equivalent if they are continuously deformed into each other by adding the *same* extra bands to the coupled Hamiltonian. In other words, the stable equivalence implies $(\mathcal{H}_+,\mathcal{H}_-)\sim(\mathcal{H}_+\oplus\mathcal{H}_{\rm ext},\mathcal{H}_-\oplus\mathcal{H}_{\rm ext})$ with an extra band $\mathcal{H}_{\rm ext}$.

7.1.1 $\mathbb{Z}$ ($2\mathbb{Z}$) invariant

First, consider non particle-hole symmetric Hamiltonians. We assume here that $\mathcal{H}_+$ and $\mathcal{H}_-$ have the same matrix dimension. Denoting the numbers of empty (occupied) states of $\mathcal{H}_\pm$ by $n_\pm$ ($m_\pm$), the topological nature of the coupled Hamiltonians can be characterized by n_+-m_+ and n_--m_- since there appears a band crossing the Fermi level when these numbers are changed. Adding trivial p empty bands and q occupied ones to the coupled Hamiltonian, we also have the stable equivalence

Table 2.4: Topological periodic table for topological insulators and superconductors.[4, 5, 11] The superscripts on $\mathbb{Z}$ and $\mathbb{Z}_2$ specify the integral representation of the corresponding topological indices. $\mathbb{Z}^{(\mathrm{Ch})}$ and $\mathbb{Z}^{(\mathrm{W})}$ are given by the Chern number Eq.(2.7.7) and the winding number Eq.(2.7.12), respectively. $\mathbb{Z}_2^{(\mathrm{CS})}$ and $\mathbb{Z}_2^{(\mathrm{CS_T})}$ represent the Chern-Simons integral Eq.(2.7.18) without and with the time-reversal constraint Eq.(2.7.22), respectively. $\mathbb{Z}_2^{(\mathrm{FK})}$ denotes the Fu-Kane invariant Eq.(2.7.21). The $\mathbb{Z}_2$ invariants without any superscript are not expressed by these integrals, but they can be defined operationally by the dimensional reduction or the Moore-Balents argument.

AZ class	TRS	PHS	CS	$\mathcal{C}_s$ or $\mathcal{R}_s$	$\delta=0$	$\delta=1$	$\delta=2$	$\delta=3$	$\delta=4$	$\delta=5$	$\delta=6$	$\delta=7$
A	0	0	0	$\mathcal{C}_0$	$\mathbb{Z}^{(\mathrm{Ch})}$	0	$\mathbb{Z}^{(\mathrm{Ch})}$	0	$\mathbb{Z}^{(\mathrm{Ch})}$	0	$\mathbb{Z}^{(\mathrm{Ch})}$	0
AIII	0	0	1	$\mathcal{C}_1$	0	$\mathbb{Z}^{(\mathrm{W})}$	0	$\mathbb{Z}^{(\mathrm{W})}$	0	$\mathbb{Z}^{(\mathrm{W})}$	0	$\mathbb{Z}^{(\mathrm{W})}$
AI	1	0	0	$\mathcal{R}_0$	$\mathbb{Z}^{(\mathrm{Ch})}$	0	0	0	$2\mathbb{Z}^{(\mathrm{Ch})}$	0	$\mathbb{Z}_2^{(\mathrm{FK})}$	$\mathbb{Z}_2^{(\mathrm{CS})}$
BDI	1	1	1	$\mathcal{R}_1$	$\mathbb{Z}_2$	$\mathbb{Z}^{(\mathrm{W})}$	0	0	0	$2\mathbb{Z}^{(\mathrm{W})}$	0	$\mathbb{Z}_2$
D	0	1	0	$\mathcal{R}_2$	$\mathbb{Z}_2$	$\mathbb{Z}_2^{(\mathrm{CS})}$	$\mathbb{Z}^{(\mathrm{Ch})}$	0	0	0	$2\mathbb{Z}^{(\mathrm{Ch})}$	0
DIII	-1	1	1	$\mathcal{R}_3$	0	$\mathbb{Z}_2^{(\mathrm{CS_T})}$	$\mathbb{Z}_2^{(\mathrm{FK})}$	$\mathbb{Z}^{(\mathrm{W})}$	0	0	0	$2\mathbb{Z}^{(\mathrm{W})}$
AII	-1	0	0	$\mathcal{R}_4$	$2\mathbb{Z}^{(\mathrm{Ch})}$	0	$\mathbb{Z}_2^{(\mathrm{FK})}$	$\mathbb{Z}_2^{(\mathrm{CS})}$	$\mathbb{Z}^{(\mathrm{Ch})}$	0	0	0
CII	-1	-1	1	$\mathcal{R}_5$	0	$2\mathbb{Z}^{(\mathrm{W})}$	0	$\mathbb{Z}_2$	$\mathbb{Z}_2$	$\mathbb{Z}^{(\mathrm{W})}$	0	0
C	0	-1	0	$\mathcal{R}_6$	0	0	$2\mathbb{Z}^{(\mathrm{Ch})}$	0	$\mathbb{Z}_2$	$\mathbb{Z}_2^{(\mathrm{CS})}$	$\mathbb{Z}^{(\mathrm{Ch})}$	0
CI	1	-1	1	$\mathcal{R}_7$	0	0	0	$2\mathbb{Z}^{(\mathrm{W})}$	0	$\mathbb{Z}_2^{(\mathrm{CS_T})}$	$\mathbb{Z}_2^{(\mathrm{FK})}$	$\mathbb{Z}^{(\mathrm{W})}$

between these numbers,

$$(n_+ - m_+, n_- - m_-) \sim (n_+ - m_+ + p - q, n_- - m_- + p - q). \tag{2.7.1}$$

Therefore, the topological number in zero dimension is defined as

$$Ch_0 := \frac{n_+ - m_+ - n_- + m_-}{2}, \tag{2.7.2}$$

because it should be invariant under the stable equivalence. Whereas Ch_0 can take any integer for class A and AI Hamiltonians, it takes only an even integer for class AII due to the Kramers degeneracy of the spectrum.

7.1.2 $\mathbb{Z}_2$ invariant

For Hamiltonians with PHS satisfying $C^2 = 1$, the following $\mathbb{Z}_2$ invariant can be introduced

$$\nu_0 = \mathrm{sgn}\left[\mathrm{Pf}(\mathcal{H}_+\tau_x)\right] \mathrm{sgn}\left[\mathrm{Pf}(\mathcal{H}_-\tau_x)\right], \tag{2.7.3}$$

with $C = \tau_x\mathcal{K}$: First, PHS implies $\mathcal{H}_\pm\tau_x = -(\mathcal{H}_\pm\tau_x)^T$, which enables us to define the Pfaffian of $\mathcal{H}_\pm\tau_x$. Then, from the relation

$$[\mathrm{Pf}(\mathcal{H}_\pm\tau_x)]^* = \mathrm{Pf}(\mathcal{H}_\pm^*\tau_x) = \mathrm{Pf}(\tau_x^T(\mathcal{H}_\pm\tau_x)^T\tau_x) = \mathrm{Pf}(\mathcal{H}_\pm\tau_x) \tag{2.7.4}$$

the sign of $\mathrm{Pf}(\mathcal{H}_{\pm}\tau_x)$ is quantized as ± 1. Taking into account the stable equivalence, we find that each of $\mathrm{Pf}(\mathcal{H}_{\pm}\tau_x)$ does not give a $\mathbb{Z}_2$ invariant, but their product ν_0 defines it.

In AZ classes, BDI and D in zero dimension support this $\mathbb{Z}_2$ invariant. Class DIII also has PHS with $C^2 = 1$, but ν_0 becomes trivial in this case because of the Kramers degeneracy.

7.2 Chern number and winding number

Here we summarize the analytic expressions of integer $\mathbb{Z}$ topological invariants, i.e. the Chern numbers in even-dimensions, and the winding numbers in odd-dimensions.

7.2.1 Q-function

It is useful to introduce the so called "Q-function"[4] defined by

$$Q(\boldsymbol{k},\boldsymbol{r}) = \sum_{E_\alpha(\boldsymbol{k},\boldsymbol{r})>E_{\mathrm{F}}} |u_\alpha(\boldsymbol{k},\boldsymbol{r})\rangle \langle u_\alpha(\boldsymbol{k},\boldsymbol{r})| - \sum_{E_\alpha(\boldsymbol{k},\boldsymbol{r})<E_{\mathrm{F}}} |u_\alpha(\boldsymbol{k},\boldsymbol{r})\rangle \langle u_\alpha(\boldsymbol{k},\boldsymbol{r})|, \tag{2.7.5}$$

where $|u_\alpha(\boldsymbol{k},\boldsymbol{r})\rangle$ is an eigenstate of $\mathcal{H}(\boldsymbol{k},\boldsymbol{r})$ with an eigen energy $E_\alpha(\boldsymbol{k},\boldsymbol{r})$. The Q-function is nothing but the flattened Hamiltonian of $\mathcal{H}(\boldsymbol{k})$, and it has the following properties:

$$Q^2(\boldsymbol{k},\boldsymbol{r}) = 1, \quad Q(\boldsymbol{k},\boldsymbol{r})\,|u_\alpha(\boldsymbol{k},\boldsymbol{r})\rangle = \begin{cases} |u_\alpha(\boldsymbol{k},\boldsymbol{r})\rangle, & (E_\alpha(\boldsymbol{k},\boldsymbol{r}) > E_{\mathrm{F}}) \\ -|u_\alpha(\boldsymbol{k},\boldsymbol{r})\rangle, & (E_\alpha(\boldsymbol{k},\boldsymbol{r}) < E_{\mathrm{F}}) \end{cases}. \tag{2.7.6}$$

The symmetry of the Q-function is the same as the original Hamiltonian $\mathcal{H}(\boldsymbol{k},\boldsymbol{r})$.

7.2.2 Chern number

In the $2n$-dimensional base space, the n-th Chern number Ch_n is defined by

$$Ch_n = \frac{1}{n!}\left(\frac{i}{2\pi}\right)^n \int \mathrm{tr}\mathcal{F}^n, \tag{2.7.7}$$

with $\mathcal{F} = d\mathcal{A} + \mathcal{A}\wedge\mathcal{A}$. Here $\mathcal{A}_{\alpha\beta} = \langle u_\alpha | du_\beta\rangle$ is the connection of occupied states $|u_\alpha(\boldsymbol{k},\boldsymbol{r})\rangle$ of $\mathcal{H}(\boldsymbol{k},\boldsymbol{r})$, and the trace is taken for all occupied states. The Chern number is rewritten as

$$Ch_n = -\frac{1}{2^{2n+1}}\frac{1}{n!}\left(\frac{i}{2\pi}\right)^n \int \mathrm{tr}Q(dQ)^{2n}. \tag{2.7.8}$$

It is also useful to express the Chern number in terms of the Green function,[90] $G(\omega,\boldsymbol{k},\boldsymbol{r}) = [i\omega - \mathcal{H}(\boldsymbol{k},\boldsymbol{r})]^{-1}$, when we discuss the electromagnetic and/or heat responses. The Chern number is recast into

$$Ch_n = -\frac{n!}{(2\pi i)^{n+1}\,(2n+1)!}\int \mathrm{tr}\left[GdG^{-1}\right]^{2n+1}. \tag{2.7.9}$$

Although the Chern number can be defined in any even dimensions, symmetry of the system sometimes prohibits a non-zero Chern number. For example, consider an antiunitary symmetry

$$A\mathcal{H}(\boldsymbol{k}_\parallel,\boldsymbol{k}_\perp)A^{-1} = \mathcal{H}(\boldsymbol{k}_\parallel,-\boldsymbol{k}_\perp). \tag{2.7.10}$$

Since the Q-function has the same symmetry, $AQ(\boldsymbol{k}_\parallel, \boldsymbol{k}_\perp)A^{-1} = Q(\boldsymbol{k}_\parallel, -\boldsymbol{k}_\perp)$, we find

$$\begin{aligned} Ch_n &= -\frac{1}{2^{2n+1}}\frac{1}{n!}\left(\frac{i}{2\pi}\right)^n \int \mathrm{tr}\left[A^{-1}Q(\boldsymbol{k}_\parallel, -\boldsymbol{k}_\perp)dQ(\boldsymbol{k}_\parallel, -\boldsymbol{k}_\perp)^{2n}A\right] \\ &= -\frac{1}{2^{2n+1}}\frac{1}{n!}\left(\frac{i}{2\pi}\right)^n \int \mathrm{tr}\left[Q^*(\boldsymbol{k}_\parallel, -\boldsymbol{k}_\perp)dQ^*(\boldsymbol{k}_\parallel, -\boldsymbol{k}_\perp)^{2n}\right] \\ &= -\frac{(-1)^{2n-d_\parallel}}{2^{2n+1}}\frac{1}{n!}\left(\frac{i}{2\pi}\right)^n \int \mathrm{tr}\left[Q^*(\boldsymbol{k})dQ^*(\boldsymbol{k})^{2n}\right] \\ &= (-1)^{n-d_\parallel}Ch_n^*. \\ &= (-1)^{n-d_\parallel}Ch_n, \end{aligned} \tag{2.7.11}$$

where we have used the fact that Ch_n is an integer in the last line. The above equation yields $Ch_n = 0$ if $n = d_\parallel + 1 \pmod 2$.

7.2.3 Winding number

In the $2n+1$-dimensional base space, the winding number is defined by,

$$N_{2n+1} = \frac{n!}{2(2\pi i)^{n+1}(2n+1)!}\int \mathrm{tr}\Gamma\left(\mathcal{H}^{-1}d\mathcal{H}\right)^{2n+1}, \tag{2.7.12}$$

if the Hamiltonian $\mathcal{H}(\boldsymbol{k}, \boldsymbol{r})$ has CS, $\Gamma\mathcal{H}(\boldsymbol{k}, \boldsymbol{r})\Gamma^{-1} = -\mathcal{H}(\boldsymbol{k}, \boldsymbol{r})$. Equivalently, the winding number (2.7.12) is expressed by the Q-function,

$$N_{2n+1} = \frac{(-1)^n n!}{2(2\pi i)^{n+1}(2n+1)!}\int \mathrm{tr}\Gamma Q\left(dQ\right)^{2n+1}. \tag{2.7.13}$$

In the diagonal base of $\Gamma = \mathrm{diag}(1, -1)$, the Q-function is off-diagonal,

$$Q(\boldsymbol{k}, \boldsymbol{r}) = \begin{pmatrix} 0 & q(\boldsymbol{k}, \boldsymbol{r}) \\ q^\dagger(\boldsymbol{k}, \boldsymbol{r}) & 0 \end{pmatrix}, \tag{2.7.14}$$

so the winding number N_{2n+1} is simplified as

$$N_{2n+1} = \frac{n!}{(2\pi i)^{n+1}(2n+1)!}\int \mathrm{tr}\left[qdq^\dagger\right]^{2n+1}. \tag{2.7.15}$$

In a manner similar to the Chern numbers, symmetry of the system sometimes prohibits a non-zero winding number. For example, the antiunitary symmetry in Eq.(2.7.10) leads

$$\begin{aligned} N_{2n+1} &= \frac{(-1)^n n!}{2(2\pi i)^{n+1}(2n+1)!}\int \mathrm{tr}\left[\Gamma A^{-1}Q(\boldsymbol{k}_\parallel, -\boldsymbol{k}_\perp)dQ(\boldsymbol{k}_\parallel, -\boldsymbol{k}_\perp)^{2n+1}A\right] \\ &= \frac{\eta_\Gamma(-1)^n n!}{2(2\pi i)^{n+1}(2n+1)!}\int \mathrm{tr}\left[\Gamma Q^*(\boldsymbol{k}_\parallel, -\boldsymbol{k}_\perp)dQ^*(\boldsymbol{k}_\parallel, -\boldsymbol{k}_\perp)^{2n+1}\right] \\ &= \frac{\eta_\Gamma(-1)^{2n+1-d_\parallel}(-1)^n n!}{2(2\pi i)^{n+1}(2n+1)!}\int \mathrm{tr}\left[\Gamma Q^*(\boldsymbol{k})dQ^*(\boldsymbol{k})^{2n+1}\right] \\ &= (-1)^{n-d_\parallel}\eta_\Gamma N_{2n+1}^* \\ &= (-1)^{n-d_\parallel}\eta_\Gamma N_{2n+1}, \end{aligned} \tag{2.7.16}$$

where $\eta_\Gamma = \pm$ specifies the commutation(+) or anti-commutation(-) relation between Γ and A. Hence, $N_{2n+1} = 0$ when $n = d_\parallel + (\eta_\Gamma - 1)/2 \pmod 2$.

7.2.4 $2\mathbb{Z}$ topological invariant

In the real AZ classes, there are two integer K-groups, $K_{\mathbb{R}}(s;d,D) = \mathbb{Z}$ for $s = d - D \pmod 8$ and $K_{\mathbb{R}}(s;d,D) = 2\mathbb{Z}$ for $s = d - D + 4 \pmod 8$, where "$2\mathbb{Z}$" means that the corresponding Chern number defined by Eq.(2.7.7) or the winding number defined by Eq.(2.7.12)) takes an even integer. Here, we outline the proof why the topological number becomes even when $s = d - D + 4 \pmod 8$ and $d \geq 1$.

Consider a Hamiltonian $\mathcal{H}(\boldsymbol{k}, \boldsymbol{r})$ in real AZ class with $s = d - D + 4 \pmod 8$. Choosing one of the momenta as the polar angle θ of the base space S^{d+D} and denoting the rest momenta by $\boldsymbol{k}'$, AZ symmetries are expressed as $T\mathcal{H}(\theta, \boldsymbol{k}', \boldsymbol{r})T^{-1} = \mathcal{H}(\pi - \theta, -\boldsymbol{k}', \boldsymbol{r})$, $C\mathcal{H}(\theta, \boldsymbol{k}', \boldsymbol{r})C^{-1} = -\mathcal{H}(\pi - \theta, -\boldsymbol{k}', \boldsymbol{r})$, and $\Gamma\mathcal{H}(\theta, \boldsymbol{k}', \boldsymbol{r})\Gamma^{-1} = -\mathcal{H}(\theta, \boldsymbol{k}', \boldsymbol{r})$. Thus, the Hamiltonian on the equator, $\mathcal{H}(\theta = \pi/2, \boldsymbol{k}', \boldsymbol{r})$, retains all the AZ symmetries that the original Hamiltonian $\mathcal{H}(\boldsymbol{k}, \boldsymbol{r})$ has. Furthermore, the equator Hamiltonian is found to be topologically trivial, since its K-group is given as $K_{\mathbb{R}}(s; d - 1, D) = K_{\mathbb{R}}(s - d + 1 + D; 0, 0) = \pi_0(\mathcal{R}_5) = 0$ when $s = d - D + 4 \pmod 8$. This means that we can pinch the $(d + D)$-dimensional sphere S^{d+D} on the equator by deforming the equator Hamiltonian into a constant Hamiltonian without breaking the symmetries.

After the pinching, the north and south hemispheres turn into a couple of $(d + D)$-dimensional spheres S^{d+D}, and the original Hamiltonian reduces to a couple of Hamiltonians in complex AZ class with the same $s = d - D + 4 \pmod 8$. Since their K-groups obey $K_{\mathbb{C}}(s; d, D) = K_{\mathbb{C}}(s - d + D; 0, 0) = \pi_0(\mathcal{C}_4) = \mathbb{Z}$, the couple of Hamiltonian have definite integer topological numbers $N_{\rm north}$ and $N_{\rm south}$, which are defined by Eq. (2.7.7) or Eq. (2.7.12). These topological numbers, however, are not independent. Because TRS and/or PHS in the original Hamiltonian exchange the north and south hemispheres, $N_{\rm north}$ and $N_{\rm south}$ must be the same. Consequently, the topological number of the original Hamiltonian, which is given by the sum of $N_{\rm north}$ and $N_{\rm south}$, must be even,

7.3 $\mathbb{Z}_2$ topological invariant

In this appendix we summarize various arguments and formulas to define $\mathbb{Z}_2$ invariants. i.e. the dimensional reduction,[13, 6] the Moore-Balents argument, [91] and the integral formulas.

7.3.1 Dimensional reduction

In our topological periodic tables, a sequence of $\mathbb{Z}_2$ indices follows a $\mathbb{Z}$ index as the dimension of the system decreases. This structure makes it possible to define the corresponding $\mathbb{Z}_2$ invariants by dimensional reduction:[13, 6] Let us consider a $(d+2)$-dimensional Hamiltonian $\mathcal{H}(\boldsymbol{k}, k_{d+1}, k_{d+2}, \boldsymbol{r})$ that is characterized by the $\mathbb{Z}$ index mentioned in the above. Then, we can construct maps from this Hamiltonian to one and two lower dimensional Hamiltonians, by considering $\mathcal{H}(\boldsymbol{k}, k_{d+1}, 0, \boldsymbol{r})$ and $\mathcal{H}(\boldsymbol{k}, 0, 0, \boldsymbol{r})$, respectively. These maps define surjective homomorphic maps from $\mathbb{Z}$ to $\mathbb{Z}_2$. As a result, the first and second descendant $\mathbb{Z}_2$ invariants , $\nu_{\rm 1st}$ and $\nu_{\rm 2nd}$, of the lower dimensional Hamiltonians are obtained as

$$(-1)^{\nu_{\rm 1st}} = (-1)^{\nu_{\rm 2nd}} = (-1)^N, \tag{2.7.17}$$

where N is the integer topological invariant of $\mathcal{H}(\boldsymbol{k}, k_{d+1}, k_{d+2}, \boldsymbol{r})$. N is the Chern number Eq.(2.7.7) for non-chiral class or the winding number Eq. (2.7.12) for chiral class.

7.3.2 Moore-Balents argument for second descendant $\mathbb{Z}_2$ index

For the second descendant $\mathbb{Z}_2$ index ($d = s + D - 2$) of Table 2.4 with $d \geq 1$, there is another operational definition of the $\mathbb{Z}_2$ invariant, which was first discussed by Moore and Balents.[91] Consider a Hamiltonian $\mathcal{H}(\boldsymbol{k}, \boldsymbol{r})$ in real AZ class with $d = s + D - 2$. Choosing one of the momenta as the polar angle θ of the base sphere S^{d+D} and denoting the rest by $\boldsymbol{k}'$, the AZ symmetries are expressed as $T\mathcal{H}(\theta, \boldsymbol{k}', \boldsymbol{r})T^{-1} = \mathcal{H}(\pi - \theta, -\boldsymbol{k}', \boldsymbol{r})$, $C\mathcal{H}(\theta, \boldsymbol{k}', \boldsymbol{r})C^{-1} = -\mathcal{H}(\pi - \theta, -\boldsymbol{k}', \boldsymbol{r})$, and $\Gamma\mathcal{H}(\theta, \boldsymbol{k}', \boldsymbol{r})\Gamma^{-1} = -\mathcal{H}(\theta, \boldsymbol{k}', \boldsymbol{r})$. Then, take only the north hemisphere ($0 \leq \theta \leq \pi/2$) of the system. Although TRS and/or PHS cannot be retained only on the north hemisphere, they are retained at its boundary, i.e. the equator. Indeed the Hamiltonian on the equator $\mathcal{H}(\theta = \pi/2, \boldsymbol{k}', \boldsymbol{r})$ has the same symmetry of the original Hamiltonian $\mathcal{H}(\boldsymbol{k}, \boldsymbol{r})$, and thus its K-group is $K_{\mathbb{R}}(s; d-1, D) = \pi_0(\mathcal{R}_3) = 0$.

To define the topological number, we introduce another hemisphere in the following manner. As mentioned in the above, the K-group of the equator Hamiltonian is trivial. Therefore the equator Hamiltonian can smoothly shrink into a point $\mathcal{H}_0$ with keeping the AZ symmetry of the $(d-1)$-dimensional momentum space. This deformation defines a Hamiltonian $\tilde{\mathcal{H}}(\theta, \boldsymbol{k}', \boldsymbol{r})$ on a new hemisphere, say, a new south hemisphere, where the new Hamiltonian interpolates $\mathcal{H}(\theta = \pi/2, \boldsymbol{k}', \boldsymbol{r})$ at the equator ($\theta = \pi/2$) to $\mathcal{H}_0$ at the south pole ($\theta = \pi$). Note here that θ of $\tilde{\mathcal{H}}(\theta, \boldsymbol{k}', \boldsymbol{r})$ is just an interpolating parameter, and thus it transforms trivially under the AZ symmetries as $T\tilde{\mathcal{H}}(\theta, \boldsymbol{k}', \boldsymbol{r})T^{-1} = \tilde{\mathcal{H}}(\theta, -\boldsymbol{k}', \boldsymbol{r})$, $C\tilde{\mathcal{H}}(\theta, \boldsymbol{k}', \boldsymbol{r})C^{-1} = -\tilde{\mathcal{H}}(\theta, -\boldsymbol{k}', \boldsymbol{r})$, and $\Gamma\tilde{\mathcal{H}}(\theta, \boldsymbol{k}', \boldsymbol{r})\Gamma^{-1} = -\tilde{\mathcal{H}}(\theta, \boldsymbol{k}', \boldsymbol{r})$.

Now define the topological number. Sewing the new south and the original north hemispheres together, we have a Hamiltonian on a sphere. In contrast to the original Hamiltonian, the resultant Hamiltonian no longer has TRS and/or PHS since θ transforms differently in the north hemisphere and the south hemisphere. It belongs to a complex AZ class (A or AIII), so it can host a nonzero integer topological number N given by the Chern number $Ch_{(d+D)/2}$ or the winding number N_{d+D}. Its value, however, depends on the choice of the interpolating Hamiltonian $\tilde{\mathcal{H}}(\theta, \boldsymbol{k}', \boldsymbol{r})$ in general. Therefore, N itself does not characterize the topological nature of the original Hamiltonian. Nevertheless, its parity $(-1)^N$ is uniquely determined: Take another interpolating Hamiltonian $\tilde{\mathcal{H}}'(\theta, \boldsymbol{k}', \boldsymbol{r})$ which may give a different integer N'. The difference between N and N' can be evaluated as the topological number of the Hamiltonian that is obtained by sewing the hemispheres of $\tilde{\mathcal{H}}(\theta, \boldsymbol{k}', \boldsymbol{r})$ and $\tilde{\mathcal{H}}'(\theta, \boldsymbol{k}', \boldsymbol{r})$ together. In this case, the combined Hamiltonian keeps TRS and/or PHS which are the same as those of the original Hamiltonian except the $\boldsymbol{r}$-type transformation of θ. Therefore, its K-group is $K_{\mathbb{R}}(s, d-1, D+1) = \pi_0(R_4) = 2\mathbb{Z}$, which implies that $N - N'$ must be even. As a result, the parity $(-1)^N$ is unique, i.e. $(-1)^N = (-1)^{N'}$. The parity defines the $\mathbb{Z}_2$ invariant of the original Hamiltonian.

7.3.3 Chern-Simons invariant for first descendant $\mathbb{Z}_2$ index in odd-dimensional non-chiral real class

The integral representation of the first descendant $\mathbb{Z}_2$ invariant in non-chiral real class is given by the Chern-Simons form. [13] Consider a Hamiltonian $\mathcal{H}(\boldsymbol{k}, \boldsymbol{r})$ on the base space S^{d+D} with odd $d + D$. The $\mathbb{Z}_2$ topological invariant is given by

$$\nu = \frac{2}{((d+D+1)/2)!}\left(\frac{i}{2\pi}\right)^{(d+D+1)/2}\int_{S^{d+D}} CS_{d+D} \pmod 2. \tag{2.7.18}$$

Here CS_{d+D} is the Chern-Simons $(d+D)$-form given by [92]

$$CS_{2n+1} = (n+1)\int_0^1 dt \mathrm{tr}\left(\mathcal{A}(td\mathcal{A} + t^2\mathcal{A}^2)^n\right) \tag{2.7.19}$$

where $\mathcal{A}_{\alpha\beta}(\boldsymbol{k},\boldsymbol{r}) = \langle u_\alpha(\boldsymbol{k},\boldsymbol{r})|du_\beta(\boldsymbol{k},\boldsymbol{r})\rangle$ is the connection defined by occupied states $|u_\alpha(\boldsymbol{k},\boldsymbol{r})\rangle$. Some of lower dimensional Chern-Simons forms are

$$\begin{aligned} CS_1 &= \mathrm{tr}\mathcal{A}, \\ CS_3 &= \mathrm{tr}\left(\mathcal{A}d\mathcal{A} + \frac{2}{3}\mathcal{A}^3\right), \\ CS_5 &= \mathrm{tr}\left(\mathcal{A}(d\mathcal{A})^2 + \frac{3}{2}\mathcal{A}^3 d\mathcal{A} + \frac{3}{5}\mathcal{A}^5\right). \end{aligned} \tag{2.7.20}$$

Here phases of the occupied states should be globally defined on the overall parameter manifold S^{d+D} so as the connection $\mathcal{A}$ is non-singular. The $\mathbb{Z}_2$ nontriviality of this integral is ensured by the dimensional reduction discussed in Sec.7.3.1.

The Chern-Simons invariant characterizes the real AZ classes with $(s,\delta) = (2n, 2n-1)$ (mod 8) in Table 2.4.

7.3.4 Fu-Kane invariant for first and second descendant $\mathbb{Z}_2$ indices in even-dimensional TRS class

In the presence of TRS, the $\mathbb{Z}_2$ invariant can be introduced as [93]

$$\nu = \frac{1}{((d+D)/2)!}\left(\frac{i}{2\pi}\right)^{(d+D)/2}\left[\int_{S^{d+D}_{1/2}} \mathrm{tr}\mathcal{F}^{(d+D)/2} - \oint_{\partial S^{d+D}_{1/2}} CS_{d+D-1}\right] \pmod 2, \tag{2.7.21}$$

where $S^{d+D}_{1/2}$ is a (north) hemisphere of S^{d+D} and $\partial S^{d+D}_{1/2} \cong S^{d+D-1}$ is the equator. We suppose here that the north hemisphere and the south one are exchanged by TRS, but the equator is invariant. The valence band wave functions of the Chern-Simons form in Eq.(2.7.21) must be smoothly defined on the equator $\partial S^{d+D}_{1/2}$ (not on the hemisphere $S^{d+D}_{1/2}$). An appropriate gauge condition is needed to obtain the $\mathbb{Z}_2$ nontriviality, and thus we impose the time-reversal constraint for the valence band Bloch wave functions $\{|u_n(\boldsymbol{k},\boldsymbol{r})\rangle\}$ as [93]

$$w_{mn}(\boldsymbol{k},\boldsymbol{r}) = \langle u_m(-\boldsymbol{k},\boldsymbol{r})|Tu_n(\boldsymbol{k},\boldsymbol{r})\rangle \equiv \text{const.} \tag{2.7.22}$$

on the equator $(\boldsymbol{k},\boldsymbol{r}) \in \partial S^{d+D}_{1/2}$. The $\mathbb{Z}_2$ invariant Eq.(2.7.21) picks up an obstruction to choosing the gauge satisfying (2.7.22) on overall Brillouin zone.

In Table 2.4, the Fu-Kane invariant characterizes the real AZ classes with $(s,\delta) = (4n+3, 4n+2)$ (mod 8) and those with $(s,\delta) = (4n+4, 4n+2)$ (mod 8). Note that the Fu-Kane invariant is not applicable to class BDI and CII, since the presence of CS that commutes with TRS makes the integral Eq.(2.7.21) trivial.

7.3.5 Constrained Chern-Simons invariant for second descendant $\mathbb{Z}_2$ index in odd-dimensional chiral TRS class

Consider a Hamiltonian $\mathcal{H}(\boldsymbol{k},\boldsymbol{r})$ on the base space S^{d+D} with odd $d+D$. If the Hamiltonian has CS and TRS that anti-commute with each other, then the $\mathbb{Z}_2$ invariant of the Hamiltonian can be

given in a form of the Chern-Simons integral: To see this, first consider the dimension raising map in Eq.(2.6.5),

$$\mathcal{H}(\boldsymbol{k},\boldsymbol{r},\theta)=\sin\theta\mathcal{H}(\boldsymbol{k},\boldsymbol{r})+\cos\theta\Gamma. \tag{2.7.23}$$

Since the mapped Hamiltonian on S^{d+D+1} has TRS and is even-dimensional, we can define the Fu-Kane $\mathbb{Z}_2$ invariant of $\mathcal{H}(\theta,\boldsymbol{k},\boldsymbol{r})$ as

$$\nu=\frac{1}{((d+D+1)/2)!}\left(\frac{i}{2\pi}\right)^{(d+D+1)/2}\left[\int_{S^{d+D+1}_{1/2}}\mathrm{tr}\mathcal{F}^{(d+D+1)/2}-\oint_{\partial S^{d+D+1}_{1/2}}CS_{d+D}\right]\pmod 2. \tag{2.7.24}$$

It is convenient to choose a $\boldsymbol{k}$-type θ and take the equator as $\theta=\pi/2$. Then, we can show that the first term of Eq.(2.7.24) is identically zero due to TRS and CS of $\mathcal{H}(\boldsymbol{k},\boldsymbol{r})$.[11] Also the equator is nothing but the original base space S^{d+D}, Eq.(2.7.24) is recast into

$$\nu=\frac{1}{((d+D+1)/2)!}\left(\frac{i}{2\pi}\right)^{(d+D+1)/2}\int_{S^{d+D}}CS_{d+D}\pmod 2, \tag{2.7.25}$$

with the time-reversal constraint Eq.(2.7.22) on $(\boldsymbol{k},\boldsymbol{r})\in S^{d+D}$.[11] Note here that Eq.(2.7.25) is a half of Eq.(2.7.18) so the additional gauge constraint Eq.(2.7.22) is necessary to obtain the $\mathbb{Z}_2$ nontriviality.

The constrained Chern-Simons invariant characterizes the real AZ classes with $(s,\delta)=(4n+3,4n+1)\pmod 8$ in Table 2.4.

Chapter 3

Topological phases with order-two point group symmetry

In this chapter, we provide the complete classification of topological crystalline insulators and superconductors with an additional order-two point group symmetry. The symmetry we consider is general, and it includes global Z_2 symmetry, reflection, two-fold rotation, inversion, and their magnetic point group symmetries. In the cases of the order-two symmetries, the topological classification is replaced by the extension problem of the Clifford algebras. The topological classification indicates that topological defect gapless states can be considered as boundary gapless states in lower dimensional systems. The resultant topological periodic table shows a novel periodicity in the number of the flipped coordinates under the order-two additional spatial symmetry, in addition to the Bott-periodicity in the space dimensions. Using the new topological periodic table, various symmetry protected topological gapless modes at topological defects are identified in a unified manner. In addition, we also present a topological classification of Fermi points (for example, Weyl semimetals and superconductors, and Dirac semimetals) in the crystalline insulators and superconductors. The bulk topological classification and the Fermi point classification show the bulk-boundary correspondence in terms of the K-theory.

The organization of this chapter is as follows. In Sec. 1, we introduce the order-two point group symmetries and their representations of defect Hamiltonians. Our main results are summarized in Sec. 2. We show relations between K-groups with different order-two additional spatial symmetries and dimensions. The derivation and proof are given in Sec. 3. The classifying spaces of AZ classes with additional order-two symmetry are summarized in Sec. 4. In Sec. 5, we discuss properties of the obtained K-groups in the presence of additional symmetry. A novel periodicity in the number of flipped coordinates under the additional symmetry is pointed out. We also find that the K-groups naturally implement topological defects as boundaries of lower dimensional crystalline insulators/superconductors. Crystalline weak topological indices are argued in Sec. 6. We also apply our formalism to a classification of Fermi point protected by additional order-two symmetry in Sec. 7. By combing the results in Secs. 2 and 7, the bulk-boundary correspondence of K-groups are presented. We conclude the present chapter with some discussions in Sec. 8.

1 Order-two point group symmetries

In addition to the Altland-Zirnbauer (AZ) symmetries, i.e. time-reversal symmetry (TRS), particle-hole symmetry (PHS), and chiral symmetry (CS), we assume an additional symmetry of Hamiltonians. As an additional symmetry, we consider general order-two (magnetic) point group symmetry. Order-two point group symmetry S implies that the symmetry operation in twice trivially acts on spatial coordinate,

$$S : (\boldsymbol{x}_\parallel, \boldsymbol{x}_\perp) \mapsto (-\boldsymbol{x}_\parallel, \boldsymbol{x}_\perp) \tag{3.1.1}$$

with $\boldsymbol{x}_\parallel = (x_1, x_2, \cdots, x_{d_\parallel})$ and $\boldsymbol{x}_\perp = (x_{d_\parallel+1}, x_{d_\parallel+2} \cdots, x_d)$. The order-two point group symmetry includes reflection, two-fold spatial rotation and inversion. It also permits global $\boldsymbol{Z}_2$ symmetry such as a two-fold spin rotation. The anti-unitary case admits order-two magnetic point group symmetries. Under an order-two spatial symmetry, the momentum $\boldsymbol{k}$ in the base space of the Hamiltonian transforms as

$$\boldsymbol{k} \to \begin{cases} (-\boldsymbol{k}_\parallel, \boldsymbol{k}_\perp), & \text{for } S = U \\ (\boldsymbol{k}_\parallel, -\boldsymbol{k}_\perp), & \text{for } S = A \end{cases}, \tag{3.1.2}$$

with $\boldsymbol{k}_\parallel = (k_1, k_2, \cdots, k_{d_\parallel})$ and $\boldsymbol{k}_\perp = (k_{d_\parallel+1}, k_{d_\parallel+2} \cdots, k_d)$. Here S can be either unitary U or anti-unitary A. Note that like time-reversal operator, the anti-linearity of A results in the minus sign of the transformation law of $\boldsymbol{k}$.

In contrast to non-spatial AZ symmetries, the spatial coordinate $\boldsymbol{r}$ of the D-dimensional sphere surrounding a topological defect also transforms non-trivially under order-two spatial symmetry. To determine the transformation law, we specify the coordinate $\boldsymbol{r}$ of the D-dimensional sphere. First, to keep the additional symmetry, the topological defect should be invariant under S. Therefore, the additional symmetry S maps the D-dimensional sphere (with a radius $a > 0$) given by

$$\boldsymbol{n}^2 = a^2, \quad \boldsymbol{n} = (n_1, n_2, \cdots, n_{D+1}), \tag{3.1.3}$$

into itself, inducing the transformation

$$\boldsymbol{n} \to (-\boldsymbol{n}_\parallel, \boldsymbol{n}_\perp), \tag{3.1.4}$$

with $\boldsymbol{n}_\parallel = (n_1, n_2, \cdots, n_{D_\parallel})$ and $\boldsymbol{n}_\perp = (n_{D_\parallel+1}, n_{D_\parallel+2} \cdots, n_{D+1})$. When $D_\parallel \leq D$, we can introduce the coordinate $\boldsymbol{r}$ of the D-dimensional sphere by the stereographic projection of $\boldsymbol{n}$ as shown in Fig. 3.1,

$$r_i = \frac{n_i}{a - n_{D+1}}, \quad (i = 1, \cdots D), \tag{3.1.5}$$

which gives a simple transformation law of $\boldsymbol{r}$ as

$$\boldsymbol{r} \to (-\boldsymbol{r}_\parallel, \boldsymbol{r}_\perp), \tag{3.1.6}$$

with $\boldsymbol{r}_\parallel = (r_1, r_2, \cdots, r_{D_\parallel})$ and $\boldsymbol{r}_\perp = (r_{D_\parallel+1}, r_{D_\parallel+2} \cdots, r_D)$. Below, we assume $D_\parallel \leq D$, since the bulk-boundary correspondence for topological defects works only in this case. The assumption $D_\parallel \leq D$ implies that there is at least one unchanged coordinate, i.e. x_{D+1}, against the order-two point group transformation.

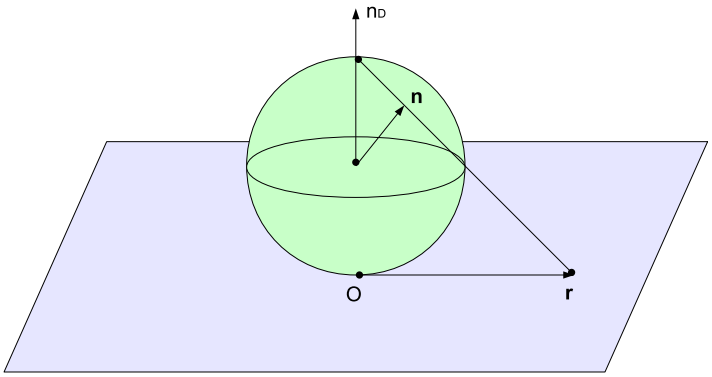

Figure 3.1: A stereographic projection of the sphere S^D.

Now the order-two unitary symmetry is expressed as

$$U\mathcal{H}(\boldsymbol{k},\boldsymbol{r})U^{-1} = \mathcal{H}(-\boldsymbol{k}_\parallel, \boldsymbol{k}_\perp, -\boldsymbol{r}_\parallel, \boldsymbol{r}_\perp), \tag{3.1.7}$$

and the order-two anti-unitary symmetry is

$$A\mathcal{H}(\boldsymbol{k},\boldsymbol{r})A^{-1} = \mathcal{H}(\boldsymbol{k}_\parallel, -\boldsymbol{k}_\perp, -\boldsymbol{r}_\parallel, \boldsymbol{r}_\perp). \tag{3.1.8}$$

Here $\mathcal{H}(\boldsymbol{k},\boldsymbol{r})$ is the defect Hamiltonian introduced in the previous chapter (eq. (2.6.1)). We suppose that

$$S^2 = \epsilon_S = \pm 1, \quad (S = U \text{ or } A), \tag{3.1.9}$$

and S commutes or anticommutes with coexisting AZ symmetries,

$$ST = \eta_T TS, \quad SC = \eta_C CS, \quad S\Gamma = \eta_\Gamma \Gamma S. \tag{3.1.10}$$

where $\eta_T = \pm 1$, $\eta_C = \pm 1$, and $\eta_\Gamma = \pm 1$. For a faithful representation of order-two symmetry, the sign ϵ_S of S^2 must be 1, but a spinor representation of rotation makes it possible to obtain $\epsilon_S = -1$. For instance, two-fold spin rotation $S = e^{i\pi s_i/2}$ $(i = 1, 2, 3)$ obeys $S^2 = -1$. Note that when $S = U$, we can set $\epsilon_S = 1$ by multiplying S by the imaginary unit i, but this changes the (anti-)commutation relations with T and/or C at the same time.

Our classification framework also works even for order-two *anti-symmetry* $\overline{S}$ defined by

$$\overline{U}\mathcal{H}(\boldsymbol{k},\boldsymbol{r})\overline{U}^{-1} = -\mathcal{H}(-\boldsymbol{k}_\parallel, \boldsymbol{k}_\perp, -\boldsymbol{r}_\parallel, \boldsymbol{r}_\perp), \tag{3.1.11}$$

$$\overline{A}\mathcal{H}(\boldsymbol{k},\boldsymbol{r})\overline{A}^{-1} = -\mathcal{H}(\boldsymbol{k}_\parallel, -\boldsymbol{k}_\perp, -\boldsymbol{r}_\parallel, \boldsymbol{r}_\perp), \tag{3.1.12}$$

where $\overline{S}$ can be either unitary $\overline{U}$ or anti-unitary $\overline{A}$. Such an anti-symmetry can be realized by combining any of order-two symmetries with CS or PHS. In a similar manner as S, we define $\epsilon_{\overline{S}}$, $\overline{\eta}_T$, $\overline{\eta}_C$ and $\overline{\eta}_\Gamma$ by

$$(\overline{S})^2 = \epsilon_{\overline{S}}, \quad \overline{S}T = \overline{\eta}_T T\overline{S}, \quad \overline{S}C = \overline{\eta}_C C\overline{S}, \quad \overline{S}\Gamma = \overline{\eta}_\Gamma \Gamma\overline{S}. \tag{3.1.13}$$

The existence of an order-two spatial symmetry S gives additional constraints on the classifying space. In the subsequent sections, we provide the resulting K-group of the homotopy classification.

2 K-group in the presence of additional symmetry: additional symmetry class

In this section we present the results of topological classification of topological crystalline insulators and superconductors and their topological defects protected by an additional order-two point group symmetry. The derivation and proof are given in the appended paper (Ref. [38]). We briefly sketch a proof in the subsection 3.

The topological classification for order-two point group symmetries is divided into the three pieces:

(i) Complex AZ classes with additional order-two unitary symmetry

(ii) Complex AZ classes with additional order-two antiunitary symmetry

(iii) Real AZ classes with additional order-two symmetry

We give their topological classification classification below. We introduce a useful parameter t refereed to as "additional symmetry class" which is an analogy to AZ symmetry classes, and characterizes types of additional symmetries.

2.1 Complex AZ classes with additional order-two unitary symmetry

The complex AZ classes consist of class A and class AIII. In class AIII Hamiltonians are imposed by CS, $\Gamma\mathcal{H}(\boldsymbol{k},\boldsymbol{r})\Gamma^{-1} = -\mathcal{H}(\boldsymbol{k},\boldsymbol{r})$. Now we impose an additional order-two symmetry/antisymmetry,

$$\begin{cases} U\mathcal{H}(\boldsymbol{k},\boldsymbol{r})U^{-1} = \mathcal{H}(-\boldsymbol{k}_\parallel,\boldsymbol{k}_\perp,-\boldsymbol{r}_\parallel,\boldsymbol{r}_\perp), & \text{(symmetry)} \\ \bar{U}\mathcal{H}(\boldsymbol{k},\boldsymbol{r})\bar{U}^{-1} = -\mathcal{H}(-\boldsymbol{k}_\parallel,\boldsymbol{k}_\perp,-\boldsymbol{r}_\parallel,\boldsymbol{r}_\perp), & \text{(antisymmetry)} \end{cases} \tag{3.2.1}$$

on complex AZ classes. Since there is no anti-unitary symmetry, a phase factor of U and $\bar{U}$ do not change the topological classification, and thus the sign of U^2 and $(\bar{U})^2$ can be fixed to be 1. For class AIII, we specify the commutation/anti-commutation relation between U and Γ ($\bar{U}$ and Γ) by U_{η_Γ} ($\bar{U}_{\eta_\Gamma}$). Note that $\bar{U}_{\eta_\Gamma}$ in class AIII is essentially the same as U_{η_Γ} because they can be converted to each other by the relation

$$\bar{U}_{\eta_\Gamma} = \Gamma U_{\eta_\Gamma}. \tag{3.2.2}$$

We denote the obtained K-group by

$$K^U_{\mathbb{C}}(s,t;d,d_\parallel,D,D_\parallel). \tag{3.2.3}$$

Here d (D) is the total space dimension (defect co-dimension), and $d_\parallel$ ($D_\parallel$) is the number of the flipping momenta (defect surrounding parameters) under the additional symmetry transformation, as was introduced in Sec.1. The label $s = 0, 1 \pmod 2$ indicates the AZ class ($s = 0$ for class A and $s = 1$ for class AIII) to which the Hamiltonian belongs, and $t = 0, 1 \pmod 2$ specifies the coexisting additional unitary symmetry as in Table. 3.1.

We can prove the following relation: [38]

$$K^U_{\mathbb{C}}(s,t;d,d_\parallel,D,D_\parallel) = K^U_{\mathbb{C}}(s-d+D,t-d_\parallel+D_\parallel;0,0,0,0). \tag{3.2.4}$$

Table 3.1: Possible types ($t = 0, 1 \pmod 2$) of order-two additional unitary symmetries in complex AZ class ($s = 0, 1 \pmod 2$). U and $\bar{U}$ represent symmetry and antisymmetry, respectively. The subscript of U_{η_Γ} and $\bar{U}_{\eta_\Gamma}$ specifies the relation $\Gamma U = \eta_\Gamma U \Gamma$. Symmetries in the same parenthesis are equivalent because of Eq. (3.2.2).

s	AZ class	$t=0$	$t=1$
0	A	U	$\bar{U}$
1	AIII	$(U_+, \bar{U}_+)$	$(U_-, \bar{U}_-)$

This relation implies that topological natures of the system can be deduced from those in 0-dimension. As we show in the section 4, the classifying spaces of the 0-dimensional K-group reduce to complex Clifford algebra, and we can obtain [68, 38]

$$\begin{cases} K^U_{\mathbb{C}}(s, t=0; 0,0,0,0) = \pi_0(\mathcal{C}_s \times \mathcal{C}_s) = \pi_0(\mathcal{C}_s) \oplus \pi_0(\mathcal{C}_s), \\ K^U_{\mathbb{C}}(s, t=1; 0,0,0,0) = \pi_0(\mathcal{C}_{s+1}). \end{cases} \tag{3.2.5}$$

where $\mathcal{C}_s (s = 0, 1)$ represents the classifying space of complex AZ classes. (See Table 2.2.)

2.2 Complex AZ classes with additional order-two antiunitary symmetry

Next, we consider order-two *anti-unitary* symmetry A or $\overline{A}$ as an additional symmetry:

$$\begin{cases} A\mathcal{H}(\boldsymbol{k}, \boldsymbol{r})A^{-1} = \mathcal{H}(\boldsymbol{k}_\parallel, -\boldsymbol{k}_\perp, -\boldsymbol{r}_\parallel, \boldsymbol{r}_\perp), & \text{(symmetry)} \\ \overline{A}\mathcal{H}(\boldsymbol{k}, \boldsymbol{r})\overline{A}^{-1} = -\mathcal{H}(\boldsymbol{k}_\parallel, -\boldsymbol{k}_\perp, -\boldsymbol{r}_\parallel, \boldsymbol{r}_\perp), & \text{(antisymmetry)} \end{cases} \tag{3.2.6}$$

As listed in Table 3.2, two different order-two anti-unitary symmetries $A^\pm$ and their corresponding anti-symmetries $\overline{A}^\pm$ are possible in class A, depending on the sign of A^2 or $(\overline{A})^2$, i.e. $(A^{\epsilon_A})^2 = \epsilon_A$, $(\overline{A}^{\epsilon_A})^2 = \epsilon_A$. In a similar manner, class AIII have two different types of additional anti-unitary symmetries, $A^{\epsilon_A}_{\eta_\Gamma}$ ($\epsilon_A = \pm 1, \eta_A = \pm 1$), and their corresponding anti-symmetries, $\overline{A}^{\epsilon_A}_{\eta_\Gamma}$ ($\epsilon_A = \pm 1, \eta_A = \pm 1$), where ϵ_A represents the sign of A^2 or $(\overline{A})^2$ and η_Γ indicates the commutation ($\eta_\Gamma = 1$) or the anti-commutation ($\eta_\Gamma = -1$) relation between A and Γ or those between A and Γ. Note that $A^{\epsilon_A}_{\eta_\Gamma}$ and $\overline{A}^{\epsilon_A \eta_\Gamma}_{\eta_\Gamma}$ are equivalent in class AIII since they can be related to each other as

$$A^{\epsilon_A}_{\eta_\Gamma} = \Gamma \overline{A}^{\epsilon_A \eta_\Gamma}_{\eta_\Gamma}. \tag{3.2.7}$$

The existence of the anti-unitary symmetry introduces *real* structures in complex AZ classes. Actually, in Eq. (3.2.6) by regarding $(\boldsymbol{k}_\perp, \boldsymbol{r}_\parallel)$ as "momenta", and $(\boldsymbol{k}_\parallel, \boldsymbol{r}_\perp)$ as "spatial coordinates", A and $\overline{A}$ can be considered as usual TRS and PHS in AZ classes, respectively. From this identification, a system in complex AZ class with an additional anti-unitary symmetry can be mapped into a real AZ class, as summarized in Table 3.2. As a result, the K-group of Hamiltonians with the symmetry s ($s = 0, 1, 2, \ldots, 7 \pmod 8$) of Table 3.2

$$K^A_{\mathbb{C}}(s; d, d_\parallel, D, D_\parallel), \tag{3.2.8}$$

reduces to the K-group of real AZ classes in Eq. (2.6.13), [38]

$$K^A_{\mathbb{C}}(s; d, d_\parallel, D, D_\parallel) = K_{\mathbb{R}}(s; d - d_\parallel + D_\parallel, D - D_\parallel + d_\parallel). \tag{3.2.9}$$

Table 3.2: Possible types ($s = 0, 1, \ldots, 7$ (mod 8)) of order-two additional anti-unitary symmetries in complex AZ class. A and $\bar{A}$ represent symmetry and anti-symmetry, respectively. The superscript of A^{ϵ_A} and $A^{\epsilon_A}_{\eta_\Gamma}$ represent the sign of the square $A^2 = \epsilon_A$, and the subscript of $A^{\epsilon_A}_{\eta_\Gamma}$ specifies the (anti-)commutation relation $\Gamma A = \eta_\Gamma A \Gamma$. Symmetries in the same parenthesis are equivalent because of Eq. (3.2.7).

s	AZ class	Coexisting symmetry	Mapped AZ class
0	A	A^+	AI
1	AIII	$(A^+_+,\ \bar{A}^+_+)$	BDI
2	A	$\bar{A}^+$	D
3	AIII	$(A^-_-,\bar{A}^+_-)$	DIII
4	A	A^-	AII
5	AIII	$(A^-_+,\ \bar{A}^-_+)$	CII
6	A	$\bar{A}^-$	C
7	AIII	$(A^+_-,\ \bar{A}^-_-)$	CI

where d (D) is the total space dimension (defect co-dimension), and $d_\parallel$ ($D_\parallel$) is the number of the flipping momentum (defect surrounding parameter) under the additional symmetry transformation. From Eq. (2.6.13), we have

$$K^A_{\mathbb{C}}(s; d, d_\parallel, D, D_\parallel) = K^A_{\mathbb{C}}(s - d + D + 2(d_\parallel - D_\parallel); 0, 0, 0, 0), \tag{3.2.10}$$

with

$$K^A_{\mathbb{C}}(s; 0, 0, 0, 0) = \pi_0(\mathcal{R}_s). \tag{3.2.11}$$

2.3 Real AZ classes with additional order-two symmetry

Hamiltonians in eight real AZ classes are invariant under TRS, $T\mathcal{H}(\boldsymbol{k}, \boldsymbol{r})T^{-1} = \mathcal{H}(-\boldsymbol{k}, \boldsymbol{r})$, and/or PHS, $C\mathcal{H}(\boldsymbol{k}, \boldsymbol{r})C^{-1} = -\mathcal{H}(-\boldsymbol{k}, \boldsymbol{r})$. In addition to TRS and/or PHS, we enforce one of order-two unitary/antiunitary spatial symmetries, U, $\bar{U}$, A, and $\bar{A}$ on the Hamiltonians,

$$\begin{cases} U\mathcal{H}(\boldsymbol{k}, \boldsymbol{r})U^{-1} = \mathcal{H}(-\boldsymbol{k}_\parallel, \boldsymbol{k}_\perp, -\boldsymbol{r}_\parallel, \boldsymbol{r}_\perp), & (\text{ unitary symmetry }) \\ \bar{U}\mathcal{H}(\boldsymbol{k}, \boldsymbol{r})\bar{U}^{-1} = -\mathcal{H}(-\boldsymbol{k}_\parallel, \boldsymbol{k}_\perp, -\boldsymbol{r}_\parallel, \boldsymbol{r}_\perp), & (\text{ unitary antisymmetry }) \\ A\mathcal{H}(\boldsymbol{k}, \boldsymbol{r})A^{-1} = \mathcal{H}(\boldsymbol{k}_\parallel, -\boldsymbol{k}_\perp, -\boldsymbol{r}_\parallel, \boldsymbol{r}_\perp), & (\text{ antiunitary symmetry }) \\ \bar{A}\mathcal{H}(\boldsymbol{k}, \boldsymbol{r})\bar{A}^{-1} = -\mathcal{H}(\boldsymbol{k}_\parallel, -\boldsymbol{k}_\perp, -\boldsymbol{r}_\parallel, \boldsymbol{r}_\perp). & (\text{ antiunitary antisymmetry }) \end{cases} \tag{3.2.12}$$

In class AI and AII, which support TRS, we have the following equivalence relations between the additional symmetries,

$$\begin{cases} U^{\epsilon_U}_{\eta_T} = iU^{-\epsilon_U}_{-\eta_T} = TA^{\eta_T\epsilon_T\epsilon_U}_{\eta_T} = iTA^{\eta_T\epsilon_T\epsilon_U}_{-\eta_T}, \\ \bar{U}^{\epsilon_U}_{\eta_T} = i\bar{U}^{-\epsilon_U}_{-\eta_T} = T\bar{A}^{\eta_T\epsilon_T\epsilon_U}_{\eta_T} = iT\bar{A}^{\eta_T\epsilon_T\epsilon_U}_{-\eta_T}, \end{cases} \tag{3.2.13}$$

where the superscript $\epsilon_S = \pm$ of S ($S = U, \bar{U}, A, \bar{A}$) denotes the sign of S^2, and the subscript η_T of S specifies the commutation ($\eta_T = +$) or anti-commutation ($\eta_T = -$) relation between S and T. In

Table 3.3: Possible types ($t = 0, 1, 2, 3$ (mod 4)) of order-two additional symmetries in real AZ class ($s = 0, 1, \ldots, 7$ (mod 8)). U and $\bar{U}$ represent unitary symmetry and anti-symmetry, respectively, and A and $\bar{A}$ represent anti-unitary symmetry and anti-symmetry, respectively. The superscript of S ($S = U, \bar{U}, A, \bar{A}$) indicates the sign of S^2, and the subscript of S specifies the commutation(+)/anti-commutation(-) relation between S and TRS and/or PHS. For BDI, DIII, CII and CI, where both TRS and PHS exist, S has two subscripts, in which the first one specifies the (anti-)commutation relation between S and T and the second one specifies that between S and C. Symmetries in the same parenthesis are equivalent because of Eqs. (3.2.13), (3.2.14) and (3.2.15).

s	AZ class	$t=0$	$t=1$	$t=2$	$t=3$
0	AI	$(U_+^+,\, U_-^-)$ $(A_+^+,\, A_-^+)$	$(\bar{U}_-^+,\, \bar{U}_+^-)$ $(\bar{A}_+^-,\, \bar{A}_-^-)$	$(U_-^+,\, U_+^-)$ $(A_-^-,\, A_+^-)$	$(\bar{U}_+^+,\, \bar{U}_-^-)$ $(\bar{A}_+^+,\, \bar{A}_-^+)$
1	BDI	$(U_{++}^+,\, U_{--}^-,\, \bar{U}_{++}^+,\, \bar{U}_{--}^-)$ $(A_{++}^+,\, A_{--}^+,\, \bar{A}_{++}^+,\, \bar{A}_{--}^+)$	$(U_{+-}^+,\, U_{-+}^-,\, \bar{U}_{-+}^+,\, \bar{U}_{+-}^-)$ $(A_{+-}^+,\, A_{-+}^+,\, \bar{A}_{-+}^-,\, \bar{A}_{+-}^-)$	$(U_{-+}^+,\, U_{++}^-,\, \bar{U}_{--}^+,\, \bar{U}_{++}^-)$ $(A_{--}^-,\, A_{++}^-,\, \bar{A}_{--}^-,\, \bar{A}_{++}^-)$	$(U_{-+}^+,\, U_{+-}^-,\, \bar{U}_{+-}^+,\, \bar{U}_{-+}^-)$ $(A_{-+}^-,\, A_{+-}^-,\, \bar{A}_{+-}^+,\, \bar{A}_{-+}^+)$
2	D	$(U_+^+,\, U_-^-)$ $(\bar{A}_+^+,\, \bar{A}_-^+)$	$(\bar{U}_-^+,\, \bar{U}_+^-)$ $(A_+^+,\, A_-^+)$	$(U_-^+,\, U_+^-)$ $(\bar{A}_-^-,\, \bar{A}_+^-)$	$(\bar{U}_+^+,\, \bar{U}_-^-)$ $(A_+^-,\, A_-^-)$
3	DIII	$(U_{++}^+,\, U_{--}^-,\, \bar{U}_{++}^-,\, \bar{U}_{--}^+)$ $(A_{++}^-,\, A_{--}^-,\, \bar{A}_{++}^+,\, \bar{A}_{--}^+)$	$(U_{-+}^+,\, U_{+-}^-,\, \bar{U}_{-+}^+,\, \bar{U}_{+-}^-)$ $(A_{-+}^+,\, A_{+-}^+,\, \bar{A}_{+-}^+,\, \bar{A}_{-+}^+)$	$(U_{--}^+,\, U_{++}^-,\, \bar{U}_{--}^-,\, \bar{U}_{++}^+)$ $(A_{--}^+,\, A_{++}^+,\, \bar{A}_{--}^-,\, \bar{A}_{++}^-)$	$(U_{+-}^+,\, U_{-+}^-,\, \bar{U}_{+-}^+,\, \bar{U}_{-+}^-)$ $(A_{+-}^-,\, A_{-+}^-,\, \bar{A}_{+-}^-,\, \bar{A}_{-+}^-)$
4	AII	$(U_+^+,\, U_-^-)$ $(A_+^-,\, A_-^-)$	$(\bar{U}_-^+,\, \bar{U}_+^-)$ $(\bar{A}_-^+,\, \bar{A}_+^+)$	$(U_-^+,\, U_+^-)$ $(A_-^+,\, A_+^+)$	$(\bar{U}_+^+,\, \bar{U}_-^-)$ $(\bar{A}_+^-,\, \bar{A}_-^-)$
5	CII	$(U_{++}^+,\, U_{--}^-,\, \bar{U}_{++}^+,\, \bar{U}_{--}^-)$ $(A_{++}^-,\, A_{--}^-,\, \bar{A}_{++}^-,\, \bar{A}_{--}^-)$	$(U_{+-}^+,\, U_{-+}^-,\, \bar{U}_{-+}^+,\, \bar{U}_{+-}^-)$ $(A_{+-}^-,\, A_{-+}^-,\, \bar{A}_{-+}^+,\, \bar{A}_{+-}^+)$	$(U_{-+}^+,\, U_{++}^-,\, \bar{U}_{--}^+,\, \bar{U}_{++}^-)$ $(A_{--}^+,\, A_{++}^+,\, \bar{A}_{--}^+,\, \bar{A}_{++}^+)$	$(U_{-+}^+,\, U_{+-}^-,\, \bar{U}_{+-}^+,\, \bar{U}_{-+}^-)$ $(A_{-+}^+,\, A_{+-}^+,\, \bar{A}_{+-}^-,\, \bar{A}_{-+}^-)$
6	C	$(U_+^+,\, U_-^-)$ $(\bar{A}_+^-,\, \bar{A}_-^-)$	$(\bar{U}_+^+,\, \bar{U}_-^-)$ $(A_+^-,\, A_-^-)$	$(U_-^+,\, U_+^-)$ $(\bar{A}_-^+,\, \bar{A}_+^+)$	$(\bar{U}_-^+,\, \bar{U}_+^-)$ $(A_-^+,\, A_+^+)$
7	CI	$(U_{++}^+,\, U_{--}^-,\, \bar{U}_{++}^-,\, \bar{U}_{--}^+)$ $(A_{++}^+,\, A_{--}^+,\, \bar{A}_{++}^-,\, \bar{A}_{--}^-)$	$(U_{-+}^+,\, U_{+-}^-,\, \bar{U}_{-+}^+,\, \bar{U}_{+-}^-)$ $(A_{-+}^-,\, A_{+-}^-,\, \bar{A}_{-+}^-,\, \bar{A}_{+-}^-)$	$(U_{--}^+,\, U_{++}^-,\, \bar{U}_{--}^-,\, \bar{U}_{++}^+)$ $(A_{--}^-,\, A_{++}^-,\, \bar{A}_{--}^+,\, \bar{A}_{++}^+)$	$(U_{+-}^+,\, U_{-+}^-,\, \bar{U}_{+-}^+,\, \bar{U}_{-+}^-)$ $(A_{+-}^+,\, A_{-+}^+,\, \bar{A}_{+-}^+,\, \bar{A}_{-+}^+)$

a similar manner, in class D and C, PHS leads to the following equivalence relations

$$\begin{cases} U_{\eta_C}^{\epsilon_U} = iU_{-\eta_C}^{-\epsilon_U} = C\bar{A}_{\eta_C}^{\eta_C\epsilon_C\epsilon_U} = iC\bar{A}_{-\eta_C}^{-\eta_C}, \\ \bar{U}_{\eta_C}^{\epsilon_U} = i\bar{U}_{-\eta_C}^{-\epsilon_U} = CA_{\eta_C}^{\eta_C\epsilon_C\epsilon_U} = iCA_{-\eta_C}^{\eta_C\epsilon_C\epsilon_U}, \end{cases} \tag{3.2.14}$$

where the superscript $\epsilon_S = \pm$ denotes the sign of S^2 and the subscript $\eta_C = \pm$ denotes the commutation ($\eta_C = +$) or anti-commutation ($\eta_C = -$) relation between S and C. Finally, in class BDI, DIII, CII and CI, we obtain

$$\begin{cases} U_{\eta_T,\eta_C}^{\epsilon_U} = iU_{-\eta_T,-\eta_C}^{-\epsilon_U} = TA_{\eta_T,\eta_C}^{\eta_T\epsilon_T\epsilon_U} = iTA_{-\eta_T,-\eta_C}^{\eta_T\epsilon_T\epsilon_U} = C\bar{A}_{\eta_T,\eta_C}^{\eta_C\epsilon_C\epsilon_U} = iC\bar{A}_{-\eta_T,-\eta_C}^{\eta_C\epsilon_C\epsilon_U}, \\ \bar{U}_{\eta_T,\eta_C}^{\epsilon_U} = i\bar{U}_{-\eta_T,-\eta_C}^{-\epsilon_U} = T\bar{A}_{\eta_T,\eta_C}^{\eta_T\epsilon_T\epsilon_U} = iT\bar{A}_{-\eta_T,-\eta_C}^{\eta_T\epsilon_T\epsilon_U}, = CA_{\eta_T,\eta_C}^{\eta_C\epsilon_C\epsilon_U} = iCA_{-\eta_T,-\eta_C}^{\eta_C\epsilon_C\epsilon_U}. \end{cases} \tag{3.2.15}$$

These equivalence relations classify order-two symmetries into four families ($t = 0, 1, 2, 3$), as summarized in Table 3.3. Here one should note that unitary symmetries can be converted into to

anti-unitary ones by multiplying TRS or PHS. Therefore, the presence of a unitary symmetry for real AZ classes gives the same K-groups as those with an additional anti-unitary symmetry.

We denote the K-group for real AZ class ($s = 0, 1, \ldots, 7$ (mod 8)) with additional order-two unitary (anti-unitary) symmetry ($t = 0, 1, 2, 3$ (mod 4)) as

$$K^U_{\mathbb{R}}(s, t; d, d_{\|}, D, D_{\|}), \quad (K^A_{\mathbb{R}}(s, t; d, d_{\|}, D, D_{\|})), \tag{3.2.16}$$

where d (D) is the total space dimension (defect co-dimension), and $d_{||}$ ($D_{||}$) is the number of the flipping momentum (defect surrounding parameter) against the additional symmetry transformation. The equivalence between unitary and anti-unitary symmetries for real AZ classes implies

$$K^U_{\mathbb{R}}(s, t; d, d_{\|}, D, D_{\|}) = K^A_{\mathbb{R}}(s, t; d, d_{\|}, D, D_{\|}). \tag{3.2.17}$$

We can show the following relation: [38]

$$K^{U/A}_{\mathbb{R}}(s, t; d, d_{\|}, D, D_{\|}) = K^{U/A}_{\mathbb{R}}(s - d + D, t - d_{\|} + D_{\|}; 0, 0, 0, 0). \tag{3.2.18}$$

In the section 4, we show [68, 38]

$$\begin{cases} K^{U/A}_{\mathbb{R}}(s, t = 0; 0, 0, 0, 0) = \pi_0(\mathcal{R}_s \times \mathcal{R}_s) = \pi_0(\mathcal{R}_s) \oplus \pi_0(\mathcal{R}_s), \\ K^{U/A}_{\mathbb{R}}(s, t = 1; 0, 0, 0, 0) = \pi_0(\mathcal{R}_{s-1}), \\ K^{U/A}_{\mathbb{R}}(s, t = 2; 0, 0, 0, 0) = \pi_0(\mathcal{C}_s), \\ K^{U/A}_{\mathbb{R}}(s, t = 3; 0, 0, 0, 0) = \pi_0(\mathcal{R}_{s+1}), \end{cases} \tag{3.2.19}$$

where $\mathcal{R}_s$ ($s = 0, 1, \ldots, 7$ (mod 8)) and $\mathcal{C}_s$ ($s = 0, 1$ (mod 2)) represent the classifying spaces of the real and complex AZ classes.

3 Dimensional hierarchy with order-two additional symmetry

In this section, we briefly illustrate a proof of Eqs. (3.2.4) and (3.2.18) which establish the relations between the K-groups of topological crystalline insulators and superconductors with order-two additional symmetry in different dimensions.

For simplicity, we only consider the cases of the complex AZ classes (3.2.4). For the real AZ classes, we can show (3.2.18) in a way similar to that of the complex AZ classes. [38] For the complex classes, due to the absence of antiunitary symmetry, the momentum $\boldsymbol{k}$ and coordinate parameters $\boldsymbol{r}$ cannot be distinguished from each other. Therefore, we have

$$K^U_{\mathbb{C}}(s, t; d, d_{\|}, D, D_{\|}) = K^U_{\mathbb{C}}(s, t; d + D, d_{\|} + D_{\|}, 0, 0). \tag{3.3.1}$$

We can also derive the following dimensional hierarchy,

$$\begin{aligned} K^U_{\mathbb{C}}(s, t; d, d_{\|}, 0, 0) &= K^U_{\mathbb{C}}(s + 1, t; d + 1, d_{\|}, 0, 0) \\ &= K^U_{\mathbb{C}}(s + 1, t + 1; d + 1, d_{\|} + 1, 0, 0), \end{aligned} \tag{3.3.2}$$

which leads to Eq.(3.2.4).

To prove Eq.(3.3.2), we use the dimension-raising maps, Eqs. (2.6.5) and (2.6.6), and their inverses, Eqs. (2.6.7) and (2.6.9). These maps determine uniquely how order-two unitary symmetry

of an original Hamiltonian acts on the mapped Hamiltonian, and as a result, we can obtain the relation between the K-groups. For instance, a Hamiltonian $\mathcal{H}_{\rm A}(\boldsymbol{k})$ in class A ($s=0$) is mapped into a Hamiltonian $\mathcal{H}_{\rm AIII}(\boldsymbol{k},\theta)$ in class AIII ($s=1$) with CS $\Gamma = \mathbf{1}\otimes\tau_x$ by the dimension-raising map

$$\begin{cases} \mathcal{H}_{\rm AIII}(\boldsymbol{k},\theta) = \sin\theta\mathcal{H}_{\rm A}(\boldsymbol{k})\otimes\tau_z + \cos\theta\mathbf{1}\otimes\tau_y, \\ \Gamma\mathcal{H}_{\rm AIII}(\boldsymbol{k},\theta)\Gamma^{-1} = -\mathcal{H}_{\rm AIII}(\boldsymbol{k},\theta), \quad \Gamma = \mathbf{1}\otimes\tau_x. \end{cases} \tag{3.3.3}$$

If the class A Hamiltonian $\mathcal{H}_{\rm A}(\boldsymbol{k})$ has an additional unitary symmetry U, which is labeled by $(s,t)=(0,0)$ in Table 3.1,

$$U\mathcal{H}_{\rm A}(\boldsymbol{k})U^{-1} = \mathcal{H}_{\rm A}(-\boldsymbol{k}_\parallel,\boldsymbol{k}_\perp), \quad (s=0,t=0), \tag{3.3.4}$$

then the mapped class AIII Hamiltonian $\mathcal{H}_{\rm AIII}(\boldsymbol{k},\theta)$ also has the corresponding symmetries,

$$(U\otimes\tau_0)\mathcal{H}_{\rm AIII}(\boldsymbol{k},\theta)(U\otimes\tau_0)^{-1} = \mathcal{H}_{\rm AIII}(-\boldsymbol{k}_\parallel,\boldsymbol{k}_\perp,\theta), \tag{3.3.5}$$

$$(U\otimes\tau_z)\mathcal{H}_{\rm AIII}(\boldsymbol{k},\theta)(U\otimes\tau_z)^{-1} = \mathcal{H}_{\rm AIII}(-\boldsymbol{k}_\parallel,\boldsymbol{k}_\perp,\pi-\theta). \tag{3.3.6}$$

The former (latter) symmetry $U\otimes\tau_0$ ($U\otimes\tau_z$) defines U_+ (U_-) in Table 3.1, which belongs to $(s,t)=(1,0)$ [$(s,t)=(1,1)$] in Table 3.1, because it (anti-)commutes with the chiral operator $\Gamma=\mathbf{1}\otimes\tau_x$. [1] Also, in the former (latter) case, the trivial (non-trivial) transformation of θ under the mapped symmetry implies that θ must be considered as a $\boldsymbol{k}_\perp$-type ($\boldsymbol{k}_\parallel$-type) variable for the mapped symmetry. Therefore, Eq.(3.3.3) provides the K-group homomorphisms

$$K^U_{\mathbb{C}}(0,0;d,d_\parallel,0,0) \to \begin{cases} K^U_{\mathbb{C}}(1,0;d+1,d_\parallel,0,0) & \text{for } U\otimes\tau_0 \\ K^U_{\mathbb{C}}(1,1;d+1,d_\parallel+1,0,0) & \text{for } U\otimes\tau_z \end{cases} \tag{3.3.7}$$

for the mapped additional symmetry (3.3.6). Note that it is not obvious that the homomorphisms (3.3.7) show isomorphisms. In such cases, we also find that the dimension-lowering maps Eqs.(2.6.7) and (2.6.9) provide the inverse of these mappings. [2] Thus, (3.3.7) is a K-group isomorphism.

In a similar manner, one can specify how other unitary symmetries in Table 3.1 are mapped, and how θ transforms under the mapped symmetries, as summarized in Table 3.4. Consequently, we have isomorphism between Hamiltonians with different (s,t)s' of Table 3.1, in the meaning of stable equivalence, which establishes the K-group isomorphism of Eq.(3.3.2).

Also, we can show the dimensional hierarchy for real AZ classes with order-two point group symmetry as [38]

$$\begin{aligned} K^{U/A}_{\mathbb{R}}(s,t;d,d_\parallel,D,D_\parallel) &= K^{U/A}_{\mathbb{R}}(s+1,t;d+1,d_\parallel,D,D_\parallel) \\ &= K^{U/A}_{\mathbb{R}}(s-1,t;d,d_\parallel,D+1,D_\parallel) \\ &= K^{U/A}_{\mathbb{R}}(s+1,t+1;d+1,d_\parallel+1,D,D_\parallel) \\ &= K^{U/A}_{\mathbb{R}}(s-1,t-1;d,d_\parallel,D+1,D_\parallel+1), \end{aligned} \tag{3.3.8}$$

which leads Eq.(3.2.18).

[1] Note that the antisymmetries $U\otimes\tau_x$ and $U\otimes\tau_y$ are equivalent to the symmetries $U\otimes\tau_0$ and $U\otimes\tau_z$, respectively.

[2] A simple criterion of the existence of an inverse homomorphism for order-two symmetries is that a order-two symmetry has fixed point in the base space S^d. An exception is an inversion symmetry $\boldsymbol{n}\mapsto-\boldsymbol{n}$ ($\boldsymbol{n}\in S^d$) where the inversion transformation has no fixed point.

Table 3.4: The isomorphism from $K^U_{\mathbb{C}}(s,t,d,d_\parallel,0,0)$ to $K^U_{\mathbb{C}}(s+1,t,d+1,d_\parallel,0,0)$ and $K^U_{\mathbb{C}}(s+1,t+1,d+1,d_\parallel+1,0,0)$.

AZ Class	t	Symmetry	Hamiltonian mapping	Type of θ	Mapped AZ class	Γ	Mapped t	Mapped symmetry
A	0	U	$\sin\theta\mathcal{H}_{\rm A}(\boldsymbol{k})\otimes\tau_z+\cos\theta\mathbf{1}\otimes\tau_y$	$\boldsymbol{k}_\perp$	AIII	$\mathbf{1}\otimes\tau_x$	0	$U_+=U\otimes\tau_0$
	1	$\bar{U}$		$\boldsymbol{k}_\perp$			1	$U_-=\bar{U}\otimes\tau_y$
	0	U		$\boldsymbol{k}_\parallel$			1	$U_-=U\otimes\tau_z$
	1	$\bar{U}$		$\boldsymbol{k}_\parallel$			0	$U_+=\bar{U}\otimes\tau_x$
AIII	0	U_+	$\sin\theta\mathcal{H}_{\rm AIII}(\boldsymbol{k})+\cos\theta\Gamma$	$\boldsymbol{k}_\perp$	A		0	$U=U_+$
	1	U_-		$\boldsymbol{k}_\perp$			1	$\bar{U}=i\Gamma U_-$
	0	U_+		$\boldsymbol{k}_\parallel$			1	$\bar{U}=\Gamma U_+$
	1	U_-		$\boldsymbol{k}_\parallel$			0	$U=U_-$

4 Classifying space of AZ classes with additional symmetry

To specify the topological classification with an additional symmetry, we have to determine the classifying spaces of 0-dimensional Hamiltonians with an additional symmetry, which leads to the K-groups as (3.2.5) and (3.2.19). The classifying spaces of the AZ classes without additional symmetry were given in Table 2.2. In this section, we show classifying spaces in the presence of additional symmetry. [68]

Here we need to consider only additional unitary symmetries: For complex AZ classes, the classifying spaces in the presence of an antiunitary symmetry are obtained as those of real AZ classes without additional symmetry, as is shown in Sec.2.2. For real AZ classes, antiunitary symmetries are converted into unitary symmetries (See Table 3.3).

4.1 Complex AZ classes with additional order-two unitary symmetry

In complex AZ classes, the presence of an additional unitary symmetry affects on the extension in two possible manners:

- $(t=0)$ Decoupling of the Clifford algebra
- $(t=1)$ Adding another generator of the Clifford algebra

Here t represents the additional symmetry class introduced in Table 3.1. We summarize the extensions and classifying spaces of complex AZ classes with an additional unitary symmetry in Table 3.5. The effect of an additional symmetry in complex AZ classes is summarized as follows:

$$\mathcal{C}_s \to \begin{cases} \mathcal{C}_s\times\mathcal{C}_s & (t=0) \\ \mathcal{C}_{s+1} & (t=1) \end{cases} \tag{3.4.1}$$

For example, let us consider class AIII. The additional symmetry class $t=0$ is represented by the U_+ symmetry:

$$\Gamma\mathcal{H}\Gamma^{-1}=-\mathcal{H},\quad U_+\mathcal{H}U_+^{-1}=\mathcal{H},\quad [U_+,\Gamma]=0. \tag{3.4.2}$$

U_+ commutes with both $\mathcal{H}$ and Γ, which implies representation of the Hamiltonian $\mathcal{H}$ follows the extension of the Clifford algebra

$$\{\Gamma\} \otimes U_+ \to \{\mathcal{H}, \Gamma\} \otimes U_+, \tag{3.4.3}$$

of which classifying space is given by a double $\mathcal{C}_1$, $\mathcal{C}_1 \times \mathcal{C}_1$. On the other hand, the additional symmetry class $t = 1$ is represented by the $\overline{U}_-$ symmetry:

$$\Gamma\mathcal{H}\Gamma^{-1} = -\mathcal{H}, \quad \overline{U}_-\mathcal{H}\overline{U}_-^{-1} = -\mathcal{H}, \quad \{\overline{U}_-, \Gamma\} = 0. \tag{3.4.4}$$

$\overline{U}_-$ anticommutes with both $\mathcal{H}$ and Γ, which implies representation of the Hamiltonian $\mathcal{H}$ follows the extension of the Clifford algebra

$$\{\Gamma, \overline{U}_-\} \to \{\mathcal{H}, \Gamma, \overline{U}_-\}, \tag{3.4.5}$$

oh which classifying space is given by shifting $\mathcal{C}_1$ by 1, $\mathcal{C}_2 \cong \mathcal{C}_0$.

4.2 Real AZ classes with additional order-two symmetry

In real AZ classes, the presence of an additional unitary symmetry affects on the extension in four possible manners:

- $(t = 0)$ Decoupling of the Clifford algebra
- $(t = 1)$ Adding another generator e with $e^2 = -1$
- $(t = 2)$ Inducing a complex structure
- $(t = 3)$ Adding another generator e with $e^2 = 1$

Here t represents the additional symmetry class introduced in Table 3.3. We summarize the extensions and classifying spaces of ral AZ classes with an additional unitary symmetry in Table 3.5. The effect of an additional symmetry in real AZ classes is summarized as follows:

$$\mathcal{R}_s \to \begin{cases} \mathcal{R}_s \times \mathcal{R}_s & (t = 0) \\ \mathcal{R}_{s-1} & (t = 1) \\ \mathcal{C}_s & (t = 2) \\ \mathcal{R}_{s+1} & (t = 3) \end{cases} \tag{3.4.6}$$

Let us comment on the complexification which occurs in the additional symmetry class with $t = 2$. In this case, the additional symmetry U is labeled by U_+^-/U_{++}^- for TRS or/and PHS AZ classes, i.e., U commutes with all the real AZ symmetry operators and Hamiltonian, and $U^2 = -1$, which implies that U plays a role of the imaginary constant in the real algebra. Thus, we get an isomorphism

$$Cl_{p,q} \otimes_{\mathbb{R}} Cl_{1,0} \cong Cl_{p+q}, \tag{3.4.7}$$

where Cl_{p+q} is the complex Clifford algebra.

Table 3.5: Classifying spaces of AZ classes with additional order-two symmetry. [68, 38] In the fifth column, J is the pure imaginary constant.

AZ class	t	Symmetry	Generator	Extension	Classifying space
A	0	U	$U \to \{H\} \otimes U$	$Cl_1 \to Cl_1 \otimes Cl_1$	$\mathcal{C}_0 \times \mathcal{C}_0$
A	1	$\bar{U}$	$\{\bar{U}\} \to \{H, \bar{U}\}$	$Cl_1 \to Cl_2$	$\mathcal{C}_1$
AIII	0	U_+	$\{\Gamma\} \otimes U_+ \to \{H, \Gamma\} \otimes U_+$	$Cl_1 \otimes Cl_1 \to Cl_2 \otimes Cl_1$	$\mathcal{C}_1 \times \mathcal{C}_1$
AIII	1	$\bar{U}_-$	$\{\Gamma, \bar{U}_-\} \to \{H, \Gamma, \bar{U}_-\}$	$Cl_2 \to Cl_3$	$\mathcal{C}_0$
AI	0	U_+^+	$\{\emptyset; T, JT\} \otimes U_+^+ \to \{JH; T, JT\} \otimes U_+^+$	$Cl_{0,2} \otimes Cl_{0,1} \to Cl_{1,2} \otimes Cl_{0,1}$	$\mathcal{R}_0 \times \mathcal{R}_0$
AI	1	$\bar{U}_-^+$	$\{\emptyset; T, JT, \bar{U}_-^+\} \to \{JH; T, JT, \bar{U}_-^+\}$	$Cl_{0,3} \to Cl_{1,3}$	$\mathcal{R}_7$
AI	2	U_+^-	$\{\emptyset; T, JT\} \otimes U_+^- \to \{JH; T, JT\} \otimes U_+^-$	$Cl_{0,2} \otimes Cl_{1,0} \to Cl_{1,2} \otimes Cl_{1,0}$	$\mathcal{C}_0$
AI	3	$\bar{U}_-^-$	$\{\bar{U}_-^-; T, JT\} \to \{JH, \bar{U}_-^-; T, JT\}$	$Cl_{1,2} \to Cl_{2,2}$	$\mathcal{R}_1$
BDI	0	U_{++}^+	$\{JCT; C, JC\} \otimes U_{++}^+ \to \{H, JCT; C, JC\} \otimes U_{++}^+$	$Cl_{1,2} \otimes Cl_{0,1} \to Cl_{1,3} \otimes Cl_{0,1}$	$\mathcal{R}_1 \times \mathcal{R}_1$
BDI	1	$\bar{U}_{+-}^-$	$\{JCT, \bar{U}_{+-}^-; C, JC\} \to \{JCT, \bar{U}_{+-}^-; H, C, JC\}$	$Cl_{2,2} \to Cl_{2,3}$	$\mathcal{R}_0$
BDI	2	U_{++}^-	$\{JCT; C, JC\} \otimes U_{++}^- \to \{H, JCT; C, JC\} \otimes U_{++}^-$	$Cl_{1,2} \otimes Cl_{1,0} \to Cl_{1,3} \otimes Cl_{1,0}$	$\mathcal{C}_1$
BDI	3	$\bar{U}_{+-}^+$	$\{JCT; C, JC, \bar{U}_{+-}^+\} \to \{JCT; H, C, JC, \bar{U}_{+-}^+\}$	$Cl_{1,3} \to Cl_{1,4}$	$\mathcal{R}_2$
D	0	U_+^+	$\{\emptyset; C, JC\} \otimes U_+^+ \to \{\emptyset; H, C, JC\} \otimes U_+^+$	$Cl_{0,2} \otimes Cl_{0,1} \to Cl_{0,3} \otimes Cl_{0,1}$	$\mathcal{R}_2 \times \mathcal{R}_2$
D	1	$\bar{U}_-^-$	$\{\bar{U}_-^-; C, JC\} \to \{\bar{U}_-^-; H, C, JC\}$	$Cl_{1,2} \to Cl_{1,3}$	$\mathcal{R}_1$
D	2	U_+^-	$\{\emptyset; C, JC\} \otimes U_+^- \to \{\emptyset; H, C, JC\} \otimes U_+^-$	$Cl_{0,2} \otimes Cl_{1,0} \to Cl_{0,3} \otimes Cl_{1,0}$	$\mathcal{C}_0$
D	3	$\bar{U}_-^+$	$\{\emptyset; C, JC, \bar{U}_-^+\} \to \{\emptyset; H, C, JC, \bar{U}_-^+\}$	$Cl_{0,3} \to Cl_{0,4}$	$\mathcal{R}_3$
DIII	0	U_{++}^+	$\{\emptyset; C, JC, JCT\} \otimes U_{++}^+ \to \{\emptyset; H, C, JC, JCT\} \otimes U_{++}^+$	$Cl_{0,3} \otimes Cl_{0,1} \to Cl_{0,4} \otimes Cl_{0,1}$	$\mathcal{R}_3 \times \mathcal{R}_3$
DIII	1	$\bar{U}_{+-}^-$	$\{\bar{U}_{+-}^-; C, JC, JCT\} \to \{\bar{U}_{+-}^-; H, C, JC, JCT\}$	$Cl_{1,3} \to Cl_{1,4}$	$\mathcal{R}_2$
DIII	2	U_{++}^-	$\{\emptyset; C, JC, JCT\} \otimes U_{++}^- \to \{\emptyset; H, C, JC, JCT\} \otimes U_{++}^-$	$Cl_{0,3} \otimes Cl_{1,0} \to Cl_{0,4} \otimes Cl_{1,0}$	$\mathcal{C}_1$
DIII	3	$\bar{U}_{+-}^+$	$\{\emptyset; C, JC, JCT, \bar{U}_{+-}^+\} \to \{\emptyset; H, C, JC, JCT, \bar{U}_{+-}^+\}$	$Cl_{0,4} \to Cl_{0,5}$	$\mathcal{R}_4$
AII	0	U_+^+	$\{T, JT; \emptyset\} \otimes U_+^+ \to \{JH, T, JT; \emptyset\} \otimes U_+^+$	$Cl_{2,0} \otimes Cl_{0,1} \to Cl_{3,0} \otimes Cl_{0,1}$	$\mathcal{R}_4 \times \mathcal{R}_4$
AII	1	$\bar{U}_-^+$	$\{T, JT; \bar{U}_-^+\} \to \{JH, T, JT; \bar{U}_-^+\}$	$Cl_{2,1} \to Cl_{3,1}$	$\mathcal{R}_3$
AII	2	U_+^-	$\{T, JT; \emptyset\} \otimes U_+^- \to \{JH, T, JT; \emptyset\} \otimes U_+^-$	$Cl_{2,0} \otimes Cl_{1,0} \to Cl_{3,0} \otimes Cl_{1,0}$	$\mathcal{C}_0$
AII	3	$\bar{U}_-^-$	$\{T, JT, \bar{U}_-^-; \emptyset\} \to \{JH, T, JT, \bar{U}_-^-; \emptyset\}$	$Cl_{3,0} \to Cl_{4,0}$	$\mathcal{R}_5$
CII	0	U_{++}^+	$\{C, JC, JCT; \emptyset\} \otimes U_{++}^+ \to \{C, JC, JCT; H\} \otimes U_{++}^+$	$Cl_{3,0} \otimes Cl_{0,1} \to Cl_{3,1} \otimes Cl_{0,1}$	$\mathcal{R}_5 \times \mathcal{R}_5$
CII	1	$\bar{U}_{+-}^-$	$\{C, JC, JCT, \bar{U}_{+-}^-; \emptyset\} \to \{C, JC, JCT, \bar{U}_{+-}^-; H\}$	$Cl_{4,0} \to Cl_{4,1}$	$\mathcal{R}_4$
CII	2	U_{++}^-	$\{C, JC, JCT; \emptyset\} \otimes U_{++}^- \to \{C, JC, JCT; H\} \otimes U_{++}^-$	$Cl_{3,0} \otimes Cl_{1,0} \to Cl_{3,1} \otimes Cl_{1,0}$	$\mathcal{C}_1$
CII	3	$\bar{U}_{+-}^+$	$\{C, JC, JCT; \bar{U}_{+-}^+\} \to \{C, JC, JCT; H, \bar{U}_{+-}^+\}$	$Cl_{3,1} \to Cl_{3,2}$	$\mathcal{R}_6$
C	0	U_+^+	$\{C, JC; \emptyset\} \otimes U_+^+ \to \{C, JC; H\} \otimes U_+^+$	$Cl_{2,0} \otimes Cl_{0,1} \to Cl_{2,1} \otimes Cl_{0,1}$	$\mathcal{R}_6 \times \mathcal{R}_6$
C	1	$\bar{U}_-^-$	$\{C, JC, \bar{U}_-^-; \emptyset\} \to \{C, JC, \bar{U}_-^-; H\}$	$Cl_{3,0} \to Cl_{3,1}$	$\mathcal{R}_5$
C	2	U_+^-	$\{C, JC; \emptyset\} \otimes U_+^- \to \{C, JC; H\} \otimes U_+^-$	$Cl_{2,0} \otimes Cl_{1,0} \to Cl_{2,1} \otimes Cl_{1,0}$	$\mathcal{C}_0$
C	3	$\bar{U}_-^+$	$\{C, JC; \bar{U}_-^+\} \to \{C, JC; H, \bar{U}_-^+\}$	$Cl_{2,1} \to Cl_{2,2}$	$\mathcal{R}_7$
CI	0	U_{++}^+	$\{C, JC; JCT\} \otimes U_{++}^+ \to \{C, JC; H, JCT\} \otimes U_{++}^+$	$Cl_{2,1} \otimes Cl_{0,1} \to Cl_{2,2} \otimes Cl_{0,1}$	$\mathcal{R}_7 \times \mathcal{R}_7$
CI	1	$\bar{U}_{+-}^-$	$\{C, JC, \bar{U}_{+-}^-; JCT\} \to \{C, JC, \bar{U}_{+-}^-; H, JCT\}$	$Cl_{3,1} \to Cl_{3,2}$	$\mathcal{R}_6$
CI	2	U_{++}^-	$\{C, JC; JCT\} \otimes U_{++}^- \to \{C, JC; H, JCT\} \otimes U_{++}^-$	$Cl_{2,1} \otimes Cl_{1,0} \to Cl_{2,2} \otimes Cl_{1,0}$	$\mathcal{C}_1$
CI	3	$\bar{U}_{+-}^+$	$\{C, JC; JCT, \bar{U}_{+-}^+\} \to \{C, JC; H, JCT, \bar{U}_{+-}^+\}$	$Cl_{2,2} \to Cl_{2,3}$	$\mathcal{R}_0$

5 Properties of K-group with an additional order-two point group symmetry

5.1 Periodicity in flipped dimensions

The K-groups (3.2.4), (3.2.10), and (3.2.18) have common general properties. First, the K-groups do not depend on d, D, $d_\parallel$ and $D_\parallel$ separately, but they depend on their differences $\delta = d - D$ and $\delta_\parallel = d_\parallel - D_\parallel$. [38] Second, in addition to the mod 2 or mod 8 Bott-periodicity in space dimension δ, there exists a novel periodic structure in flipped dimensions $\delta_\parallel$, due to two-fold or fourfold periodicity in type t of additional symmetries. [38] Consequently, the presence of order-two additional symmetry provides four different families of periodic tables for topological crystalline insulators and superconductors and their topological defects:

- (i) $\delta_\parallel = 0$ family: The additional symmetry in this family includes non-spatial unitary symmetry such as two-fold spin rotation, where no spatial parameter is flipped in the bulk.
- (ii) $\delta_\parallel = 1$ family: This family includes bulk topological phases protected by reflection symmetry, where one direction of the momenta is flipped.
- (iii) $\delta_\parallel = 2$ family: Bulk topological phases protected by two-fold spatial rotation are categorized into this family.
- (iv) $\delta_\parallel = 3$ family: Inversion symmetric bulk topological phases are classified into this family.

Note that the correspondence between these additional symmetries and the families is shifted by $D_\parallel$ in the presence of topological defects. In the next chapter, we give periodic tables for those families and some concrete examples.

5.2 Defect gapless states as boundary gapless states

The differences $\delta = d - D$ and $\delta_\parallel = d_\parallel - D_\parallel$ have simple graphical meanings: First, we notice that a topological defect surrounded by S^D in d-dimensions defines a $(\delta-1)$-dimensional submanifold, since D is the defect codimension. For instance, a line defect in three dimensions has $\delta = 2$ ($d = 3$,$D = 1$), and thus it defines one-dimensional submanifold. Then, we also find that $\delta_\parallel$ indicates the number of flipped coordinates of the submanifold under the additional symmetry. For instance, see topological defects in $\delta_\parallel = 0$ family, illustrated in Fig. 4.1. Although the surrounding parameters of the topological defects transform nontrivially under the additional reflection or two-fold rotation, we find that the defects themselves are unaffected by the additional symmetries. In a similar manner, for topological defects of $\delta_\parallel = 1$ ($\delta_\parallel = 2$) family in Fig. 4.2 (Fig. 4.3), one-direction (two-directions) in the defect submanifold is (are) flipped under additional symmetries. In other words, additional symmetries in $\delta_\parallel = 1$ ($\delta_\parallel = 2$) family act on defect submanifolds in the same manner as reflection (two-fold rotation) whatever the original transformations are.

These graphical meanings provide a natural explanation why the K-groups depend solely on δ and $\delta_\parallel$: As first suggested by Read and Green,[37] the $(\delta - 1)$-dimensional defect submanifold can be considered as a boundary of a δ-dimensional insulator/superconductor. Then, the above geometrical observation implies that additional symmetries induce an effective symmetry with $\delta_\parallel$ flipped directions in the $(\delta - 1)$-dimensional defect submanifold, and thus also induce the same effective symmetry in the δ-dimensional insulator/superconductor. Consequently, the K-group of

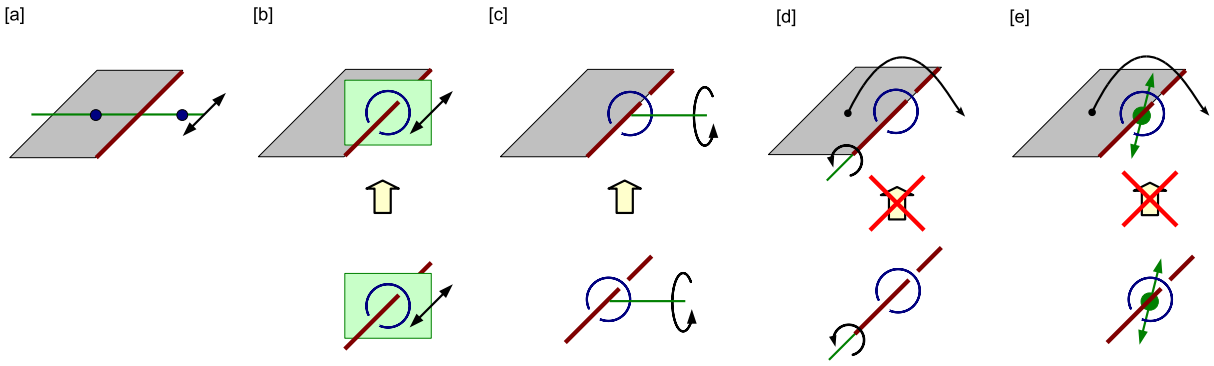

Figure 3.2: Line defects with additional order-two point group symmetry.

the topological defect reduces to that of the δ-dimensional crystalline insulator/superconductor with the $\delta_\parallel$ flipped additional symmetry.

For example, let us consider $(\delta, \delta_\parallel) = (2, 1)$ family which represents topological gapless states localized at line defects with a reflection-like symmetry on the defect. Fig. 3.2 [a-c] show examples of gapless states belonging to this family in lower-dimensions:

- [a] A boundary gapless state with refection symmetry $(d = 2, D = 0, d_\parallel = 1, D_\parallel = 0)$
- [b] A vortex gapless state with refection symmetry where the reflection plane is parallel to the vortex $(d = 3, D = 1, d_\parallel = 1, D_\parallel = 0)$
- [c] A vortex gapless state with two-fold rotation symmetry where the rotation axis is perpendicular to the vortex $(d = 3, D = 1, d_\parallel = 2, D_\parallel = 1)$

On the 2-dimensional planes in the upper figures in Fig. 3.2 [a-c], all the point group symmetries act on their planes as an effective reflection symmetry. If such effective symmetries obey the same representation, their topological classifications are the same, which is a physical meaning of the dimensional hierarchies (3.2.4), (3.2.10), and (3.2.18).

Also, It turns out that for topological protection of defect gapless states it is required that the condition $D_\parallel \leq D$ is satisfied, i.e., inversion symmetry-like point group symmetries on the defect surrounding sphere S^D does not protect gapless states. Since there is no δ-dimensional insulators in which their boundaries does not break the point group symmetry. [3] For example, let us consider

- [d] A vortex with two-fold rotation symmetry where the rotation axis is parallel the vortex
- [e] A vortex with inversion symmetry

as shown in Fig. 3.2 [d], [e]. The upper figures of [d], [e] show that the 2-dimensional planes with the boundary do not close under the point group transformations, which implies the such symmetries do not protect defect gapless states.

[3] In fact, we can prove isomorphisms (3.2.4), (3.2.10) and (3.2.18) only for the cases of $D_\parallel \leq D$.

6 Weak crystalline topological indices

Up to now, we have treated the base space of Hamiltonians as a $(d+D)$-dimensional sphere S^{d+D}. For band insulators, however, the actual base space is a direct product of a d-dimensional torus T^d and a D-dimensional sphere S^D, i.e. $T^d \times S^D$, because of the periodic structure of the Brillouin zone. The torus manifold gives rise to an extra topological structure. For example, the K-group of d-dimensional topological band insulators ($D=0$) in the real AZ class s ($s=0,1,\cdots,7$) is given as[5]

$$K_{\mathbb{R}}(s;T^d) \cong \pi_0(\mathcal{R}_{s-d}) \bigoplus_{q=1}^{d-1} \binom{d}{q} \pi_0(\mathcal{R}_{s-d+q}), \quad (d \geq 1). \tag{3.6.1}$$

The first term reproduces the K-group of the Hamiltonians on S^d, i.e. $K_{\mathbb{R}}(s;d,D=0)$, but there are extra terms that define weak topological indices. Here Eq. (3.6.1) does not include 0-dimensional indices $\pi_0(\mathcal{R}_s)$ since the base space d-dimensional torus T^d does not have Z_2 distinct parts.[94]

The extra terms in the presence of additional symmetry are more complicated than those of the above case because there are two different choices of lowering dimension, i.e. the parameters which is flipped by the additional symmetry transformation or not. The complete K-group for topological crystalline band insulators and superconductors in complex AZ classes with additional unitary symmetry is given by

$$\begin{aligned} &K^U_{\mathbb{C}}(s,t;T^d) \\ &\cong \bigoplus_{0\leq q_\perp \leq d-d_\parallel, 0\leq q_\parallel \leq d_\parallel, 0\leq q_\perp+q_\parallel \leq d-1} \binom{d-d_\parallel}{q_\perp} \binom{d_\parallel}{q_\parallel} K^U_{\mathbb{C}}(s,t;d-q_\perp-q_\parallel, d_\parallel-q_\parallel,0,0), \quad (d\geq 1) \end{aligned} \tag{3.6.2}$$

where $s=0,1$ and $t=0,1$ denote the AZ class and the unitary symmetry in Table 3.1. Similar results are obtained for those with additional antiunitary symmetry and those in real AZ classes.

To illustrate weak crystalline topological indices, consider an odd-parity superconductor in 3-dimensions. The full K-group on the torus T^3 is given by

$$\begin{aligned} &K^U_{\mathbb{R}}(s=2,t=2;d=3,d_\parallel=3,0,0;T^3) \\ &= K^U_{\mathbb{R}}(s=2,t=2;d=3,d_\parallel=3,0,0;S^3)(=\mathbb{Z}) \\ &\quad \bigoplus_{i=1}^{3} K^U_{\mathbb{R}}(s=2,t=2;d=2,d_\parallel=2,0,0;S^2_i) \left(=\bigoplus^{3}(\mathbb{Z}\oplus\mathbb{Z})\right) \\ &\quad \bigoplus_{i=1}^{3} K^U_{\mathbb{R}}(s=2,t=2;d=1,d_\parallel=1,0,0;S^1_i) \left(=\bigoplus^{3}\mathbb{Z}\right) \\ &= \bigoplus^{10}\mathbb{Z}, \end{aligned} \tag{3.6.3}$$

where S^2_i and S^1_i denote 2-dimensional and 1-dimensional spheres that are obtained as high symmetric submanifolds of the torus. This equation implies that there are ten $\mathbb{Z}$ crystalline topological indices. Among them, three indices are the weak first Chern numbers defined at fixed k_i plane T^2_i

$(i = x, y, z)$ in the Brillouin zone,

$$Ch_1^i = \frac{i}{2\pi}\frac{\epsilon_{ijk}}{2}\int_{T_i^2} \mathrm{tr}\mathcal{F}_{jk}(\boldsymbol{k}) \quad (i = x, y, z). \tag{3.6.4}$$

The other seven $\mathbb{Z}$ indices are defined at the eight symmetric points Γ_i $(i = 1, \dots 8)$ of inversion, which satisfy $\boldsymbol{k} = -\boldsymbol{k} + \boldsymbol{G}$ with a reciprocal vector $\boldsymbol{G}$. In the cubic lattice, these Γ_i are $\Gamma_1 = (0,0,0), \Gamma_2 = (\pi,0,0), \Gamma_3 = (0,\pi,0), \Gamma_4 = (0,0,\pi), \Gamma_5 = (\pi,\pi,0), \Gamma_6 = (\pi,0,\pi), \Gamma_7 = (0,\pi,\pi)$, and $\Gamma_8 = (\pi,\pi,\pi)$. The seven $\mathbb{Z}$ indices are

$$[\Gamma_{i,8}] = \#\Gamma_i^+ - \#\Gamma_8^+ = -(\#\Gamma_i^- - \#\Gamma_8^-), \quad (i = 1, \dots, 7), \tag{3.6.5}$$

where $\#\Gamma_i^\pm$ is the number of negative energy states with parity $\tilde{P} = \pm$ at Γ_i. Here we have used the relation $\#\Gamma_i^+ + \#\Gamma_i^- = \#\Gamma_j^+ + \#\Gamma_j^-$ for full gapped systems.

7 Topological classification of Fermi points with additional order-two point group symmetry

7.1 K-group of Fermi points

So far, we have argued topological classification of crystalline insulators and superconductors and their topological defects in the presence of an additional order-two symmetry. In this section, we will show that a similar but a slightly different argument works for classification of topological stable Fermi points in the momentum space.

The topological classification of Fermi points is done by the homotopy classification of Hamiltonians $\mathcal{H}(\boldsymbol{\kappa})$ where $\boldsymbol{\kappa} = (\kappa_1, \kappa_2, \cdots, \kappa_d)$ is coordinates of a d-dimensional sphere S^d surrounding Fermi points in the momentum space. Since the Hamiltonian $\mathcal{H}(\boldsymbol{\kappa})$ defines a map from S^d to a classifying space like classification of topological insulators, a similar K-group argument applies to the classification of Fermi points eventually. However, as is shown below, the application is not straightforward but a careful treatment of symmetry is needed.

The obstruction encountered here is non-trivial transformation of $\boldsymbol{\kappa} \in S^d$ under symmetry: Consider a Fermi point located at the origin in $(d+1)$-dimensions. A d-dimensional sphere S^d, which is defined as $\boldsymbol{k}^2 = k_1^2 + k_2^2 + \cdots k_{d+1}^2 = \epsilon^2$, encloses the Fermi point. Although $\boldsymbol{k}$ transforms as $\boldsymbol{k} \to -\boldsymbol{k}$ under TRS and/or PHS, any d-dimensional coordinates $\boldsymbol{\kappa} = (\kappa_1, \dots, \kappa_d)$ of S^d does not transform such a simple way. Therefore, one cannot directly apply our arguments so far to the Fermi points.

The key to resolve this difficulty is the dimension-raising map introduced in Sec.6.2 in Chap. 2: Formally, one can raise the dimension of the surrounding d-dimensional sphere, and map isomorphically a Hamiltonian $\mathcal{H}(\boldsymbol{\kappa})$ on S^d into $\mathcal{H}(\boldsymbol{\kappa}, \kappa_{d+1})$ on S^{d+1}. Then, topological classification of the original Hamiltonian $\mathcal{H}(\boldsymbol{\kappa})$ reduces to that of the mapped Hamiltonian $\mathcal{H}(\boldsymbol{\kappa}, \kappa_{d+1})$, which is found to be done in the framework developed so far.

The map from $\mathcal{H}(\boldsymbol{\kappa})$ to $\mathcal{H}(\boldsymbol{\kappa}, \kappa_{d+1})$ is constructed as follows. If the original Hamiltonian supports CS Γ, then the map is

$$\mathcal{H}_{\mathrm{nc}}(\boldsymbol{\kappa}, \kappa_{d+1} = \theta) = \sin\theta\mathcal{H}_{\mathrm{c}}(\boldsymbol{\kappa}) + \cos\theta\Gamma, \quad \theta \in [0, \pi] \tag{3.7.1}$$

and if not, then

$$\mathcal{H}_{\mathrm{c}}(\boldsymbol{\kappa}, \kappa_{d+1} = \theta) = \sin\theta\mathcal{H}_{\mathrm{nc}}(\boldsymbol{\kappa}) \otimes \tau_z + \cos\theta\mathbf{1} \otimes \tau_y, \quad \theta \in [0, \pi] \tag{3.7.2}$$

where the subscripts c and nc of $\mathcal{H}$ denote the presence and absence of CS, respectively. (The chiral operator of the latter Hamiltonian $\mathcal{H}_{\rm c}(\boldsymbol{\kappa}, \kappa_{d+1})$ is given by $\mathbf{1} \otimes \tau_x$.) Since $\mathcal{H}(\boldsymbol{\kappa}, \kappa_{d+1}) = $ const. at $\kappa_{d+1} = 0$ and $\kappa_{d+1} = \pi$, the d-dimensional sphere $\boldsymbol{\kappa} \in S^d$ can be contracted into a point either at $\kappa_{d+1} = 0$ and $\kappa_{d+1} = \pi$. The resultant space of $(\boldsymbol{\kappa}, \kappa_{d+1})$ is identified as a $(d+1)$-dimensional sphere S^{d+1} where $\boldsymbol{\kappa} \in S^d$ and κ_{d+1} parametrize the "circles of latitude" and the "meridian" of the $(d+1)$-dimensional sphere, respectively, and $\kappa_{d+1} = 0$ and $\kappa_{d+1} = \pi$ point to the "north and south poles". Because the inverse map also can be constructed in the meaning of stable equivalence, as explained in Sec.6.3 in Chap. 2, the topological nature of the mapped Hamiltonian is the same as that of the original one.

Let us now define TRS and/or PHS in the mapped Hamiltonian. To define them, we need to determine the transformation law of the new variable κ_{d+1} under these symmetries, since κ_{d+1} is an artificial variable, and thus no a priori transformation law is given. A convenient way is to treat the new variable κ_{d+1} as $\boldsymbol{r}$-type, which means that κ_{d+1} is invariant under TRS and/or PHS.

From the construction, it is evident that the TRS and/or PHS for the original Hamiltonian induce a two fold rotation of the $(d+1)$-dimensional sphere: If one represents the $(d+1)$-dimensional sphere S^{d+1} as $k_1^2 + k_2^2 \cdots + k_{d+1}^2 + k_{d+2}^2 = \epsilon^2$, TRS and/or PHS act as $(k_1, k_2, \cdots, k_{d+1}, k_{d+2}) \to (-k_1, -k_2, \cdots, -k_{d+1}, k_{d+2})$ in a suitable basis. Then, the following new reparametrization of S^{d+1}

$$\kappa_i = \frac{k_i}{\epsilon + k_{d+2}}, \quad (i = 1, \cdots, d+1), \tag{3.7.3}$$

simplifies the transformation law of $(\boldsymbol{\kappa}, \kappa_{d+1})$ as $(\boldsymbol{\kappa}, \kappa_{d+1}) \to (-\boldsymbol{\kappa}, -\kappa_{d+1})$. Therefore, the mapped Hamiltonian is categorized as a Hamiltonian discussed in Sec. 2.

Here note that the mapped Hamiltonian $\mathcal{H}(\boldsymbol{\kappa}, \kappa_{D+1})$ supports a different set of AZ symmetries than the original one since it loses or obtains CS. With a careful analysis of the symmetry, we find that the dimension-raising map shifts s of the K-groups of the original Hamiltonians by -1. Therefore, denoting the K-group of the Fermi point in AZ class s as $K_{\mathbb{F}}^{\rm FP}(s, d)$, we obtain

$$K_{\mathbb{F}}^{\rm FP}(s, d) = K_{\mathbb{F}}(s-1, d+1), \quad (\mathbb{F} = \mathbb{C}, \mathbb{R}), \tag{3.7.4}$$

where the right hand side is *the K-group of topological insulator and superconductors in AZ class s*. This relation reproduces the previous classification of the Fermi points by Hořava [95] and Zhao-Wang. [96, 97]

We can also classify Fermi points stabilized by an additional symmetry besides AZ symmetries: Under the assumption that the Fermi points are enclosed by a d-dimensional sphere S^d and they are invariant under the symmetries we consider, the K-groups for the Fermi points can be related to *the K-groups for $(d+1)$ dimensional topological crystalline insulators and superconductors in the presence of an additional symmetry*:

$$\begin{aligned}
K_{\mathbb{C}}^{U;{\rm FP}}(s, t; d, d_\parallel) &= K_{\mathbb{C}}^{U}(s-1, t; d+1, d_\parallel, 0, 0), \\
K_{\mathbb{C}}^{A;{\rm FP}}(s; d, d_\parallel) &= K_{\mathbb{C}}^{A}(s-1; d+1, d_\parallel, 0, 0), \\
K_{\mathbb{R}}^{U/A;{\rm FP}}(s, t; d, d_\parallel) &= K_{\mathbb{R}}^{U/A}(s-1, t; d+1, d_\parallel, 0, 0),
\end{aligned} \tag{3.7.5}$$

where $d_\parallel$ is the number of flipped momenta under the additional symmetry.

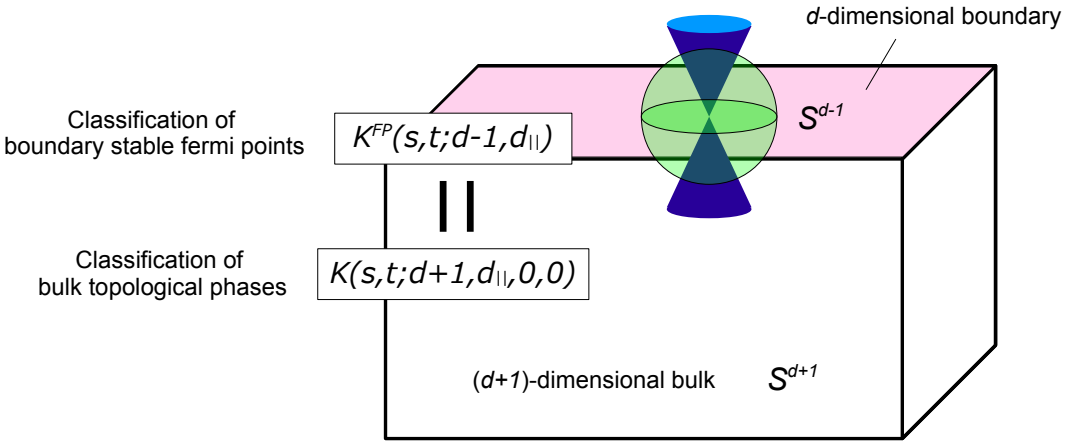

Figure 3.3: Bulk-boundary correspondence of topological crystalline phases with order-two point group symmetry.

7.2 Bulk-boundary correspondence of K-groups

Equations (3.7.4) and (3.7.5) provide a novel realization of the bulk-boundary correspondence, [29, 10, 98, 99, 97] in terms of the K-theory. First, consider Eq.(3.7.4). From the dimensional hierarchy in Eqs. (2.6.10) and (2.6.11), Eq.(3.7.4) is recast into

$$K_{\mathbb{F}}^{\mathrm{FP}}(s,d) = K_{\mathbb{F}}(s,d+2). \tag{3.7.6}$$

The relation (3.7.6) is nothing but the bulk-boundary correspondence: While the right hand side provides a bulk topological number of a $(d+2)$-dimensional insulator or superconductor, the left hand side ensures the existence of topologically stable surface Fermi points enclosed by a sufficiently large S^d in the $(d+1)$-dimensional surface momentum space.

In a similar manner, we can obtain the bulk-boundary correspondence of the K-group in the presence of an additional symmetry. From the dimensional hierarchy Eqs. (3.3.2) and (3.3.8) in the presence of additional symmetry, we obtain

$$\begin{aligned}
K_{\mathbb{C}}^{U;\mathrm{FP}}(s,t;d,d_{\|}) &= K_{\mathbb{C}}^{U}(s,t;d+2,d_{\|},0,0),\\
K_{\mathbb{C}}^{A;\mathrm{FP}}(s;d,d_{\|}) &= K_{\mathbb{C}}^{A}(s;d+2,d_{\|},0,0),\\
K_{\mathbb{R}}^{U/A;\mathrm{FP}}(s,t;d,d_{\|}) &= K_{\mathbb{R}}^{U/A}(s,t;d+2,d_{\|},0,0),
\end{aligned} \tag{3.7.7}$$

where the right hand sides represent bulk $(d+2)$-dimensional topological numbers of topological crystalline insulators and superconductors and the left hand sides give d-dimensional topological numbers of the corresponding $(d+1)$-dimensional surface states as shown in Fig. 3.3. Both topological numbers ensure the stability of topological crystalline phases.

Note that the number of the flipped momentum $d_\parallel$ is the same in the both sides of Eq.(3.7.7). Otherwise, the boundary breaks the additional symmetry in the bulk, and thus the bulk-boundary correspondence does not hold anymore.

7.3 Inversion symmetric Fermi points

To obtain the bulk-boundary correspondence, at least one-direction in the bulk should not be flipped under the additional symmetry. Indeed, if this happens, surfaces normal to the non-flipped direction preserve the additional symmetry. This condition implies that Eq.(3.7.7) holds only when $d_\parallel \leq d+1$.

Here note that the possible $d_\parallel$ can be larger than d, i.e. $d_\parallel = d+1$. In this case, the left hand side of Eq.(3.7.7) implies that the number of flipped coordinates of S^d surrounding Fermi points becomes larger than the total dimension d of S^d. This can be understood as follows. As was mentioned above, the bulk-boundary correspondence holds only for the surface normal to a non-flipped direction of the additional symmetry. Therefore, when $d_\parallel = d+1$, the additional symmetry flips all directions parallel to the surface. In other words, the additional symmetry induces inversion $\boldsymbol{k} \to -\boldsymbol{k}$ on the surface. In a manner similar to TRS and PHS, while the d-dimensional sphere surrounding Fermi points, $\boldsymbol{k}^2 \equiv k_1^2 + k_2^2 + \cdots + k_{d+1}^2 = \epsilon^2$, preserves the inversion symmetry, any d-dimensional coordinates $\boldsymbol{\kappa}$ of S^d transforms nontrivially under the inversion. This makes it possible to realize $d_\parallel > d$. As well as TRS and PHS, the dimension-raising is needed to obtain a simple transformation law of the surrounding coordinates.

We notice that such an inversion symmetric Fermi point may support a topological number in a unusual manner. For example, consider an inversion symmetric Fermi point in class AIII with $d = 0$, $d_\parallel = 1$ and U_+. From Eq.(3.7.7), the relevant K-group $K_{\mathbb{C}}^{U;FP}(1,0;0,1)$ is evaluated as $K_{\mathbb{C}}^{U}(1,0;2,1,0,0) = \pi_0(\mathcal{C}_0) = \mathbb{Z}$. Therefore, the Fermi point can be topologically stable. Indeed, such a topologically stable Fermi point is realize in the following model

$$\mathcal{H}(k) = \sigma_x k, \tag{3.7.8}$$

with the chiral operator $\Gamma = \sigma_z$ and inversion operator $U = \sigma_z$,

$$\{\Gamma, \mathcal{H}\} = 0, \quad U\mathcal{H}(k)U^\dagger = \mathcal{H}(-k). \tag{3.7.9}$$

The energy of this model is given by $E(k) = \pm k$, and thus there exists an inversion symmetric Fermi point at $k = 0$. Although the Fermi point can be gapped by the mass terms $m\sigma_y$ and $m'\sigma_z$, these terms are not allowed by the chiral and inversion symmetries. Therefore, the Fermi point is symmetry-protected. The Hamiltonian of the Fermi point is given by

$$\mathcal{H}(\kappa_0 = \pm) = \pm\sigma_z, \tag{3.7.10}$$

where the "sphere" surrounding the Fermi point consists of just two points $\kappa_0 = \pm$ in the present case.

To calculate the topological number of this class of model, we use the Hamiltonian mapped by the dimension raising,

$$\mathcal{H}(\kappa_0 = \pm, \kappa_1 = \theta) = \sin\theta\mathcal{H}(\kappa_0 = \pm) + \cos\theta\Gamma, \quad \theta \in [0, \pi]. \tag{3.7.11}$$

Inversion of the original Hamiltonian induces the following additional symmetry,

$$U\mathcal{H}(+,\theta)U^\dagger = \mathcal{H}(-,\theta). \tag{3.7.12}$$

Since the mapped Hamiltonian commutes with U at the high-symmetric points of this symmetry, i.e. at $\theta = 0, \pi$, the energy eigenstates at these points are decomposed into two subsets with different eigenvalues of U. Then, we can introduce a topological number by

$$N = \frac{(N_+(0) - N_-(0)) - (N_+(\pi) - N_-(\pi))}{2} = N_+(0) - N_+(\pi), \tag{3.7.13}$$

where $N_\pm$ is the number of negative energy states with the eigenvalue $U = \pm$. We find that $N = 1$ in the above model (3.7.8), which ensures topological stability of the Fermi point at $k = 0$.

Here note that at the high-symmetric points, the mapped Hamiltonian reduces to the chiral operator $\pm\Gamma$ of the original Hamiltonian. Therefore, in contrast to ordinary topological numbers, the topological number of the inversion symmetric Fermi point is not directly evaluated from the original Hamiltonian $\mathcal{H}(\kappa_0 = \pm)$, but it is implicitly encoded in the chiral operator Γ.

Now let see how the topological number of the chiral operator stabilizes the Fermi points. In general, a Fermi point of this class is described by the following Dirac Hamiltonian

$$\mathcal{H} = \gamma k, \tag{3.7.14}$$

with the chiral operator Γ and the inversion U

$$\{\Gamma, \mathcal{H}\} = 0, \quad U\mathcal{H}(k)U^\dagger = \mathcal{H}(-k), \quad [U, \Gamma] = 0. \tag{3.7.15}$$

If the Fermi point at $k = 0$ is topologically unstable, then there exists a mass term M consistent with Eq.(3.7.15). As the mass term satisfies

$$\{\gamma, M\} = 0, \quad \{\Gamma, M\} = 0, \quad [U, M] = 0, \tag{3.7.16}$$

it defines an extra CS Γ' by $\Gamma' = M/\sqrt{M^2}$. The existence of the extra CS, however, implies that N of Γ must be zero. Actually, using Γ', one can interpolate $\Gamma(0) = \Gamma$ and $\Gamma(\pi) = -\Gamma$ smoothly by $\Gamma(t) = \Gamma\cos t + \Gamma'\sin t$, which means $N = 0$ since Γ and $-\Gamma$ have an opposite topological number. As a result, we can conclude that the topological number must be zero to obtain a gap of the Fermi point.

Recently, topological fermi points protected by chiral symmetry Γ and inversion symmetry U with $[\Gamma, U] = 0$ were fully developed in Ref. [100].

8 Conclusion

In this chapter, we present a topological classification of crystalline insulators and superconductors and their topological defects that support order-two additional symmetry, besides AZ symmetries. The additional symmetry includes spin-rotation, reflection, π-rotation, and inversion. Their magnetic point group symmetries are also included. Using the dimensional hierarchy of K-groups, we can reduce the topological classification of Hamiltonians into that of simple matrices in 0-dimension. The obtained results are summarized in Eqs. (3.2.4), (3.2.10) and (3.2.18). These K-groups suggest that defect zero modes can be considered as boundary states of lower-dimensional crystalline insulators and superconductors. We also classify Fermi points stabilized by the additional symmetry, and derive the K-theory version of the bulk-boundary correspondence. Various symmetry protected topological phases and gapless modes are identified and discussed in a unified framework.

While we have completed a topological classification of crystalline insulators and superconductors with order-two additional symmetry, the full classification of topological crystalline insulators and superconductors has not been yet done. General crystalline symmetries admit higher-order symmetries such as C_n-rotation ($n = 3, 4, 6$), which are also responsible for non-trivial topological phases. [18, 101, 101, 102, 103, 104, 105, 106, 100] Even for these higher-order symmetries, the dimensional hierarchy of K-groups may hold as Thom isomorphism, and thus a similar K-theory approach is applicable,[85, 86, 81, 82] but we need a more sophisticated representation theory beyond the Clifford algebra in order to clarify these topological structures systematically.

Chapter 4

Periodic table in the presence of additional order-two symmetry

In the previous chapter, we have presented the K-groups for topological crystalline insulators and superconductors and their topological defects protected by order-two additional symmetry. The K-groups give exhaustive topological periodic tables for the symmetry protected topological phases. We clarify the Abelian group structures such as $\mathbb{Z}$ or $\mathbb{Z}_2$. Whereas we do not give all of the explicit expressions of the corresponding topological invariants, we illustrate how the topological tables work by using concrete examples. In the following sections, we focus on additional unitary and antiunitary symmetries. We omit here classification tables for additional antisymmetries because most of antisymmetries reduce to unitary or antiunitary symmetries by the symmetry equivalence relation.[1] Also, we omit antiunitary symmetry in the time-reversal symmetric AZ classes because antiunitary symmetry naturally realizes as a combination of time-reversal and point group symmetries, i.e. magnetic point group symmetry, in TRS broken systems.

Due to the 4-fold periodicity in the number of the flipped coordinates under the order-two additional point group symmetry, topological periodic tables are divided into four families: Z_2 global ($\delta_\parallel = 0$), reflection ($\delta_\parallel = 1$), two-fold rotation ($\delta_\parallel = 2$), and inversion ($\delta_\parallel = 3$). The resultant distinct symmetry classes consist of the (27×4)-fold classes for an additional order-two point group symmetry and the (10×4)-fold classes for an additional order-two magnetic point group symmetry.

1 Z_2 global family ($\delta_\parallel = 0$)

In this section, we consider additional symmetries with $\delta_\parallel = 0 \pmod 4$. In condensed matter contexts, relevant symmetries include order-two global symmetry such two-fold spin rotation ($d_\parallel = D_\parallel = 0$), reflection with a line and point defect in the mirror plane ($d_\parallel = D_\parallel = 1$), two-fold spatial rotation with a point defect on the rotation axis ($d_\parallel = D_\parallel = 2$), as illustrated in Fig. 4.1. We summarize the classification table for $\delta_\parallel = 0 \pmod 4$ with order-two unitary symmetries in Table 4.1 and that with antiunitary symmetries in Table 4.2, respectively.

[1] An unitary antisymmetry in class A, AI, and AII does not reduce to a conventional symmetry, but the realization of such antisymmetry is difficult in the condensed matter systems.

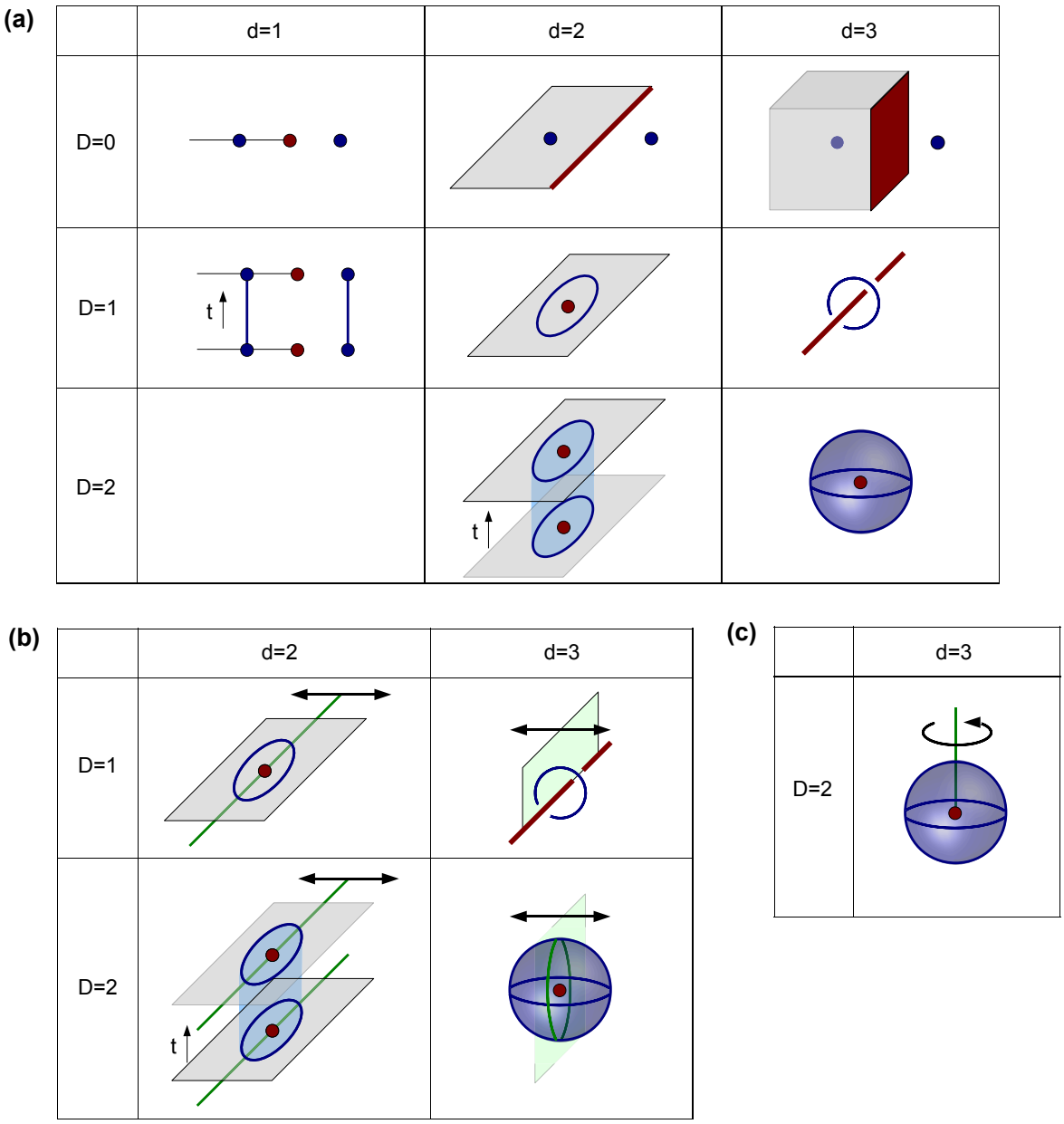

Figure 4.1: Topological defects and adiabatic pump protected by order-two additional symmetries with $\delta_{\|} = d_{\|} - D_{\|} = 0$. The additional symmetries are (a) global $\boldsymbol{Z}_2$ symmetry, (b) reflection symmetry and (c) π-rotation symmetry, respectively. The spatial position of topological defects is unchanged under the symmetry transformation of $\delta_{\|} = 0$ family. [38]

Table 4.1: Classification table for topological crystalline insulators and superconductors and their topological defects in the presence of order-two additional unitary symmetry with flipped parameters $\delta_\parallel \equiv d_\parallel - D_\parallel = 0 \pmod 4$. Here $\delta = d - D$.

Symmetry	Class	$\mathcal{C}_q$ or $\mathcal{R}_q$	$\delta=0$	$\delta=1$	$\delta=2$	$\delta=3$	$\delta=4$	$\delta=5$	$\delta=6$	$\delta=7$
U	A	$\mathcal{C}_0\times\mathcal{C}_0$	$\mathbb{Z}\oplus\mathbb{Z}$	0	$\mathbb{Z}\oplus\mathbb{Z}$	0	$\mathbb{Z}\oplus\mathbb{Z}$	0	$\mathbb{Z}\oplus\mathbb{Z}$	0
U_+	AIII	$\mathcal{C}_1\times\mathcal{C}_1$	0	$\mathbb{Z}\oplus\mathbb{Z}$	0	$\mathbb{Z}\oplus\mathbb{Z}$	0	$\mathbb{Z}\oplus\mathbb{Z}$	0	$\mathbb{Z}\oplus\mathbb{Z}$
U_-	AIII	$\mathcal{C}_0$	$\mathbb{Z}$	0	$\mathbb{Z}$	0	$\mathbb{Z}$	0	$\mathbb{Z}$	0
$U_+^+, U_-^-, U_{++}^+, U_{--}^-$	AI	$\mathcal{R}_0\times\mathcal{R}_0$	$\mathbb{Z}\oplus\mathbb{Z}$	0	0	0	$2\mathbb{Z}\oplus2\mathbb{Z}$	0	$\mathbb{Z}_2\oplus\mathbb{Z}_2$	$\mathbb{Z}_2\oplus\mathbb{Z}_2$
	BDI	$\mathcal{R}_1\times\mathcal{R}_1$	$\mathbb{Z}_2\oplus\mathbb{Z}_2$	$\mathbb{Z}\oplus\mathbb{Z}$	0	0	0	$2\mathbb{Z}\oplus2\mathbb{Z}$	0	$\mathbb{Z}_2\oplus\mathbb{Z}_2$
	D	$\mathcal{R}_2\times\mathcal{R}_2$	$\mathbb{Z}_2\oplus\mathbb{Z}_2$	$\mathbb{Z}_2\oplus\mathbb{Z}_2$	$\mathbb{Z}\oplus\mathbb{Z}$	0	0	0	$2\mathbb{Z}\oplus2\mathbb{Z}$	0
	DIII	$\mathcal{R}_3\times\mathcal{R}_3$	0	$\mathbb{Z}_2\oplus\mathbb{Z}_2$	$\mathbb{Z}_2\oplus\mathbb{Z}_2$	$\mathbb{Z}\oplus\mathbb{Z}$	0	0	0	$2\mathbb{Z}\oplus2\mathbb{Z}$
	AII	$\mathcal{R}_4\times\mathcal{R}_4$	$2\mathbb{Z}\oplus2\mathbb{Z}$	0	$\mathbb{Z}_2\oplus\mathbb{Z}_2$	$\mathbb{Z}_2\oplus\mathbb{Z}_2$	$\mathbb{Z}\oplus\mathbb{Z}$	0	0	0
	CII	$\mathcal{R}_5\times\mathcal{R}_5$	0	$2\mathbb{Z}\oplus2\mathbb{Z}$	0	$\mathbb{Z}_2\oplus\mathbb{Z}_2$	$\mathbb{Z}_2\oplus\mathbb{Z}_2$	$\mathbb{Z}\oplus\mathbb{Z}$	0	0
	C	$\mathcal{R}_6\times\mathcal{R}_6$	0	0	$2\mathbb{Z}\oplus2\mathbb{Z}$	0	$\mathbb{Z}_2\oplus\mathbb{Z}_2$	$\mathbb{Z}_2\oplus\mathbb{Z}_2$	$\mathbb{Z}\oplus\mathbb{Z}$	0
	CI	$\mathcal{R}_7\times\mathcal{R}_7$	0	0	0	$2\mathbb{Z}\oplus2\mathbb{Z}$	0	$\mathbb{Z}_2\oplus\mathbb{Z}_2$	$\mathbb{Z}_2\oplus\mathbb{Z}_2$	$\mathbb{Z}\oplus\mathbb{Z}$
U_{+-}^+, U_{-+}^-	BDI	$\mathcal{R}_0$	$\mathbb{Z}$	0	0	0	$2\mathbb{Z}$	0	$\mathbb{Z}_2$	$\mathbb{Z}_2$
U_{-+}^+, U_{+-}^-	DIII	$\mathcal{R}_2$	$\mathbb{Z}_2$	$\mathbb{Z}_2$	$\mathbb{Z}$	0	0	0	$2\mathbb{Z}$	0
U_{+-}^+, U_{-+}^-	CII	$\mathcal{R}_4$	$2\mathbb{Z}$	0	$\mathbb{Z}_2$	$\mathbb{Z}_2$	$\mathbb{Z}$	0	0	0
U_{-+}^+, U_{+-}^-	CI	$\mathcal{R}_6$	0	0	$2\mathbb{Z}$	0	$\mathbb{Z}_2$	$\mathbb{Z}_2$	$\mathbb{Z}$	0
U_-^+, U_+^-	AI, D, AII, C	$\mathcal{C}_0$	$\mathbb{Z}$	0	$\mathbb{Z}$	0	$\mathbb{Z}$	0	$\mathbb{Z}$	0
U_{--}^+, U_{++}^-	BDI, DIII, CII, CI	$\mathcal{C}_1$	0	$\mathbb{Z}$	0	$\mathbb{Z}$	0	$\mathbb{Z}$	0	$\mathbb{Z}$
U_{-+}^+, U_{+-}^-	BDI	$\mathcal{R}_2$	$\mathbb{Z}_2$	$\mathbb{Z}_2$	$\mathbb{Z}$	0	0	0	$2\mathbb{Z}$	0
U_{+-}^+, U_{-+}^-	DIII	$\mathcal{R}_4$	$2\mathbb{Z}$	0	$\mathbb{Z}_2$	$\mathbb{Z}_2$	$\mathbb{Z}$	0	0	0
U_{-+}^+, U_{+-}^-	CII	$\mathcal{R}_6$	0	0	$2\mathbb{Z}$	0	$\mathbb{Z}_2$	$\mathbb{Z}_2$	$\mathbb{Z}$	0
U_{+-}^+, U_{-+}^-	CI	$\mathcal{R}_0$	$\mathbb{Z}$	0	0	0	$2\mathbb{Z}$	0	$\mathbb{Z}_2$	$\mathbb{Z}_2$

1.1 Spin Chern insulator (U_+^- in class AII)

The simplest example of the symmetry protected topological phases is a quantum spin Hall insulator preserving the z-component of spin. [107] The system has TRS, and it is also invariant under the two-fold spin rotation along the z-axis,which is generated by $U = is_z$. Since the additional symmetry $U = is_z$ commutes with T, the system is categorized into class AII with U_+^- in 2-dimensions. Thus the topological nature is characterized by $\mathbb{Z}$, as is seen in Table 4.1.

The corresponding topological number is known as the spin Chern number: In the presence of non-spatial unitary symmetry $U = is_z$, the Hamiltonian $\mathcal{H}(k_x, k_y)$ of the system can be block-diagonal in the eigen basis of U with the eigenvalue $U = \pm i$. The anti-unitarity of T implies that TRS do not close in the each eigen sector, so each block of the Hamiltonian loses a real structure caused by TRS. In other words, $U = is_z$ plays a role of the imaginary unit i. Such an effect is called as *complexification*, which induces a complex structure in real AZ class. As a result, change of symmetry class, AII $\to$ A, occurs. The class A Hamiltonian is obtained by *forgetting* the real structure,

$$\tilde{\mathcal{H}}(k_x, k_y) := \frac{1}{2}\mathrm{Tr}_s\left[s_z \mathcal{H}(k_x, k_y)\right], \tag{4.1.1}$$

and the topological invariant is given by the 1st Chern character,

$$Ch_1 = \frac{i}{2\pi}\int \mathrm{tr}\tilde{\mathcal{F}}, \tag{4.1.2}$$

where $\tilde{\mathcal{F}}$ is the Berry curvature of the complexified Hamiltonian $\tilde{\mathcal{H}}(k_x, k_y)$. The topological invariant Eq. (4.1.2) is the spin Chern number.

To illustrate the complexification and the spin Chern number, consider the model Hamiltonian given by

$$\begin{aligned}\mathcal{H}(k_x, k_y) &= m(k_x, k_y)\sigma_z + vk_x\sigma_x s_z + vk_y\sigma_y,\\ m(k_x, k_y) &= m_0 - m_2(k_x^2 + k_y^2),\end{aligned} \tag{4.1.3}$$

where m_0 is the a mass, and v is a velocity. Here we have also introduced a cut-off m_2. In terms of $U = is_z$, the Hamiltonian is rewritten as $\mathcal{H}(\boldsymbol{k}) = m(\boldsymbol{k})\sigma_z - ivk_x\sigma_x U + vk_y\sigma_y$, and thus the complexified Hamiltonian, $\tilde{\mathcal{H}}(\boldsymbol{k}) = m(\boldsymbol{k})\sigma_z + vk_x\sigma_x + vk_y\sigma_y$, is given by replacing U with i. The spin Chern number Ch_1 of this model is $\mathrm{sgn}(m_0 m_2)$.

1.2 Mirror-odd two-dimensional topological superconductor (U_- in class D)

Consider a time-reversal broken (class D) superconductor in 2 dimensions:

$$\mathcal{H}_{\mathrm{BdG}}(k_x, k_y) = \begin{pmatrix} \epsilon(k_x, k_y) & \Delta(k_x, k_y) \\ \Delta^\dagger(k_x, k_y) & -\epsilon^T(-k_x, -k_y) \end{pmatrix} \tag{4.1.4}$$

As an additional symmetry, we assume here the mirror reflection symmetry with respect to the xy-plane. The reflection symmetry implies $M\epsilon(\boldsymbol{k})M^\dagger = \epsilon(\boldsymbol{k})$ with $M = is_z$, but the gap function $\Delta(\boldsymbol{k})$ can be mirror-even, $M\Delta(\boldsymbol{k})M^T = \Delta(\boldsymbol{k})$, or mirror-odd, $M\Delta(\boldsymbol{k})M^T = -\Delta(\boldsymbol{k})$. Even in the latter case, the BdG Hamiltonian can be invariant under the mirror reflection by performing simultaneously the $U(1)$ gauge symmetry $\Delta(\boldsymbol{k}) \to \Delta(\boldsymbol{k})e^{i\theta}$ with $\theta = \pi$.

First, examine the mirror odd case. In this case, the BdG Hamiltonian $\mathcal{H}_{\mathrm{BdG}}(\boldsymbol{k})$ commutes with $\tilde{M} = is_z\tau_0$. Since $\tilde{M}$ anticommutes with PHS, $C = \tau_x\mathcal{K}$, the additional symmetry $\tilde{M}$ is identified with U_- in class D. From Table 4.1, the topological index is $\mathbb{Z}\oplus\mathbb{Z}$.

The $\mathbb{Z}\oplus\mathbb{Z}$ structure can be understood as a pair of spinless class D superconductors: From the commutation relation $[\mathcal{H}(\boldsymbol{k}), \tilde{M}] = 0$, the BdG Hamiltonian can be block-diagonal into a pair of spinless systems with different eigen values of $\tilde{M} = \pm i$. The anti-unitarity of C and the anti-commutation relation $\{C, \tilde{M}\} = 0$ imply that each spinless system retains PHS, and thus it can be considered as a spinless class D superconductor. Since each 2-dimensional class D superconductor is characterized by the 1st Chern number, we obtain the $\mathbb{Z}\oplus\mathbb{Z}$ structure.

The model Hamiltonian is given by

$$\begin{aligned}\mathcal{H}_{\mathrm{BdG}}(k_x, k_y) &= \begin{pmatrix} \frac{k^2}{2m} - \mu - h_z s_z & \frac{\Delta_p}{k_{\mathrm{F}}}(k_x s_x + k_y s_y)is_y \\ -is_y\frac{\Delta_p}{k_{\mathrm{F}}}(k_x s_x + k_y s_y) & -\frac{k^2}{2m} + \mu + h_z s_z \end{pmatrix}\\ &= \left(\frac{k^2}{2m} - \mu\right)\tau_z - h_z s_z\tau_z - \frac{\Delta_p}{k_{\mathrm{F}}}k_x s_z\tau_x - \frac{\Delta_p}{k_{\mathrm{F}}}k_y\tau_y,\end{aligned} \tag{4.1.5}$$

where we have introduced the Zeeman term $h_z s_z$ in order to break TRS. In the diagonal basis with $\tilde{M} = \pm i$, we have

$$\mathcal{H}^{\pm}_{\mathrm{BdG}}(k_x, k_y) = \left(\frac{k^2}{2m} - \mu \mp h_z\right)\tau_z \mp \frac{\Delta_p}{k_{\mathrm{F}}}k_x\tau_x - \frac{\Delta_p}{k_{\mathrm{F}}}k_y\tau_y, \tag{4.1.6}$$

where each of $\mathcal{H}^{\pm}_{\rm BdG}(k_x,k_y)$ supports PHS, i.e. $C\mathcal{H}^{\pm}_{\rm BdG}(\boldsymbol{k})C^{-1}=-\mathcal{H}^{\pm}_{\rm BdG}(-\boldsymbol{k})$. The topological invariant for each sector is

$$Ch_1^{\pm}=\frac{i}{2\pi}\int {\rm tr}\mathcal{F}^{\pm}, \tag{4.1.7}$$

where $\mathcal{F}^{\pm}$ is the Berry curvature of $\mathcal{H}^{\pm}_{\rm BdG}(k_x,k_y)$. The Abelian group $\mathbb{Z}\oplus\mathbb{Z}$ is characterized by the two integers (Ch_1^+,Ch_1^-). Note that Ch_1^+ and Ch_1^- can be different from each other by adjusting h_z, which also confirms the direct sum structure of $\mathbb{Z}\oplus\mathbb{Z}$.

The presence of a vortex shifts δ as $\delta=1$. From Table 4.1, the topological index of the vortex is given by $\mathbb{Z}_2\oplus\mathbb{Z}_2$. In a thin film of ^{3}He-A under perpendicular Zeeman fields, one can create an integer quantum vortex, in which a pair of Majorana zero mode exist due to the mirror symmetry. The mirror protected Majorana zero mode gives rise to non-Abelian statistics of integer quantum vortices.[108]

1.3 Mirror-even two-dimensional topological superconductor (U_+^- in class D)

Now consider the mirror even case, where the mirror reflection operator for the BdG Hamiltonian is given by $\tilde{M}=is_z\tau_z$. From the commutation relation between $\tilde{M}$ and C, $\tilde{M}$ is identified as U_+^- in class D. The topological index is $\mathbb{Z}$.

Again the BdG Hamiltonian $\mathcal{H}_{\rm BdG}(\boldsymbol{k})$ can be block-diagonal in the eigen basis of $\tilde{M}$. However, in contrast to the mirror odd case, each spinless sector does not support PHS, and thus it belongs to class A. Moreover, because the spinless sectors are exchanged by C to keep PHS in the whole system, they cannot be independent, and thus they should have the essentially same structure. Hence, the topological index is not a direct sum, $\mathbb{Z}\oplus\mathbb{Z}$, but a single $\mathbb{Z}$.

The model Hamiltonian is given by

$$\begin{aligned}\mathcal{H}_{\rm BdG}(k_x,k_y) &= \begin{pmatrix}\frac{k^2}{2m}-\mu-h_zs_z & i\frac{\Delta_p}{k_{\rm F}}(k_x+ik_y)s_zs_y\\ -is_y\frac{\Delta_p}{k_{\rm F}}(k_x-ik_y)s_z & -\frac{k^2}{2m}+\mu+h_zs_z\end{pmatrix}\\ &= \left(\frac{k^2}{2m}-\mu\right)\tau_z-h_zs_z\tau_z+\frac{\Delta_p}{k_{\rm F}}k_xs_x\tau_x-\frac{\Delta_p}{k_{\rm F}}k_ys_x\tau_y.\end{aligned} \tag{4.1.8}$$

In the diagonal basis of $M_{\rm BdG}=\pm i$, we obtain

$$\mathcal{H}^{\pm}_{\rm BdG}(k_x,k_y)=\left(\frac{k^2}{2m}-\mu\right)\tau_z\pm h_z\tau_0+\frac{\Delta_p}{k_{\rm F}}k_x\tau_x-\frac{\Delta_p}{k_{\rm F}}k_y\tau_y. \tag{4.1.9}$$

Contrary to the mirror odd case, the Zeeman field h_z merely shifts the origin of energy, so the first Chern numbers $Ch_1^{\pm}$ of the two sectors coincide, i.e. $Ch_1^+=Ch_1^-$.

1.4 Superconducting nanowire with Rashba SO interaction and Zeeman fields (A_+^+, A_-^+ in class D)

Consider a time-reversal broken (class D) superconductor with the spin-orbit interaction in 1-dimension,[109, 110]

$$\mathcal{H}_{\rm BdG}(k_x) = \begin{pmatrix}\frac{k_x^2}{2m}-\mu+\lambda k_xs_y+\boldsymbol{h}\cdot\boldsymbol{s} & \Delta is_y\\ -is_y\Delta & -\frac{k_x^2}{2m}+\mu-\lambda k_xs_y-\boldsymbol{h}\cdot\boldsymbol{s}^T\end{pmatrix} \tag{4.1.10}$$

$$= \left(\frac{k_x^2}{2m}-\mu\right)\tau_z+\lambda k_xs_y\tau_z-\Delta s_y\tau_y+h_xs_x\tau_z+h_ys_y+h_zs_z\tau_z, \tag{4.1.11}$$

Table 4.2: Classification table for topological crystalline insulators and superconductors and their topological defects in the presence of order-two additional antiunitary symmetry with flipped parameters $\delta_\parallel = d_\parallel - D_\parallel = 0 \pmod 4$. Here $\delta = d - D$.

Symmetry	Class	$\mathcal{C}_q$ or $\mathcal{R}_q$	$\delta=0$	$\delta=1$	$\delta=2$	$\delta=3$	$\delta=4$	$\delta=5$	$\delta=6$	$\delta=7$
A^+	A	$\mathcal{R}_0$	$\mathbb{Z}$	0	0	0	$2\mathbb{Z}$	0	$\mathbb{Z}_2$	$\mathbb{Z}_2$
A^-	A	$\mathcal{R}_4$	$2\mathbb{Z}$	0	$\mathbb{Z}_2$	$\mathbb{Z}_2$	$\mathbb{Z}$	0	0	0
A^+_+	AIII	$\mathcal{R}_1$	$\mathbb{Z}_2$	$\mathbb{Z}$	0	0	0	$2\mathbb{Z}$	0	$\mathbb{Z}_2$
A^-_-	AIII	$\mathcal{R}_3$	0	$\mathbb{Z}_2$	$\mathbb{Z}_2$	$\mathbb{Z}$	0	0	0	$2\mathbb{Z}$
A^-_+	AIII	$\mathcal{R}_5$	0	$2\mathbb{Z}$	0	$\mathbb{Z}_2$	$\mathbb{Z}_2$	$\mathbb{Z}$	0	0
A^+_-	AIII	$\mathcal{R}_7$	0	0	0	$2\mathbb{Z}$	0	$\mathbb{Z}_2$	$\mathbb{Z}_2$	$\mathbb{Z}$
A^+_+, A^+_-	D	$\mathcal{R}_1$	$\mathbb{Z}_2$	$\mathbb{Z}$	0	0	0	$2\mathbb{Z}$	0	$\mathbb{Z}_2$
A^-_+, A^-_-	C	$\mathcal{R}_5$	0	$2\mathbb{Z}$	0	$\mathbb{Z}_2$	$\mathbb{Z}_2$	$\mathbb{Z}$	0	0
A^-_+, A^-_-	D	$\mathcal{R}_3$	0	$\mathbb{Z}_2$	$\mathbb{Z}_2$	$\mathbb{Z}$	0	0	0	$2\mathbb{Z}$
A^+_+, A^+_-	C	$\mathcal{R}_7$	0	0	0	$2\mathbb{Z}$	0	$\mathbb{Z}_2$	$\mathbb{Z}_2$	$\mathbb{Z}$

where $\lambda k_x s_y \tau_z$ is the Rashba spin-orbit interaction term, Δ is an s-wave pairing, and $\boldsymbol{h}$ is the Zeeman field. Equation (4.1.11) is the low-energy effective Hamiltonian describing a 1-dimensional nanowire with the Rashba spin-orbit interaction and a proximity induced s-wave superconductivity. In the absence of the Zeeman field, TRS, $T = is_y\mathcal{K}$, and mirror reflection symmetry with respect to zx-plane, $\mathcal{M}_{zx} = is_y$, are preserved. The Zeeman field breaks both TRS and the mirror reflection symmetry, however, if $h_y = 0$ it retains an antiunitary symmetry which is obtained as their combination $A = \mathcal{M}_{zx}T = \mathcal{K}$:[111] $A\mathcal{H}(-k_x)A^{-1} = \mathcal{H}(k_x)$. This system hosts topological superconductivity when $|\boldsymbol{h}| > \sqrt{\Delta^2 + \mu^2}$. [112, 113]

As the symmetry operator A commutes with the particle-hole transformation $C = \tau_x\mathcal{K}$, it is labeled as A^+_+ in class D of Table 4.2. The anti-symmetry $A = \mathcal{K}$ defines an emergent spinless TRS [114, 115, 111] because of $A^2 = 1$, which changes the AZ symmetry class effectively as D $\to$ BDI. The topological number $\mathbb{Z}$ in Table 4.2 (A^+_+ in class D with $\delta = 1$) is the winding number of the emergent class BDI,

$$N_1 = \frac{1}{4\pi i}\int \mathrm{tr}\left[\tau_x \mathcal{H}^{-1} d\mathcal{H}\right], \tag{4.1.12}$$

with the chiral operator $\tau_x = CA$. Note that since the emergent class BDI is not accidental but it is originated from the symmetry of the configuration, the same topological characterization works even for multi-band nanowires as far as the wire configuration respects the symmetry [111].

In the above, we have assumed an s-wave pairing, but even for other unconventional pairings,[116, 117] one can obtain a similar topological characterization if the gap function has a definite parity under the mirror reflection with respect to the zx plane: If the pairing is even under the mirror reflection $\mathcal{M}_{zx}$, the same antiunitary symmetry A^+_+ characterizes the system, but even if the pairing is mirror-odd, a similar emergent TRS is obtained as $A = \tau_z\mathcal{K}$ by combining TRS and the mirror operator of this case $\mathcal{M}_{zx} = is_y\tau_z$ [83]. Because the particle-hole transformation $C = \tau_x\mathcal{K}$ anti-commutes with the latter A, it is labeled as A^+_- in class D of Table 4.2. The corresponding topological number is $\mathbb{Z}$ again in 1-dimension.

1.5 Vortex in two-dimensional superconductors with magnetic in-plane reflection symmetry (A_+^+, A_-^+ in class D)

Consider a 2-dimensional time-reversal invariant superconductor,

$$\mathcal{H}_{\rm BdG}(k_x,k_y)=\begin{pmatrix}\epsilon(k_x,k_y) & \Delta(k_x,k_y)\\ \Delta^\dagger(k_x,k_y) & -\epsilon^T(-k_x,-k_y)\end{pmatrix}, \tag{4.1.13}$$

with in-plane mirror reflection symmetry that flips the x-direction. The mirror symmetry implies

$$M_x\epsilon(k_x,k_y)M_x^\dagger=\epsilon(-k_x,k_y),\quad M_x=is_x, \tag{4.1.14}$$

in the normal part, but in a manner similar to Sec. 1.2, two different realizations (mirror even and mirror odd) are possible in the gap function

$$M_x\Delta(k_x,k_y)M_x^T=\pm\Delta(-k_x,k_y), \tag{4.1.15}$$

due to the U(1) gauge symmetry. The mirror symmetry is summarized as

$$\tilde{M}_x\mathcal{H}_{\rm BdG}(k_x,k_y)\tilde{M}_x^\dagger=\mathcal{H}_{\rm BdG}(-k_x,k_y), \tag{4.1.16}$$

with $\tilde{M}_x=is_x\tau_z$ ($\tilde{M}_x=is_x\tau_0$) for the mirror even (odd) gap function.

Now explore topological properties of a vortex in this system. Applying a magnetic field normal to the system, one can create a vortex. The adiabatic (semiclassical) BdG Hamiltonian with a vortex is given by

$$\mathcal{H}_{\rm BdG}(k_x,k_y,\phi)=\begin{pmatrix}\epsilon(k_x,k_y) & \Delta(k_x,k_y,\phi)\\ \Delta^\dagger(k_x,k_y,\phi) & -\epsilon^T(-k_x,-k_y)\end{pmatrix}, \tag{4.1.17}$$

where ϕ denotes the angle around the vortex measured from the y-axis. Since ϕ transforms as $\phi\to-\phi$ under the mirror reflection, the vortex configuration $\Delta(k_x,k_y,\phi)\sim\Delta(k_x,k_y)e^{i\phi}$ breaks the mirror reflection symmetry as well as TRS, but the combination of these two symmetries remains,

$$A_x\mathcal{H}_{\rm BdG}(k_x,k_y,\phi)A_x^{-1}=\mathcal{H}_{\rm BdG}(k_x,-k_y,-\phi) \tag{4.1.18}$$

with $A_x=T\tilde{M}_x$. The magnetic in-plane reflection symmetry A_x is labeled as A_-^+ or A_+^+ in class D of Table 4.2, and thus the topological index of the vortex ($\delta=1$, $\delta_\parallel=0$) is given by $\mathbb{Z}$.

A vortex in 2-dimensional chiral p_x+ip_y superconductors also has the same magnetic in-plane reflection symmetry. Although chiral p_x+ip_y gap functions explicitly break TRS as well as the in-plane reflection symmetry, they preserve the magnetic in-plane reflection symmetry up to the U(1) gauge symmetry. Consequently, a vortex also preserves the magnetic in-plane reflection symmetry, and thus the topological index of the vortex is also given by $\mathbb{Z}$.

In the mirror-symmetric subspace defined by $k_x=0$, $\phi=0$ or $k_x=0$, $\phi=\pi$, the magnetic in-plane reflection symmetry in class D implies the presence of CS,

$$\Gamma_x\mathcal{H}(0,k_y,\phi)\Gamma_x^{-1}=\mathcal{H}(0,k_y,\phi),\quad(\phi=0,\pi) \tag{4.1.19}$$

where $\Gamma_x=CA_x$ with the particle-hole operator C. Using CS, one can define two 1-dimensional winding numbers as

$$N_1^{\phi=0,\pi}=\frac{1}{4\pi i}\int{\rm tr}[\Gamma_x\mathcal{H}_{\rm BdG}^{-1}(0,k_y,\phi)d_{k_y}\mathcal{H}_{\rm BdG}(0,k_y,\phi)]\big|_{\phi=0,\pi}. \tag{4.1.20}$$

Among these two $\mathbb{Z}$ indices, only the difference is relevant to topologically stable zero modes in the vortex. Indeed if they are the same, i.e. $N_1^0 = N_1^\pi$, the vortex can be smoothly deformed into the bulk without a topological obstruction, and thus vortex zero modes, even if they exist, disappear. This means that the $\mathbb{Z}$ index of the vortex, which ensures the topological stability of vortex zero modes, is proportional to $N_1^0 - N_1^\pi$.

To determine the proportional constant, consider a representative Hamiltonian with the same magnetic in-plane reflection symmetry,

$$\mathcal{H}_1 = \begin{pmatrix} \frac{k^2}{2m} - \mu & i\Delta e^{i\phi}(k_x + ik_y) \\ -i\Delta e^{-i\phi}(k_x - ik_y) & -\frac{k^2}{2m} + \mu \end{pmatrix}, \tag{4.1.21}$$

where the particle-hole transformation and the magnetic reflection are given by $C = \tau_x K$ and $A = \tau_z K$, respectively. This model supports a single zero mode localized at the vortex,[118] and its topological index is

$$(N_1^0, N_1^\pi)\big|_{\mathcal{H}_1} = (1, -1). \tag{4.1.22}$$

Therefore, in order for the $\mathbb{Z}$ index of the vortex, N_1^{vortex}, to be equal to the number of vortex zero modes, the proportional constant should be $1/2$,

$$N_1^{\text{vortex}} = \frac{N_1^0 - N_1^\pi}{2}. \tag{4.1.23}$$

2 Reflection family ($\delta_\parallel = 1$)

In this section, we consider additional symmetries with $\delta_\parallel = 1 \pmod 4$. In condensed matter contexts, relevant symmetries include reflection symmetry ($d_\parallel = 1, D_\parallel = 0$) and π-rotation symmetry with one flipping defect surrounding parameter ($d_\parallel = 2, D_\parallel = 1$) as shown in Fig. 4.2. A common nature of the $\delta_\parallel = 1$ family is that the additional symmetries act on defect submanifolds as reflection. We summarize the classification table for $\delta_\parallel = 1 \pmod 4$ with additional unitary symmetry in Table 4.3 and that with antiunitary symmetry in Table 4.4, respectively. A complete classification of the bulk topological phase with reflection symmetry was given by Chiu et al. [119], and Morimoto-Furusaki [68]. New results are the classification of topological defects, and that with antiunitary symmetry. In the following sections, we illustrate some examples.

2.1 Topological number $\mathbb{Z} \oplus \mathbb{Z}$

First, we give a concrete expression of the topological number $\mathbb{Z} \oplus \mathbb{Z}$ in Table 4.3. This number is denoted by "$\mathbb{Z}^1$" in the classification table by Chiu, et. al. [119] The topological number consists of two topological invariants. For odd (even) spatial dimensions d, one is the winding number N_{2n+1} (the Chern character), and the other is the mirror Chern number (the mirror winding number). While the former topological invariant can be defined without the additional symmetry, the latter cannot.

For example, we consider class AIII system with a U_- additional symmetry in 3 dimensions. The Hamiltonian has the following symmetry:

$$\Gamma\mathcal{H}(k_x, k_y, k_z)\Gamma^{-1} = -\mathcal{H}(k_x, k_y, k_z), \tag{4.2.1}$$

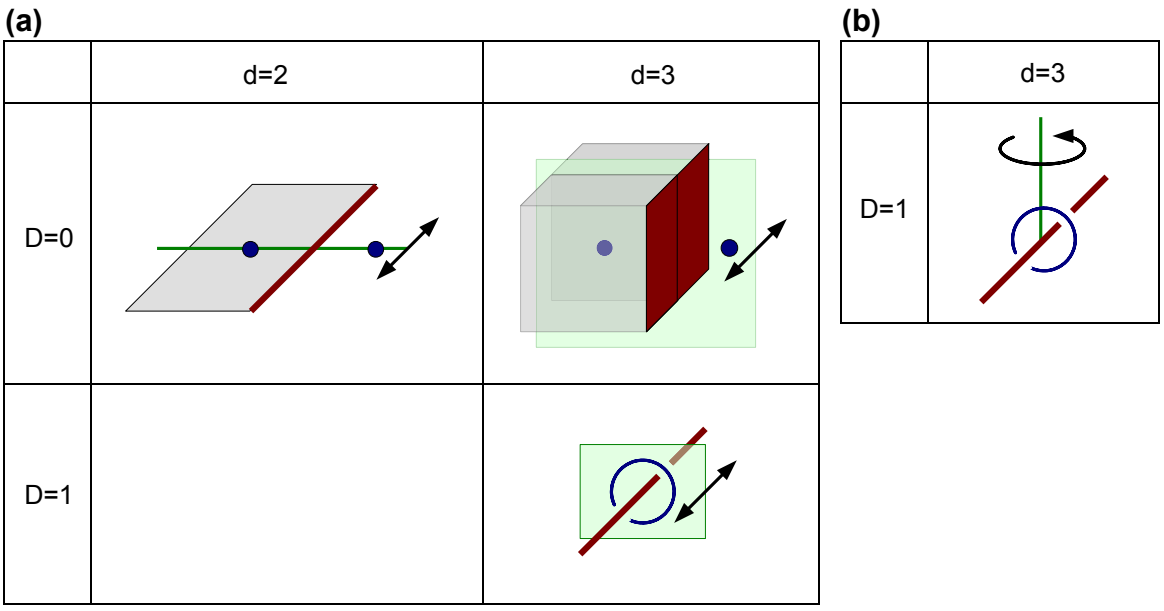

Figure 4.2: Topological defects protected by order-two additional symmetries with $\delta_{\|} = d_{\|} - D_{\|} = 1$. The additional symmetries are (a) reflection symmetry and (b) π-rotation symmetry, respectively. The spatial position of topological defects is transformed as reflection under the symmetry transformation of $\delta_{\|} = 1$ family. [38]

$$U\mathcal{H}(k_x, k_y, k_z)U^{-1} = \mathcal{H}(-k_x, k_y, k_z), \quad \{U, \Gamma\} = 0. \tag{4.2.2}$$

The winding number is defined as

$$N_3 = \frac{1}{48\pi^2} \int_{S^3} \mathrm{tr}\Gamma \left[\mathcal{H}^{-1} d\mathcal{H}\right]^3. \tag{4.2.3}$$

Note that reflection symmetry U_- does not eliminate the winding number because $U\Gamma U^{-1} = -\Gamma$ and $U\left[\mathcal{H}^{-1}d\mathcal{H}\right]^3 U^{-1} = -\left[\mathcal{H}^{-1}d\mathcal{H}\right]^3$.

In addition to N_3, we can introduce the first Chern number on the mirror invariant plane with $k_x = 0$: On the mirror invariant plane, the Hamiltonian $\mathcal{H}(0, k_y, k_z)$ can be block diagonal in the basis of eigenstates of $U = \pm$ since it commutes with U, i.e. $[U, \mathcal{H}(0, k_y, k_z)] = 0$. Then the first Chern number is defined as

$$Ch_1^{\pm} = \frac{i}{2\pi} \int_{S^2} \mathrm{tr}\mathcal{F}^{\pm}, \tag{4.2.4}$$

where $\mathcal{F}^{\pm}$ is the Berry curvature of the Hamiltonian $\mathcal{H}(0, k_y, k_z)$ in the $U = \pm$ sector. Here note that the two Chern numbers Ch_1^+ and Ch_1^- are not independent. In fact, the total first Chern number should be trivial in the sense of strong topological index in three dimensions, $Ch_1^+ + Ch_1^- = 0$ [120]. Hence the meaningful topological invariant is only the difference between Ch_1^+ and Ch_2^-,

$$N_{M\mathbb{Z}} = \frac{Ch_1^+ - Ch_1^-}{2}. \tag{4.2.5}$$

Table 4.3: Classification table for topological crystalline insulators and superconductors and their topological defects in the presence of order-two additional unitary symmetry with flipped parameters $\delta_\parallel = d_\parallel - D_\parallel = 1 \pmod 4$. Here $\delta = d - D$.

Symmetry	Class	$\mathcal{C}_q$ or $\mathcal{R}_q$	$\delta=0$	$\delta=1$	$\delta=2$	$\delta=3$	$\delta=4$	$\delta=5$	$\delta=6$	$\delta=7$
U	A	$\mathcal{C}_1$	0	$\mathbb{Z}$	0	$\mathbb{Z}$	0	$\mathbb{Z}$	0	$\mathbb{Z}$
U_+	AIII	$\mathcal{C}_0$	$\mathbb{Z}$	0	$\mathbb{Z}$	0	$\mathbb{Z}$	0	$\mathbb{Z}$	0
U_-	AIII	$\mathcal{C}_1 \times \mathcal{C}_1$	0	$\mathbb{Z}\oplus\mathbb{Z}$	0	$\mathbb{Z}\oplus\mathbb{Z}$	0	$\mathbb{Z}\oplus\mathbb{Z}$	0	$\mathbb{Z}\oplus\mathbb{Z}$
$U_+^+, U_-^-, U_{++}^+, U_{--}^-$	AI	$\mathcal{R}_1$	$\mathbb{Z}_2$	$\mathbb{Z}$	0	0	0	$2\mathbb{Z}$	0	$\mathbb{Z}_2$
	BDI	$\mathcal{R}_2$	$\mathbb{Z}_2$	$\mathbb{Z}_2$	$\mathbb{Z}$	0	0	0	$2\mathbb{Z}$	0
	D	$\mathcal{R}_3$	0	$\mathbb{Z}_2$	$\mathbb{Z}_2$	$\mathbb{Z}$	0	0	0	$2\mathbb{Z}$
	DIII	$\mathcal{R}_4$	$2\mathbb{Z}$	0	$\mathbb{Z}_2$	$\mathbb{Z}_2$	$\mathbb{Z}$	0	0	0
	AII	$\mathcal{R}_5$	0	$2\mathbb{Z}$	0	$\mathbb{Z}_2$	$\mathbb{Z}_2$	$\mathbb{Z}$	0	0
	CII	$\mathcal{R}_6$	0	0	$2\mathbb{Z}$	0	$\mathbb{Z}_2$	$\mathbb{Z}_2$	$\mathbb{Z}$	0
	C	$\mathcal{R}_7$	0	0	0	$2\mathbb{Z}$	0	$\mathbb{Z}_2$	$\mathbb{Z}_2$	$\mathbb{Z}$
	CI	$\mathcal{R}_0$	$\mathbb{Z}$	0	0	0	$2\mathbb{Z}$	0	$\mathbb{Z}_2$	$\mathbb{Z}_2$
U_{+-}^+, U_{-+}^-	BDI	$\mathcal{R}_1 \times \mathcal{R}_1$	$\mathbb{Z}_2\oplus\mathbb{Z}_2$	$\mathbb{Z}\oplus\mathbb{Z}$	0	0	0	$2\mathbb{Z}\oplus 2\mathbb{Z}$	0	$\mathbb{Z}_2\oplus\mathbb{Z}_2$
U_{-+}^+, U_{+-}^-	DIII	$\mathcal{R}_3 \times \mathcal{R}_3$	0	$\mathbb{Z}_2\oplus\mathbb{Z}_2$	$\mathbb{Z}_2\oplus\mathbb{Z}_2$	$\mathbb{Z}\oplus\mathbb{Z}$	0	0	0	$2\mathbb{Z}\oplus 2\mathbb{Z}$
U_{+-}^+, U_{-+}^-	CII	$\mathcal{R}_5 \times \mathcal{R}_5$	0	$2\mathbb{Z}\oplus 2\mathbb{Z}$	0	$\mathbb{Z}_2\oplus\mathbb{Z}_2$	$\mathbb{Z}_2\oplus\mathbb{Z}_2$	$\mathbb{Z}\oplus\mathbb{Z}$	0	0
U_{-+}^+, U_{+-}^-	CI	$\mathcal{R}_7 \times \mathcal{R}_7$	0	0	0	$2\mathbb{Z}\oplus 2\mathbb{Z}$	0	$\mathbb{Z}_2\oplus\mathbb{Z}_2$	$\mathbb{Z}_2\oplus\mathbb{Z}_2$	$\mathbb{Z}\oplus\mathbb{Z}$
$U_-^+, U_+^-, U_{--}^+, U_{++}^-$	AI	$\mathcal{R}_7$	0	0	0	$2\mathbb{Z}$	0	$\mathbb{Z}_2$	$\mathbb{Z}_2$	$\mathbb{Z}$
	BDI	$\mathcal{R}_0$	$\mathbb{Z}$	0	0	0	$2\mathbb{Z}$	0	$\mathbb{Z}_2$	$\mathbb{Z}_2$
	D	$\mathcal{R}_1$	$\mathbb{Z}_2$	$\mathbb{Z}$	0	0	0	$2\mathbb{Z}$	0	$\mathbb{Z}_2$
	DIII	$\mathcal{R}_2$	$\mathbb{Z}_2$	$\mathbb{Z}_2$	$\mathbb{Z}$	0	0	0	$2\mathbb{Z}$	0
	AII	$\mathcal{R}_3$	0	$\mathbb{Z}_2$	$\mathbb{Z}_2$	$\mathbb{Z}$	0	0	0	$2\mathbb{Z}$
	CII	$\mathcal{R}_4$	$2\mathbb{Z}$	0	$\mathbb{Z}_2$	$\mathbb{Z}_2$	$\mathbb{Z}$	0	0	0
	C	$\mathcal{R}_5$	0	$2\mathbb{Z}$	0	$\mathbb{Z}_2$	$\mathbb{Z}_2$	$\mathbb{Z}$	0	0
	CI	$\mathcal{R}_6$	0	0	$2\mathbb{Z}$	0	$\mathbb{Z}_2$	$\mathbb{Z}_2$	$\mathbb{Z}$	0
U_{-+}^+, U_{+-}^-	BDI, CII	$\mathcal{C}_1$	0	$\mathbb{Z}$	0	$\mathbb{Z}$	0	$\mathbb{Z}$	0	$\mathbb{Z}$
U_{+-}^+, U_{-+}^-	DIII, CI	$\mathcal{C}_1$	0	$\mathbb{Z}$	0	$\mathbb{Z}$	0	$\mathbb{Z}$	0	$\mathbb{Z}$

Consequently, the K-group is characterized by N_3 and $N_{M\mathbb{Z}}$:

$$(N_3, N_{M\mathbb{Z}}) \in \mathbb{Z}\oplus\mathbb{Z}. \tag{4.2.6}$$

2.2 Mirror reflection symmetric vortex in three-dimensional superconductors (U_-^- in class D)

Mirror reflection symmetry may protect Majorana gapless modes propagating a vortex in 3 dimensions. Consider a superconductor in 3 dimensions,

$$\mathcal{H}_{\mathrm{BdG}}(\boldsymbol{k}) = \begin{pmatrix} \epsilon(\boldsymbol{k}) & \Delta(\boldsymbol{k}) \\ \Delta^\dagger(\boldsymbol{k}) & -\epsilon^T(-\boldsymbol{k}) \end{pmatrix}. \tag{4.2.7}$$

As was mentioned in Sec. 1.2, mirror reflection symmetry with respect to the xy-plane implies that the normal part is invariant under the mirror reflection

$$M_{xy}\epsilon(k_x,k_y,k_z)M_{xy}^\dagger = \epsilon(k_x,k_y,-k_z), \quad M_{xy} = is_z \tag{4.2.8}$$

Table 4.4: Classification table for topological crystalline insulators and superconductors and their topological defects in the presence of order-two additional antiunitary symmetry with flipped parameters $\delta_\parallel = d_\parallel - D_\parallel = 1 \pmod 4$. Here $\delta = d - D$.

Symmetry	Class	$\mathcal{C}_q$ or $\mathcal{R}_q$	$\delta=0$	$\delta=1$	$\delta=2$	$\delta=3$	$\delta=4$	$\delta=5$	$\delta=6$	$\delta=7$
A^+	A	$\mathcal{R}_2$	$\mathbb{Z}_2$	$\mathbb{Z}_2$	$\mathbb{Z}$	0	0	0	$2\mathbb{Z}$	0
A^-	A	$\mathcal{R}_6$	0	0	$2\mathbb{Z}$	0	$\mathbb{Z}_2$	$\mathbb{Z}_2$	$\mathbb{Z}$	0
A^+_+	AIII	$\mathcal{R}_3$	0	$\mathbb{Z}_2$	$\mathbb{Z}_2$	$\mathbb{Z}$	0	0	0	$2\mathbb{Z}$
A^-_-	AIII	$\mathcal{R}_5$	0	$2\mathbb{Z}$	0	$\mathbb{Z}_2$	$\mathbb{Z}_2$	$\mathbb{Z}$	0	0
A^-_+	AIII	$\mathcal{R}_7$	0	0	0	$2\mathbb{Z}$	0	$\mathbb{Z}_2$	$\mathbb{Z}_2$	$\mathbb{Z}$
A^+_-	AIII	$\mathcal{R}_1$	$\mathbb{Z}_2$	$\mathbb{Z}$	0	0	0	$2\mathbb{Z}$	0	$\mathbb{Z}_2$
A^+_+, A^+_-	D	$\mathcal{R}_2 \times \mathcal{R}_2$	$\mathbb{Z}_2 \oplus \mathbb{Z}_2$	$\mathbb{Z}_2 \oplus \mathbb{Z}_2$	$\mathbb{Z} \oplus \mathbb{Z}$	0	0	0	$2\mathbb{Z} \oplus 2\mathbb{Z}$	0
A^-_+, A^-_-	C	$\mathcal{R}_6 \times \mathcal{R}_6$	0	0	$2\mathbb{Z} \oplus 2\mathbb{Z}$	0	$\mathbb{Z}_2 \oplus \mathbb{Z}_2$	$\mathbb{Z}_2 \oplus \mathbb{Z}_2$	$\mathbb{Z} \oplus \mathbb{Z}$	0
A^-_+, A^-_-	D	$\mathcal{C}_0$	$\mathbb{Z}$	0	$\mathbb{Z}$	0	$\mathbb{Z}$	0	$\mathbb{Z}$	0
A^+_+, A^+_-	C	$\mathcal{C}_0$	$\mathbb{Z}$	0	$\mathbb{Z}$	0	$\mathbb{Z}$	0	$\mathbb{Z}$	0

but the gap function can be either mirror even or mirror odd

$$M_{xy}\Delta(k_x, k_y, k_z)M_{xy}^T = \pm\Delta(k_x, k_y, -k_z). \tag{4.2.9}$$

When the gap function is mirror even (mirror odd), $\mathcal{H}_{\mathrm{BdG}}(\boldsymbol{k})$ obeys

$$\tilde{M}_{xy}\mathcal{H}_{\mathrm{BdG}}(k_x, k_y, k_z)\tilde{M}_{xy}^\dagger = \mathcal{H}_{\mathrm{BdG}}(k_x, k_y, -k_z), \tag{4.2.10}$$

with $\tilde{M}_{xy} = \mathrm{diag}(M_{xy}, M_{xy}^*) = is_z\tau_z$ ($\tilde{M}_{xy} = \mathrm{diag}(M_{xy}, -M_{xy}^*) = is_z\tau_0$).

A straight vortex extended in the z-direction does not break the mirror reflection symmetry. For the adiabatic BdG Hamiltonian with the vortex, the mirror symmetry is expressed as

$$\tilde{M}_{xy}\mathcal{H}_{\mathrm{BdG}}(k_x, k_y, k_z, \phi)\tilde{M}_{xy}^\dagger = \mathcal{H}_{\mathrm{BdG}}(k_x, k_y, -k_z, \phi), \tag{4.2.11}$$

where ϕ is the angle around the vortex. For mirror even gap superconductors, $\tilde{M}_{xy} = is_z\tau_z$ is labeled as U^-_+ in class D, while for mirror odd superconductors, $\tilde{M}_{xy} = is_z\tau_0$ is labeled as U^-_- in class D. Since $\delta = 2$ and $\delta_\parallel = 1$, the topological index of the vortex is 0 for mirror even gap functions and $\mathbb{Z}_2$ for mirror odd gap functions. See Table 4.3.

The $\mathbb{Z}_2$ index in the mirror odd case is given in the following manner. On the mirror symmetric subspace with $k_z = 0$, the BdG Hamiltonian commutes with $\tilde{M}_{xy}$, and thus it is decomposed into two mirror eigensectors with $M_{xy} = \pm i$,

$$\mathcal{H}_{\mathrm{BdG}}(k_x, k_y, 0, \phi) = \begin{pmatrix} \mathcal{H}^i_{\mathrm{BdG}}(k_x, k_y, 0, \phi) & \\ & \mathcal{H}^{-i}_{\mathrm{BdG}}(k_x, k_y, 0, \phi) \end{pmatrix}. \tag{4.2.12}$$

Each mirror subsector is mapped to itself by the particle-hole transformation due to the anticommutation relation $\{C, \tilde{M}_{xy}\} = 0$ in the mirror odd case. Therefore it supports its own PHS, which enables us to define the mirror $\mathbb{Z}_2$ numbers by

$$\nu_{\pm i} = 2 \cdot \frac{1}{2}\left(\frac{i}{2\pi}\right)^2 \int Q_3^{\pm i} \pmod 2. \tag{4.2.13}$$

Here $Q_3^{\pm}$ is the Chern-Simons 3-form, $Q_3 = \mathrm{tr}\left[\mathcal{A}d\mathcal{A} + \frac{2}{3}\mathcal{A}^3\right]$, of the $M_{xy} = \pm i$ sector, and the integral is performed on the 3-dimensional sphere of (k_x, k_y, ϕ). We can also show that the sum of the mirror $\mathbb{Z}_2$ numbers is trivial, i.e. $\nu_i + \nu_{-i} = 0 \pmod 2$: First of all, the sum of the mirror $\mathbb{Z}_2$ numbers coincides with the integral of the Chern-Simon 3-form of *the total Hamiltonian*, which can be defined on any 3-dimensional sphere of (k_x, k_y, ϕ) even with a nonzero k_z. Moreover, the latter integral is also quantized to be 0 or 1 (mod.2) and is independent of k_z because of the combined symmetry of PHS and the mirror reflection symmetry. Its value, however, should be zero, since the Hamiltonian is smoothly connected into a topologically trivial one by taking $k_z \to \infty$. As a result, the sum of the mirror $\mathbb{Z}_2$ numbers is also zero. This means that we have only a single independent $\mathbb{Z}_2$ number.

We can also show that when the $\mathbb{Z}_2$ number is nontrivial, there are a pair of Majorana gapless modes propagating the vortex. For instance, consider a vortex (o-vortex) in ^{3}He-B phase.[121, 122] The adiabatic Hamiltonian describing the o-vortex is

$$\mathcal{H}_{\mathrm{BdG}}(k_x, k_y, k_z, \phi) = \begin{pmatrix} \frac{k^2}{2m} - \mu & \frac{\Delta e^{i\phi}}{k_F}\boldsymbol{k}\cdot\boldsymbol{s}is_y \\ -is_y\frac{\Delta e^{-i\phi}}{k_F}\boldsymbol{k}\cdot\boldsymbol{s} & -\frac{k^2}{2m} + \mu \end{pmatrix}, \tag{4.2.14}$$

which reduces to

$$\mathcal{H}^{\pm i}_{\mathrm{BdG}}(k_x, k_y, 0, \phi) = \begin{pmatrix} \frac{k^2}{2m} - \mu & \frac{\Delta e^{i\phi}}{k_F}(\mp k_x + ik_y) \\ \frac{\Delta e^{-i\phi}}{k_F}(\mp k_x - ik_y) & -\frac{k^2}{2m} + \mu \end{pmatrix}. \tag{4.2.15}$$

when $k_z = 0$. Since each mirror subsector is nothing but a spinless chiral p-wave superfluid with a vortex, it supports a zero mode, which gives a pair of propagating modes totally. The topological invariant is $\nu_i = 1 \pmod 2$. We also find that our $\mathbb{Z}_2$ number ensures the existence of similar vortex gapless modes [123, 124] in an odd-parity superconducting states of $\mathrm{UPt_3}$[125, 126, 127] and $\mathrm{Cu}_x\mathrm{Bi_2Se_3}$.[69, 55, 56, 128, 23, 129]

2.3 $2\mathbb{Z}$ chiral doublet edge modes protected by the antiunitary reflection symmetry (A^- in class A)

From Table 4.4, 2-dimensional class A insulators with an antiunitary reflection symmetry A^- are topologically characterized by an even integer $2\mathbb{Z}$, which implies that topologically protected edge modes appear in a pair. This can be understood by quasi Kramers degeneracy originated from the antiunitary reflection symmetry.

To illustrate this, consider an antiunitary reflection symmetry

$$A\mathcal{H}(k_x, k_y)A^{-1} = \mathcal{H}(k_x, -k_y). \tag{4.2.16}$$

Note here that it corresponds to reflection of x, $x \to -x$ since anti-unitarity changes the sign of momentum $\boldsymbol{k}$. An edge parallel to the x-direction preserves the reflection symmetry, and thus if the first Chern number of the system is non-zero, there exists a chiral edge state a_{k_x} described by the effective Hamiltonian,

$$H = \sum_{k_x} vk_x a^\dagger_{k_x} a_{k_x}. \tag{4.2.17}$$

In a manner similar to the Kramers theorem, one can prove that the antiunitary reflection symmetry with $A^2 = -1$ results in degeneracy of the edge state, but in contrast to TRS, the resultant degenerate states b_{k_x} have the same energy dispersion, since the antiunitary reflection A acts as

$$a_{k_x} \to b_{k_x}, \quad b_{k_x} \to -a_{k_x}. \tag{4.2.18}$$

Indeed, the antiunitary invariance of H leads to double chiral edge modes with the same energy dispersion:

$$H = \sum_{k_x} v k_x \left(a^\dagger_{k_x} a_{k_x} + b^\dagger_{k_x} b_{k_x} \right). \tag{4.2.19}$$

Correspondingly, the first Chern number of the system should be an even integer.

2.4 $\mathbb{Z}\oplus\mathbb{Z}$ superconductor protected by emergent spinless reflection TRS (A^+_+, A^+_- in class D)

2-dimensional class D superconductors with an antiunitary reflection symmetry with $A^2 = 1$ are characterized by a set of topological numbers $\mathbb{Z} \oplus \mathbb{Z}$. (See A^+_-, A^+_- in class D with $\delta = 2$ of Table 4.4.) The PHS and the antiunitary symmetry are expressed as

$$\begin{aligned} &C\mathcal{H}(-k_x, -k_y)C^{-1} = -\mathcal{H}(k_x, k_y), \\ &A\mathcal{H}(k_x, -k_y)A^{-1} = \mathcal{H}(k_x, k_y), \quad A^2 = 1, \end{aligned} \tag{4.2.20}$$

where the reflection in the x-direction has been assumed. One of the topological numbers is the 1st Chern character Ch_1, which can be nonzero even in the presence of the antiunitary reflection. The other is the winding number N_1 defined on the high-symmetric line $k_x = 0$, where the Hamiltonian $\mathcal{H}(0, k_y)$ effectively supports the class BDI symmetry if one identifies A with TRS. The K-group $\mathbb{Z} \oplus \mathbb{Z}$ is spanned by the basis $e_1 = (Ch_1 = 1, N_1 = 1)$ and $e_2 = (Ch_1 = -1, N_1 = 1)$ where the representative Hamiltonians $\mathcal{H}^{(Ch_1, N_1)}$ are given by

$$\mathcal{H}^{(\pm 1,1)}(k_x, k_y) = \pm k_x \tau_y + k_y \tau_x + [m - \epsilon(k_x^2 + k_y^2)]\tau_z, \tag{4.2.21}$$

with $C = \tau_x \mathcal{K}$, $A = \tau_z \mathcal{K}$, and $m, \epsilon > 0$.

Combining the representative Hamiltonians in the above,

$$\begin{pmatrix} \mathcal{H}^{(1,1)}(k_x, k_y) & 0 \\ 0 & \mathcal{H}^{(-1,1)}(k_x, k_y) \end{pmatrix}, \tag{4.2.22}$$

one obtains the system with $(Ch_1 = 0, N_1 = 2)$. This system hosts a helical gapless Majorana state protected by the reflection symmetry A.

2.5 Vortex in 3-dimensional superconductors with magnetic π-rotation symmetry (A^+_+, A^+_- in class D)

Consider a 3-dimensional time-reversal invariant superconductor (or superfluid) with an additional π-rotation symmetry. If one creates a vortex in this system, it breaks TRS, but if the vortex is straight and perpendicular to the rotation axis of the π-rotation, as illustrated in Fig.4.2 (b), the system can be invariant under the combination of time-reversal and the π-rotation.

Supposing a vortex extended in the z-direction and the magnetic π-rotation around the x-axis, the magnetic π-rotation symmetry A is expressed as

$$A\mathcal{H}_{\rm BdG}(k_x,k_y,k_z,\phi)A^{-1}=\mathcal{H}_{\rm BdG}(-k_x,k_y,k_z,-\phi),\quad A=\tau_z s_z\mathcal{K}, \tag{4.2.23}$$

where $\mathcal{H}_{\rm BdG}(k_x,k_y,k_z,\phi)$ is the BdG Hamiltonian with a vortex, and ϕ is the angle around the vortex measured from the x-axis. Since A anticommutes with $C=\tau_x\mathcal{K}$, it is labeled as A^+_- with $\delta=2$ and $\delta_\parallel=1$ ($d=3$, $D=1$, $d_\parallel=2$ and $D_\parallel=1$) in class D. From Table 4.4, the topological index is $\mathbb{Z}\oplus\mathbb{Z}$. One of the $\mathbb{Z}$ indices is the second Chern number

$$Ch_2=\frac{1}{2}\left(\frac{i}{2\pi}\right)^2\int {\rm tr}\mathcal{F}^2 \tag{4.2.24}$$

where $\mathcal{F}=\mathcal{F}(\boldsymbol{k},\phi)$ is the Berry curvature of $\mathcal{H}_{\rm BdG}(k_x,k_y,k_z,\phi)$, and the trace is taken for all negative energy states. The other $\mathbb{Z}$ index is defined on the $k_z=0$ plane. On the $k_z=0$ plane, the magnetic π-rotation coincides with the magnetic in-plane reflection, and thus the BdG Hamiltonian is topologically the same as that in Sec. 1.5. Consequently, the BdG Hamiltonian is chiral symmetric at $\phi=0,\pi$, and zero modes with $k_z=0$ localized at the vortex are characterized by

$$N_1^{\rm strong}=\frac{N_1^0-N_1^\pi}{2}, \tag{4.2.25}$$

where $N_1^{0/\pi}$ is given by

$$N_1^{0/\pi}=\frac{1}{4\pi i}\int {\rm tr}\Gamma\mathcal{H}^{-1}_{\rm BdG}(k_x,0,0,0/\pi)d\mathcal{H}_{\rm BdG}(k_x,0,0,0/\pi), \tag{4.2.26}$$

with the chiral operator $\Gamma=s_z\tau_y$.

When these $\mathbb{Z}$ indices are nonzero, the bulk-boundary correspondence implies that there exist 1-dimensional gapless Majorana modes propagating the vortex. These gapless modes propagate upward or downward, and we call the former mode as right mover and the latter as left mover. Also, thanks to the CS above, each gapless state has a definite chirality of Γ at $k_z=0$. Hence, a gapless state localized at the vortex has two characters (α,Γ), where $\alpha(=\mathrm{R},\mathrm{L})$ denotes the direction of the movement and Γ denotes the chirality of Γ at $k_z=0$. If we express the number of vortex gapless states with (α,Γ) by $N(\alpha,\Gamma)$, then, Ch_2 and $N_1^{\rm strong}$ are related to $N(\alpha,\Gamma)$ as

$$\begin{aligned} Ch_2&=N(\mathrm{R},+)+N(\mathrm{R},-)-N(\mathrm{L},+)-N(\mathrm{L},-),\\ N_1^{\rm strong}&=N(\mathrm{R},+)-N(\mathrm{R},-)+N(\mathrm{L},+)-N(\mathrm{L},-). \end{aligned} \tag{4.2.27}$$

Such a magnetic π-rotation symmetric vortex can be realized in ^{3}He-B phase[121] or $Cu_xBi_2Se_3$.[69, 55, 56, 128, 23, 129]

3 Two-fold rotation family ($\delta_\parallel=2$)

In this section, we discuss topological phases protected by additional symmetries with $\delta_\parallel=2$ (mod 4). Relevant systems are π-rotation symmetric insulators and their surface defects ($d_\parallel=2$, $D_\parallel=0$) illustrated in Fig. 4.3. We summarize the classification table for $d_\parallel=2$ (mod 4) with additional unitary symmetry in Table 4.5 and that with additional antiunitary symmetry in Table 4.6, respectively.

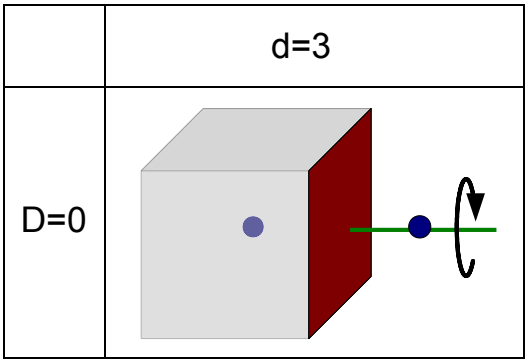

Figure 4.3: Topological defects protected by order-two additional symmetry with $\delta_{\parallel} = d_{\parallel} - D_{\parallel} = 2$. The additional symmetry is (a) π-rotation symmetry. The spatial position of topological defects is transformed as π-rotation under the symmetry transformation of $\delta_{\parallel} = 2$ family. [38]

3.1 π-rotation Chern number and π-rotation winding number

In a manner similar to the mirror Chern number and the mirror winding number, we can define the *π-rotation Chern number* and the *π-rotation winding number* in the presence of two-fold (π) rotation symmetry.

To define these topological numbers, we first introduce π-rotation subsectors. The presence of π-rotation symmetry implies

$$U\mathcal{H}(k_x, k_y, \boldsymbol{k}_\perp)U^{-1} = \mathcal{H}(-k_x, -k_y, \boldsymbol{k}_\perp). \tag{4.3.1}$$

On the symmetric subspace $k_x = k_y = 0$ of π-rotation, the Hamiltonian is decomposed into two π-rotation subsectors which are eigenstates of U,

$$\mathcal{H}(0, 0, \boldsymbol{k}_\perp) = \mathcal{H}_+(0, 0, \boldsymbol{k}_\perp) \oplus \mathcal{H}_-(0, 0, \boldsymbol{k}_\perp), \tag{4.3.2}$$

since the Hamiltonian commutes with U on the π-rotation invariant subspace.

In even $2n$-dimensions, we can define the π-rotation Chern number by

$$Ch^{\Pi}_{n-1} := \frac{Ch^{+}_{n-1} - Ch^{-}_{n-1}}{2}, \tag{4.3.3}$$

where $Ch^{\pm}_{n-1}$ is the $(n-1)$-th Chern number of $\mathcal{H}_\pm(0, 0, \boldsymbol{k}_\perp)$. Since the original Chern number is identically zero in the presence of TRS or CS in $(4p-2)$-dimensions, or in the presence of PHS in $4p$-dimensions, the meaningful π-rotation Chern number can be obtained only when $\mathcal{H}_\pm(0, 0, \boldsymbol{k}_\perp)$ does not have such symmetries. For example, consider a π-rotation symmetric class DIII system in 4 dimensions. There are four types of π-rotation with $U^2 = 1$: U^{+}_{++}, U^{+}_{--}, U^{+}_{+-}, U^{+}_{-+}. In the former two cases, U^{+}_{++}, U^{+}_{--}, the π-rotation Chern number is identically zero because the π-rotation subsectors support CS in 2 dimensions, i.e. $[\Gamma, \mathcal{H}_\pm(0, 0, \boldsymbol{k}_\perp)] = 0$ with $\Gamma = CT$. U^{+}_{+-} also forbids a non-zero π-rotation Chern number because TRS in 2 dimensions remains in the π-rotation

Table 4.5: Classification table for topological crystalline insulators and superconductors and their topological defects in the presence of order-two additional unitary symmetry with flipped parameters $\delta_\parallel = d_\parallel - D_\parallel = 2 \pmod 4$. Here $\delta = d - D$.

Symmetry	Class	$\mathcal{C}_q$ or $\mathcal{R}_q$	$\delta=0$	$\delta=1$	$\delta=2$	$\delta=3$	$\delta=4$	$\delta=5$	$\delta=6$	$\delta=7$
U	A	$\mathcal{C}_0\times\mathcal{C}_0$	$\mathbb{Z}\oplus\mathbb{Z}$	0	$\mathbb{Z}\oplus\mathbb{Z}$	0	$\mathbb{Z}\oplus\mathbb{Z}$	0	$\mathbb{Z}\oplus\mathbb{Z}$	0
U_+	AIII	$\mathcal{C}_1\times\mathcal{C}_1$	0	$\mathbb{Z}\oplus\mathbb{Z}$	0	$\mathbb{Z}\oplus\mathbb{Z}$	0	$\mathbb{Z}\oplus\mathbb{Z}$	0	$\mathbb{Z}\oplus\mathbb{Z}$
U_-	AIII	$\mathcal{C}_0$	$\mathbb{Z}$	0	$\mathbb{Z}$	0	$\mathbb{Z}$	0	$\mathbb{Z}$	0
U_+^+, U_-^-	AI, D, AII, C	$\mathcal{C}_0$	$\mathbb{Z}$	0	$\mathbb{Z}$	0	$\mathbb{Z}$	0	$\mathbb{Z}$	0
U_{++}^+, U_{--}^-	BDI, DIII, CII, CI	$\mathcal{C}_1$	0	$\mathbb{Z}$	0	$\mathbb{Z}$	0	$\mathbb{Z}$	0	$\mathbb{Z}$
U_{+-}^+, U_{-+}^-	BDI	$\mathcal{R}_2$	$\mathbb{Z}_2$	$\mathbb{Z}_2$	$\mathbb{Z}$	0	0	0	$2\mathbb{Z}$	0
U_{-+}^+, U_{+-}^-	DIII	$\mathcal{R}_4$	$2\mathbb{Z}$	0	$\mathbb{Z}_2$	$\mathbb{Z}_2$	$\mathbb{Z}$	0	0	0
U_{+-}^+, U_{-+}^-	CII	$\mathcal{R}_6$	0	0	$2\mathbb{Z}$	0	$\mathbb{Z}_2$	$\mathbb{Z}_2$	$\mathbb{Z}$	0
U_{-+}^+, U_{+-}^-	CI	$\mathcal{R}_0$	$\mathbb{Z}$	0	0	0	$2\mathbb{Z}$	0	$\mathbb{Z}_2$	$\mathbb{Z}_2$
$U_-^+, U_+^-, U_{--}^+, U_{++}^-$	AI	$\mathcal{R}_0\times\mathcal{R}_0$	$\mathbb{Z}\oplus\mathbb{Z}$	0	0	0	$2\mathbb{Z}\oplus2\mathbb{Z}$	0	$\mathbb{Z}_2\oplus\mathbb{Z}_2$	$\mathbb{Z}_2\oplus\mathbb{Z}_2$
	BDI	$\mathcal{R}_1\times\mathcal{R}_1$	$\mathbb{Z}_2\oplus\mathbb{Z}_2$	$\mathbb{Z}\oplus\mathbb{Z}$	0	0	0	$2\mathbb{Z}\oplus2\mathbb{Z}$	0	$\mathbb{Z}_2\oplus\mathbb{Z}_2$
	D	$\mathcal{R}_2\times\mathcal{R}_2$	$\mathbb{Z}_2\oplus\mathbb{Z}_2$	$\mathbb{Z}_2\oplus\mathbb{Z}_2$	$\mathbb{Z}\oplus\mathbb{Z}$	0	0	0	$2\mathbb{Z}\oplus2\mathbb{Z}$	0
	DIII	$\mathcal{R}_3\times\mathcal{R}_3$	0	$\mathbb{Z}_2\oplus\mathbb{Z}_2$	$\mathbb{Z}_2\oplus\mathbb{Z}_2$	$\mathbb{Z}\oplus\mathbb{Z}$	0	0	0	$2\mathbb{Z}\oplus2\mathbb{Z}$
	AII	$\mathcal{R}_4\times\mathcal{R}_4$	$2\mathbb{Z}\oplus2\mathbb{Z}$	0	$\mathbb{Z}_2\oplus\mathbb{Z}_2$	$\mathbb{Z}_2\oplus\mathbb{Z}_2$	$\mathbb{Z}\oplus\mathbb{Z}$	0	0	0
	CII	$\mathcal{R}_5\times\mathcal{R}_5$	0	$2\mathbb{Z}\oplus2\mathbb{Z}$	0	$\mathbb{Z}_2\oplus\mathbb{Z}_2$	$\mathbb{Z}_2\oplus\mathbb{Z}_2$	$\mathbb{Z}\oplus\mathbb{Z}$	0	0
	C	$\mathcal{R}_6\times\mathcal{R}_6$	0	0	$2\mathbb{Z}\oplus2\mathbb{Z}$	0	$\mathbb{Z}_2\oplus\mathbb{Z}_2$	$\mathbb{Z}_2\oplus\mathbb{Z}_2$	$\mathbb{Z}\oplus\mathbb{Z}$	0
	CI	$\mathcal{R}_7\times\mathcal{R}_7$	0	0	0	$2\mathbb{Z}\oplus2\mathbb{Z}$	0	$\mathbb{Z}_2\oplus\mathbb{Z}_2$	$\mathbb{Z}_2\oplus\mathbb{Z}_2$	$\mathbb{Z}\oplus\mathbb{Z}$
U_{-+}^+, U_{+-}^-	BDI	$\mathcal{R}_0$	$\mathbb{Z}$	0	0	0	$2\mathbb{Z}$	0	$\mathbb{Z}_2$	$\mathbb{Z}_2$
U_{+-}^+, U_{-+}^-	DIII	$\mathcal{R}_2$	$\mathbb{Z}_2$	$\mathbb{Z}_2$	$\mathbb{Z}$	0	0	0	$2\mathbb{Z}$	0
U_{-+}^+, U_{+-}^-	CII	$\mathcal{R}_4$	$2\mathbb{Z}$	0	$\mathbb{Z}_2$	$\mathbb{Z}_2$	$\mathbb{Z}$	0	0	0
U_{+-}^+, U_{-+}^-	CI	$\mathcal{R}_6$	0	0	$2\mathbb{Z}$	0	$\mathbb{Z}_2$	$\mathbb{Z}_2$	$\mathbb{Z}$	0

subsectors, because of $[U,T]=0$. A nonzero π-rotation Chern number is possible only in the last case U_{-+}^+ since no AZ symmetry remains in π-rotation subsectors.

On the other hand, the π-rotation winding number can be defined in odd $(2n+1)$-dimensions. In order to define the π-rotation winding number, we need CS that commutes with π-rotation, $[U,\Gamma]=0$. In this case, CS remains even in the π-rotation subsectors. Then, the winding number $N_{2n+1}^{\pm}$ for each π-rotation subsector is given by

$$N_{2n-1}^{\pm} = \frac{n!}{(2\pi i)^n (2n)!} \int \mathrm{tr}\Gamma \left[\mathcal{H}_{\pm}^{-1} d\mathcal{H}_{\pm}\right]^{2n-1}, \tag{4.3.4}$$

with $\mathcal{H}_{\pm} = \mathcal{H}_{\pm}(0,0,\boldsymbol{k}_\perp)$. The π-rotation winding number N_{2n-1}^{Π} is defined as the difference between N_{2n-1}^{+} and N_{2n-1}^{-}:

$$N_{2n-1}^{\Pi} := \frac{N_{2n-1}^{+} - N_{2n-1}^{-}}{2}. \tag{4.3.5}$$

3.2 $\mathbb{Z}_2$ topological insulator protected by the magnetic π-rotation symmetry (A^+ in class A)

Here we demonstrate a topologically nontrivial phase which is protected by the combined symmetry of time-reversal and a π-rotation. The combined antiunitary symmetry we consider is $A = -iUT =$

Table 4.6: Classification table for topological crystalline insulators and superconductors and their topological defects in the presence of order-two additional antiunitary symmetry with flipped parameters $\delta_\parallel = d_\parallel - D_\parallel = 2 \pmod 4$. Here $\delta = d - D$.

Symmetry	Class	$\mathcal{C}_q$ or $\mathcal{R}_q$	$\delta=0$	$\delta=1$	$\delta=2$	$\delta=3$	$\delta=4$	$\delta=5$	$\delta=6$	$\delta=7$
A^+	A	$\mathcal{R}_4$	$2\mathbb{Z}$	0	$\mathbb{Z}_2$	$\mathbb{Z}_2$	$\mathbb{Z}$	0	0	0
A^-	A	$\mathcal{R}_0$	$\mathbb{Z}$	0	0	0	$2\mathbb{Z}$	0	$\mathbb{Z}_2$	$\mathbb{Z}_2$
A^+_+	AIII	$\mathcal{R}_5$	0	$2\mathbb{Z}$	0	$\mathbb{Z}_2$	$\mathbb{Z}_2$	$\mathbb{Z}$	0	0
A^-_-	AIII	$\mathcal{R}_7$	0	0	0	$2\mathbb{Z}$	0	$\mathbb{Z}_2$	$\mathbb{Z}_2$	$\mathbb{Z}$
A^-_+	AIII	$\mathcal{R}_1$	$\mathbb{Z}_2$	$\mathbb{Z}$	0	0	0	$2\mathbb{Z}$	0	$\mathbb{Z}_2$
A^+_-	AIII	$\mathcal{R}_3$	0	$\mathbb{Z}_2$	$\mathbb{Z}_2$	$\mathbb{Z}$	0	0	0	$2\mathbb{Z}$
A^+_+, A^+_-	D	$\mathcal{R}_3$	0	$\mathbb{Z}_2$	$\mathbb{Z}_2$	$\mathbb{Z}$	0	0	0	$2\mathbb{Z}$
A^-_+, A^-_-	C	$\mathcal{R}_7$	0	0	0	$2\mathbb{Z}$	0	$\mathbb{Z}_2$	$\mathbb{Z}_2$	$\mathbb{Z}$
A^-_+, A^-_-	D	$\mathcal{R}_1$	$\mathbb{Z}_2$	$\mathbb{Z}$	0	0	0	$2\mathbb{Z}$	0	$\mathbb{Z}_2$
A^+_+, A^+_-	C	$\mathcal{R}_5$	0	$2\mathbb{Z}$	0	$\mathbb{Z}_2$	$\mathbb{Z}_2$	$\mathbb{Z}$	0	0

$s_x\mathcal{K}$ where $U = is_z$ is the π-rotation around the z-axis and $T = is_y\mathcal{K}$ is time-reversal. In 3 dimensions, the antiunitary symmetry implies

$$A\mathcal{H}(k_x, k_y, k_z)A^{-1} = \mathcal{H}(k_x, k_y, -k_z). \tag{4.3.6}$$

The antiunitary symmetry A is categorized as A^+ because of $A^2 = 1$, and thus the topological index is $\mathbb{Z}_2$ in 3 dimensions, as is shown in Table 4.6 of class A with A^+. The $\mathbb{Z}_2$ topological invariant is defined by the Chern-Simons 3-form,

$$\nu = 2 \cdot \frac{1}{2}\left(\frac{i}{2\pi}\right)^2 \int \mathrm{tr}\left(\mathcal{A}d\mathcal{A} + \frac{2}{3}\mathcal{A}^3\right) \pmod 2. \tag{4.3.7}$$

The model Hamiltonian of this topological phase is given by

$$\mathcal{H}(k_x, k_y, k_z) = s_x\sigma_0(k_x - h) + s_y\sigma_0 k_y + s_z\sigma_z k_z + s_z\sigma_y m(k), \quad m(k) = m_0 - ((k_x - h)^2 + k_y^2 + k_z^2), \tag{4.3.8}$$

where we have introduced orbital degrees of freedom σ_μ, and the antiunitary operator A acts on the orbital space trivially as $A = s_x\sigma_0\mathcal{K}$. The sign of m_0 provides the $\mathbb{Z}_2$ number of the above model: When m_0 is positive (negative), the system is topologically non-trivial (trivial). Indeed, the non-trivial $\mathbb{Z}_2$ number implies the existence of a gapless Dirac fermion on a surface parallel to the z-axis, which preserves the π-rotation symmetry above. The wave function of the surface Dirac fermion localized at $z = 0$ is solved as

$$\boldsymbol{\varphi}(z) = (e^{\kappa_+ z} - e^{\kappa_- z}) \begin{pmatrix} 1 \\ -1 \end{pmatrix}_\sigma \otimes u_s(k_x, k_y) \tag{4.3.9}$$

with the boundary condition $\boldsymbol{\varphi}(0) = \boldsymbol{\varphi}(-\infty) = 0$, where $\kappa_\pm = 1/2 \pm \sqrt{-m_0 + (k_x - h)^2 + k_y^2 + 1/4}$ and $(1, 1)^T_\sigma$ is the spinor in the orbital space. The spinor $u_{s=\pm}$ in the spin space satisfies

$$\mathcal{H}^{\mathrm{D}}(k_x, k_y)u_\pm = \pm\sqrt{(k_x - h)^2 + k_y^2}\,u_\pm \tag{4.3.10}$$

where $\mathcal{H}^{\rm D}(k_x, k_y)$ is the low energy effective Hamiltonian of the Dirac fermion.

$$\mathcal{H}^{\rm D}(k_x, k_y) = s_x(k_x - h) + s_y k_y, \tag{4.3.11}$$

Here note that m_0 needs to be positive in order to satisfy the boundary condition $\boldsymbol{\varphi}(0) = \boldsymbol{\varphi}(-\infty) = 0$. Otherwise, κ_- becomes negative even for small $k_x - h$ and k_y, and thus $\boldsymbol{\varphi}(z)$ never converges when $z \to -\infty$.

The $\mathbb{Z}_2$ character of this phase is also evident in the surface state. From the additional symmetry of the low energy effective surface Hamiltonian

$$A\mathcal{H}^{\rm D}(k_x, k_y)A^{-1} = \mathcal{H}^{\rm D}(k_x, k_y), \quad A = s_x\mathcal{K}, \tag{4.3.12}$$

the Berry phase $\gamma(C)$, which is defined as a line integral along the path C enclosing a degenerate point of a surface state

$$\gamma(C) = i \oint_C {\rm tr}\mathcal{A}, \tag{4.3.13}$$

is quantized as $e^{i\gamma(C)} = \pm 1$. The Berry phase defines a $\mathbb{Z}_2$ number of the surface state. Using the Berry curvature $\mathcal{A}$ of the Dirac fermion,

$$\mathcal{A} = u_-^\dagger du_-, \tag{4.3.14}$$

with u_- in Eq.(4.3.10), we find that the surface Dirac fermion supports a non-trivial $\mathbb{Z}_2$ number, i.e. $e^{i\gamma(C)} = -1$, and thus it cannot be gapped into a topologically trivial state as far as the additional symmetry is preserved.

3.3 ^{3}He-B slab with parallel magnetic fields (A_+^+ in class D)

In superfluid ^{3}He-B, the gap function $\hat{\Delta} = i(\Delta/k_{\rm F})\boldsymbol{k}\cdot\boldsymbol{s}s_y$ preserves the $SO_{L+S}(3)$ rotation symmetry as well as TRS. [130] The presence of a surface partially breaks the $SO_{L+S}(3)$ rotation symmetry, but it still preserves the $SO_{L+S}(2)$ rotation normal to the surface, say the spin-orbit rotation around z-axis.

If we apply magnetic field parallel to the surface (say in the y-direction), both TRS and the $SO_{L+S}(2)$ symmetry are broken. However, the magnetic π-rotation symmetry, which operator acts as combination of time-reversal and the π-rotation of $SO(2)_{L+S}$, remains. It defines the antiunitary symmetry

$$A\mathcal{H}_{\rm BdG}(k_x, k_y, -k_z)A^{-1} = \mathcal{H}_{\rm BdG}(k_x, k_y, k_z), \tag{4.3.15}$$

for the BdG Hamiltonian

$$\mathcal{H}_{\rm BdG}(k_x, k_y, k_z) = \begin{pmatrix} \frac{k^2}{2m} - \mu + h_x s_x + h_y s_y & \frac{\Delta}{k_F}\boldsymbol{k}\cdot\boldsymbol{s}is_y \\ -\frac{\Delta}{k_F}is_y\boldsymbol{k}\cdot\boldsymbol{s} & -\frac{k^2}{2m} + \mu - h_x s_x + h_y s_y \end{pmatrix}, \tag{4.3.16}$$

where $A = TU(\pi) = is_x\tau_z\mathcal{K}$ with $T = is_y\tau_0\mathcal{K}$ and $U(\pi) = is_z\tau_z \in SO_{L+S}(2)$. Considering the sign of A^2 and the commutation relation between A and PHS, we find that the additional symmetry is labeled as A_+^+ in the class D of Table 4.6. In 3 dimensions, the topological index of this system is $\mathbb{Z}$.

The $\mathbb{Z}$ index is the 1-dimensional π-rotation winding number.

$$N_1 = \frac{1}{4\pi i}\int \mathrm{tr}\left[\Gamma \mathcal{H}_{\mathrm{BdG}}^{-1}(0,0,k_z) d\mathcal{H}_{\mathrm{BdG}}(0,0,k_z)\right], \tag{4.3.17}$$

with $\Gamma = -AC = s_x\tau_y$. For the BdG Hamiltonian (4.3.16) with small h_y, $N_1 = -2\mathrm{sgn}(\Delta)$. The non-trivial value of N_1 explains the reason why helical surface Majorana fermions in ^{3}He-B can stay gapless under magnetic fields parallel to the surface:[131] Although the class DIII topological superconductivity of ^{3}He-B is lost by magnetic fields breaking TRS, the additional magnetic π-rotation symmetry gives an extra topological superconductivity to ^{3}He-B.

3.4 Inversion symmetric quantum (spin) Hall states (U in class A, U_+^+ in class AII)

Here we consider inversion symmetric quantum Hall states which satisfy

$$P\mathcal{H}(k_x,k_y)P^{-1} = \mathcal{H}(-k_x,-k_y), \quad P^2 = 1. \tag{4.3.18}$$

Since the inversion P is labeled as U in class A of Table 4.5, its topological index is $\mathbb{Z}\oplus\mathbb{Z}$. One of the $\mathbb{Z}$ indices is the first Chern number $Ch_1 = i/(2\pi)\int \mathrm{tr}\mathcal{F}$, which is directly related to the Hall conductance σ_{xy} of the system as $\sigma_{xy} = (e^2/h)Ch_1$.[14, 15] The other $\mathbb{Z}$ index is defined at symmetric points of inversion, i.e. $\boldsymbol{k} = (0,0) \equiv \Gamma_0$ and $\boldsymbol{k} = \infty \equiv \Gamma_\infty$: As the Hamiltonian $\mathcal{H}(\Gamma_i)$ at Γ_i $(i = 0, \infty)$ commutes with P, it can be block-diagonal into two subsectors with different parity $P = \pm$

$$\mathcal{H}(\Gamma_i) = \mathcal{H}_{P=+}(\Gamma_i) \oplus \mathcal{H}_{P=-}(\Gamma_i) \tag{4.3.19}$$

Now let us denote $\#\Gamma_i^\pm$ to be the number of occupied states of $\mathcal{H}_{P=\pm}(\Gamma_i)$. Although a set of numbers $\{\#\Gamma_i^\pm\}$ characterizes the Hamiltonian, there are some constraints. First, for a full gapped system, the total number of occupied states is momentum-independent, so we have

$$\#\Gamma_0^+ + \#\Gamma_0^- = \#\Gamma_\infty^+ + \#\Gamma_\infty^- \tag{4.3.20}$$

Furthermore, by adding $p^\pm$ trivial bands with $P = \pm$, we find that two sets of numbers, $\{\#\Gamma_i^\pm\}$ and $\{\#\Gamma_i^\pm + p^\pm\}$, specify the same stable-equivalent Hamiltonian. Consequently, the topological index, which should be unchanged under the stable equivalence, is given by

$$[\Gamma_{0,\infty}] = \#\Gamma_0^+ - \#\Gamma_\infty^+ = -(\#\Gamma_0^- - \#\Gamma_\infty^-). \tag{4.3.21}$$

It has been known that the following formula holds between Ch_1 and $[\Gamma_{0,\infty}]$[132, 133, 134],

$$(-1)^{Ch_1} = (-1)^{[\Gamma_{0,\infty}]}. \tag{4.3.22}$$

We find that the K-theory simplifies the derivation of this formula: Let us consider two representative Hamiltonians of quantum Hall states

$$\begin{aligned} \mathcal{H}_1 &= k_x\sigma_x + k_y\sigma_x + (1 - k_x^2 - k_y^2)\sigma_z, \\ \mathcal{H}_2 &= k_x\sigma_x - k_y\sigma_x + (1 - k_x^2 - k_y^2)\sigma_z, \end{aligned} \tag{4.3.23}$$

with $P = \sigma_z$, which topological indices are $(Ch_1, [\Gamma_{0,\infty}])|_{\mathcal{H}_1} = (1, -1)$ and $(Ch_1, [\Gamma_{0,\infty}])|_{\mathcal{H}_2} = (-1, -1)$, respectively. Then, because any inversion symmetric quantum Hall state $\mathcal{H}$ is stable-equivalent to a direct sum of $\mathcal{H}_1$ and $\mathcal{H}_2$,

$$[\mathcal{H}] = l_1[\mathcal{H}_1] \oplus l_2[\mathcal{H}_2], \tag{4.3.24}$$

its topological numbers, $(Ch_1, [\Gamma_{0,\infty}])|_{\mathcal{H}} = (l_1 - l_2, -l_1 - l_2)$, obey Eq.(4.3.22) as $(-1)^{Ch_1} = (-1)^{l_1 - l_2} = (-1)^{-l_1 - l_2} = (-1)^{[\Gamma_{0,\infty}]}$.

If we consider an inversion symmetric quantum spin Hall state, instead of a quantum Hall state, the system also supports TRS. In this case, P is labeled as U_+^+ in class AII of Table 4.5. Now the topological index reduces to $\mathbb{Z}$, since TRS makes Ch_1 to be zero. In a manner similar to Eq.(4.3.21), the remaining topological index is given by

$$[\Gamma_{0,\infty}] = \frac{\#\Gamma_0^+ - \#\Gamma_\infty^+}{2} = -\frac{\#\Gamma_0^- - \#\Gamma_\infty^-}{2}. \tag{4.3.25}$$

Here, in comparison with Eq.(4.3.21), the $\mathbb{Z}$ index in Eq.(4.3.25) is divided by 2, in order to remove the trivial factor 2 caused by the Kramers degeneracy.

Like ordinary quantum spin Hall states, we can also introduce the Kane-Mele $\mathbb{Z}_2$ invariant $(-1)^\nu$[48], but it is written by $[\Gamma_{0,\infty}]$,

$$(-1)^\nu = (-1)^{[\Gamma_{0,\infty}]}. \tag{4.3.26}$$

as was shown by Fu and Kane[52]. Again, the K-theory provides a simple derivation of this formula: Using a representative Hamiltonian of inversion symmetric quantum spin Hall states

$$\mathcal{H}_1 = k_x s_x \sigma_x + k_y s_y \sigma_x + (1 - k_x^2 - k_y^2)\sigma_z, \quad T = i s_y \mathcal{K}, \quad P = \sigma_z, \tag{4.3.27}$$

with the topological indices $((-1)^\nu, [\Gamma_{0,\infty}])|_{\mathcal{H}_1} = (-1, -1)$, the K-theory implies that any inversion symmetric quantum spin Hall state $\mathcal{H}$ is stable-equivalent to a direct sum of $\mathcal{H}_1$,

$$[\mathcal{H}] = l_1[\mathcal{H}_1]. \tag{4.3.28}$$

Therefore, the topological indices of $\mathcal{H}$ is given by $((-1)^\nu, [\Gamma_{0,\infty}])|_{\mathcal{H}} = ((-1)^{l_1}, -l_1)$, and thus Eq.(4.3.26) holds. This parity formula is useful to evaluate the $\mathbb{Z}_2$ invariant of real materials [135].

3.5 Odd parity superconductors in two dimensions (U_-^+ in class D)

Now consider topological properties of odd parity superconductors in 2 dimensions,[136, 132] where the normal dispersions are inversion symmetric, $P\epsilon(-\boldsymbol{k})P^\dagger = \epsilon(\boldsymbol{k})$, and the pairing functions are odd under inversion, $P\hat{\Delta}(-\boldsymbol{k})P^T = -\hat{\Delta}(\boldsymbol{k})$, with a unitary matrix P. Combining with $U(1)$ gauge symmetry, the inversion symmetry of the BdG Hamiltonian

$$\mathcal{H}_{\rm BdG}(\boldsymbol{k}) = \begin{pmatrix} \epsilon(\boldsymbol{k}) & \hat{\Delta}(\boldsymbol{k}) \\ \hat{\Delta}^\dagger(\boldsymbol{k}) & -\epsilon^T(-\boldsymbol{k}) \end{pmatrix} \tag{4.3.29}$$

is expressed as

$$\tilde{P}\mathcal{H}_{\rm BdG}(-\boldsymbol{k})\tilde{P}^\dagger = \mathcal{H}_{\rm BdG}(\boldsymbol{k}), \quad \tilde{P} = {\rm diag}(P, -P^*). \tag{4.3.30}$$

Because $\tilde{P}^2 = 1$ and $\{\tilde{P}, C\} = 0$, $\tilde{P}$ is labeled as U_-^+ in class D. From Table 4.5, its topological index is $\mathbb{Z} \oplus \mathbb{Z}$ in 2 dimensions. Like an inversion symmetric quantum Hall state, one of the $\mathbb{Z} \oplus \mathbb{Z}$ index is the first Chern number $Ch_1 = i/(2\pi) \int \mathrm{tr}\mathcal{F}$, and the other is defined at the symmetric points $\boldsymbol{k} = (0,0) \equiv \Gamma_0$ and $\boldsymbol{k} = \infty \equiv \Gamma_\infty$ of inversion. Denoting the number of negative energy states with parity $\pm$ at Γ_i as $\#\Gamma_i^\pm$, the latter topological index is given by

$$[\Gamma_{0,\infty}] = \#\Gamma_0^+ - \#\Gamma_\infty^+ = -(\#\Gamma_0^- - \#\Gamma_\infty^-). \tag{4.3.31}$$

Furthermore, we can also show

$$(-1)^{Ch_1} = (-1)^{[\Gamma_{0,\infty}]}, \tag{4.3.32}$$

in a manner similar to Eq.(4.3.22).[132]

For ordinary odd-parity superconductors, the gap functions at Γ_i are often identically zero or they are much smaller than the energy scale of the normal part. The energy hierarchy between the normal and superconducting states simplifies the evaluation of $[\Gamma_{0,\infty}]$:[136, 132] Under these situations, without closing the bulk gap, $\Delta(\Gamma_i)$ can be neglected in $\mathcal{H}(\Gamma_i)$,

$$\mathcal{H}(\Gamma_i) = \begin{pmatrix} \epsilon(\Gamma_i) & 0 \\ 0 & -\epsilon^T(\Gamma_i) \end{pmatrix}, \tag{4.3.33}$$

and thus the normal dispersion $\epsilon(\Gamma_i)$ determines the BdG spectrum at Γ_i: By using an eigenstate $|\varphi_i\rangle$ of $\epsilon(\Gamma_i)$, a negative energy state of $\mathcal{H}(\Gamma_i)$ is given by $(|\varphi_i\rangle, 0)^t$ $[(0, |\varphi_i^*\rangle)^t]$ if the state $|\varphi_i\rangle$ is below (above) the Fermi level. Therefore, we obtain

$$\#\Gamma_i^\sigma = \#\epsilon_-^\sigma(\Gamma_i) + \#\epsilon_+^{-\sigma}(\Gamma_i) \tag{4.3.34}$$

where $\#\epsilon_-^\sigma(\Gamma_i)$ $[\#\epsilon_+^\sigma(\Gamma_i)]$ denotes the number of $P = \sigma$ bands in the normal state below (above) the Fermi level. Consequently, $[\Gamma_{0,\infty}]$ is recast into

$$\begin{aligned} [\Gamma_{0,\infty}] &= \#\epsilon_-^+(\Gamma_0) + \#\epsilon_+^-(\Gamma_0) - \#\epsilon_-^+(\Gamma_\infty) - \#\epsilon_+^-(\Gamma_\infty) \\ &= \#\epsilon_-^+(\Gamma_0) - \#\epsilon_-^+(\Gamma_\infty) - [\#\epsilon_-^-(\Gamma_0) - \#\epsilon_-^-(\Gamma_\infty)] \\ &= [\epsilon_-^+(\Gamma_{0,\infty})] - [\epsilon_-^-(\Gamma_{0,\infty})] \end{aligned} \tag{4.3.35}$$

where $[\epsilon_-^\sigma(\Gamma_{0,\infty})] \equiv \#\epsilon_-^\sigma(\Gamma_0) - \#\epsilon_-^\sigma(\Gamma_\infty)$, and we have used the relation $\#\epsilon_-^\sigma(\Gamma_0) + \#\epsilon_+^\sigma(\Gamma_0) = \#\epsilon_-^\sigma(\Gamma_\infty) + \#\epsilon_+^\sigma(\Gamma_\infty)$. From Eqs. (4.3.32) and (4.3.35), the parity of the first Chern number is also evaluated as [136, 132]

$$(-1)^{Ch_1} = (-1)^{[\epsilon_-^+(\Gamma_{0,\infty})] + [\epsilon_-^-(\Gamma_{0,\infty})]} = (-1)^{N_\mathrm{F}}, \tag{4.3.36}$$

where N_F is the number of the Fermi surfaces enclosing Γ_0.

The Fermi surface formula (4.3.36) enables us to predict topological superconductivity of odd parity superconductors without detailed knowledge of the gap function. In particular, remembering that when $(-1)^{Ch_1} = -1$ a vortex hosts a single Majorana zero mode so to obey the non-Abelian anyon statistics[37, 137], Eq.(4.3.36) provide a simple criterion for non-Abelian topological order:[132] If N_F is odd, then the odd-parity superconductor is in non-Abelian topological phase.

If odd parity superconductors support TRS, $\tilde{P}$ is labeled as U_{+-}^+ in class DIII of Table 4.5, and thus the topological index reduces to a single $\mathbb{Z}$ in 2 dimensions. This is because Ch_1 vanishes due

to TRS. Removing the trivial factor 2 caused by the Kramers degeneracy, the remaining topological index is given by

$$[\Gamma_{0,\infty}] = \frac{\#\Gamma_0^+ - \#\Gamma_\infty^+}{2} = -\frac{\#\Gamma_0^- - \#\Gamma_\infty^-}{2}. \tag{4.3.37}$$

We can also introduce the Kane-Mele $\mathbb{Z}_2$ invariant $(-1)^\nu$ as in the case of quantum spin Hall states. In a manner similar to Eq.(4.3.36), for weak coupling odd-parity Cooper pairs, it is evaluated by the number $N_{\rm F}$ of the Fermi surfaces enclosing Γ_0,[132]

$$(-1)^\nu = (-1)^{N_{\rm F}/2}, \tag{4.3.38}$$

where the Kramers degeneracy in $N_{\rm F}$ is taken into account. This formula is also useful to clarify the topological superconductivity of time-reversal invariant odd parity superconductors.

4 Inversion family ($\delta_\parallel = 3$)

Here we consider additional symmetries with $\delta_\parallel = 3$ (mod 4). In condensed matter systems, relevant symmetry is inversion. We summarize the classification table for $\delta_\parallel = 3$ with order-two unitary symmetry in Table 4.7 and that with order-two antiunitary symmetry in Table 4.8, respectively.

4.1 Inversion symmetric topological insulators (U in class A, U_+^+ in class AII)

Class A systems in 3 dimensions cannot host a strong topological phase in general. However, the presence of inversion symmetry admits a strong crystalline $\mathbb{Z}$ topological index. [27, 133, 134] The inversion symmetry is expressed as

$$P\mathcal{H}(-\boldsymbol{k})P^{-1} = \mathcal{H}(\boldsymbol{k}) \tag{4.4.1}$$

with a unitary matrix P. Since P is labeled as U in class A of Table 4.7, its topological index is given by $\mathbb{Z}$ in 3 dimensions. The $\mathbb{Z}$ index is defined at symmetric points of inversion, $\boldsymbol{k} = (0,0,0) \equiv \Gamma_0$ and $\boldsymbol{k} = \infty \equiv \Gamma_\infty$ in a manner similar to the 2-dimensional case discussed in Sec.3.4. Since the Hamiltonian commutes with P at $\boldsymbol{k} = \Gamma_i$ $(i = 0, \infty)$, the Hamiltonian is decomposed into two eigensectors of $P = \pm$ as $\mathcal{H}(\Gamma_i) = \mathcal{H}_{P=+}(\Gamma_i) \oplus \mathcal{H}_{P=-}(\Gamma_i)$. Then, the $\mathbb{Z}$ index is defined by the number $\#\Gamma_i^\pm$ of occupied states with parity $P = \pm$ at Γ_i. Using the same argument in Sec.3.4, we have $\#\Gamma_0^+ + \#\Gamma_0^- = \#\Gamma_\infty^+ + \#\Gamma_\infty^-$, and the stable equivalence implies that the index $\mathbb{Z}$ depends only on the difference $(\#\Gamma_0^+ - \#\Gamma_0^-) - (\#\Gamma_\infty^+ - \#\Gamma_\infty^-)$. In 3 dimensions, however, there exists an extra global constraint: By regarding k_z in $\mathcal{H}(\boldsymbol{k})$ as a parameter, one can define the first Chern number $Ch_1(k_z)$, but for a full gapped system in S^3, it must be zero since the 2-dimensional system, which is obtained by fixing k_z of S^3 in the momentum space, smoothly goes to a topologically trivial state as $k_z \to \infty$. This means that $Ch_1(k_z = 0) = 0$ on the inversion symmetric 2-dimensional plane at $k_z = 0$. Therefore, from Eq.(4.3.22), $\#\Gamma_0^+ - \#\Gamma_\infty^+$ must be even. Taking into account this constraint, the $\mathbb{Z}$ index is defined as

$$[\Gamma_{0,\infty}] = \frac{\#\Gamma_0^+ - \#\Gamma_\infty^+}{2}. \tag{4.4.2}$$

For inversion symmetric insulators, the magnetoelectric polarizability,

$$P_3 = \frac{-1}{8\pi^2}\int \mathrm{tr}\left(\mathcal{A}d\mathcal{A} + \frac{2}{3}\mathcal{A}^3\right) \quad \text{(mod. 1)} \tag{4.4.3}$$

Table 4.7: Classification table for topological crystalline insulators and superconductors and their topological defects in the presence of order-two additional unitary symmetry with flipped parameters $\delta_\parallel = d_\parallel - D_\parallel = 3 \pmod 4$. Here $\delta = d - D$.

Symmetry	Class	$\mathcal{C}_q$ or $\mathcal{R}_q$	$\delta=0$	$\delta=1$	$\delta=2$	$\delta=3$	$\delta=4$	$\delta=5$	$\delta=6$	$\delta=7$
U	A	$\mathcal{C}_1$	0	$\mathbb{Z}$	0	$\mathbb{Z}$	0	$\mathbb{Z}$	0	$\mathbb{Z}$
U_+	AIII	$\mathcal{C}_0$	$\mathbb{Z}$	0	$\mathbb{Z}$	0	$\mathbb{Z}$	0	$\mathbb{Z}$	0
U_-	AIII	$\mathcal{C}_1 \times \mathcal{C}_1$	0	$\mathbb{Z}\oplus\mathbb{Z}$	0	$\mathbb{Z}\oplus\mathbb{Z}$	0	$\mathbb{Z}\oplus\mathbb{Z}$	0	$\mathbb{Z}\oplus\mathbb{Z}$
$U_+^+, U_-^-, U_{++}^+, U_{--}^-$	AI	$\mathcal{R}_7$	0	0	0	$2\mathbb{Z}$	0	$\mathbb{Z}_2$	$\mathbb{Z}_2$	$\mathbb{Z}$
	BDI	$\mathcal{R}_0$	$\mathbb{Z}$	0	0	0	$2\mathbb{Z}$	0	$\mathbb{Z}_2$	$\mathbb{Z}_2$
	D	$\mathcal{R}_1$	$\mathbb{Z}_2$	$\mathbb{Z}$	0	0	0	$2\mathbb{Z}$	0	$\mathbb{Z}_2$
	DIII	$\mathcal{R}_2$	$\mathbb{Z}_2$	$\mathbb{Z}_2$	$\mathbb{Z}$	0	0	0	$2\mathbb{Z}$	0
	AII	$\mathcal{R}_3$	0	$\mathbb{Z}_2$	$\mathbb{Z}_2$	$\mathbb{Z}$	0	0	0	$2\mathbb{Z}$
	CII	$\mathcal{R}_4$	$2\mathbb{Z}$	0	$\mathbb{Z}_2$	$\mathbb{Z}_2$	$\mathbb{Z}$	0	0	0
	C	$\mathcal{R}_5$	0	$2\mathbb{Z}$	0	$\mathbb{Z}_2$	$\mathbb{Z}_2$	$\mathbb{Z}$	0	0
	CI	$\mathcal{R}_6$	0	0	$2\mathbb{Z}$	0	$\mathbb{Z}_2$	$\mathbb{Z}_2$	$\mathbb{Z}$	0
U_{+-}^+, U_{-+}^-	BDI, CII	$\mathcal{C}_1$	0	$\mathbb{Z}$	0	$\mathbb{Z}$	0	$\mathbb{Z}$	0	$\mathbb{Z}$
U_{-+}^+, U_{+-}^-	DIII, CI	$\mathcal{C}_1$	0	$\mathbb{Z}$	0	$\mathbb{Z}$	0	$\mathbb{Z}$	0	$\mathbb{Z}$
$U_-^+, U_+^-, U_{--}^+, U_{++}^-$	AI	$\mathcal{R}_1$	$\mathbb{Z}_2$	$\mathbb{Z}$	0	0	0	$2\mathbb{Z}$	0	$\mathbb{Z}_2$
	BDI	$\mathcal{R}_2$	$\mathbb{Z}_2$	$\mathbb{Z}_2$	$\mathbb{Z}$	0	0	0	$2\mathbb{Z}$	0
	D	$\mathcal{R}_3$	0	$\mathbb{Z}_2$	$\mathbb{Z}_2$	$\mathbb{Z}$	0	0	0	$2\mathbb{Z}$
	DIII	$\mathcal{R}_4$	$2\mathbb{Z}$	0	$\mathbb{Z}_2$	$\mathbb{Z}_2$	$\mathbb{Z}$	0	0	0
	AII	$\mathcal{R}_5$	0	$2\mathbb{Z}$	0	$\mathbb{Z}_2$	$\mathbb{Z}_2$	$\mathbb{Z}$	0	0
	CII	$\mathcal{R}_6$	0	0	$2\mathbb{Z}$	0	$\mathbb{Z}_2$	$\mathbb{Z}_2$	$\mathbb{Z}$	0
	C	$\mathcal{R}_7$	0	0	0	$2\mathbb{Z}$	0	$\mathbb{Z}_2$	$\mathbb{Z}_2$	$\mathbb{Z}$
	CI	$\mathcal{R}_0$	$\mathbb{Z}$	0	0	0	$2\mathbb{Z}$	0	$\mathbb{Z}_2$	$\mathbb{Z}_2$
U_{-+}^+, U_{+-}^-	BDI	$\mathcal{R}_1 \times \mathcal{R}_1$	$\mathbb{Z}_2\oplus\mathbb{Z}_2$	$\mathbb{Z}\oplus\mathbb{Z}$	0	0	0	$2\mathbb{Z}\oplus 2\mathbb{Z}$	0	$\mathbb{Z}_2\oplus\mathbb{Z}_2$
U_{+-}^+, U_{-+}^-	DIII	$\mathcal{R}_3 \times \mathcal{R}_3$	0	$\mathbb{Z}_2\oplus\mathbb{Z}_2$	$\mathbb{Z}_2\oplus\mathbb{Z}_2$	$\mathbb{Z}\oplus\mathbb{Z}$	0	0	0	$2\mathbb{Z}\oplus 2\mathbb{Z}$
U_{-+}^+, U_{+-}^-	CII	$\mathcal{R}_5 \times \mathcal{R}_5$	0	$2\mathbb{Z}\oplus 2\mathbb{Z}$	0	$\mathbb{Z}_2\oplus\mathbb{Z}_2$	$\mathbb{Z}_2\oplus\mathbb{Z}_2$	$\mathbb{Z}\oplus\mathbb{Z}$	0	0
U_{+-}^+, U_{-+}^-	CI	$\mathcal{R}_7 \times \mathcal{R}_7$	0	0	0	$2\mathbb{Z}\oplus 2\mathbb{Z}$	0	$\mathbb{Z}_2\oplus\mathbb{Z}_2$	$\mathbb{Z}_2\oplus\mathbb{Z}_2$	$\mathbb{Z}\oplus\mathbb{Z}$

with the Berry connection $\mathcal{A}$ of $\mathcal{H}(\boldsymbol{k})$, also defines a topological invariant: Because P_3 is defined modulo integer and $P_3 \to -P_3$ under inversion, the value of P_3 is quantized to be 0, 1/2 for inversion symmetric insulators, which means that $(-1)^{2P_3}$ defines a $\mathbb{Z}_2$ invariant. This $\mathbb{Z}_2$ invariant, however, is not independent of $[\Gamma_{0,\infty}]$. It holds that

$$(-1)^{2P_3} = (-1)^{[\Gamma_{0,\infty}]}. \tag{4.4.4}$$

Therefore, the $\mathbb{Z}$ index $[\Gamma_{0,\infty}]$ fully characterizes the topological phase of 3-dimensional inversion symmetric insulators, as indicated by Table 4.7.

If we impose TRS on inversion symmetric insulators, P is labeled as U_+^+ in class AII of Table 4.7. The topological index in 3 dimensions is $\mathbb{Z}$, which is defined in a manner similar to Eq.(4.4.2).

$$[\Gamma_{0,\infty}] = \frac{\#\Gamma_0^+ - \#\Gamma_\infty^+}{2}. \tag{4.4.5}$$

Note here that in contrast to the 2-dimensional case in Sec.3.4, the Kramers degeneracy does not impose an extra constraint because of the global constraint mentioned in the above.

Table 4.8: Classification table for topological crystalline insulators and superconductors and their topological defects in the presence of order-two additional antiunitary symmetry with flipped parameters $\delta_\parallel = d_\parallel - D_\parallel = 3 \pmod 4$. Here $\delta = d - D$.

Symmetry	Class	$\mathcal{C}_q$ or $\mathcal{R}_q$	$\delta=0$	$\delta=1$	$\delta=2$	$\delta=3$	$\delta=4$	$\delta=5$	$\delta=6$	$\delta=7$
A^+	A	$\mathcal{R}_6$	0	0	$2\mathbb{Z}$	0	$\mathbb{Z}_2$	$\mathbb{Z}_2$	$\mathbb{Z}$	0
A^-	A	$\mathcal{R}_2$	$\mathbb{Z}_2$	$\mathbb{Z}_2$	$\mathbb{Z}$	0	0	0	$2\mathbb{Z}$	0
A^+_+	AIII	$\mathcal{R}_7$	0	0	0	$2\mathbb{Z}$	0	$\mathbb{Z}_2$	$\mathbb{Z}_2$	$\mathbb{Z}$
A^-_-	AIII	$\mathcal{R}_1$	$\mathbb{Z}_2$	$\mathbb{Z}$	0	0	0	$2\mathbb{Z}$	0	$\mathbb{Z}_2$
A^-_+	AIII	$\mathcal{R}_3$	0	$\mathbb{Z}_2$	$\mathbb{Z}_2$	$\mathbb{Z}$	0	0	0	$2\mathbb{Z}$
A^+_-	AIII	$\mathcal{R}_5$	0	$2\mathbb{Z}$	0	$\mathbb{Z}_2$	$\mathbb{Z}_2$	$\mathbb{Z}$	0	0
A^+_+, A^+_-	D	$\mathcal{C}_0$	$\mathbb{Z}$	0	$\mathbb{Z}$	0	$\mathbb{Z}$	0	$\mathbb{Z}$	0
A^-_+, A^-_-	C	$\mathcal{C}_0$	$\mathbb{Z}$	0	$\mathbb{Z}$	0	$\mathbb{Z}$	0	$\mathbb{Z}$	0
A^-_+, A^-_-	D	$\mathcal{R}_2 \times \mathcal{R}_2$	$\mathbb{Z}_2 \oplus \mathbb{Z}_2$	$\mathbb{Z}_2 \oplus \mathbb{Z}_2$	$\mathbb{Z} \oplus \mathbb{Z}$	0	0	0	$2\mathbb{Z} \oplus 2\mathbb{Z}$	0
A^+_+, A^+_-	C	$\mathcal{R}_6 \times \mathcal{R}_6$	0	0	$2\mathbb{Z} \oplus 2\mathbb{Z}$	0	$\mathbb{Z}_2 \oplus \mathbb{Z}_2$	$\mathbb{Z}_2 \oplus \mathbb{Z}_2$	$\mathbb{Z} \oplus \mathbb{Z}$	0

Like an ordinary topological insulator, TRS also admits to define the 3-dimensional $\mathbb{Z}_2$ invariant. [91, 135, 138] However, it is not independent of $[\Gamma_{0,\infty}]$ again. Indeed, the $\mathbb{Z}_2$ invariant can be expressed in terms of the magnetoelectric polarizability,[139]

$$(-1)^\nu = (-1)^{2P_3}, \tag{4.4.6}$$

and thus Eq.(4.4.4) leads to

$$(-1)^\nu = (-1)^{[\Gamma_{0,\infty}]}. \tag{4.4.7}$$

By using the relation $\#\Gamma_0^+ + \#\Gamma_0^- = \#\Gamma_\infty^+ + \#\Gamma_\infty^-$ that holds for full gapped systems, this equation is recast into

$$(-1)^\nu = (-1)^{(\#\Gamma_0^- + \#\Gamma_\infty^-)/2}. \tag{4.4.8}$$

This is the Fu-Kane's parity formula for the $\mathbb{Z}_2$ invariant.[52]

4.2 Odd parity superconductors in three dimensions (U^+_- in class D, U^+_{+-} in class DIII)

We examine here topological phases in 3-dimensional odd parity superconductors. As in 2 dimensions discussed in Sec.3.5, the inversion $\tilde{P}$ of the BdG Hamiltonian anticommutes with $C = \tau_x\mathcal{K}$, and thus it is labeled as U^+_- in class D of Table 4.7. In 3 dimensions, the topological index is $\mathbb{Z}$. The $\mathbb{Z}$ index is defined at symmetric points, $\boldsymbol{k} = (0,0,0) \equiv \Gamma_0$ and $\boldsymbol{k} = \infty \equiv \Gamma_\infty$, in a manner similar to that for 3-dimensional inversion symmetric topological insulators discussed in Sec.4.1,

$$[\Gamma_{0,\infty}] = \frac{\#\Gamma_0^+ - \#\Gamma_\infty^+}{2}. \tag{4.4.9}$$

where $\#\Gamma_i^\pm$ is the number of negative energy states with parity $\tilde{P} = \pm$ at Γ_i. As well as inversion symmetric topological insulators, we can also introduce a $\mathbb{Z}_2$ index $(-1)^{2P_3}$ with the gravitomagnetoelectric polarizability P_3 defined by Eq.(4.4.3) for the BdG Hamiltonian, but it is not independent

of $[\Gamma_{0,\infty}]$, again. The relation

$$(-1)^{2P_3} = (-1)^{[\Gamma_{0,\infty}]} \tag{4.4.10}$$

holds, and thus the present topological phase is fully characterized by $[\Gamma_{0,\infty}]$. The formula Eq.(4.4.10) is useful to discuss the heat response of odd-parity superconductors by using the axion-type low energy effective Hamiltonian. [75, 140, 76, 73]

Using an argument given in Sec. 3.5, for weak pairing odd parity superconductors, one can evaluate $[\Gamma_{0,\infty}]$ by the electron spectrum in the normal state,

$$[\Gamma_{0,\infty}] = \frac{[\#\epsilon_-^+(\Gamma_0) - \#\epsilon_-^+(\Gamma_0)] - [\#\epsilon_-^+(\Gamma_\infty) - \#\epsilon_-^+(\Gamma_\infty)]}{2} \tag{4.4.11}$$

where $\#\epsilon_-^\pm(\Gamma_i)$ denotes the number of $P = \pm$ bands in the normal state below the Fermi level at Γ_i. (P is the inversion operator acting on electron in the normal state. See Sec. 3.5.)

If an odd parity superconductor has TRS as well, then $\tilde{P}$ is labeled as U_{+-}^+ in class DIII. As is seen in Table 4.7, its topological number is enriched as $\mathbb{Z} \oplus \mathbb{Z}$ in 3 dimensions. One of the $\mathbb{Z}$ indices is $[\Gamma_{0,\infty}]$ in Eq.(4.4.9), and the additional $\mathbb{Z}$ index is the 3-dimensional winding number N_3 in class DIII. Although the parity of N_3 is equal to the parity of $[\Gamma_{0,\infty}]$ [132, 55],

$$(-1)^{N_3} = (-1)^{[\Gamma_{0,\infty}]}, \tag{4.4.12}$$

a full description of the present topological phase needs both of $[\Gamma_{0,\infty}]$ and N_3. We can also relate the parity of N_3 to the gravitomagnetoelectric polarization P_3 as $(-1)^{2P_3} = (-1)^{N_3}$.[6, 73]

In a weak pairing odd parity superconductor, from Eq.(4.4.11), the formula Eq.(4.4.12) is recast into

$$(-1)^{N_3} = (-1)^{[\sum_{\sigma=\pm} \#\epsilon_-^\sigma(\Gamma_0) - \sum_{\sigma=\pm} \#\epsilon_-^\sigma(\Gamma_\infty)]/2} = (-1)^{N_{\rm F}/2}, \tag{4.4.13}$$

where $N_{\rm F}$ is the number of the Fermi surfaces enclosing Γ_0.[132, 55] Note here that $N_{\rm F}$ is even due to the Kramers degeneracy. This formula means that an odd parity superconductor automatically realizes topological superconductivity with non-zero N_3 if it has the Fermi surface with odd $N_{\rm F}/2$. Although a boundary breaks inversion symmetry, the Fermi surface criterion for topological odd-parity superconductivity predicts the existence of surface helical Majorana fermions since N_3 itself is well-defined even in the presence of boundary.

4.3 $\mathbb{Z}_2$ topological phase protected by antiunitary inversion symmetry in three-dimensional class AIII system (A_-^+ in class AIII)

Finally, we examine a three-dimensional class AIII system with an additional antiunitary inversion symmetry A_-^+. As a class AIII system, the winding number N_3 can be introduced by $N_3 = 1/(48\pi^2) \int \mathrm{tr}[\Gamma(\mathcal{H}^{-1}d\mathcal{H})^3]$, but the presence of A_-^+ makes N_3 identically zero because it imposes the constraint $A\Gamma(\mathcal{H}^{-1}d\mathcal{H})^3A^{-1} = -\Gamma(\mathcal{H}^{-1}d\mathcal{H})^3$ on the integral. Alternatively, one can introduce the following $\mathbb{Z}_2$ topological invariant: Because the additional antiunitary inversion

$$A\mathcal{H}(\boldsymbol{k})A^{-1} = \mathcal{H}(\boldsymbol{k}), \quad \{A, \Gamma\} = 0, \quad A^2 = 1, \tag{4.4.14}$$

acts in the same way as the time-reversal in the *coordinate* space, the system can be identified with those in class CI with three coordinate parameters. Therefore, the alternative topological number can be introduced as the third homotopy group of the classifying space of class CI, i.e. $\pi_3(\mathcal{R}_7) = \mathbb{Z}_2$, which reproduces the topological index in Table 4.8.

Chapter 5

Electromagnetic and thermal responses of chiral topological insulators and superconductors

The physical implication of the winding number, which characterizes topological insulators and superconductors with the chiral symmetry in odd spatial dimensions, is discussed. We clarify that the winding number can appear in electromagnetic and thermal responses in a certain class of heterostructure systems. It is also proposed that the Z non-triviality can be detected in the bulk "chiral polarization", which is induced by magnetic field.

1 Chiral symmetry and winding number

The relation between topological invariants and physical observable quantities is a fundamental issue of topological phases. For instance, the Chern number appears as the quantized Hall conductivity in the quantum Hall effect [14], and the Z_2 invariant of a time-reversal invariant (TRI) topological insulator (TI) in 3 dimensions can be detected in axion electromagnetic responses [13]. The correspondence between bulk topological invariants and electromagnetic (or thermal) responses naturally arises from the existence of underlying low-energy effective topological field theories [13].

However, it is not clear that the physical meaning of other topological invariants. Especially, for the case of topological phases characterized by Z invariants in odd spatial dimensions, this point has not yet been fully understood. These classes include 3-dimensional TRI superconductors and 3-dimensional (3D) chiral-symmetric (CS) TIs which have the sublattice symmetry. It is noted that all of these classes possess the chiral symmetry:

$$\Gamma\mathcal{H}(\boldsymbol{k})\Gamma^{-1} = -\mathcal{H}(\boldsymbol{k}) \tag{5.1.1}$$

with Γ a unitary operator, which enable to define a topological invariant referred to as the winding number,

$$N_3 = \frac{1}{48\pi^2}\int_{BZ} \mathrm{tr}\ \Gamma[\mathcal{H}^{-1}d\mathcal{H}]^3. \tag{5.1.2}$$

A general framework which relates the winding number to electromagnetic or thermal responses is still lacking, and desired.

2 Z_2 characterization of winding number

We would like to comment about Z_2 characterization of the winding number. The Z_2 part of the winding number is captured in the axion field theory as in the case of TRI Z_2 TIs, the action of which is given by [13, 75],

$$S_{\rm axion} = \frac{e^2}{2\pi\hbar c}\int dtd^3xP_3\boldsymbol{E}\cdot\boldsymbol{B}, \tag{5.2.1}$$

where

$$P_3 = \frac{1}{8\pi^2}\int_{BZ}{\rm tr}\left[\mathcal{A}d\mathcal{A} - \frac{2i}{3}\mathcal{A}^3\right] \tag{5.2.2}$$

is the magnetoelectric polarization expressed by the Chern-Simons 3-form with Berry connection $\mathcal{A}_{nm}(\boldsymbol{k}) = i\langle u_n(\boldsymbol{k})|du_m(\boldsymbol{k})\rangle$ for occupied states $|u_n(\boldsymbol{k})\rangle$. Because of chiral symmetry, P_3 takes only two values, i.e. $P_3 = \frac{N_3}{2}$ (mod 1) where N_3 is the integer-valued winding number [6]. Thus, the above field theory captures only Z_2 part of the winding number, and fails to describe the Z nontrivial character [141]. The same problem also occurs for class DIII topological superconductors (TSCs), as previously noticed by Wang and his coworkers [140]. For this case, Wang et al. presented an argument based on an effective theory for surface Majorana fermions.

3 Bulk winding number and magnetoelectric polarization in chiral symmetric TIs

We, first, consider the approach based on heterostructure systems. To explain our approach in a concrete way, we consider 3D chiral-symmetric TIs, i.e. a class AIII systems. The following argument is straightforwardly extended to the case of class DIII TSCs. A key idea is to consider a heterostructure system which consists of the 3D CS TI and a chiral-symmetry-broken (CSB) trivial insulator with the Hamiltonian, as depicted in FIG. 5.1(a). Here, the trivial insulator means that $P_3 = 0$ in the bulk. [1] For instance, we can consider the CSB trivial insulator with inversion symmetry in the bulk which ensures $P_3 = 0$. To deal with spatially varying heterostructure systems, we utilize an adiabatic approach. That is, as long as there is a finite energy gap which separates the ground state and the first excited states, the interface structure can be smoothly deformed to the slowly varying one. In the slowly varying structure, the position operator $\hat{z}$ in the Hamiltonian can be treated as a parameter (adiabatic parameter) independent of 3D momentum $\boldsymbol{k}$, which parametrizes the spatial inhomogeneity of the heterostructure. Then, the magnetoelectric polarization $P_3(z)$ is constructed from the adiabatic Hamiltonian of the heterostructure system, $\tilde{H}(\boldsymbol{k}, z)$. $\tilde{H}(\boldsymbol{k}, z)$ interpolates between the bulk Hamiltonian of the CS TI, $H(\boldsymbol{k})$, and that of the CSB trivial insulator, $H_{\rm CSB}(\boldsymbol{k})$, when z is varied; i.e. $\tilde{H}(\boldsymbol{k}, z) = H(\boldsymbol{k})$ when z is a point in the bulk of the CS TI, and $\tilde{H}(\boldsymbol{k}, z) = H_{\rm CSB}(\boldsymbol{k})$ when z in the bulk of the CSB trivial insulator. The adiabatic approach was exploited before to derive electromagnetic responses of the TRI Z_2 TIs from the axion field theory [13, 11]. Our strategy is to extend the adiabatic argument for the Z_2 non-triviality to the Z nontrivial electromagnetic responses. We, first consider the quantum anomalous Hall effect. We note that in

[1] Generally, it is possible that $P_3 \neq 0$ even for a trivial insulator when both time-reversal symmetry and inversion symmetry are broken. We do not consider such a specific case in our scenario.

the heterostructure junction system, the anomalous Hall effect caused by surface Dirac fermions is obtained by integrating z-direction under a z-independent electromagnetic field,

$$S_{surf}[A(t,x,y)] = \frac{e^2}{2\pi\hbar c}\left(\int_{z_0,C}^{z_1} dz \frac{dP_3(z)}{dz}\right)\int dt d^2x \epsilon_{\mu\nu\rho} A_\mu \partial_\nu A_\rho. \tag{5.3.1}$$

Here z_0 (z_1) is a point in the CS TI (CSB trivial insulator), and C is a path of z-integral. Hence the Hall conductivity is given by,

$$\sigma_{\rm H} = \frac{e^2}{2\pi\hbar}\int_{z_0,C}^{z_1} dz \frac{dP_3(z)}{dz} = \frac{e^2}{h}\int_{z_0,C}^{z_1} dP_3(z). \tag{5.3.2}$$

There are two important remarks. First, although the magnetoelectric polarization P_3 is gauge-invariant only for mod 1, the line integral of a small difference of $P_3(z)$ is fully gauge-invariant. Second, $\sigma_{\rm H}$ is determined not only by the bulk magnetoelectric polarization at the point z_0 and that at the point z_1, but also by a homologous equivalence class of the path C. This means that $\sigma_{\rm H}$ depends on the microscopic structure of the interface, and is not protected solely by the bulk topology. The concrete path C is determined by the signs of the mass gaps of Dirac fermions on the surface of the CS TI. In our system, the mass gaps are generated by the chiral-symmetry breaking field induced by the CSB trivial insulator at the surface. [2] Here, we consider the case that the sign of the chiral-symmetry breaking field, and hence, that of the induced mass gaps are uniform on the interface between the CS TI and the CSB trivial insulator. More precisely, the Hamiltonian $H_{\rm CSB}(\boldsymbol{k})$ satisfying this condition is generally expressed as $H_{\rm CSB}(\boldsymbol{k}) = H_0(\boldsymbol{k}) + \alpha(\boldsymbol{k})\Gamma$ where $\alpha(\boldsymbol{k}) > 0$ (or < 0) for any $\boldsymbol{k}$, and Γ is the chiral symmetry operator mentioned before, and $H_0(\boldsymbol{k})$ does not generate mass gaps of the surface Dirac fermions. It is noted that Γ itself plays the role of a chiral-symmetry breaking field. Then the winding number N_3 for $H(\boldsymbol{k})$ and the magnetoelectric polarization $P_3(z)$ for the adiabatic Hamiltonian $\tilde{H}(\boldsymbol{k}, z)$ satisfies the following relation,

$$\int_{z_0,C}^{z_1} dP_3(z) = \pm\frac{N_3}{2}. \tag{5.3.3}$$

This relation is one of our central new findings. The derivation of Eq. (5.3.3) is presented in Appendix A.1.

Using Eqs.(5.3.3) and (5.3.2) together, we can readily obtain the remarkable result that the winding number N_3 can appear in the quantized Hall conductivity for the heterostructure system depicted in FIG.5.1(a),

$$\sigma_{\rm H} = \pm\frac{e^2}{2h}N_3. \tag{5.3.4}$$

Hence, the Z non-triviality of CS TIs can be detected experimentally in this electromagnetic response.

We can also apply the formula (5.3.3) to the investigation on topological magnetoelectric effects which are characterized not by the Z_2 invariant, but by the Z invariant N_3. Let us consider the

[2] $H_{\rm CSB}$ may contain terms proportional to an identity matrix in the sublattice space, which break chiral symmetry, but do not generate mass gaps of the surface Dirac fermions. Since such terms merely shift the chemical potential, and do not affect our argument, we neglect them.

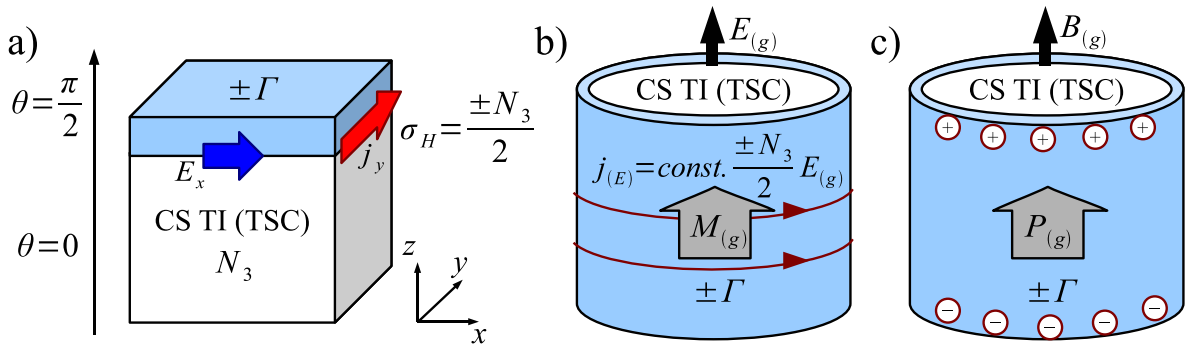

Figure 5.1: Heterostructure composed of a CS TI (or a CS TSC) and trivial insulators (or superconductors) with Hamiltonian $H = \pm\Gamma$. Red arrows represent charge (or energy) currents. In (b) and (c), we assume CS TI (TSC) is coated by a CSB trivial insulator (SC) so that the interface structure has a finite energy gap anywhere. [73]

heterostructure system depicted in FIG.5.1(b) and (c), which consists of a cylindrical CS TI with its surface coated by a CSB trivial insulators. From Eq. (5.3.3), the magnetoelectric polarization of the CS TI coated by the CSB trivial insulator is given by $P_3 = P_3(z = z_1) - \int_{z_0,C}^{z_1} dP_3(z) = \mp\frac{N_3}{2}$, which leads the magnetoelectric effect, $\boldsymbol{P} = -\frac{e^2}{hc}P_3\boldsymbol{B}$ and $\boldsymbol{M} = -\frac{e^2}{hc}P_3\boldsymbol{E}$, [13] i.e.,

$$\boldsymbol{P} = \pm\frac{e^2}{2hc}N_3\boldsymbol{B}, \quad \boldsymbol{M} = \pm\frac{e^2}{2hc}N_3\boldsymbol{E}. \tag{5.3.5}$$

Here, $\boldsymbol{E}$ and $\boldsymbol{B}$ are an electric field and a magnetic field applied parallel to the axis of the cylinder. The winding number successfully appears in the above magnetoelectric responses. It is noted that if the system is extended without open boundaries and possesses translational symmetry, magnetoelectric polarization (5.2.2) is gauge-dependent under large gauge transformation so that $P_3 \mapsto P_3 + n$ where n is integer. $P_3 = \mp\frac{N_3}{2}$ in Eq. (5.3.5) implies that the particular choice of the configuration of the heterostructure as depicted in FIG.5.1(b) and (c) corresponds to the particular choice of the gauge that can extract the winding number of the TI in the heterostructure system.

4 Case of time-reversal invariant topological superconductors

The above argument is also applicable to class DIII TRI TSCs in 3 dimensions. In the case of TSCs with spin-triplet pairing, since both charge and spin are not conserved, it is difficult to detect the topological character in electromagnetic responses. However, instead, thermal responses can be a good probe for the topological nontriviality, because surface Majorana fermions still preserve energy. An effective low energy theory for the thermal responses of TSCs is the gravitational axion

field theory described by the action [75, 76], [3]

$$S = \frac{\pi k_B^2 T^2}{12\hbar v} \int dt d^3x P_3(x) \boldsymbol{E}_g \cdot \boldsymbol{B}_g \tag{5.4.1}$$

where $\boldsymbol{E}_g$ is a gravitoelectric field which play the same role as temperature gradient $-\boldsymbol{\nabla} T/T$, and $\boldsymbol{B}_g$ is a gravitomagnetic field, which is in analogy with a magnetic field of electromagnetism, and v is the fermi velocity. Because of time-reversal symmetry, P_3 in the above action (5.4.1), takes only two values, i.e. 0 or 1/2, implying the Z_2 non-triviality, and hence Eq.(5.4.1) is an incomplete description for the Z nontrivial TSCs. However, as in the case of class AIII TIs discussed above, the winding number N_3 can be detected as thermal responses in a certain class of heterostructure system. In the case of class AIII TIs, an important role is played by the chiral-symmetry-breaking field Γ. Similarly, also in the case of TRI TSCs, the winding number appears in the heterostructure system composed of a TRI TSC and a trivial phase with broken chiral-symmetry. For a p-wave TSC which is realized in ^{3}He, $Cu_xBi_2Se_3$ and Li_2Pt_3B, the chiral-symmetry-breaking field is nothing but an s-wave pairing gap with broken time reversal symmetry. This is easily seen from the fact that the s-wave pairing term of the Hamiltonian is expressed as $\mathrm{Re}\Delta_s \tau_y \sigma_y + \mathrm{Im}\Delta_s \Gamma$ where Δ_s is the s-wave gap, and τ_μ (σ_μ) is the Pauli matrix for particle-hole (spin) space, and the chiral symmetry operator Γ is expressed as $\Gamma = \tau_x \sigma_y$. When the imaginary part of Δ_s is nonzero, this term breaks chiral-symmetry. Thus, Eq.(5.3.3) is applicable for the heterostructure system composed of a TRI TSC and a trivial s-wave SC with broken time-reversal symmetry, as long as the real part of the s-wave gap does not yield gap-closing. For the system depicted in FIGs.1(a), (b) and (c) the quantum anomalous thermal Hall effect and the topological gravitomagetoelectric effects associated with the winding number are realized. Combining the gravitational axion field theory (5.4.1) and the relation (5.3.3), we obtain the quantum anomalous thermal Hall conductivity,

$$\kappa_{xy} = \frac{\pi^2 k_{\mathrm{B}}^2 T}{12h} N_3, \tag{5.4.2}$$

realized for the system shown in FIG.1(a). This result essentially coincides with that obtained by Wang et al. from the argument based on surface Majorana fermions [140]. We can also obtain the gravitomagnetoelectric effects,

$$\boldsymbol{P}_g = \pm \frac{\pi^2 k_{\mathrm{B}}^2 T^2}{12hv} N_3 \boldsymbol{B}_g, \quad \boldsymbol{M}_g = \pm \frac{\pi^2 k_{\mathrm{B}}^2 T^2}{12hv} N_3 \boldsymbol{E}_g, \tag{5.4.3}$$

realized for the system shown in FIG.1(b) and (c). The first equation of Eq.(5.4.3) implies that circulating energy current flows surrounding the axis of the cylinder induces the energy (or thermal) polarization, resulting in nonzero temperature gradient along the axis. The winding number explicitly appears in this thermal response.

[3] The derivation of the gravitoelectromagnetic axion action (8) by Nomura et al. [76] is based on the anomalous thermal Hall effect on the surface of TSC with a finite energy gap. On the other hand, Stone pointed out that the uniform gravitational field cannot produce a nontrivial Riemann curvature in the gravitational instanton term which is the source of the anomalous thermal Hall current [142]. Thus, it is not yet clear how the axion action (8) can be related to the gravitational anomaly in $(3+1)$ dimensions discussed in [75, 140]. However, a recent careful analysis [77, 143] which includes energy magnetization corrections revealed that bulk thermal Hall currents in 2-dimensional gapped systems can be induced by temperature gradient, supporting the argument in [76]. Thus, we believe that, as done in the main text, it is legitimate to discuss the thermal Hall effect and gravitomagnetoelectric effects as bulk effects in gapped systems on the basis of Eq. (8), though the clarification of the topological origin of (8) needs further investigation. Also, we note that Hidaka et al. [144] proposed another origin of the gravitational axion action, which is based on the Nier-Yahn term [145].

5 Chiral polarization and the winding number

Hitherto, we have explored the Z topological responses in heterostructure junction systems in which the winding number successfully emerges as the quantum Hall effect and the topological magnetoelectric effect. However, it is still desirable to establish a direct connection between the winding number and the bulk physical quantities, as in the case of the quantum Hall effect in a 2-dimensional electron gas and Z_2 TIs. We pursue this possibility here. For this purpose, we introduce the chiral polarization defined by,

$$\boldsymbol{P}^5 = \frac{e}{V_c} \sum_{n \in \text{occupied}} \langle w_n | \hat{\boldsymbol{X}}^5 | w_n \rangle, \tag{5.5.1}$$

where $|w_n\rangle$ is the Wannier function, V_c is the unit cell volume, and $\hat{\boldsymbol{X}}^5$ is the projected chiral position operator defined by $\hat{X}^5_\mu = P\Gamma\hat{r}_\mu P$ with $\hat{\boldsymbol{r}}$ a position operator and P the projection to the occupies states. Generally, to construct the Wannier function localized exponentially in real space, we need the absence of gauge obstruction of the Bloch wave function, i.e., vanishing of Chern number $C_{ij}/(2\pi i) = \int_{BZ} d^3k/(2\pi)^3 \mathrm{tr}\mathcal{F}_{ij} = 0$ [146]. In chiral symmetric systems, the Chern numbers C_{ij} are zeroes, [4] and hence the exponentially localized Wannier functions are always well defined. Eq. (5.5.1) is similar to charge polarization, but an important difference is that the chiral symmetry operator Γ is inserted in (5.5.1). For the class AIII TIs and the class BDI TIs with two sub-lattice structures, $\boldsymbol{P}^5$ represents a difference of charge polarization between two sub-lattices. It is noted that in contrast to charge polarization which depends on the choice of gauge, $\boldsymbol{P}^5$ is gauge-invariant, since the gauge ambiguity cancels out between the two sub-lattice contributions explained in Appendix. As will be shown below, $\boldsymbol{P}^5$ is a key bulk quantity which can be related to the winding number. Actually, in the case of 1-dimensional (1D) systems, $\boldsymbol{P}^5$ is expressed by the 1D winding number N_1 as,

$$P^5 = -\frac{N_1 e}{2}, \tag{5.5.2}$$

which is shown in Appendix. For instance, for the 1D BDI class TIs such as the Su-Schrieffer-Heeger model of polyacetylene, Eq.(5.5.2) represents fractional charges which appear at open edges of the system. Eq.(5.5.2) is derived from non-trivial algebraic properties satisfied by $\hat{\boldsymbol{X}}^5$, which can be regarded as a generalization of the commutation relation of the projected position operator $P\hat{\boldsymbol{r}}P$ (See Appendix). In the 3D case, this algebra also yields an interesting result that the winding number N_3 is expressed by the Nambu three bracket of $\hat{\boldsymbol{X}}^5$[147], which recently attracts much attentions in connection with the density algebra in 3D TIs [148, 149]. However, we have not yet succeeded to relate the Nambu bracket to any physical quantities in condensed matter systems. Thus, we here take a different approach for the 3D case. In fact, in the case of 3D AIII TIs, on the assumption that the occupied and unoccupied Wannier states satisfy the chiral symmetry $|w_{\bar{n}}\rangle = \Gamma |w_n\rangle$ ($\bar{n} \in$ unoccupied, $n \in$ occupied), a more remarkable and useful relation between $\boldsymbol{P}^5$ and the winding number N_3 can be derived; $\boldsymbol{P}^5$ can be induced by an applied magnetic field, in

[4] From the chiral symmetry, we can choose the unoccupied states $|\bar{n}\rangle = \Gamma|n\rangle$, then the Chern number of the *unoccupied* state, $\bar{C}h_{ij}$ is identical with one of the occupied state Ch_{ij}: $\bar{C}h_{ij} = Ch_{ij}$ because $\mathrm{tr}\mathcal{F}^{(\bar{n})}_{ij} = i\langle\partial_i\bar{n}|\partial_j\bar{n}\rangle - (i \leftrightarrow j) = i\langle\partial_i n|\partial_j n\rangle - (i \leftrightarrow j) = \mathrm{tr}\mathcal{F}^{(n)}_{ij}$. On the other hand, the sum of the Chern number for all bands is zero: $Chij + \bar{C}h_{ij} = 0$ because $\sum_n \mathrm{tr}\mathcal{F}^{(n)} = \sum_n i\langle\partial_i n|\partial_j n\rangle - (i \leftrightarrow j) = -i\sum_{mn}[\langle n|\partial_j m\rangle\langle m|\partial_j n\rangle - (i \leftrightarrow j)] = 0$. Hence $Ch_{ij} = 0$.

analogy with the topological magnetoelectric effect, and furthermore, N_3 appears in the response function. From the first-order perturbative calculation with respect to a magnetic field, we obtain,

$$\boldsymbol{P}^5 = -\frac{e^2}{2hc} N_3 \boldsymbol{B}. \tag{5.5.3}$$

This is proved in Appendix. Thus, the winding number can be detected as the chiral polarization induced by a magnetic field. This is another main result of this paper.

It is expected that an analogous effect may be realized in 3D TRI TSCs. In the case of TSCs, to explore topological characters, we need to consider thermal responses, instead of electromagnetic ones. However, we have not yet succeeded to obtain thermal analogue of Eq.(5.5.3). Furthermore, it is highly non-trivial what $\boldsymbol{P}^5$ means for the case of superconductors. These are important open issues which should be addressed in the near future.

6 Conclusion

We have clarified that the Z non-triviality of 3D TRI TSCs and TIs with sub-lattice symmetry can appear in electromagnetic and thermal responses of heterostructure systems which consist of the TSCs or TIs and CSB trivial s-wave superconductors or band insulators. We have also established the relation between the bulk winding number and the bulk chiral polarization, which may be utilized for experimental detection of the Z non-triviality.

A Appendix

A.1 The derivation of Eq. (5.3.3)

In this section, we present a detailed derivation of Eq. (5.3.3). We calculate the continuous change of the magnetoelectric polarization $P_3(z)$ between the chiral-symmetric topological insulator $H(\boldsymbol{k})$ with winding number N_3 and chiral-symmetry-broken trivial insulator $H_{CSB}(\boldsymbol{k}) = H_0(\boldsymbol{k}) + \alpha(\boldsymbol{k})\Gamma$ with a trivial magnetoelectric polarization $P_3 = 0$. As noted in the main text, we assume that $\alpha(\boldsymbol{k}) > 0$ (or < 0) for any $\boldsymbol{k}$, and $H_0(\boldsymbol{k})$ does not generate mass gaps. Thus all of the signs of the mass gaps of the surface Dirac fermions are determined by the sign of $\alpha(\boldsymbol{k})$. Since the value of $\int_{z_0,C}^{z_1} dP_3(z)$ is adiabatically protected against smooth deformation of surface structure which does not close the energy gap, it is sufficient for our purpose to consider a flat band system, and assume, without loss of generality, that the spatial inhomogeneity of the heterostructure system is sufficiently slow, allowing the semiclassical treatment of the spatially varying parameter. Then, the Hamiltonian of our system is expressed by

$$\tilde{H}(\boldsymbol{k}, \theta) = \cos\theta Q(\boldsymbol{k}) \pm \sin\theta\Gamma, \tag{5.A.1}$$

where $Q(\boldsymbol{k})$ is the "Q-function" defined by $Q(\boldsymbol{k}) = 1 - 2P(\boldsymbol{k})$ with $P(\boldsymbol{k})$ the projection to occupied bands of $H(\boldsymbol{k})$. The continuous change of the magnetoelectric polarization $P_3(z)$ is given by,

$$\int_{z_0,C}^{z_1} dP_3(z) = \int_0^{\frac{\pi}{2}} d\theta \frac{dP_3(\theta)}{d\theta} = \frac{1}{8\pi^2} \int_{\theta=0}^{\theta=\frac{\pi}{2}} \int_{BZ} \mathrm{tr}\mathcal{F}^2(\boldsymbol{k}, \theta), \tag{5.A.2}$$

where $P_3(\theta)$ is the magnetoelectric polarization of $\tilde{H}(\boldsymbol{k}, \theta)$, $\mathcal{F} = d\mathcal{A} + \mathcal{A} \wedge \mathcal{A}$ is the Berry curvature, and $\mathcal{A}(\boldsymbol{k}, \theta) = i \langle \tilde{u}(\boldsymbol{k}, \theta) | d\tilde{u}(\boldsymbol{k}, \theta) \rangle$ is the Berry connection for the occupied states $|\tilde{u}(\boldsymbol{k}, \theta)\rangle$ of the semiclassical Hamiltonian $\tilde{H}(\boldsymbol{k}, \theta)$.

Note that the Q-function of $\tilde{H}(\boldsymbol{k},\theta)$ is equivalent to $\tilde{H}(\boldsymbol{k},\theta)$ itself as shown below. The occupied states $|\tilde{u}(\boldsymbol{k},\theta)\rangle$ of $\tilde{H}(\boldsymbol{k},\theta)$ are given by

$$|\tilde{u}(\boldsymbol{k},\theta)\rangle = \cos\frac{\theta}{2}|u(\boldsymbol{k})\rangle \mp \sin\frac{\theta}{2}\Gamma|u(\boldsymbol{k})\rangle \tag{5.A.3}$$

with $|u(\boldsymbol{k})\rangle$ the occupied states of $Q(\boldsymbol{k})$, $Q(\boldsymbol{k})|u(\boldsymbol{k})\rangle = -|u(\boldsymbol{k})\rangle$. Then the Q-function of $\tilde{H}(\boldsymbol{k},\theta)$ is

$$\tilde{Q}(\boldsymbol{k},\theta) = 1 - 2\tilde{P}(\boldsymbol{k},\theta) = 1 - 2\sum_{u\in occupied}(|\tilde{u}(\boldsymbol{k},\theta)\rangle\langle\tilde{u}(\boldsymbol{k},\theta)|) = \cos\theta Q(\boldsymbol{k}) \pm \sin\theta\Gamma. \tag{5.A.4}$$

Here, we have used the relation $\Gamma P(\boldsymbol{k}) + P(\boldsymbol{k})\Gamma = \Gamma$ obtained from the chiral symmetry.

We now calculated the right-hand side of (5.A.2). Generally, the Chern form $\mathrm{tr}\mathcal{F}^n$ can be written in terms of the gauge invariant Q-function. In the case of $n = 2$, we have,

$$\mathrm{tr}\mathcal{F}^2(\boldsymbol{k},\theta) = \frac{1}{2^5}\mathrm{tr}\left[\tilde{Q}(\boldsymbol{k},\theta)\left(d\tilde{Q}(\boldsymbol{k},\theta)\right)^4\right]. \tag{5.A.5}$$

Dividing the external differential d into $(d_{\boldsymbol{k}}, d_\theta) = (d_{k_x}, d_{ky}, d_{k_z}, d_\theta)$, and using Eq.(5.A.4), we rewrite the right-hand side of Eq.(5.A.5) as,

$$\mathrm{tr}\left[\tilde{Q}\left(d\tilde{Q}\right)^4\right] = \pm 4\ \mathrm{tr}\left[\Gamma Q(\boldsymbol{k})\left(d_{\boldsymbol{k}}Q(\boldsymbol{k})\right)^3\right] \wedge \cos^3\theta d\theta. \tag{5.A.6}$$

For the basis in which Γ is represented as $\Gamma = \begin{pmatrix} 1 & 0 \\ 0 & -1 \end{pmatrix}$, $Q(\boldsymbol{k})$ is expressed as $Q(\boldsymbol{k}) = \begin{pmatrix} 0 & q(\boldsymbol{k}) \\ q^\dagger(\boldsymbol{k}) & 0 \end{pmatrix}$ with a unitary matrix $q(\boldsymbol{k})$. Then, from Eqs. (5.A.5) and (5.A.6), we have

$$\frac{1}{8\pi^2}\mathrm{tr}\mathcal{F}^2(\boldsymbol{k},\theta) = \pm\frac{1}{32\pi^2}\mathrm{tr}\left[q^\dagger(\boldsymbol{k})d_{\boldsymbol{k}}q(\boldsymbol{k})\right]^3 \wedge \cos^3\theta d\theta. \tag{5.A.7}$$

Hence the change of the magnetoelectric polarization (5.A.2) is given by

$$\int_{z_0,C}^{z_1} dP_3(z) = \pm\frac{1}{32\pi^2}\int_{BZ}\mathrm{tr}\left[q^\dagger(\boldsymbol{k})d_{\boldsymbol{k}}q(\boldsymbol{k})\right]^3\int_{\theta=0}^{\theta=\frac{\pi}{2}}\cos^3\theta d\theta = \pm\frac{1}{2}N_3, \tag{5.A.8}$$

where $N_3 = \frac{1}{24\pi^2}\int_{BZ}\mathrm{tr}\left[q^\dagger(\boldsymbol{k})d_{\boldsymbol{k}}q(\boldsymbol{k})\right]^3$ is the winding number characterizing the ground state topology of the chiral symmetric topological insulator.

A.2 The derivation of Eq. (5.5.2) and some algebraic properties of projected chiral position operator

In this section, we will derive Eq. (5.5.2). For this purpose, we, first, explain some important features of the projected chiral position operator $\hat{X}^5_\mu$ which hold both in 1D and 3D systems. $\hat{X}^5_\mu$ has some similarity with the projected position operator $\hat{X}_\mu = P\hat{r}_\mu P$ where $P = \sum_{n\in\mathrm{occupied}}\sum_{\boldsymbol{k}\in\mathcal{BZ}}|\phi_{n\boldsymbol{k}}\rangle\langle\phi_{n\boldsymbol{k}}|$ is a projector on the occupied bands. It is useful for the following argument to summarize some basic properties of $\hat{X}_\mu$ here. On the basis of Bloch states $|\phi_{n\boldsymbol{k}}\rangle$, $\hat{X}_\mu$ is represented as

$$\left\langle\phi_{n\boldsymbol{k}}\middle|\hat{X}_\mu\middle|\phi_{m\boldsymbol{k}'}\right\rangle = \left(i\delta_{nm}\frac{\partial}{\partial k_\mu} + \mathcal{A}_{nm,\mu}(\boldsymbol{k})\right)\delta_{\boldsymbol{k},\boldsymbol{k}'}, \tag{5.A.9}$$

where $\mathcal{A}_{nm,\mu}(\boldsymbol{k}) = i\left\langle n_{\boldsymbol{k}}\middle|\frac{\partial m_{\boldsymbol{k}}}{\partial k_\mu}\right\rangle$ with $|n_{\boldsymbol{k}}\rangle = e^{-i\boldsymbol{k}\cdot\boldsymbol{r}}|\phi_{n\boldsymbol{k}}\rangle$ is the Berry connection. Then the non-commutativity of the projected position operator $\hat{X}_\mu$ yields

$$\left\langle \phi_{n\boldsymbol{k}}\middle|\left[\hat{X}_\mu,\hat{X}_\nu\right]\middle|\phi_{m\boldsymbol{k}'}\right\rangle = i\mathcal{F}_{nm,\mu\nu}(\boldsymbol{k})\delta_{\boldsymbol{k},\boldsymbol{k}'}, \tag{5.A.10}$$

where $\mathcal{F}_{\mu\nu}(\boldsymbol{k}) = \partial_\mu\mathcal{A}_\nu - \partial_\nu\mathcal{A}_\mu + [\mathcal{A}_\mu,\mathcal{A}_\nu]$ is the non-Abelian Berry curvature arising in multi-band systems. Under a gauge transformation of the occupied Bloch states

$$\Psi(\boldsymbol{k}) = \{|n_{\boldsymbol{k}}\rangle, |m_{\boldsymbol{k}}\rangle, \cdots\}_{n,m,\cdots\in occ} \mapsto \Psi(\boldsymbol{k})U(\boldsymbol{k}) \tag{5.A.11}$$

with a unitary matrix $U(\boldsymbol{k})$, the Berry curvature $\mathcal{F}$ is transformed as $\mathcal{F} \mapsto U^\dagger\mathcal{F}U$, hence a nontrivial gauge dependence do not exist.

We now apply a similar argument to the projected chiral position operator defined by

$$\hat{X}^5_\mu := P\Gamma\hat{r}_\mu P. \tag{5.A.12}$$

The representation of $\hat{X}^5_\mu$ on the basis of Bloch states is given by

$$\left\langle \phi_{n\boldsymbol{k}}\middle|\hat{X}^5_\mu\middle|\phi_{m\boldsymbol{k}'}\right\rangle = i\left\langle n_{\boldsymbol{k}}\middle|\Gamma\middle|\frac{\partial m_{\boldsymbol{k}}}{\partial k_\mu}\right\rangle\delta_{\boldsymbol{k},\boldsymbol{k}'}. \tag{5.A.13}$$

Note that $\langle\phi_{n\boldsymbol{k}}|\Gamma|\phi_{m\boldsymbol{k}'}\rangle$ vanishes when both $|\phi_{n\boldsymbol{k}}\rangle$ and $|\phi_{m\boldsymbol{k}'}\rangle$ are occupied states, because of the chiral symmetry. We denote $\tilde{X}^5_{nm,\mu}(\boldsymbol{k}) := i\left\langle n_{\boldsymbol{k}}\middle|\Gamma\middle|\frac{\partial m_{\boldsymbol{k}}}{\partial k_\mu}\right\rangle$ or $\tilde{X}^5_\mu(\boldsymbol{k}) := i\Psi^\dagger(\boldsymbol{k})\Gamma\partial_\mu\Psi(\boldsymbol{k})$ in matrix representation, Hereafter, $\tilde{X}^5_\mu(\boldsymbol{k})$ is referred to as the projected chiral position. Under a gauge transformation $\Psi(\boldsymbol{k}) \mapsto \Psi(\boldsymbol{k})U(\boldsymbol{k})$, $\tilde{X}^5_\mu(\boldsymbol{k})$ transforms as

$$\tilde{X}^5_\mu(\boldsymbol{k}) \mapsto iU^\dagger(\boldsymbol{k})\Psi^\dagger(\boldsymbol{k})\Gamma\partial_\mu\{\Psi(\boldsymbol{k})U(\boldsymbol{k})\} = U^\dagger(\boldsymbol{k})\tilde{X}^5_\mu(\boldsymbol{k})U(\boldsymbol{k}). \tag{5.A.14}$$

Thus, Here, we used $\langle n_{\boldsymbol{k}}|\Gamma|m_{\boldsymbol{k}}\rangle = 0$ for the n,m occupied bands. Hence, in the chiral symmetric systems, the projected chiral position $\tilde{X}^5_\mu(\boldsymbol{k})$ is gauge invariant in the same way as the Berry curvature $\mathcal{F}_{\mu\nu}(\boldsymbol{k})$, in sharp contrast to the projected position which is gauge-dependent. Furthermore, the commutator of the projected chiral position yields the Berry curvature,

$$\left[\tilde{X}^5_\mu,\tilde{X}^5_\nu\right] = -\Psi^\dagger\Gamma\partial_\mu\Psi\Psi^\dagger\Gamma\partial_\nu\Psi - (\mu\leftrightarrow\nu) = -i\mathcal{F}_{\mu\nu}. \tag{5.A.15}$$

Here we used $1 = \Psi\Psi^\dagger + \Gamma\Psi\Psi^\dagger\Gamma$.

We also remark that the winding number is written as the integral of the $(2n+1)$-bracket of the projected chiral position over the Brillouin zone :

$$N_{2n+1} = \frac{-i^n}{\pi^{n+1}(2n+1)!!}\int_{BZ}\mathrm{tr}\left[\tilde{X}^5_1,\tilde{X}^5_2,\cdots,\tilde{X}^5_{2n+1}\right] \tag{5.A.16}$$

where $[X_1,X_2,\cdots,X_{2n+1}] = \epsilon_{\mu_1\mu_2\cdots\mu_{2n+1}}X_{\mu_1}X_{\mu_2}\cdots X_{\mu_{2n+1}}$ is the $(2n+1)$-bracket, and μ_i run over $1,2,\cdots,2n+1$. Note that when $n=1$ (i.e. N_3), $[X_1,X_2,X_3]$ is the Nambu bracket. This expression of the winding number is analogous to the relation between the Chern number and non-commutativity of the projected position operator. Eq.(5.A.16) directly follows from (2.7.13). The

matrix element of $dQ = d\left(1 - 2\sum_{n\in occupied} |n\rangle\langle n|\right) = -2\sum_{n\in occupied}(|dn\rangle\langle n| + |n\rangle\langle dn|)$ on the basis of the occupied states $|n\rangle$ and unoccupied states $|\bar{n}\rangle = \Gamma|n\rangle$ are

$$\begin{aligned} dQ \to \begin{pmatrix} \langle n|dQ|n'\rangle & \langle n|dQ|\bar{n}'\rangle \\ \langle \bar{n}|dQ|n'\rangle & \langle \bar{n}|dQ|\bar{n}'\rangle \end{pmatrix} &= \begin{pmatrix} 0 & 2\langle n|\Gamma|dn'\rangle \\ -2\langle n|\Gamma|dn'\rangle & 0 \end{pmatrix} \\ &= -2i\tau_2\langle n|\Gamma|dn'\rangle = -2\tau_2\tilde{X}^5_{nn',\mu}\, dk_\mu \end{aligned} \tag{5.A.17}$$

where $\boldsymbol{\tau} = (\tau_1, \tau_2, \tau_3)$ is the Pauli matrices in the occupied-unoccupied space. In the same way, Γ and Q is written as

$$\Gamma \to \begin{pmatrix} \langle n|\Gamma|n'\rangle & \langle n|\Gamma|\bar{n}'\rangle \\ \langle \bar{n}|\Gamma|n'\rangle & \langle \bar{n}|\Gamma|\bar{n}'\rangle \end{pmatrix} = \begin{pmatrix} 0 & \delta_{nn'} \\ \delta_{nn'} & 0 \end{pmatrix} = \tau_1\delta_{nn'}, \tag{5.A.18}$$

$$Q \to \begin{pmatrix} \langle n|Q|n'\rangle & \langle n|Q|\bar{n}'\rangle \\ \langle \bar{n}|Q|n'\rangle & \langle \bar{n}|Q|\bar{n}'\rangle \end{pmatrix} = \begin{pmatrix} -\delta_{nn'} & 0 \\ 0 & \delta_{nn'} \end{pmatrix} = -\tau_3\delta_{nn'}. \tag{5.A.19}$$

By using (5.A.17), (5.A.18) and (5.A.19), we can write the winding number (2.7.13) as

$$\begin{aligned} N_{2n+1} &= \frac{(-1)^n}{(2\pi i)^{n+1}2^{n+1}(2n+1)!!}\int_{BZ} \mathrm{tr}\ \Gamma Q(\boldsymbol{k})\,[dQ(\boldsymbol{k})]^{2n+1} \\ &= \frac{(-1)^n}{(2\pi i)^{n+1}2^{n+1}(2n+1)!!}\int_{BZ} \mathrm{tr}\left[\tau_1(-\tau_3)\left(-2\tau_2\tilde{X}^5_{\mu_1}\, dk_{\mu_2}\right)\wedge\cdots\wedge\left(-2\tau_2\tilde{X}^5_{\mu_{2n+1}}\, dk_{\mu_{2n+1}}\right)\right] \\ &= \frac{(-1)^{n+1}}{(\pi i)^n(2n+1)!!}\int_{BZ} \mathrm{tr}\left[\tilde{X}^5_{\mu_1}\tilde{X}^5_{\mu_2}\cdots\tilde{X}^5_{\mu_{2n+1}}\right] dk_{\mu_1}\wedge\cdots\wedge dk_{\mu_{2n+1}} \end{aligned} \tag{5.A.20}$$

Thus, we arrive at (5.A.16).

In the case of the 1-dimensional systems, the winding number

$$N_1 = -\frac{1}{\pi}\int_{BZ} \mathrm{tr}\ \tilde{X}^5(\boldsymbol{k}) \tag{5.A.21}$$

is directly related to the chiral polarization defined by (5.5.1). For the Wannier function localized at the site R, (5.5.1) is

$$P^5 = \frac{e}{V_cN_c}\sum_{n\in occupied}\sum_{k,k'}\left\langle \phi_{nk}\middle| e^{ikR}\Gamma\hat{x}e^{-ik'R}\middle|\phi_{nk'}\right\rangle = \frac{e}{2\pi}\int_{BZ} dk\ \mathrm{tr}\ \tilde{X}^5(k) = -\frac{N_1e}{2}, \tag{5.A.22}$$

where N_c is the number of unit cell. Thus we obtain Eq.(5.5.2).

To close this section, we would like to comment on an implication of (5.A.16) to the 3D case. In this case, from Eq.(5.A.16), the winding number N_3 is expressed in terms of the Nambu bracket. This implies that N_3 may be related to a physical quantity described by the Nambu dynamics [147]. However, we do not know any examples in condensed matter systems which are described by the Nambu mechanics, and also quantum version of the Nambu mechanics is not well understood. We have not yet succeeded to obtain any insight from the study in this direction. Thus, we consider a different approach to relate the 3D winding number N_3 to a physical quantity, as explained in the main text and the following section.

A.3 The derivation of Eq. (5.5.3)

In this section, we derive Eq.(5.5.3) on the assumption that the occupied and unoccupied Wannier states satisfy the chiral symmetry $|w_{\bar{n}\boldsymbol{R}}\rangle = \Gamma\,|w_{n\boldsymbol{R}}\rangle$ ($\bar{n} \in$ unoccupied, $n \in$ occupied). This is equivalent to the gauge fixing condition $|\phi_{\bar{n}\boldsymbol{k}}\rangle = \Gamma\,|\phi_{n\boldsymbol{k}}\rangle$ for unoccupied and occupied Bloch states. Our derivation of Eq.(5.5.3) is based on the perturbation formalism developed by Kita-Arai [150] for the Wannier function under the magnetic field. Generally, to construct the exponentially localized Wannier function, we need the absence of gauge obstruction of the Bloch wave function, i.e., vanishing of Chern number $C_{ij}/(2\pi i) = \int_{BZ} d^3k/(2\pi)^3 \mathrm{tr}\mathcal{F}_{ij} = 0$. In chiral symmetric systems, the Chern numbers C_{ij} are zeroes, and hence the exponentially localized Wannier functions are always well defined.

The chiral charge polarization in the case with no magnetic field introduced in the main text is

$$\boldsymbol{P}^5_{(\boldsymbol{B}=\boldsymbol{0})} = \frac{e}{V_c}\sum_{n\in occ}\langle w_{n\boldsymbol{R}}|\Gamma\hat{\boldsymbol{r}}|w_{n\boldsymbol{R}}\rangle\,, \tag{5.A.23}$$

where $|w_{n\boldsymbol{R}}\rangle$ is the Wannier function localized at a site $\boldsymbol{R}$ constructed from the n-th occupied band,

$$|w_{n\boldsymbol{R}}\rangle = \frac{1}{\sqrt{N_c}}\sum_{\boldsymbol{k}} e^{-i\boldsymbol{k}\cdot\boldsymbol{R}}\,|\phi_{n\boldsymbol{k}}\rangle\,, \tag{5.A.24}$$

where N_c is the number of unit cells. Now, we will calculate the first order perturbative corrections to $\boldsymbol{P}^5$ with respect to an applied uniform magnetic field $\boldsymbol{B}$. First, we introduce modified Wannier states $|w'_{n\boldsymbol{R}}\rangle$ defined by [151]

$$w'_{n\boldsymbol{R}}(\boldsymbol{r}) = e^{iI_{\boldsymbol{r}\boldsymbol{R}}}w_{n\boldsymbol{R}}(\boldsymbol{r}), \tag{5.A.25}$$

where $I_{\boldsymbol{r}\boldsymbol{R}}$ is the Peierls phase

$$I_{\boldsymbol{r}\boldsymbol{R}} = \frac{e}{\hbar c}\int_{\boldsymbol{R}}^{\boldsymbol{r}} d\boldsymbol{r}'\cdot\boldsymbol{A}(\boldsymbol{r}') \tag{5.A.26}$$

with $d\boldsymbol{r}'$ the straight line path from $\boldsymbol{R}$ to $\boldsymbol{r}$. The modified Wannier states $|w'_{n\boldsymbol{R}}\rangle$ form a complete set, though they are not orthonormal for the case with a finite magnetic field. To orthonormalize them, we need to include corrections from other sites and other bands to $|w'_{n\boldsymbol{R}}\rangle$. Then, the orthonormal modified Wannier function is expressed as,

$$|\varphi_{n\boldsymbol{R}}\rangle = \sum_{n'\boldsymbol{R}}|w'_{n'\boldsymbol{R}'}\rangle\,S_{n'\boldsymbol{R}',n\boldsymbol{R}}, \tag{5.A.27}$$

for which $\langle\varphi_{n\boldsymbol{R}}|\varphi_{n'\boldsymbol{R}'}\rangle = \delta_{nn'}\delta_{\boldsymbol{R}\boldsymbol{R}'}$ is satisfied. Thus, the chiral charge polarization under an applied magnetic field is given by

$$\boldsymbol{P}^5 = \frac{e}{V_c}\sum_{n\in occ}\langle\varphi_{n\boldsymbol{R}}|\Gamma\hat{\boldsymbol{r}}|\varphi_{n\boldsymbol{R}}\rangle\,. \tag{5.A.28}$$

From Ref. [150], in the cases of a uniform magnetic field, $S_{n'\boldsymbol{R}',n\boldsymbol{R}}$ is expanded up to the first order in $\boldsymbol{B}$:

$$S_{n'\boldsymbol{R}',n\boldsymbol{R}} = \delta_{nn'}\delta_{\boldsymbol{R}\boldsymbol{R}'} - \frac{ie}{4\hbar c}B_i\epsilon_{ijl}\frac{e^{iI_{\boldsymbol{R}'\boldsymbol{R}}}}{N_c}\sum_{\boldsymbol{k}} e^{i\boldsymbol{k}\cdot(\boldsymbol{R}'-\boldsymbol{R})}\,\langle\partial_j n'_{\boldsymbol{k}}|\partial_l n_{\boldsymbol{k}}\rangle\,, \tag{5.A.29}$$

where $|n_{\boldsymbol{k}}\rangle = e^{-i\boldsymbol{k}\cdot\hat{\boldsymbol{r}}}|\phi_{n\boldsymbol{k}}\rangle$. We denote $|\varphi_{n\boldsymbol{R}}\rangle = |w'_{n\boldsymbol{R}}\rangle + |\delta w'_{n\boldsymbol{R}}\rangle$. Then, the correction term of the chiral polarization is

$$\delta \boldsymbol{P}^5 = \frac{e}{V_c}\sum_{n\in occ}\left[\langle w'_{n\boldsymbol{R}}|\Gamma\hat{\boldsymbol{r}}|w'_{n\boldsymbol{R}}\rangle - \langle w_{n\boldsymbol{R}}|\Gamma\hat{\boldsymbol{r}}|w_{n\boldsymbol{R}}\rangle\right] + \frac{e}{V_c}\sum_{n\in occ}\left[\langle w'_{n\boldsymbol{R}}|\Gamma\hat{\boldsymbol{r}}|\delta w'_{n\boldsymbol{R}}\rangle + c.c.\right]. \quad (5.A.30)$$

The first term vanishes since the Peierls phases of $|w'_{n\boldsymbol{R}}\rangle$ are canceled out in $\langle w'_{n\boldsymbol{R}}|\Gamma\hat{\boldsymbol{r}}|w'_{n\boldsymbol{R}}\rangle$. The second term is recast into the following form with the use of (5.A.29),

$$\langle w'_{n\boldsymbol{R}}|\Gamma\hat{\boldsymbol{r}}|\delta w'_{n\boldsymbol{R}}\rangle = -\frac{ie}{4\hbar c}B_i\epsilon_{ijl}\sum_{n'\boldsymbol{R}'}\langle w_{n\boldsymbol{R}}|\Gamma\hat{\boldsymbol{r}}|w_{n'\boldsymbol{R}'}\rangle\frac{1}{N_c}\sum_{\boldsymbol{k}}e^{i\boldsymbol{k}\cdot(\boldsymbol{R}'-\boldsymbol{R})}\langle\partial_j n'_{\boldsymbol{k}}|\partial_l n_{\boldsymbol{k}}\rangle. \quad (5.A.31)$$

Here, we omitted the Peierls phases since they are higher order corrections. On the other hand, the factor $\langle w_{n\boldsymbol{R}}|\Gamma\hat{\boldsymbol{r}}|w_{n'\boldsymbol{R}'}\rangle$ is expressed as,

$$\begin{aligned}\langle w_{n\boldsymbol{R}}|\Gamma\hat{\boldsymbol{r}}|w_{n'\boldsymbol{R}'}\rangle &= \frac{1}{N_c}\sum_{\boldsymbol{k},\boldsymbol{k}'}e^{i\boldsymbol{k}\cdot\boldsymbol{R}}\langle\phi_{n\boldsymbol{k}}|\Gamma\hat{\boldsymbol{r}}|\phi_{n'\boldsymbol{k}'}\rangle e^{-i\boldsymbol{k}'\cdot\boldsymbol{R}'}\\ &= \boldsymbol{R}\delta_{\bar{n}n'}\delta_{\boldsymbol{R},\boldsymbol{R}'} + \frac{1}{N_c}\sum_{\boldsymbol{k}}e^{i\boldsymbol{k}\cdot(\boldsymbol{R}-\boldsymbol{R}')}i\langle n_{\boldsymbol{k}}|\Gamma|\boldsymbol{\nabla}n'_{\boldsymbol{k}}\rangle,\end{aligned} \quad (5.A.32)$$

where $\bar{n}$ is a label for an unoccupied state and we fixed the gauge of $|\phi_{\bar{n}}\rangle$ satisfying $|\phi_{\bar{n}}\rangle = \Gamma|\phi_n\rangle$ with $|\phi_n\rangle$ an occupied state. From (5.A.31) and (5.A.32), we have,

$$\langle w'_{n\boldsymbol{R}}|\Gamma\hat{\boldsymbol{r}}|\delta w'_{n\boldsymbol{R}}\rangle = -\frac{ie}{4\hbar c}B_i\epsilon_{ijl}\frac{1}{N_c}\sum_{\boldsymbol{k}}\left[\boldsymbol{R}\langle\partial_j n'_{\boldsymbol{k}}|\Gamma|\partial_l n_{\boldsymbol{k}}\rangle + \sum_{n'}i\langle n_{\boldsymbol{k}}|\Gamma|\boldsymbol{\nabla}n'_{\boldsymbol{k}}\rangle\langle\partial_j n'_{\boldsymbol{k}}|\partial_l n_{\boldsymbol{k}}\rangle\right]. \quad (5.A.33)$$

The first term vanishes because it is the total derivative : $\epsilon_{ijl}\langle\partial_j n_{\boldsymbol{k}}|\Gamma|\partial_l n_{\boldsymbol{k}}\rangle = \epsilon_{ijl}\partial_j\{\langle n_{\boldsymbol{k}}|\Gamma|\partial_l n_{\boldsymbol{k}}\rangle\}$. Hence we obtain,

$$\begin{aligned}\delta\boldsymbol{P}^5 &= \frac{e^2}{4\hbar c}B_i\epsilon_{ijl}\frac{1}{N_cV_c}\sum_{n\in occ}\sum_{n'\boldsymbol{k}}\langle n_{\boldsymbol{k}}|\Gamma|\boldsymbol{\nabla}n'_{\boldsymbol{k}}\rangle\langle\partial_j n'_{\boldsymbol{k}}|\partial_l n_{\boldsymbol{k}}\rangle + c.c.\\ &= \frac{e^2}{2\hbar c}B_i\epsilon_{ijl}\int\frac{d^3\boldsymbol{k}}{(2\pi)^3}\mathrm{tr}\left[\Psi^\dagger\Gamma\boldsymbol{\nabla}\Psi\partial_j\Psi^\dagger\partial_l\Psi + \Psi^\dagger\boldsymbol{\nabla}\Psi\partial_j\Psi^\dagger\Gamma\partial_l\Psi\right],\end{aligned} \quad (5.A.34)$$

where $\Psi = \{|n_1\rangle, |n_2\rangle, \cdots\}_{n_i\in occ}$ and we omit the parameter $\boldsymbol{k}$.

From this expression, we find that $\alpha_{ij} = \frac{\delta P^5_i}{\delta B_j}$ is proportional to δ_{ij}. For instance, we consider an off-diagonal component,

$$\begin{aligned}\alpha_{xy} &= \frac{e^2}{2\hbar c}\epsilon_{yjl}\int\frac{d^3\boldsymbol{k}}{(2\pi)^3}\mathrm{tr}\left[\Psi^\dagger\Gamma\partial_x\Psi\partial_j\Psi^\dagger\partial_l\Psi + \Psi^\dagger\partial_x\Psi\partial_j\Psi^\dagger\Gamma\partial_l\Psi\right]\\ &= \frac{e^2}{2\hbar c}\int\frac{d^3\boldsymbol{k}}{(2\pi)^3}\mathrm{tr}\left[\Psi^\dagger\Gamma\partial_x\Psi\partial_z\Psi^\dagger\partial_x\Psi - \Psi^\dagger\Gamma\partial_x\Psi\partial_x\Psi^\dagger\partial_z\Psi + \Psi^\dagger\partial_x\Psi\partial_z\Psi^\dagger\Gamma\partial_x\Psi - \Psi^\dagger\partial_x\Psi\partial_x\Psi^\dagger\Gamma\partial_z\Psi\right].\end{aligned} \quad (5.A.35)$$

We see that on the interior of the trace in Eq.(5.A.35),

$$(1st) + (4th) = \mathrm{tr}\left[-\partial_x\Psi\partial_x\Psi^\dagger\Gamma\partial_z P\right], \quad (5.A.36)$$

and

$$(2nd) + (3rd) = \mathrm{tr}\left[-\partial_x \Psi \partial_x \Psi^\dagger \partial_z P \Gamma\right]. \tag{5.A.37}$$

Thus, we can show

$$\alpha_{xy} = \frac{e^2}{2\hbar c}\int \frac{d^3\boldsymbol{k}}{(2\pi)^3}\mathrm{tr}\left[-\partial_x \Psi \partial_x \Psi^\dagger \left(\Gamma \partial_z P + \partial_z P \Gamma\right)\right] = 0, \tag{5.A.38}$$

where, $P = \sum_{n\in occ} |n\rangle \langle n|$ is a projector to occupied bands, and we have used $d\Psi\Psi^\dagger + \Psi d\Psi^\dagger = dP$, and $\Gamma\partial_z P + \partial_z P\Gamma = \partial_z \Gamma = 0$. Hence,

$$\alpha_{ij} = \delta_{ij}\frac{e^2}{24\pi^3\hbar c}\int \mathrm{tr}\left[\Psi^\dagger \Gamma d\Psi d\Psi^\dagger d\Psi\right], \tag{5.A.39}$$

The integrand of this expression is gauge-invariant under gauge transformation $\Psi \to \Psi U$ with a unitary matrix U except for total derivative. This is seen as follows.

$$\mathrm{tr}\left[\Psi^\dagger \Gamma d\Psi d\Psi^\dagger d\Psi\right] \mapsto \mathrm{tr}\left[U^\dagger \Psi^\dagger \Gamma d(\Psi U) d(U^\dagger \Psi^\dagger) d(\Psi U)\right] = \mathrm{tr}\left[\Psi^\dagger \Gamma d\Psi d\Psi^\dagger d\Psi\right] - d\ \mathrm{tr}\left[\Psi^\dagger \Gamma d\Psi U dU^\dagger\right], \tag{5.A.40}$$

where, we have used $\Psi\Psi^\dagger\Gamma + \Gamma\Psi\Psi^\dagger = \sum_{n\in occ}\left(|n\rangle\langle n|\Gamma + \Gamma|n\rangle\langle n|\right) = \Gamma$. Hence the integral over the Brillouin zone is gauge-invariant. Now, we choose the basis, $\Psi = \frac{1}{\sqrt{2}}\begin{pmatrix} q \\ -1 \end{pmatrix}$, where, q is the off diagonal part of Q-function $Q = \begin{pmatrix} 0 & q \\ q^\dagger & 0 \end{pmatrix}$. Then

$$\alpha^i_j = -\delta^i_j \frac{e^2}{96\pi^3\hbar}\int \mathrm{tr}(q^\dagger dq)^3 = -\delta^i_j \frac{e^2}{4\pi\hbar} N_3, \tag{5.A.41}$$

where $N_3 = \frac{1}{24\pi^3}\int \mathrm{tr}(q^\dagger dq)^3$ is the winding number. Thus we arrive at Eq. (5.5.3).

Note that the magnetic induced chiral polarization represented by the first line of (5.A.34) generally depends on the gauge of the unoccupied Bloch states $|\phi_{\bar{n}\boldsymbol{k}}\rangle$, so the gauge fixing condition $|\phi_{\bar{n}\boldsymbol{k}}\rangle = \Gamma|\phi_{n\boldsymbol{k}}\rangle$ is crucial for our results.

Chapter 6

Dynamical axion phenomena in superconductors and superfluids

In this chapter, we argue dynamical axion phenomena in superconductors and superfluids in terms of the gravitoelectromagnetic topological action. The dynamical axion is induced by relative phase fluctuations between topological and s-wave superconducting orders. We show that an antisymmetric spin-orbit interaction (SOI) which induces parity-mixing of Cooper pairs enlarges the parameter region in which the dynamical axion fluctuation appears as a low-energy excitation.

The organization of this chapter is as follows. First, we give a background material and motivation in Sec. 1. In Sec. 2, we give topological θ terms that may be related to the axion physics in thermal (or gravitational) responses. In Sec. 4, we consider a concrete microscopic model of a topological superconductor (TSC) in which the dynamical action appears at a sufficiently low-energy scale compared to the bulk superconducting gap, and clarify the effect of the SOI raised by broken inversion symmetry, which makes low-energy dynamical axion more feasible. In Sec. 5, we discuss experimentally observable phenomena driven by the dynamical axion in TSC. We conclude in Sec.6 with some remarks.

1 Introduction

The topological θ term of electromagnetic fields,

$$S_{\rm axion} = \frac{\alpha}{4\pi^2}\int d^3x dt \theta(x) \boldsymbol{E}\cdot\boldsymbol{B} \tag{6.1.1}$$

describes axion electrodynamics of insulators. [13] Here $\alpha = e^2/\hbar c$ is the fine structure constant. $\theta(x)$ is a magnetoelectric polarization which reflects the nontrivial momentum space topology of band insulators. Because $\boldsymbol{E}\cdot\boldsymbol{B}$ is a total derivative, physical phenomena associated with $\mathcal{L}_{\rm top}$ arise only when θ is spatially or temporally inhomogeneous. A domain wall of θ leads to the anomalous Hall effect and the image monopole effect. [152] Thermal or quantum fluctuations of the axion field θ also yield various interesting phenomena. For example, in a time-reversal invariant $\mathbb{Z}_2$ topological insulator in 3 dimension, inter-orbital antiferromagnetic fluctuations induce the dynamical axion field, which couples with electromagnetic fields, leading to an axionic polariton under an applied magnetic field [45] and magnetic instability under an applied electrostatic field. [46]

In the case of TSCs, since charge, and also spin if the SOI presents, are not conserved, it is difficult to detect topological characters in electromagnetic responses. However, thermal responses can be good probes for topological nontriviality because energy is still conserved. TSCs with time-reversal symmetry (class DIII) in 3-spatial dimensions are classified by an integer $\mathbb{Z}$, i.e. the so-called winding number, [4] and the TSC characterized by the topological invariant N possesses N gapless Majorana fermions at open boundaries. If mass gaps are induced in surface gapless Majorana fermions, the (2+1)-dimensional surface exhibits the thermal Hall effect, which can be interpreted in the context of the thermal axion physics where the axion field θ equals to $N\pi$. [75, 140, 76] From analogy to the dynamical axion in the topological insulators, [45] one can deduce that for TSCs, the dynamical axion field in TSCs can be provided by imaginary s-wave superconducting fluctuations, which break quantization of magnetoelectric polarization and lead to dynamics of θ. [73]

In the present chapter, we discuss the axion physics in TSCs mainly focusing on its dynamical effects, i.e. fluctuations of the axion field in TSCs. We investigate low-energy excitations of the dynamical axion using a concrete model of a p-wave TSC with an s-wave channel attractive interaction which is necessary for inducing dynamics of axion. We also discuss the effect of the SOI in the case with noncentrosymmetric crystal structures, and show that the inversion-symmetry-breaking SOI enhances significantly dynamical axion fluctuations. We also discuss some implications for experimentally observable phenomena involving dynamical axion.

2 Gravitational topological action term for topological superconductors

In this section, we briefly review previous argument on topological action terms and effective internal energy related with thermal responses in TSCs, which are the basis for dynamical axion phenomena. In TSCs, a conserved quantity is energy, and hence thermal responses can be used for probing the topological nontriviality. For translational invariant superfluids, momentum is also a conserved current. Probe fields which couple with energy-momentum tensor are metric. Here we consider topological action terms which are constructed from the metric degrees of freedom, These action terms are known as the gravitational instanton term in (3+1) dimensions and the gravitational Chern-Simons (CS) term in (2+1) dimensions. Also, we introduce another type of a topological term which is related with the gravitoelectromagnetism and the torsional anomaly. [144, 153]

2.1 (2+1) dimensions

In 2-dimensional systems, TSCs characterized by the nontrivial Chern number have the gravitational CS 3 form as a low-energy effective theory, [10, 37]

$$S_{CS} = \frac{1}{4\pi}\frac{c}{24}\int d^3x \epsilon^{\mu\nu\rho}\mathrm{tr}\left(\omega_\mu \partial_\nu \omega_\rho + \frac{2}{3}\omega_\mu\omega_\nu\omega_\rho\right) \tag{6.2.1}$$

with $x = (c_0 t, \boldsymbol{r})$ where c_0 is the Fermi velocity, ω_μ the spin connections determined by the metric and $c = 1/2$, which is the central charge of the Ising conformal field theory. It has been discussed that there should be an edge channel with the central charge $c = 1/2$, which raises the thermal Hall effect in Hall-bar geometry. [37] It is important to note that the gravitational CS term (6.2.1) does not directly lead to the thermal Hall effect in (2+1) dimension, because (6.2.1) yields the energy current proportional to gradient of the Ricci tensor which corresponds to a spatially second order

differential of a temperature field. [142] In this respect, the gravitational CS action differs from the electromagnetic CS action $S_{CS} = c\frac{\alpha}{4\pi}\int d^3x\epsilon^{\mu\nu\rho}A_\mu\partial_\nu A_\rho$, which yields the Hall current proportional to electric field via a functional derivative, $j_y = c(e^2/h)E_x$.

On the other hand, a careful calculation of the thermal Hall effect including a contribution of the dia-thermal current (a change of the local thermal current operator due to an applied gravitational field), [154, 76] or equivalently, a contribution from the thermal magnetization current, [77, 143] provides the generalized Wiedemann-Franz low at low temperature, which suggests the thermal Hall effect in the (2+1) dimensional bulk system with a topological thermal coefficient defined by $j_{Hy} = \kappa_H\partial_x T$,

$$\kappa_H = c\frac{\pi^2 k_B^2 T}{3h}. \tag{6.2.2}$$

This thermal Hall conductivity agrees with the result obtained from the (1+1) dimensional edge theory. Here, we would like to note that an important role of the energy magnetization contribution can be seen in various systems. For instance, let us consider massive Weyl fermions described by the bulk Hamiltonian $\mathcal{H} = \sigma_1 k_x + \sigma_2 k_y + m\sigma_3$. In this system, the standard Kubo formula for energy current correlation functions gives no contribution, and the thermal Hall conductivity κ_H stems only from the energy magnetization.

The topological thermal Hall conductivity (6.2.2) from the (2+1) dimensional bulk calculation suggests an alternative low energy effective action describing the thermal Hall effect,

$$S_{CS} = c\frac{\pi^2 k_B^2 T^2}{6h}\int dtd^2\boldsymbol{r}\epsilon^{\mu\nu\rho}A_{E,\mu}\partial_\nu A_{E,\rho} \tag{6.2.3}$$

where $A_{E\mu} = (A_{0E}, \boldsymbol{A}_E)$ couple with an energy density $h(\boldsymbol{x})$ and an energy current density $\boldsymbol{j}_E(\boldsymbol{x})$ via $H_c = \int d^2x\,(h(\boldsymbol{x})A_{E0} - \boldsymbol{j}_E(\boldsymbol{x})\cdot\boldsymbol{A}_E)$. In the action (6.2.3), an overall coefficient has a dimension of the square of energy, which is the same as the the torsional anomaly. [153] The relation between the thermal Hall effect and the torsional anomaly was discussed by Hidaka et al. at zero temperature.[144] Also, Shi and Cheng discussed [155] the gauge invariance for $\boldsymbol{A}_E$ within a first order of $A_{E\mu}$ by using the scaling relation for the energy current density under gravitational potential. [156, 77] We could not derive the action (6.2.3) directly from microscopic Hamiltonian of electron systems coupled with gravitoelectromagnetic fields. However, we deduce it from the analogy with the relation between the (2+1) dimensional electromagnetic CS action and the electric Hall conductivity. It is still an important open issue to establish the low-energy effective field theory of the thermal Hall effect.

2.2 (3+1) dimensions

For (3+1) dimensional TSCs with time-reversal symmetry classified by the topological invariant N, a low-energy gravitational effective theory is described by the gravitational instanton term,

$$S_\theta = \frac{\theta}{1536\pi^2}\int d^4x\epsilon^{\mu\nu\rho\sigma}R^\alpha_{\beta\mu\nu}R^\beta_{\alpha\rho\sigma} \tag{6.2.4}$$

with $\theta = \pi \pmod{2\pi}$. Thus, Eq. (6.2.4) provides a $\mathbb{Z}_2$ characterization of the TSCs classified by the parity of the integer topological invariant N. For heterostructure geometry composed of the TSC and a trivial insulator (here, "trivial" means the zero axion angle), when interface Majorana

fermions are completely gapped out, the action (6.2.4) leads to the interface half integer gravitational CS action

$$S_{CS} = \frac{1}{2}\frac{1}{4\pi}\frac{c}{24}\int d^3x\epsilon^{\mu\nu\rho}\mathrm{tr}\left(\omega_\mu\partial_\nu\omega_\rho + \frac{2}{3}\omega_\mu\omega_\nu\omega_\rho\right) \tag{6.2.5}$$

with $c = (N+2M)/2$ where M is an integer depending on the microscopic structure of the interface, and determined by the signs of mass gaps of N Majorana fermions. [140, 73] It is noted that as in the case of the pure (2+1) gravitational CS action (6.2.1), the action (6.2.5) does not directly lead to the bulk thermal Hall effect.

A more preferable action describing the interface thermal Hall effect is the following gravito-electromagnetic θ term, [76]

$$S_\theta = \theta\frac{\pi k_B^2 T^2}{12h}\int dtd^3\boldsymbol{r}\boldsymbol{E}_E\cdot\boldsymbol{B}_E, \tag{6.2.6}$$

where $\boldsymbol{E}_E$ and $\boldsymbol{B}_E$ couple with the energy polarization and the energy magnetization, respectively. The topological action (6.2.6) describes a thermal topological magnetoelectric effect, i.e., the energy magnetization induced by the gravitational field: $\boldsymbol{M}_E = \theta\frac{\pi k_B^2 T^2}{12h}\boldsymbol{E}_E$, and the energy polarization induced by the gravitomagnetic field; $\boldsymbol{P}_E = \theta\frac{\pi k_B^2 T^2}{12h}\boldsymbol{B}_E$. [76] If there is a U(1) gauge structure in $\boldsymbol{E}_E, \boldsymbol{B}_E$, as in the case of the axion electrodynamics, [13] a low-energy effective action for Majorana fermions at the interface between the TSC and the trivial insulator is given by,

$$S_{CS} = \frac{c}{2}\frac{\pi^2 k_B^2 T^2}{6h}\int d^3x\epsilon^{\mu\nu\rho}A_{E,\mu}\partial_\nu A_{E,\rho}, \tag{6.2.7}$$

where $c = (N+2M)/2$.

Here we sketch the derivation of the gravitoelectromagnetic topological internal energy presented by Nomura et al. [76] The time reversal symmetric (class DIII) TSC classified by topological invariant N possesses N gapless Majorana modes localized at the boundary of the system. If mass gaps are induced in Majorana modes, each Majorana fermion gives rise to the half-integer thermal Hall effect described by the Hall conductivity $\kappa_H = \mathrm{sgn}(m)\frac{\pi^2 k_B^2 T}{12h}$ where m is the mass. They proved that the topological part of the internal energy for a TSC in a cylindrical geometry with a surface perturbation inducing mass gaps of the Majorana fermions is expressed as,

$$U_{\mathrm{top}} = -\int d^3\boldsymbol{r}\frac{k_{\mathrm{B}}^2 T}{12\hbar v^2}\theta\boldsymbol{\nabla}T\cdot\boldsymbol{\Omega}. \tag{6.2.8}$$

Here v is a velocity of surface Majorana fermion and θ is a constant determined by the sign of mass gaps of the surface Majorana fermions. They obtained this result from the calculations of the cross-correlated type response on the surface quasi-Lorentz symmetric system: (i) an angular momentum induced by the temperature gradient along z-axis, and (ii) heat population induced by mechanical rotation.

Eqs. (6.2.4), (6.2.6) and (6.2.8) imply that dynamics of the axion field θ give rise to dynamical thermal (gravitational) responses. We investigate such dynamical axion effects of TSCs in the following.

3 Basic features of class DIII topological superconductors

3.1 $\mathbb{Z}$ characterization of class DIII topological superconductors and gravito magnetoelectric polarization

In this section, we summarize some basic properties of class DIII TSCs relevant to the following argument. The topological classification of class DIII TSCs is given by integers $\mathbb{Z}$. However, the gravitational instanton term (6.2.4) describes only $\mathbb{Z}_2$ part, i.e., the parity of topological invariant. Also, the internal energy (6.2.8) is derived by assuming a priori the existence of N Majorana fermions on the surface. As in the case of the magnetoelectric polarization in topological insulators [13], in real systems, a non-topological even integer part of θ depends on the energy gap structure of the surface Majorana fermions. Hence it is possible to obtain the thermal conductivity exactly proportional to topological invariant N by using a specific perturbation which generates mass gap m_i of the i-th Majorana fermion satisfying $\sum_i \mathrm{sgn}(m_i) = N$. For this perturbation, the (gravito) magnetoelectric polarization $\theta = N\pi$. Actually, class DIII TSCs inherently have the appropriate perturbation that can be constructed from a chiral symmetric structure of class DIII TSCs: $\Gamma \mathcal{H}_{\mathrm{BdG}} \Gamma^{-1} = -\mathcal{H}_{\mathrm{BdG}}$ where Γ is determined by the combination of a time-reversal transformation and a particle-hole transformation. This perturbation is expressed as

$$V_\Gamma = \frac{\gamma}{2} \int d^3x \Psi^\dagger(\boldsymbol{x}) \Gamma \Psi(\boldsymbol{x}) \tag{6.3.1}$$

where $\Psi(\boldsymbol{x})$ is the Nambu spinor. The perturbation (6.3.1) induces the thermal Hall conductivity characterized by the topological invariant N as $\kappa_H = N\frac{\pi^2 k_B^2 T}{12h}$. [140, 73] To see the physical meaning of (6.3.1), let us consider a time-reversal symmetric superconductor. If we choose the Nambu representation $\Psi = (\psi_\uparrow, \psi_\downarrow, \psi_\downarrow^\dagger, -\psi_\uparrow^\dagger)^T$, the time-reversal transformation $\Psi \mapsto \Theta\Psi$ is given by $\Theta = i\sigma_2 K$ and the particle-hole transformation $\Psi \mapsto \Xi\Psi$ is given by $\Xi = \tau_2\sigma_2 K$ where K is a complex conjugate operator. In this Nambu bases, $\Gamma = \tau_2$ (overall sign is arbitrary), then $V = -i\gamma \int d^3x(\psi_\uparrow\psi_\downarrow - \psi_\downarrow^\dagger\psi_\uparrow^\dagger)$. Hence V is the imaginary s-wave pairing order. [140, 73] Here, we have assumed that the global phase of the bulk pairing gap is fixed to be zero. From an effective description of the surface Majorana fermions under the perturbation of V_Γ, we can get $\kappa_H = N\frac{\pi^2 k_B^2 T}{12h}$.

Also, $\sum_i \mathrm{sgn}(m_i) = N$ can be derived from the surface jump of (gravito) magnetoelectric polarization defined by the Chern-Simons 3 form,

$$\theta_{\mathrm{CS}} = 2\pi \int CS_3(\mathcal{A}) = \frac{1}{4\pi} \int \mathrm{tr}\left(\mathcal{A}d\mathcal{A} + \frac{2}{3}\mathcal{A}^3\right), \tag{6.3.2}$$

where $\mathcal{A} = \mathcal{A}_{nm}(\boldsymbol{k}) = \langle u_n(\boldsymbol{k}) | d_{\boldsymbol{k}} u_m(\boldsymbol{k})\rangle$ is the Berry connections determined by quasiparticle states of a bulk Bogoliubov-de Gennes (BdG) Hamiltonian $\mathcal{H}_{\mathrm{BdG}}(\boldsymbol{k}) |u_n(\boldsymbol{k})\rangle = -E_n(\boldsymbol{k}) |u_n(\boldsymbol{k})\rangle$. An adiabatic treatment of the surface structure between the TSC and the V_Γ perturbation yields an adiabatic Hamiltonian $\mathcal{H}_{\mathrm{BdG}}(\boldsymbol{k}, \lambda) = (1-\lambda)\mathcal{H}_{\mathrm{BdG}}(\boldsymbol{k}) + \lambda\gamma\Gamma$ ($\lambda \in [0,1]$), and gives the surface jump of (gravito) magnetoelectric polarization by $\int_{\lambda=0}^{\lambda=1} d\theta_{\mathrm{CS}}(\lambda) = \mathrm{sgn}(\gamma)N\pi$. [73] Although the magnetoelectric polarization θ_{CS} is gauge invariant only modulo 2π, the line integral of a small difference of $\theta_{\mathrm{CS}}(\lambda)$ is fully gauge invariant. The derivation of the topological internal energy (6.2.8) given by Nomura et al. is based on the surface half-integer thermal Hall effect, which limits the applicability of (6.2.8) to the case with a quantized value of θ. However, the above observation that the $\mathbb{Z}$-part of θ coincides with the surface jump of the (gravito) magnetoelectric polarization θ_{CS} defined by (6.3.2)

strongly suggests that non-quantized θ is given by $\theta_{\rm CS}$ as in the case of the axion electrodynamics. In this chapter, we *assume* the topological action

$$S_{\rm top} = -\int dt \int d^3x \frac{k_{\rm B}^2 T}{12\hbar v^2}\theta_{\rm CS}\boldsymbol{\nabla} T\cdot\boldsymbol{\Omega} \tag{6.3.3}$$

for *non-quantized* value of $\theta_{\rm CS}$, and consider phenomena raised by the dynamical axion in TSCs. Later, we identify θ with $\theta_{\rm CS}$.

Here, it is worth while mentioning the physical meaning of the non-quantized value of θ. If the surface jump of θ is $\Delta\theta$, then the surface thermal Hall conductivity κ_H is given by $\kappa_H = \Delta\theta\frac{\pi k_{\rm B}^2 T}{12h}$. In the case that $\Delta\theta/\pi$ is an integer, the surface thermal Hall conductivity can be understood as contributions of surface massive Majorana fermions which gives $\kappa_H = \frac{{\rm sgn}(m)}{2}\frac{\pi^2 k_{\rm B}^2 T}{6h}$, respectively. However, non-quantized values of κ_H cannot be derived from a pure (2+1)-dimensional surface effective theory. In fact, this comes from (3+1)-dimensional bulk wave functions.

3.2 Preliminary for dynamical axion : non-quantized axion angle for a p-wave TSC with an imaginary s-wave pairing order

As mentioned previously, the imaginary s-wave pairing order in spin-1/2 systems, or generally, the Γ-perturbation (6.3.1) induces the change of the axion angle by a quantized value $\theta = N\pi$. Hence, thermal and quantum fluctuations of the imaginary s-wave superconducting order $\delta\Delta_s^{\rm Im}$ may give rise to dynamical axion $\delta\theta$ in TSCs. One may naively expect that the opposite may be also possible, i.e., the fluctuation of the imaginary topological superconducting order $\delta\Delta_p^{\rm Im}$ in the ordinary s-wave superconductor raises the dynamical axion. However, actually, dynamical axion in the latter case is much suppressed compared to the former case. To see this, here, we consider a concrete example, the axion angle for the topological p-wave superconducting order coexisting with the imaginary s-wave order described by

$$\hat{\Delta} = \Delta_p\frac{\boldsymbol{k}}{k_F}\cdot\boldsymbol{\sigma}(i\sigma_2) + i\Delta_s^{\rm Im}(i\sigma_2), \tag{6.3.4}$$

where Δ_p and $\Delta_s^{\rm Im}$ are real constants. The corresponding bulk BdG Hamiltonian is

$$\mathcal{H}_{BdG} = \left(\frac{k^2}{2m}-\mu\right)\tau_3 + \tau_1\Delta_p\frac{\boldsymbol{k}}{k_F}\cdot\boldsymbol{\sigma} - \tau_2\Delta_s^{\rm Im} = \epsilon_F\left[\left(\frac{k^2}{k_F^2}-1\right)\tau_3 + \tau_1\frac{\Delta_p}{\epsilon_F}\frac{\boldsymbol{k}}{k_F}\cdot\boldsymbol{\sigma} - \tau_2\frac{\Delta_s^{\rm Im}}{\epsilon_F}\right], \tag{6.3.5}$$

where we choose the Nambu spinor as $\Psi = (\psi_\uparrow, \psi_\downarrow, \psi_\downarrow^\dagger, -\psi_\uparrow^\dagger)^T$. As shown in the second line of (6.3.5), the axion angle depends on the two parameters $\left(\Delta_p/\epsilon_F, \Delta_s^{\rm Im}/\epsilon_F\right)$ since the axion angle defined by (6.3.2) is independent of an overall factor of the BdG Hamiltonian and a scale of the wave number $\boldsymbol{k}$ for continuum models. It is noted that the latter simplification is not applicable to lattice systems. Parameterizing (Δ,ϕ) by $\left(\Delta_p, \Delta_s^{\rm Im}\right) = (\Delta\cos\phi, \Delta\sin\phi)$, we calculate the change of θ as a function of ϕ with a fixed value of Δ,

$$\frac{d\theta}{d\phi} = \frac{1}{16\pi}\int d^3k\ \epsilon^{\mu\nu\rho\sigma}{\rm tr}\left[\mathcal{F}_{\mu\nu}(\boldsymbol{k},\phi)\mathcal{F}_{\rho\sigma}(\boldsymbol{k},\phi)\right] = \int_0^\infty dk\frac{3\alpha^4k^2\cos^2\phi\left\{3k^2+1-\left(k^2-1\right)\cos(2\phi)\right\}}{2\left(\alpha^2\sin^2\phi+\alpha^2k^2\cos^2\phi+\left(k^2-1\right)^2\right)^{5/2}} \tag{6.3.6}$$

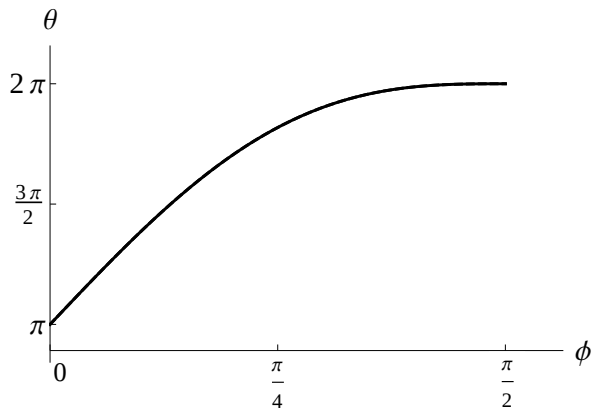

Figure 6.1: The axion angle θ as a function of ϕ for fixed gap amplitudes $\Delta/\epsilon_F = 0.003,\ 0.01,\ 0.1$. The three lines almost overlap each other. [157]

with $\alpha = \Delta/\epsilon_F$. In Fig.6.1, we show the axion angle θ as a function of ϕ for some different fixed gap amplitudes $\Delta/\epsilon_F = 0.003,\ 0.01,\ 0.1$. $\phi \sim 0$ corresponds to the imaginary s-wave pairing fluctuation in the TSC and $\phi \sim \pi/2$ corresponds to the imaginary topological pairing fluctuation in the ordinary s-wave superconductor. In this model, for a realistic value of the gap amplitude $\Delta/\epsilon_F = o(10^{-1})$, fluctuations of the imaginary s-wave pairing order in the TSC induce dynamical axion, while dynamical axion due to fluctuations of the imaginary topological pairing order in the trivial superconductor is strongly suppressed. Because of this distinctive behavior of axion angle, we only consider the fluctuation of the imaginary s-wave pairing order in the TSC in the following sections. The ratio between the fluctuation $\Delta_s^{\rm Im}$ and the dynamical axion $\delta\theta$ is

$$\delta\theta = 2\pi c \frac{\Delta_s^{\rm Im}}{\Delta_p} \tag{6.3.7}$$

with $c = O(1)$.

The consideration in this section is based on the mean-field Hamiltonian (6.3.5). The $s(p)$-wave order parameter field in (6.3.5) should be regarded as a fluctuating field in the case of the TSC (trivial superconductor), In the next section, we present more accurate and reliable calculations for order parameter fluctuations.

4 Dynamical axion in TSCs with s-wave pairing interaction

As mentioned in the previous section, for spin-1/2 superconducting systems, the imaginary s-wave superconducting fluctuation in the TSC gives rise to (gravitational) dynamical axion field in condensed matter systems. In this section, we explore properties of dynamical axion fluctuations. The action of the dynamical axion is written by

$$S_{\rm axion}[\delta\theta] = Jg^2 \int_0^\beta d\tau \int d^3x \left[(\partial_\tau \delta\theta)^2 + v_F^2 (\boldsymbol{\nabla}\delta\theta)^2 + m_\theta^2 (\delta\theta)^2 \right] \tag{6.4.1}$$

up to the second order of the fluctuation field $\delta\theta$, which amounts to the random-phase approximation (RPA). A parameter g relates the dynamical axion field $\delta\theta$ and the superconducting fluctuation

field $\delta\psi$, i.e. $\delta\theta = g\delta\psi$. Here, $\delta\psi$ may be the fluctuation of the amplitude, or the phase of the superconducting order, or the mixture of them. g can be derived by expanding Eq.(6.3.2) in terms of $\delta\psi$ up to the 1st order. The expressions of J, and the axion mass m_θ for a particular microscopic model are given in Appendix. The axion mass m_θ controls fluctuation of the dynamical axion. For the realization of dynamical axion, it is required that m_θ is smaller than the bulk superconducting gap Δ. As a concrete example, we consider a p-wave TSC system similar to the B-phase of ^{3}He. We also assume that there is an s-wave-channel pairing interaction U_s which yields s-wave superconducting fluctuations. [1] In the case with inversion symmetry, pairing states with different parity cannot be mixed with each other. Thus, in the p-wave pairing state, the s-wave superconducting order cannot develop even when U_s is nonzero. However, fluctuation of s-wave pairing order is still possible. On the other hand, in the case with broken inversion symmetry (i.e. noncentrosymmetric crystal structure), parity-mixing of p-wave pairing and s-wave pairing is induced by the antisymmetric SOI. [159] In this case, the imaginary s-wave pairing fluctuation is not independent of the p-wave pairing fluctuation. Actually, dynamical axion emerges as a fluctuation of a phase difference between s-wave and p-wave superconducting orders *a la* the Leggett mode. [74, 160] Generally, in the presence of two mean field superconducting order Δ_1, Δ_2, there are two superconducting fluctuations $\Delta_1 e^{i\theta_1}$, $\Delta_2 e^{i\theta_2}$. Intensity of the phase fluctuations is determined by a Coulomb interaction, which couples with the total phase fluctuation $\theta_1 + \theta_2$, and a scattering channel between two Cooper pairs, which couples with the relative phase fluctuation (Leggett mode) $\theta_1 - \theta_2$. It is noted that the Leggett mode has an advantage for the realization of dynamical axion because the relative phase avoids to get a plasma gap from a long-range Coulomb interaction, and thus dynamical axion can survive in the low-energy region. In the following, we consider two cases with and without the SOI, and compare properties of dynamical action for these two cases. We will find that the SOI induced by broken inversion symmetry dramatically enlarges the parameter region in which dynamical axion appears as a low-energy excitation.

4.1 Model Hamiltonian

We consider a toy model which has contact attractive interactions in both the s-wave and p-wave channels, and also the antisymmetric SOI. The Hamiltonian is

$$H = H_0 + H_s + H_p, \tag{6.4.2}$$

$$H_0 = \sum_{\boldsymbol{k}} \left[\left(\frac{k^2}{2m} - \mu \right) \delta_{\alpha\beta} + \lambda \boldsymbol{k} \cdot \boldsymbol{\sigma}_{\alpha\beta} \right] c^\dagger_{\boldsymbol{k}\alpha} c_{\boldsymbol{k}\beta}, \tag{6.4.3}$$

$$H_s = -\frac{U_s}{4V} \sum_{\boldsymbol{k}\boldsymbol{k}'\boldsymbol{q}} (i\sigma_2)_{\alpha\beta} (i\sigma_2)_{\alpha'\beta'} c^\dagger_{\boldsymbol{k}+\frac{\boldsymbol{q}}{2}\alpha} c^\dagger_{-\boldsymbol{k}+\frac{\boldsymbol{q}}{2}\beta} c_{-\boldsymbol{k}'+\frac{\boldsymbol{q}}{2}\beta'} c_{\boldsymbol{k}'+\frac{\boldsymbol{q}}{2}\alpha'}, \tag{6.4.4}$$

$$H_p = -\frac{U_p}{4V} \sum_{\boldsymbol{k}\boldsymbol{k}'\boldsymbol{q}} \left(\hat{k} \cdot \boldsymbol{\sigma} i\sigma_2 \right)_{\alpha\beta} \left(-i\sigma_2 \boldsymbol{\sigma} \cdot \hat{k}' \right)_{\alpha'\beta'} c^\dagger_{\boldsymbol{k}+\frac{\boldsymbol{q}}{2}\alpha} c^\dagger_{-\boldsymbol{k}+\frac{\boldsymbol{q}}{2}\beta} c_{-\boldsymbol{k}'+\frac{\boldsymbol{q}}{2}\beta'} c_{\boldsymbol{k}'+\frac{\boldsymbol{q}}{2}\alpha'}, \tag{6.4.5}$$

where λ is the SOI strength, U_s and $U_p < 0$ are, respectively, the s-wave and p-wave attractive interactions, and $\hat{k} = \boldsymbol{k}/k_F$ with k_F the Fermi wave number for $\lambda = 0$. We assume that the d-vector of the p-wave pairing is the same as that of the B-phase of ^{3}He, which is a typical example of a class DIII TSC. For simplicity, we ignore scatterings between the s-wave and p-wave pairs, though such

[1] We note that dynamical axion in a similar model without SOI was also studied in [158].

processes are generally allowed in the case without inversion symmetry. This treatment is justified because scattering processes mixing different parity are higher order in terms of a parameter ϵ_{SO}/ϵ_F where ϵ_{SO} is the energy scale of the SOI, and ϵ_F is the Fermi energy, satisfying $\epsilon_{SO}/\epsilon_F \ll 1$ for most of real materials. [159] The mean field order parameter is written in the following form,

$$\Delta(\boldsymbol{k}) = \Delta_s i\sigma_2 + \Delta_p \hat{k}\cdot\boldsymbol{\sigma} i\sigma_2. \tag{6.4.6}$$

$|\Delta_p| > |\Delta_s|$ corresponds to the TSC ($N = \pm 1$) and $|\Delta_p| < |\Delta_s|$ corresponds to the trivial superconductor ($N = 0$). The Hubbard-Stratonovich transformation leads to the partition function in the form,

$$Z = \int D\Delta D\Delta^* e^{-S[\Delta,\Delta^*]}, \tag{6.4.7}$$

$$S[\Delta,\Delta^*] = \int_0^\beta d\tau \int d^3x \sum_{l=s,p} \frac{|\Delta_l(x)|^2}{U_l} - \frac{1}{2}\mathrm{Trln}G^{-1}[\Delta,\Delta^*], \tag{6.4.8}$$

where

$$\begin{aligned}
&G^{-1}_{\alpha\beta}(\boldsymbol{k}_1\tau_1,\boldsymbol{k}_2\tau_2;\Delta,\Delta^*) \\
&= \begin{pmatrix} -\partial_{\tau_1}\delta_{\boldsymbol{k}_1\boldsymbol{k}_2}\delta_{\alpha\beta} - H_{\alpha\beta}(\boldsymbol{k}_1,\boldsymbol{k}_2) & -\sum_{l=s,p}\sum_{\boldsymbol{q}} \Delta_l(\tau_1,\boldsymbol{q})\varphi_{l,\boldsymbol{q}}([(\boldsymbol{k}_1\alpha)(-\boldsymbol{k}_2\beta)]) \\ -\sum_{l=s,p}\sum_{\boldsymbol{q}} \Delta^*_l(\tau_1,\boldsymbol{q})\varphi^*_{l,\boldsymbol{q}}([(\boldsymbol{k}_2\beta)(-\boldsymbol{k}_1\alpha)]) & -\partial_{\tau_1}\delta_{\boldsymbol{k}_1\boldsymbol{k}_2}\delta_{\alpha\beta} + H_{\beta\alpha}(-\boldsymbol{k}_2,-\boldsymbol{k}_1) \end{pmatrix} \delta(\tau_1-\tau_2),
\end{aligned} \tag{6.4.9}$$

with the normal part of the Hamiltonian,

$$H_{\alpha\beta}(\boldsymbol{k}_1,\boldsymbol{k}_2) = \left(\varepsilon_{\boldsymbol{k}_1}\delta_{\alpha\beta} + \lambda\hat{k}_1\cdot\boldsymbol{\sigma}_{\alpha\beta}\right)\delta_{\boldsymbol{k}_1\boldsymbol{k}_2}, \tag{6.4.10}$$

and the s-wave and p-wave pairing channel bases

$$\varphi_{s,\boldsymbol{q}}([(\boldsymbol{k}_1\alpha)(\boldsymbol{k}_2\beta)]) = \delta_{\boldsymbol{q},\boldsymbol{k}_1+\boldsymbol{k}_2}(i\sigma_2)_{\alpha\beta}, \tag{6.4.11}$$

$$\varphi_{p,\boldsymbol{q}}([(\boldsymbol{k}_1\alpha)(\boldsymbol{k}_2\beta)]) = \delta_{\boldsymbol{q},\boldsymbol{k}_1+\boldsymbol{k}_2}\left(\frac{\boldsymbol{k}_1-\boldsymbol{k}_2}{2k_F}\cdot\boldsymbol{\sigma} i\sigma_2\right)_{\alpha\beta}, \tag{6.4.12}$$

where $\boldsymbol{q}$ is a momentum of center-of-mass motion of a Cooper pair. Here, we choose the Nambu spinor as $\Psi = (\psi_\uparrow,\psi_\downarrow,\psi^*_\uparrow,\psi^*_\downarrow)^T$, and define the Fourier transformation of the superconducting fluctuations $\Delta_l(\tau,\boldsymbol{x})$ by $\Delta_l(\tau,\boldsymbol{q}) = \frac{1}{V}\int d^3x \Delta_l(\tau,\boldsymbol{x})e^{-i\boldsymbol{q}\cdot\boldsymbol{x}}$.

4.2 Case without spin-orbit interaction

First, we consider the case without the SOI, i.e., $\lambda = 0$, which corresponds to the case with inversion symmetry. The mean field free energy is obtained by setting $\Delta_l(\tau,\boldsymbol{x}) = \Delta_l = const.$:

$$\begin{aligned}
&F[\Delta,\Delta^*]/V \\
&= \frac{|\Delta_s|^2}{U_s} + \frac{|\Delta_p|^2}{U_p} - \frac{1}{2}\frac{1}{\beta V}\sum_{\omega_n\boldsymbol{k}} \ln\left[\left(\omega_n^2 + \varepsilon_{\boldsymbol{k}}^2 + |\Delta_s|^2 + (k/k_F)^2|\Delta_p|^2\right)^2 - (k/k_F)^2\left(\Delta_s^*\Delta_p + \Delta_s\Delta_p^*\right)^2\right].
\end{aligned} \tag{6.4.13}$$

From this expression, it is found that the cases of the $\pi/2$ relative phase between Δ_s and Δ_p, i.e., $\Delta_s^*\Delta_p + \Delta_s\Delta_p^* = 0$, have the lowest free energy, which means the imaginary s-wave fluctuation is larger than the real s-wave fluctuation in the bulk p-wave superconducting phase. Within approximation of $k \sim k_F$ in the sum of $\boldsymbol{k}$ in the third term in (6.4.13), we search for the free-energy minimum. We find that for $U_s > U_p$, the s-wave order trivial phase $\Delta_s \neq 0, \Delta_p = 0$ is stabilized, while for $U_s < U_p$, the topological phase with the p-wave order, i.e. $\Delta_s = 0, \Delta_p \neq 0$, realizes. As mentioned in the previous section, here, we only consider fluctuations of s-wave pairing in the bulk p-wave superconductor in the case of $U_p > U_s$. The gap equation for $\Delta_p(T)$ is derived from the free energy minimum $\frac{\partial F[\Delta_p, \Delta_s=0]}{\partial \Delta_p^*} = 0$,

$$\frac{1}{U_p} = \frac{1}{\beta V}\sum_{\omega_n, \boldsymbol{k}} \frac{(k/k_F)^2}{\omega_n^2 + \varepsilon_{\boldsymbol{k}} + (k/k_F)^2\Delta_p^2(T)}. \tag{6.4.14}$$

The action of the imaginary s-wave fluctuation is obtained by expanding (6.4.8) in terms of the imaginary part of the s-wave gap Δ_s^{Im} within the Gaussian approximation:

$$\begin{aligned} &S[\Delta_s^{\mathrm{Im}}] \\ &= J\int_0^\beta d\tau \int d^3x \left[(\partial_\tau \Delta_s^{\mathrm{Im}})^2 + v_F^2(\boldsymbol{\nabla}\Delta_s^{\mathrm{Im}})^2 + m_\theta^2(\Delta_s^{\mathrm{Im}})^2\right] \end{aligned} \tag{6.4.15}$$

where $v_F = \partial_k \varepsilon_{\boldsymbol{k}}|_{k=k_F}$ is the Fermi velocity and the definition of J and mass gap m_θ is given in Appendix. At zero temperature $T = 0$, m_θ is

$$m_\theta(T=0) = |\Delta_p|\sqrt{\frac{2}{\rho_0}\left(\frac{1}{U_s} - \frac{1}{U_p}\right)} \tag{6.4.16}$$

with $\rho_0 = 2mk_F/(2\pi)^2$ the density of state per spin. The axion mass gap is determined by the distance from the topological phase transition point $U_s = U_p$. In Fig.6.2, we show the bulk superconducting gap Δ_p and the axion mass gap m_θ at zero temperature for a fixed $\rho_0 U_p = 0.3$. It is noted that fluctuations of dynamical axion survive only in the very narrow parameter region in vicinity of the topological transition point $U_s = U_p$. Thus, the dynamical axion scenario is unlikely to realize for centrosymmetric systems with no SOI , i.e. $\lambda = 0$.

4.3 Case with spin-orbit interaction

Next, let us consider the case with the finite SOI $\lambda \neq 0$. We fix $\lambda > 0$. Due to the parity mixing, the s-wave and the p-wave superconducting orders coexist. The mean field free energy is derived by setting $\Delta_l(\tau, \boldsymbol{x}) = \Delta_l = const.$,

$$\begin{aligned} F[\Delta, \Delta^*]/V &= \frac{|\Delta_s|^2}{U_s} + \frac{|\Delta_p|^2}{U_p} \\ &- \frac{1}{2}\frac{1}{\beta V}\sum_{\omega_n \boldsymbol{k}} \ln\left(\omega_n^2 + (\varepsilon_{\boldsymbol{k}} + \lambda k)^2 + |\Delta_s + (k/k_F)\Delta_p|^2\right) - \frac{1}{2}\frac{1}{\beta V}\sum_{\omega_n \boldsymbol{k}} \ln\left(\omega_n^2 + (\varepsilon_{\boldsymbol{k}} - \lambda k)^2 + |\Delta_s - (k/k_F)\Delta_p|^2\right). \end{aligned} \tag{6.4.17}$$

The second and third terms correspond to the contribution from the inner Fermi surface and the outer Fermi surface, respectively. The gap equation is derived from a free energy minimum condition

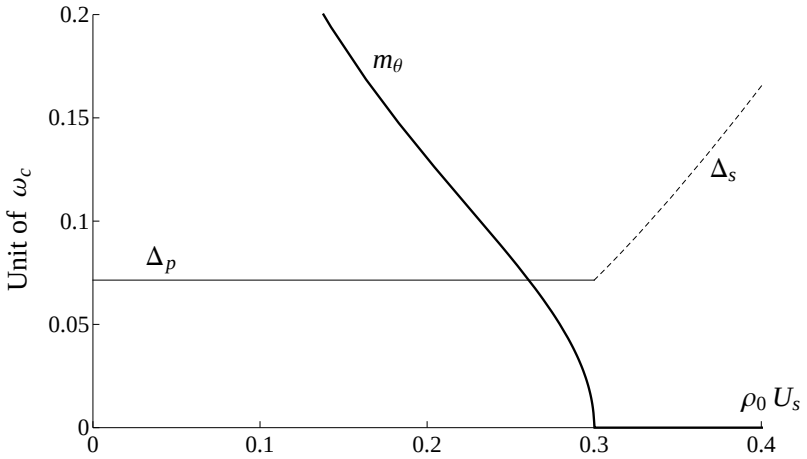

Figure 6.2: The bulk superconducting gap Δ_p/Δ_s and the axion mass gap m_θ in a unit of cutoff energy ω_c at zero temperature for a fixed value of U_p plotted against $\rho_0 U_s$. The region $0 \leq \rho_0 U_s < 0.3$ is the p-wave topological superconducting state, while the region $0.3 \leq \rho_0 U_s$ is the trivial s-wave pairing state. The first order topological phase transition occurs at $\rho_0 U_s = 0.3$ point. [157]

$\frac{\partial F}{\partial \Delta_s^*} = \frac{\partial F}{\partial \Delta_p^*} = 0$, which leads to

$$\frac{\Delta_s}{U_s} = \frac{1}{2\beta V}\sum_{\omega_n,\boldsymbol{k}} \frac{\Delta_s + (k/k_F)\Delta_p}{\omega_n^2 + (\varepsilon_{\boldsymbol{k}} + \lambda k)^2 + |\Delta_s + (k/k_F)\Delta_p|^2} + \frac{1}{2\beta V}\sum_{\omega_n,\boldsymbol{k}} \frac{\Delta_s - (k/k_F)\Delta_p}{\omega_n^2 + (\varepsilon_{\boldsymbol{k}} - \lambda k)^2 + |\Delta_s - (k/k_F)\Delta_p|^2},$$
$$\frac{\Delta_s}{U_p} = \frac{1}{2\beta V}\sum_{\omega_n,\boldsymbol{k}} \frac{\{\Delta_s + (k/k_F)\Delta_p\}(k/k_F)}{\omega_n^2 + (\varepsilon_{\boldsymbol{k}} + \lambda k)^2 + |\Delta_s + (k/k_F)\Delta_p|^2} - \frac{1}{2\beta V}\sum_{\omega_n,\boldsymbol{k}} \frac{\{\Delta_s - (k/k_F)\Delta_p\}(k/k_F)}{\omega_n^2 + (\varepsilon_{\boldsymbol{k}} - \lambda k)^2 + |\Delta_s - (k/k_F)\Delta_p|^2}. \tag{6.4.18}$$

We denote the Fermi wave numbers for the inner/outer Fermi surface as $k_{F\pm}$ where $\pm$ represent the $\boldsymbol{k}$-dependent helicities for the spin degrees of freedom, i.e. $\boldsymbol{k}\cdot\sigma = \pm k$. When the normal energy dispersion is $\varepsilon_{\boldsymbol{k}} = \frac{k^2}{2m} - \epsilon_F$, then $k_{F\pm}/k_F = \sqrt{1 + \left(\frac{\lambda}{v_F}\right)} \mp \frac{\lambda}{v_F}$ with $k_F = \sqrt{2m\varepsilon_F}$ and $v_F = \frac{k_F}{m}$. The bulk superconducting gaps for each Fermi surface are given by $\Delta_s + k_{F+}/k_F\Delta_p$ for the inner Fermi surface and $\Delta_s - k_{F-}/k_F\Delta_p$ for the outer Fermi surface. In Fig.6.3, we show the superconducting gap as a function of the SOI strength λ for a fixed value of $U_s < U_p$ at zero temperature. The small λ region corresponds to a topological phase since this region adiabatically connects to the pure p-wave topological phase. There is a topological phase transition point λ_c at which the superconducting gap for the inner Fermi surface $\Delta_s + k_{F+}/k_F\Delta_p$ closes. At the phase transition point, the magnitude of the s-wave pairing interaction U_s and that of the effective p-wave interaction $(k_{F+}/k_F)U_p$ are the same. The region for $\lambda > \lambda_c$ is the topologically trivial state since this region adiabatically connects to the ordinary s-wave superconductor $\Delta_p = 0$. To investigate properties of the dynamical axion induced by superconducting fluctuations, we only consider the topological region $\lambda < \lambda_c$.

In the case with the SOI, because of the mixing of Δ_s and Δ_p, the imaginary s-wave fluctuation is not independent of the p-wave superconducting fluctuation. As a matter of fact, the fluctuation

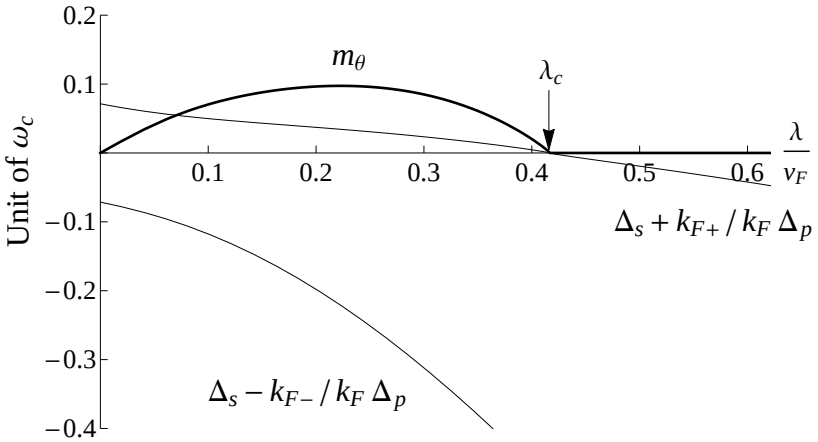

Figure 6.3: The bulk superconducting gaps $\Delta_s \pm k_{F\pm}/k_F\Delta_p$ for inner/outer band and the axion mass gap m_θ in a unit of cut off energy ω_c at zero temperature for a fixed values of $\rho_0 U_s = 0.2$ and $\rho_0 U_p = 0.3$. $\lambda = \lambda_c$ is the topological phase transition point. [157]

inducing the dynamical axion is a relative phase fluctuation between Δ_s and Δ_p. We define the relative phase θ_r by

$$\begin{aligned}\Delta_s(\tau,\boldsymbol{x}) &= \Delta_s^{\mathrm{MF}} e^{\frac{i}{2}\theta_r(\tau,\boldsymbol{x})},\\ \Delta_p(\tau,\boldsymbol{x}) &= \Delta_p^{\mathrm{MF}} e^{-\frac{i}{2}\theta_r(\tau,\boldsymbol{x})}.\end{aligned} \tag{6.4.19}$$

The action of the relative phase fluctuation is given by (6.4.8) up to the Gaussian fluctuation around the mean field solution and within the long wave-length approximation,

$$S[\theta_r] = J\int_0^\beta d\tau \int d^3x \left[(\partial_\tau\theta_r)^2 + v_F^2(\boldsymbol{\nabla}\theta_r)^2 + m_\theta^2(\theta_r)^2\right] \tag{6.4.20}$$

where $v_F = \partial_k \varepsilon_{\boldsymbol{k}}|_{k=k_F}$ is Fermi velocity and the definition of J and mass gap m_θ is given in Appendix. In Fig.6.3, we show the axion mass gap m_θ as a function of λ at zero temperature. For sufficiently small and realistic values of λ/v_F, m_θ is much smaller than the superconducting gap, and hence, the dynamical axion realizes as a low-energy excitation. Here, we have ignored parity non-conserving pairing interactions such as the scattering between s-wave Cooper pairs and p-wave Cooper pairs. Such channels induce an additional gap in the relative phase fluctuation. However, they are higher order in terms of the SOI,[159] and thus, the effect on the axion mass gap is small.

Here we remark some important features which are different from the case without the SOI. As shown in Fig.6.2, in the absence of the SOI, the axion mass gap m_θ increases quite rapidly as the distance from the topological phase transition point $U_s = U_p$ increases. Thus, in this case, the realization of the dynamical axion requires a fine tuning of the interaction strength U_s and U_p. On the other hand, in the case with the SOI, due to the finite gaps of both s-wave and p-wave superconducting orders, the relative phase can fluctuate, and for sufficiently small λ, the axion mass gap is smaller than the bulk superconducting gaps. The region where the dynamical axion survives always exists for any interaction strength satisfying $U_s < U_p$. Moreover the relative phase does not couple with a long-range Coulomb interaction. Therefore, it is free from acquiring a plasma

gap. Hence, noncentrosymmetric superconductors with the antisymmetric SOI are significantly promising systems for the realization of dynamical axion in TSCs.

5 Dynamical axion phenomena in topological superconductors

In this section, we discuss the physically observable phenomena raised by the dynamical axion via the gravitoelectromagnetic θ term (6.3.3). In the condensed matter context, in the case with the U(1) particle number conservation, the dynamical axion θ couples with electromagnetic fields via the topological θ term $S_\theta = \frac{\alpha}{32\pi^2}\int dtd^3x\theta\epsilon^{\mu\nu\rho\sigma}F_{\mu\nu}F_{\rho\sigma}$, which induces novel phenomena such as axionic polariton under an applied uniform magnetic field [45] and magnetic instability under an applied uniform electrostatic field [46]. An important question is, then, what dynamical axion phenomena are in topological superconductors or superfluids for which U(1) symmetry is broken.

We discuss the dynamical axion phenomena on the basis of the topological action (6.3.3), in which mechanical rotation couples with dynamical axion. Let us consider an increase of the moment of inertia raised by the dynamical axion fluctuation under finite temperature gradient. The real time action per unit volume for the rotation $\Omega = \dot{\phi}$ and dynamical axion $\delta\theta$ is given by

$$S[\phi, \delta\theta] = \int dt \frac{1}{2} I\dot{\phi}^2 + Jg^2 \int dt \left(\delta\dot{\theta}^2 - m_\theta^2 \delta\theta^2\right) - \frac{k_{\rm B}^2 T\nabla T}{12\hbar v^2}\int dt\dot{\phi}\delta\theta, \tag{6.5.1}$$

where I is the inertia moment per unit volume, and we assume that the temperature gradient $\boldsymbol{\nabla} T$ is parallel to $\boldsymbol{\Omega}$. Integrating out the dynamical axion fluctuation, we get an effective action for rotation only,

$$S_{\rm eff}[\phi] = \int \frac{d\omega}{2\pi}\frac{I_{\rm eff}(\omega)}{2}\omega^2|\phi(\omega)|^2 \tag{6.5.2}$$

with

$$I_{\rm eff}(\omega) = I + \frac{1}{2Jg^2m_\theta^2}\left(\frac{k_{\rm B}^2 T\nabla T}{12\hbar v^2}\right)^2 \frac{1}{1-(\omega/m_\theta)^2}. \tag{6.5.3}$$

The result implies that the mechanical rotation excites the dynamical axions via the topological coupling (6.3.3), which increase the inertia moment for a low-frequency region $\omega < m_\theta$. Let us estimate the order of the increase of the inertia moment. We approximate J, g, and v by

$$J \sim \rho = \frac{k_F^3}{8\pi^3\epsilon_F},\ g \sim \pi,\ v \sim \frac{\Delta}{\hbar k_F}, \tag{6.5.4}$$

and the bare inertia moment per unit volume by

$$I \sim M/L_z \tag{6.5.5}$$

with M the system total mass and L_z the system size in the direction parallel to the temperature gradient. Then we obtain,

$$\frac{I_{\rm eff}(\omega) - I}{I} \sim \frac{\pi}{36}\left(\frac{k_B T}{\Delta}\right)^2\left(\frac{k_B L_z\nabla T}{\Delta}\right)^2\left(\frac{\hbar}{m_\theta}\right)^2 \frac{\epsilon_F k_F}{ML_z}\frac{1}{1-(\omega/m_\theta)^2}. \tag{6.5.6}$$

The prefactor of Eq.(6.5.6) is extremely small. However, in the case of ac mechanical rotation, i.e. a shaking motion with a finite frequency ω, as ω approaches the resonance frequency m_θ, this effect becomes observable.

6 Conclusion

In this chapter, we discussed dynamical axion in topological superconductors and superfluids in terms of the gravitoelectromagnetic-type topological action (6.3.3), in which the axion and mechanical rotation are coupled under finite temperature gradient. Here, we stress that the microscopic derivation of the topological action (6.3.3) for non-quantized axion angle θ and its fluctuation $\delta\theta$ is still an open issue. We have assumed the topological action (6.3.3) and θ is determined by the Chern-Simons 3 form, $\theta = 2\pi \int CS_3(\mathcal{A})$. Under this assumption, the superconducting fluctuations which shift axion angle defined by the Chern-Simons 3 form give rise to the dynamical axion. The superconducting fluctuations inducing the dynamical axion in the topological superconductors are the time-reversal broken s-wave fluctuations in the absence of the antisymmetric SOI, and the relative phase fluctuation (Leggett mode) between p-wave and s-wave orders in the presence of the antisymmetric SOI. We found that the SOI breaking inversion symmetry enlarges the parameter region in which the dynamical axion fluctuation appears as a low-energy excitation, since the magnitude of the relative phase fluctuation is determined by the coupling strength between s-wave and p-wave Cooper pairs, i.e., the strength of the SOI. We proposed that the dynamical axion fluctuation increases the moment of inertia. If the rotation frequency ω is close to the dynamical axion fluctuation mass m_θ, this effect is observable.

Chapter 7

Conclusion

This thesis reported some theoretical studies on topological insulators and superconductors.

In Chap. 1, we introduced a basic concept of topological phases of matter. Topological phases are the gapped quantum phases which cannot adiabatically connect to a trivial phase. Topological insulators and superconductors are classes of topological phases of free fermions. Within the single particle approximation, the bulk shows no low-energy excitation because of a finite energy gap, thus, all physically observable phenomena can occur at their boundaries or topological defects. The topological nontriviality of bulk reflects an existence of robust gapless excitations at the boundaries or defects. The topological periodic table shows the fact that a defect gapless state can be considered as a boundary gapless state. The gapless excitation itself also has topological implication: stable fermi points are topological defects in momentum space. The topological classification of gapped topological phases and gapless topological phases provide a realization of the bulk-boundary correspondence in terms of the K-theory.

A space group symmetry originated from a crystalline structure gives a finer classification of topological phases, which enable some trivial phases without crystalline symmetries to be topologically nontrivial phases. The topological band theory, which was developed in Chap. 2, is a unified framework of the classification of topological crystalline insulators and superconductors. The space group symmetries besides the time-reversal symmetry and the particle-hole symmetry define some variety of the K-theory. [81, 82] The K-theory naturally provides the concept of the dimensional hierarchy: equivalent relations between different space dimensions and different symmetries, leading to the periodic table of topological insulators and superconductors, for example. To this date we wrote this thesis, there is no knowledge of an algorithmic method of the classification of topological crystalline phases for general space group symmetries. Topological crystalline phases with some simple point group symmetries have been classified. However, there are many unclassified symmetry classes, for example, topological crystalline insulators with nonsymmorphic space group symmetries, and topological superconductors with point group symmetries that do not commute with the particle-hole transformation. Sometimes, a topological classification is argued only by searching possible well-defined topological invariants. However, such strategies may have a risk that the true topological classification is missed. On the other hand the K-theory provides the exhaustive classification.

For order-two point group symmetries, we can successfully classify all the topological phases of free fermions, which was explained in Chap. 3. The order-two point group symmetries include Z_2 global spin flip, reflection, two-fold rotation, inversion, and their magnetic symmetries. Hamil-

tonians with any order-two point group symmetries are represented by the Dirac Hamiltonians, which enable us to classify the topological phases by using the Clifford algebras. Each eight (two) classifying space of the real (complex) Altland-Zirnbauer classes is changed by adding a generator of the Clifford algebra from the Z_2 additional symmetry, [68] which leads to the (4+32)-fold way of the classification table of the crystalline topological phases with an additional order-two point group symmetry. Obtained K-groups satisfy that defect zero modes can be considered as boundary states of lower-dimensional crystalline insulators and superconductors. We also classify Fermi points stabilized by the additional symmetry, and derive the K-theory version of the bulk-boundary correspondence. Various symmetry protected topological phases and gapless modes are identified and discussed in a unified framework.

The periodic tables with an additional order-two point group symmetry were presented in Chap. 4. The 10-fold symmetry classes of the periodic table [4, 5] were extended into the 27-fold symmetry classes with an additional reflection symmetry [119, 68]. These symmetry classes have been further extended into 148-fold symmetry classes with an additional order-two (magnetic) point group symmetry. [38] We illustrated how the topological tables work by using various concrete examples.

Revealing relations between bulk topological invariants and experimentally observable physical quantities is a fundamental issue of topological phases. In Chap. 5, we clarified this relation in the case of chiral symmetric topological phases in odd spatial dimensions such as time-reversal invariant topological superconductors and topological insulators with sublattice symmetry, where those relations had not been well understood. The winding number which characterizes the bulk Z nontriviality of these systems can appear in electromagnetic and thermal responses in a certain class of heterostructure systems. It is also found that the Z nontriviality can be detected in a certain polarization, "chiral polarization," which is induced by magnetic field.

A dynamical aspect of band topology has not been well understood. The dynamical axion is a topic of this. In Chap. 6, we argued a possibility of realizing dynamical axion in superconductors and superfluids, where the dynamical axion is induced by relative phase fluctuations between topological and s-wave superconducting orders. We showed that if there is an inversion-symmetry-breaking spin-orbit interaction from noncentrosymmetric crystal structure, the dynamical axion is more feasible since the parity-mixing of Cooper pairs enables a relative phase fluctuation (Leggett mode) between the even and odd parity superconducting orders.

Bibliography

[1] X.-G. Wen, *Quantum Field Theory of Many-body Systems* (Oxford University Press, 2004), ISBN 019922725X.

[2] M. Z. Hasan and C. L. Kane, Reviews of Modern Physics **82**, 3045 (2010), arXiv:1002.3895.

[3] X.-L. Qi and S.-C. Zhang, Reviews of Modern Physics **83**, 1057 (2011), arXiv:1008.2026.

[4] A. Schnyder, S. Ryu, A. Furusaki, and A. Ludwig, Physical Review B **78**, 195125 (2008), arXiv:0803.2786.

[5] A. Kitaev, AIP Conference Proceedings **22**, 22 (2009), arXiv:0901.2686.

[6] S. Ryu, A. P. Schnyder, A. Furusaki, and A. W. W. Ludwig, New Journal of Physics **12**, 065010 (2010), arXiv:0912.2157.

[7] M. F. Atiyah and D. W. Anderson, *K-Theory* (W. A. Benjamin (New York and Amsterdam), 1967).

[8] H. B. Lawson and M.-L. Michelsohn, *Spin geometry* (Oxford Univ Press, 1989), ISBN 0691085420.

[9] M. Karoubi, *K-Theory: An Introduction* (Springer, 2008), ISBN 3540798897.

[10] G. E. Volovik, *The universe in a helium droplet* (Clarendon Press, 2003), ISBN 0199564841.

[11] J. C. Y. Teo and C. L. Kane, Physical Review B **82**, 115120 (2010), arXiv:1006.0690.

[12] J. Goldstone and F. Wilczek, Physical Review Letters **47**, 986 (1981).

[13] X.-L. Qi, T. L. Hughes, and S.-C. Zhang, Physical Review B **78**, 195424 (2008), arXiv:0802.3537.

[14] D. Thouless, M. Kohmoto, M. Nightingale, and M. den Nijs, Physical Review Letters **49**, 405 (1982).

[15] M. Kohmoto, Annals of Physics **160**, 343 (1985).

[16] Q. Niu, D. Thouless, and Y.-S. Wu, Physical Review B **31**, 3372 (1985).

[17] J. Teo, L. Fu, and C. Kane, Physical Review B **78**, 045426 (2008).

[18] L. Fu, Physical Review Letters **106**, 106802 (2011), arXiv:1010.1802.

[19] R. S. K. Mong, J. H. Bardarson, and J. E. Moore, Physical Review Letters **108**, 076804 (2012), arXiv:1109.3201.

[20] Z. Ringel, Y. E. Kraus, and A. Stern, Physical Review B **86**, 045102 (2012), arXiv:1105.4351.

[21] L. Fu and C. L. Kane, Physical Review Letters **109**, 246605 (2012), arXiv:1208.3442.

[22] I. C. Fulga, B. van Heck, J. M. Edge, and A. R. Akhmerov, Physical Review B **89**, 155424 (2014), arXiv:1212.6191.

[23] T. H. Hsieh, H. Lin, J. Liu, W. Duan, A. Bansil, and L. Fu, Nature communications **3**, 982 (2012).

[24] Y. Tanaka, Z. Ren, T. Sato, K. Nakayama, S. Souma, T. Takahashi, K. Segawa, and Y. Ando, Nature Physics **8**, 800 (2012), arXiv:1206.5399.

[25] P. Dziawa, B. J. Kowalski, K. Dybko, R. Buczko, A. Szczerbakow, M. Szot, E. Lusakowska, T. Balasubramanian, B. M. Wojek, M. H. Berntsen, et al., Nature materials **11**, 1023 (2012), arXiv:1206.1705.

[26] S.-Y. Xu, C. Liu, N. Alidoust, M. Neupane, D. Qian, I. Belopolski, J. D. Denlinger, Y. J. Wang, H. Lin, L. a. Wray, et al., Nature communications **3**, 1192 (2012).

[27] A. M. Turner, Y. Zhang, and A. Vishwanath, Physical Review B **82**, 241102 (2010).

[28] F. D. M. Haldane, Physical Review Letters **61**, 2015 (1988).

[29] Y. Hatsugai, Physical Review Letters **71**, 3697 (1993).

[30] S. Ryu and Y. Hatsugai, Physical Review Letters **89**, 077002 (2002), arXiv:cond-mat/0112197.

[31] X.-L. Qi, Y.-S. Wu, and S.-C. Zhang, Physical Review B **74**, 045125 (2006), arXiv:cond-mat/0604071.

[32] R. Jackiw and P. Rossi, Nuclear Physics B **190**, 681 (1981).

[33] L. Fu and C. Kane, Physical Review Letters **100**, 096407 (2008), arXiv:0707.1692.

[34] E. Weinberg, Physical Review D **24**, 2669 (1981).

[35] A. Niemi and G. Semenoff, Nuclear Physics B **269**, 131 (1986).

[36] K. Shiozaki, T. Fukui, and S. Fujimoto, Physical Review B **86**, 125405 (2012), arXiv:1203.2086.

[37] N. Read and D. Green, Physical Review B **61**, 10267 (2000), arXiv:cond-mat/9906453.

[38] K. Shiozaki and M. Sato, Physical Review B **90**, 165114 (2014), arXiv:1403.3331.

[39] H. Nielsen and M. Ninomiya, Nuclear Physics B **193**, 173 (1981).

[40] D. Thouless, Physical Review B **27**, 6083 (1983).

[41] M. J. Rice, Physical Review Letters **49**, 1455 (1982).

[42] D. Xiao, M.-C. Chang, and Q. Niu, Reviews of Modern Physics **82**, 1959 (2010), arXiv:0907.2021.

[43] R. King-Smith and D. Vanderbilt, Physical Review B **47**, 1651 (1993).

[44] F. Wilczek, Physical Review Letters **58**, 1799 (1987).

[45] R. Li, J. Wang, X.-L. Qi, and S.-C. Zhang, Nature Physics **6**, 284 (2010), arXiv:0908.1537.

[46] H. Ooguri and M. Oshikawa, Physical Review Letters **108**, 161803 (2012), arXiv:1112.1414.

[47] K. Klitzing, G. Dorda, and M. Pepper, Physical Review Letters **45**, 494 (1980).

[48] C. L. Kane and E. J. Mele, Physical Review Letters **95**, 146802 (2005), arXiv:cond-mat/0506581.

[49] C. L. Kane and E. J. Mele, Physical Review Letters **95**, 226801 (2005), arXiv:cond-mat/0411737.

[50] B. A. Bernevig, T. L. Hughes, and S.-C. Zhang, Science (New York, N.Y.) **314**, 1757 (2006), arXiv:cond-mat/0611399.

[51] M. König, S. Wiedmann, C. Brüne, A. Roth, H. Buhmann, L. W. Molenkamp, X.-L. Qi, and S.-C. Zhang, Science (New York, N.Y.) **318**, 766 (2007), arXiv:0710.0582.

[52] L. Fu and C. Kane, Physical Review B **76**, 045302 (2007), arXiv:cond-mat/0611341.

[53] Y. Ando, Journal of the Physical Society of Japan **82**, 102001 (2013), arXiv:1304.5693.

[54] P. G. Grinevich and G. E. Volovik, Journal of Low Temperature Physics **72**, 371 (1988).

[55] L. Fu and E. Berg, Physical Review Letters **105**, 097001 (2010), arXiv:0912.3294.

[56] S. Sasaki, M. Kriener, K. Segawa, K. Yada, Y. Tanaka, M. Sato, and Y. Ando, Physical Review Letters **107**, 217001 (2011), arXiv:1108.1101.

[57] D. a. Ivanov, Physical Review Letters **86**, 268 (2001), arXiv:cond-mat/0005069.

[58] A. Kitaev, Annals of Physics **303**, 2 (2003), arXiv:quant-ph/9707021.

[59] C. Nayak, A. Stern, M. Freedman, and S. Das Sarma, Reviews of Modern Physics **80**, 1083 (2008), arXiv:0707.1889.

[60] A. P. Mackenzie and Y. Maeno, Reviews of Modern Physics **75**, 657 (2003).

[61] Z. K. Liu, B. Zhou, Y. Zhang, Z. J. Wang, H. M. Weng, D. Prabhakaran, S.-K. Mo, Z. X. Shen, Z. Fang, X. Dai, et al., Science (New York, N.Y.) **343**, 864 (2014), arXiv:1310.0391.

[62] M. Neupane, S.-Y. Xu, R. Sankar, N. Alidoust, G. Bian, C. Liu, I. Belopolski, T.-R. Chang, H.-T. Jeng, H. Lin, et al., Nature communications **5**, 3786 (2014).

[63] Z. K. Liu, J. Jiang, B. Zhou, Z. J. Wang, Y. Zhang, H. M. Weng, D. Prabhakaran, S.-K. Mo, H. Peng, P. Dudin, et al., Nature materials **13**, 677 (2014).

[64] S. Borisenko, Q. Gibson, D. Evtushinsky, V. Zabolotnyy, B. Büchner, and R. J. Cava, Physical Review Letters **113**, 027603 (2014), arXiv:1309.7978.

[65] Y. Kasahara, T. Iwasawa, H. Shishido, T. Shibauchi, K. Behnia, Y. Haga, T. Matsuda, Y. Onuki, M. Sigrist, and Y. Matsuda, Physical Review Letters **99**, 116402 (2007), arXiv:0708.1042.

[66] K. Yano, T. Sakakibara, T. Tayama, M. Yokoyama, H. Amitsuka, Y. Homma, P. Miranović, M. Ichioka, Y. Tsutsumi, and K. Machida, Physical Review Letters **100**, 017004 (2008), arXiv:0712.1376.

[67] G. Abramovici and P. Kalugin, International Journal of Geometric Methods in Modern Physics **09**, 1250023 (2012), arXiv:1101.1054.

[68] T. Morimoto and A. Furusaki, Physical Review B **88**, 125129 (2013), arXiv:1306.2505.

[69] Y. S. Hor, A. J. Williams, J. G. Checkelsky, P. Roushan, J. Seo, Q. Xu, H. W. Zandbergen, A. Yazdani, N. P. Ong, and R. J. Cava, Physical Review Letters **104**, 057001 (2010), arXiv:0909.2890.

[70] H. Yuan, D. Agterberg, N. Hayashi, P. Badica, D. Vandervelde, K. Togano, M. Sigrist, and M. Salamon, Physical Review Letters **97**, 017006 (2006), arXiv:cond-mat/0512601.

[71] W. Su, J. Schrieffer, and A. Heeger, Physical Review B **22**, 2099 (1980).

[72] A. Y. Kitaev, Physics-Uspekhi **44**, 131 (2001), arXiv:cond-mat/0010440.

[73] K. Shiozaki and S. Fujimoto, Physical Review Letters **110**, 076804 (2013), arXiv:1210.2825.

[74] A. J. Leggett, Progress of Theoretical Physics **36**, 901 (1966).

[75] S. Ryu, J. E. Moore, and A. W. W. Ludwig, Physical Review B **85**, 045104 (2012), arXiv:1010.0936.

[76] K. Nomura, S. Ryu, A. Furusaki, and N. Nagaosa, Physical Review Letters **108**, 026802 (2012), arXiv:1108.5054.

[77] T. Qin, Q. Niu, and J. Shi, Physical Review Letters **107**, 236601 (2011), arXiv:1108.3879.

[78] A. Altland and M. R. Zirnbauer, Physical Review B **55**, 1142 (1997), arXiv:cond-mat/9602137.

[79] P. Heinzner, A. Huckleberry, and M. Zirnbauer, Communications in Mathematical Physics **257**, 725 (2005), arXiv:math-ph/0411040.

[80] H. Hiller, American Mathematical Monthly **93**, 765 (1986).

[81] D. S. Freed and G. W. Moore, Annales Henri Poincaré **14**, 1927 (2013), arXiv:1208.5055.

[82] G. C. Thiang, arXiv:1406.7366.

[83] Y. Ueno, A. Yamakage, Y. Tanaka, and M. Sato, Physical Review Letters **111**, 087002 (2013), arXiv:1303.0202.

[84] J. Moore, Y. Ran, and X.-G. Wen, Physical Review Letters **101**, 186805 (2008), arXiv:0804.4527.

[85] G. Segal, Publications mathématiques de l'IHÉS **34**, 129 (1968).

[86] M. F. Atiyah and G. B. Segal, J. Differential Geom. **3**, 1 (1969).

[87] M. F. ATIYAH, The Quarterly Journal of Mathematics **17**, 367 (1966).

[88] J. L. Dupont, Mathematica Scandinavica **24**, 27 (1969).

[89] J. W. Milnor, *Morse Theory* (Princeton university press, 1963), ISBN 9780691080086.

[90] K. Ishikawa and T. Matsuyama, Zeitschrift für Physik C Particles and Fields **33**, 41 (1986).

[91] J. Moore and L. Balents, Physical Review B **75**, 121306 (2007), arXiv:cond-mat/0607314.

[92] M. Nakahara, *Geometry, topology, and physics* (CRC Press, 2003), ISBN 0750306068.

[93] L. Fu and C. Kane, Physical Review B **74**, 195312 (2006), arXiv:cond-mat/0606336.

[94] Y. Ran, arXiv:1006.5454.

[95] P. Horava, Physical Review Letters **95**, 016405 (2005), arXiv:hep-th/0503006.

[96] Y. X. Zhao and Z. D. Wang, Physical Review Letters **110**, 240404 (2013), arXiv:1211.7241.

[97] Y. X. Zhao and Z. D. Wang, Physical Review B **89**, 075111 (2014).

[98] A. M. Essin and V. Gurarie, Physical Review B **84**, 125132 (2011), arXiv:1104.1602.

[99] M. Sato, Y. Tanaka, K. Yada, and T. Yokoyama, Physical Review B **83**, 224511 (2011), arXiv:1102.1322.

[100] M. Koshino, T. Morimoto, and M. Sato, Physical Review B **90**, 115207 (2014), arXiv:1406.3094.

[101] C. Fang, M. J. Gilbert, and B. A. Bernevig, Physical Review B **86**, 115112 (2012), arXiv:1207.5767.

[102] J. C. Y. Teo and T. L. Hughes, Physical Review Letters **111**, 047006 (2013), arXiv:1208.6303.

[103] X.-j. Liu and K. T. Law, arXiv:1310.5685.

[104] W. A. Benalcazar, J. C. Y. Teo, and T. L. Hughes, Physical Review B **89**, 224503 (2014), arXiv:1311.0496.

[105] R.-x. Zhang and C.-x. Liu, arXiv:1401.6922.

[106] A. Alexandradinata, C. Fang, M. J. Gilbert, and B. A. Bernevig, Physical Review Letters **113**, 116403 (2014), arXiv:1402.6323.

[107] B. A. Bernevig and S.-C. Zhang, Physical Review Letters **96**, 106802 (2006), arXiv:cond-mat/0504147.

[108] M. Sato, A. Yamakage, and T. Mizushima, Physica E: Low-dimensional Systems and Nanostructures **55**, 20 (2014), arXiv:1305.7469.

[109] R. M. Lutchyn, J. D. Sau, and S. Das Sarma, Physical Review Letters **105**, 077001 (2010), arXiv:1002.4033.

[110] Y. Oreg, G. Refael, and F. von Oppen, Physical Review Letters **105**, 177002 (2010), arXiv:1003.1145.

[111] T. Mizushima and M. Sato, New Journal of Physics **15**, 075010 (2013), arXiv:1302.4341.

[112] M. Sato, Y. Takahashi, and S. Fujimoto, Physical Review Letters **103**, 020401 (2009), arXiv:0901.4693.

[113] M. Sato, Y. Takahashi, and S. Fujimoto, Physical Review B **82**, 134521 (2010), arXiv:1006.4487.

[114] M. Sato and S. Fujimoto, Physical Review B **79**, 094504 (2009), arXiv:0811.3864.

[115] S. Tewari and J. D. Sau, Physical Review Letters **109**, 150408 (2012), arXiv:1111.6592,.

[116] C. L. M. Wong and K. T. Law, Physical Review B **86**, 184516 (2012), arXiv:1211.0338.

[117] F. Zhang and C. L. Kane, Physical Review B **90**, 020501 (2014), arXiv:1310.5281.

[118] N. Kopnin and M. Salomaa, Physical Review B **44**, 9667 (1991).

[119] C.-k. Chiu, H. Yao, and S. Ryu, Physical Review B **88**, 075142 (2013), arXiv:1303.1843.

[120] J. E. Avron, R. Seiler, and B. Simon, Physical Review Letters **51**, 51 (1983).

[121] M. Salomaa and G. Volovik, Reviews of Modern Physics **59**, 533 (1987).

[122] M. A. Silaev, JETP Letters **90**, 391 (2009), arXiv:0907.5341.

[123] Y. Tsutsumi, M. Ishikawa, T. Kawakami, T. Mizushima, M. Sato, M. Ichioka, and K. Machida, Journal of the Physical Society of Japan **82**, 113707 (2013), arXiv:1307.1264.

[124] Y. Nagai, H. Nakamura, and M. Machida, Journal of the Physical Society of Japan **83**, 064703 (2014), arXiv:1211.0125.

[125] G. R. Stewart, Z. Fisk, J. O. Willis, and J. L. Smith, Physical Review Letters **52**, 679 (1984).

[126] Y. Machida, A. Itoh, Y. So, K. Izawa, Y. Haga, E. Yamamoto, N. Kimura, Y. Onuki, Y. Tsutsumi, and K. Machida, Physical Review Letters **108**, 157002 (2012), arXiv:1107.3082.

[127] Y. Tsutsumi, K. Machida, T. Ohmi, and M.-a. Ozaki, Journal of the Physical Society of Japan **81**, 074717 (2012), arXiv:1202.1894.

[128] L. Hao and T. K. Lee, Physical Review B **83**, 134516 (2011).

[129] A. Yamakage, K. Yada, M. Sato, and Y. Tanaka, Physical Review B **85**, 180509 (2012).

[130] D. Vollhardt and P. Wolfle, *The superfluid phases of 3He* (Francis and Taylor, London, 1990).

[131] T. Mizushima, M. Sato, and K. Machida, Physical Review Letters **109**, 165301 (2012), arXiv:1204.4780.

[132] M. Sato, Physical Review B **81**, 220504 (2010), arXiv:0912.5281.

[133] T. L. Hughes, E. Prodan, and B. A. Bernevig, Physical Review B **83**, 245132 (2011), arXiv:1010.4508.

[134] A. M. Turner, Y. Zhang, R. S. K. Mong, and A. Vishwanath, Physical Review B **85**, 165120 (2012).

[135] L. Fu, C. Kane, and E. Mele, Physical Review Letters **98**, 106803 (2007), arXiv:cond-mat/0607699.

[136] M. Sato, Physical Review B **79**, 214526 (2009), arXiv:0806.0426.

[137] R. Roy, Physical Review Letters **105**, 186401 (2010), arXiv:1001.2571.

[138] R. Roy, Physical Review B **79**, 195322 (2009), arXiv:cond-mat/0607531.

[139] Z. Wang, X.-L. Qi, and S.-C. Zhang, New Journal of Physics **12**, 065007 (2010), arXiv:0910.5954.

[140] Z. Wang, X.-L. Qi, and S.-C. Zhang, Physical Review B **84**, 014527 (2011), arXiv:1011.0586.

[141] P. Hosur, S. Ryu, and A. Vishwanath, Physical Review B **81**, 045120 (2010), arXiv:0908.2691.

[142] M. Stone, Physical Review B **85**, 184503 (2012), arXiv:1201.4095.

[143] H. Sumiyoshi and S. Fujimoto, Journal of the Physical Society of Japan **82**, 023602 (2013), arXiv:1211.5419.

[144] Y. Hidaka, Y. Hirono, T. Kimura, and Y. Minami, Progress of Theoretical and Experimental Physics **2013**, 13A02 (2012), arXiv:1206.0734.

[145] H. Nieh and M. Yan, Annals of Physics **138**, 237 (1982).

[146] C. Brouder, G. Panati, M. Calandra, C. Mourougane, and N. Marzari, Physical Review Letters **98**, 046402 (2007), arXiv:cond-mat/0606726.

[147] Y. Nambu, Physical Review D **7**, 2405 (1973).

[148] T. Neupert, L. Santos, S. Ryu, C. Chamon, and C. Mudry, Physical Review B **86**, 035125 (2012), arXiv:1202.5188.

[149] B. Estienne, N. Regnault, and B. A. Bernevig, Physical Review B **86**, 241104 (2012), arXiv:1202.5543.

[150] T. Kita and M. Arai, Journal of the Physical Society of Japan **74**, 2813 (2005), arXiv:cond-mat/0510381.

[151] J. Luttinger, Physical Review **84**, 814 (1951).

[152] X.-l. Qi, R. Li, J. Zang, and S.-c. Zhang, Science (New York, N.Y.) **323**, 1184 (2009).

[153] T. L. Hughes, R. G. Leigh, and O. Parrikar, Physical Review D **88**, 025040 (2013), arXiv:1211.6442.

[154] L. Smrcka and P. Streda, Journal of Physics C: Solid State Physics **10**, 2153 (1977).

[155] J. Shi and Z. Cheng, arXiv:1211.3633.

[156] N. R. Cooper, B. I. Halperin, and I. M. Ruzin, Physical Review B **55**, 2344 (1997), arXiv:cond-mat/9607001.

[157] K. Shiozaki and S. Fujimoto, Physical Review B **89**, 054506 (2014), arXiv:1310.4982.

[158] P. Goswami and B. Roy, Physical Review B **90**, 041301 (2014), arXiv:1307.3240.

[159] E. Bauer and M. Sigrist, *Non-centrosymmetric superconductors: introduction and overview* (Springer, 2012).

[160] S. Sharapov, V. Gusynin, and H. Beck, The European Physical Journal B **30**, 45 (2002), arXiv:cond-mat/0205131.

Acknowledgment

First of all, I would like to thank my mentor, Satoshi Fujimoto, for his help and support during my five years graduate course. I would like to express my gratitude to him for guidance, education, and patience in explaining or discussing physical topics. He always took time off for sharing valuable problems and insights of research projects. Due to his broad knowledge of condensed matter physics, I have been able to study whatever I wanted to do. I have been impressed by his point of view and vision during discussions, which formed the ways to tackle a research problem for me.

Also I would like to thank Masatoshi Sato a lot. Through the collaboration with him, I have learned many aspects of topological crystalline phases from him. His explanations have been very instructive, simple, and suggestive. His insights of our crude results have given a friendly picture, which always took me to next step.

I am deeply grateful to Takahiro Morimoto for many fruitful and stimulating discussions on the topological crystalline insulators. His valuable comments have been important for me to complete the work.

I would like to acknowledge Shinsei Ryu for helping me in my postdoctoral application and collaboration. I am indebted to his creativity and deep knowledges of physics.

I would like to thank Takahiro Fukui on the early stage of my research. Through the projects with him, I acquired basic insight and questions on topological phases of matter, which was the good starting point of my study.

I would also like to thank Kiyonori Gomi for introducing me to topological K-theory. There had been very few references connecting physical problems and mathematical knowledge. His advises have been very helpful for me and will be good guidance for my future study.

I would like to thank the faculty in the condensed matter theory group at Kyoto, Norio Kawakami, Ryusuke Ikeda, Hiroaki Ikeda, Masaki Tezuka, and Kazushi Aoyama for their help in various academic matters. Also I benefited from discussions and interactions with many inspiring colleagues and friends in the condensed matter theory group. I am especially grateful to Fuyuki Matsuda, Masaya Nakagawa, Kazuto Noda, Takuya Nomoto, Jun-ichi Ozaki, Masaru Sakaida, Atsuo Shitade, Hiroaki Sumiyoshi, Yasuhiro Tada, Rina Takashima, Shun Uchino, Suguru Ueda, Yasuhiro Yamada, and Tsuneya Yoshida for everyday discussions about physics and others. The five years I spent here were very enjoyable for them.

My graduate course owed to continuous interactions with many physicists around Japan. I would like to thank Yohei Fuji, Shunsuke Furukawa, Akira Furusaki, Taro Kimura, Shingo Kobayashi, Sho Nakosai, Muneto Nitta, Kentaro Nomura, Masahiro Sato, Shintaro Takayoshi, and Akihiro Tanaka.

I would also like to acknowledge financial support I have received over the past two years from the Japan Society for the Promotion of Science (JSPS), without which the work reported in this dissertation would not have been possible. Also I would like to thank the Grant-in-Aid for Scientific Research on innovative Areas, MEXT, Japan, "Topological Quantum Phenomena in Condensed Matter with Broken Symmetries" for my visiting at the Nagoya university for the research project with Masatoshi Sato, and many conferences in which I got many opportunities of discussion with many good physicists and encounters with inspired good rivals.

At last, I wish to express my gratitude to my parents, Shigeo Shiozaki and Chieko Shiozaki. I really benefited from their support and patience for my decision to study physics.